SOIL AND SEDIMENT POLLUTION, PROCESSES AND REMEDIATION

EDITED BY: Hongbiao Cui, Chunhao Gu, Zhu Li and Jun Zhou
PUBLISHED IN: Frontiers in Environmental Science

frontiers Research Topics

frontiers

ISSN 1664-8714
ISBN 978-2-88974-310-0
DOI 10.3389/978-2-88974-310-0

About Frontiers

Frontiers is more than just an open-access publisher of scholarly articles: it is a pioneering approach to the world of academia, radically improving the way scholarly research is managed. The grand vision of Frontiers is a world where all people have an equal opportunity to seek, share and generate knowledge. Frontiers provides immediate and permanent online open access to all its publications, but this alone is not enough to realize our grand goals.

Frontiers Journal Series

The Frontiers Journal Series is a multi-tier and interdisciplinary set of open-access, online journals, promising a paradigm shift from the current review, selection and dissemination processes in academic publishing. All Frontiers journals are driven by researchers for researchers; therefore, they constitute a service to the scholarly community. At the same time, the Frontiers Journal Series operates on a revolutionary invention, the tiered publishing system, initially addressing specific communities of scholars, and gradually climbing up to broader public understanding, thus serving the interests of the lay society, too.

Dedication to Quality

Each Frontiers article is a landmark of the highest quality, thanks to genuinely collaborative interactions between authors and review editors, who include some of the world's best academicians. Research must be certified by peers before entering a stream of knowledge that may eventually reach the public - and shape society; therefore, Frontiers only applies the most rigorous and unbiased reviews.
Frontiers revolutionizes research publishing by freely delivering the most outstanding research, evaluated with no bias from both the academic and social point of view. By applying the most advanced information technologies, Frontiers is catapulting scholarly publishing into a new generation.

What are Frontiers Research Topics?

Frontiers Research Topics are very popular trademarks of the Frontiers Journals Series: they are collections of at least ten articles, all centered on a particular subject. With their unique mix of varied contributions from Original Research to Review Articles, Frontiers Research Topics unify the most influential researchers, the latest key findings and historical advances in a hot research area! Find out more on how to host your own Frontiers Research Topic or contribute to one as an author by contacting the Frontiers Editorial Office: frontiersin.org/about/contact

SOIL AND SEDIMENT POLLUTION, PROCESSES AND REMEDIATION

Topic Editors:
Hongbiao Cui, Anhui University of Science and Technology, China
Chunhao Gu, University of Delaware, United States
Zhu Li, Institute of Soil Science, Chinese Academy of Sciences (CAS), China
Jun Zhou, University of Massachusetts Lowell, United States

Citation: Cui, H., Gu, C., Li, Z., Zhou, J., eds. (2022). Soil and Sediment Pollution, Processes and Remediation. Lausanne: Frontiers Media SA.
doi: 10.3389/978-2-88974-310-0

Table of Contents

frontiers in Environmental Science

EDITORIAL
published: 22 December 2021
doi: 10.3389/fenvs.2021.822355

Editorial: Soil and Sediment Pollution, Processes and Remediation

Hongbiao Cui[1], Jun Zhou[2], Zhu Li[3] and Chunhao Gu[4]*

[1]School of Earth and Environment, Anhui University of Science and Technology, Huainan, China, [2]Department of Environmental, Earth, and Atmospheric Sciences, University of Massachusetts, Lowell, MA, United States, [3]CAS Key Laboratory of Soil Environment and Pollution Remediation, Institute of Soil Science, Chinese Academy Sciences, Nanjing, China, [4]Delaware Environmental Institute, Department of Plant and Soil Sciences, University of Delaware, Newark, DE, United States

Keywords: pollution, remediation, soils and sediments, heavy metals, phytoremediation, security application

Editorial on the Research Topic

Soil and Sediment Pollution, Processes and Remediation

INTRODUCTION

Since the 20th century, human activities have generated a large amount of toxic organic and inorganic pollutants that have been released into earth surface environment, causing a number of environmental public health issues (Boente et al., 2017; Song et al., 2017; Sun et al., 2020; Tang et al., 2015). Many pollutants from natural or anthropogenic sources can enter soils and sediments through spills, leaks, tank and pipeline ruptures, irrigation, atmospheric transport, and other disposal pathways (Zhang et al., 2008; He et al., 2019). These pollutants can accumulate in soil and sediment systems, posing potential threats to food security, ecological and human health. Moreover, abandoned industrial sites due to weak environmental management (insufficient management, legislation and enforcement) and adjustment of urban planning or industrial structure are increasing and causes severe contamination to adjacent soils and sediments (Zhao et al., 2015). The pollution process, migration, transformation, degradation, and accumulation of toxic pollutants in soil and sediment of industrial sites are not well understood and reuse of these sites requires some *in-situ* and *ex-situ* remediation.

Before remediation, it is crucial to control the source of pollutants and prevent pollutants from entering soil and sediment. The choice of remediation technologies of contaminated soil and sediment is strongly dependent upon the types of pollutants and degree of pollution (Khalid et al., 2016; Ye et al., 2017; Zhang et al., 2021). Through remediation and risk assessment, prime land in established locations can be reused (e.g., agricultural, residential, and commercial land), thereby lowering the pressure on green land. Therefore, studies on the biogeochemical processes of soil and sediment pollution, control, and remediation are urgently needed. Since soil and sediment remediation followed by redevelopment prevent degradation of the environment, it is a topic of enormous public interest.

This Research Topic focuses on new pollutants such as antibiotics, environmental hormones, antibiotics resistance genes, pathogens, and microplastics as well as traditional heavy metals, excess nutrient microelements, and pesticides. This Research Topic covers the following themes: (a) Sources, migration, and transformation of pollutants in soils and sediments; (b) Plant and microbe response and environmental effect in polluted soils; (c) Biogeochemistry processes of pollutants between the atmosphere, organisms, water and soil/sediment systems; (d) Safe use, risk assessment and control of contaminated soil and sediment; (e) Mitigation and remediation technologies; (f) Environmental modeling of the fate and biogeochemical process of pollutants.

Highlights from Publications Featured in this Research Topic

OPEN ACCESS

Edited and reviewed by:
Oladele Ogunseitan, University of California, Irvine, United States

****Correspondence:***
Hongbiao Cui
cuihongbiao0554@163.com

Specialty section:
This article was submitted to Toxicology, Pollution and the Environment, a section of the journal Frontiers in Environmental Science

Received: *25 November 2021*
Accepted: *01 December 2021*
Published: *22 December 2021*

Citation:
Cui H, Zhou J, Li Z and Gu C (2021) Editorial: Soil and Sediment Pollution, Processes and Remediation. Front. Environ. Sci. 9:822355. doi: 10.3389/fenvs.2021.822355

Huang et al. investigated the spatial variation in Cd and Hg concentrations in farmland soils from the Poyang Lake Plain, China, and evaluated their potential ecological risks. The authors concluded that moderate pollution of Cd and Hg presented in these farmland soils where their comprehensive potential ecological risk level was generally low and mainly influenced by soil pH and total phosphorous.

Wang et al. focused on the spatial distribution of Antimony in paddy Soils from Hunan Province, China, and concluded that strong migration of antimony in horizontal direction and a decrease trend of antimony with the increase of profile depth, which was significantly affected by parent materials.

Kong and Zhang investigated the spatial distribution of five heavy metals in north of north China plain, and proposed a scheme for the regional division of the security of soil heavy metals based on the different evaluation methods.

Zou et al. investigated the effects of As and Pb on spatial variation of soil microbial community, and concluded that soil pH, total As and Pb, bioavailable As and Pb, nitrate-nitrogen (NO_3−-N) and ammonia-nitrogen (NH_4^+-N) were the most important factors in shaping the bacterial community structure.

Liu et al. predicted the transformation of Cd from soil to potato in Karst soil and discovered soil pH was the key factor influencing Cd uptake by potatoes.

Abakumov et al. quantitatively and qualitatively evaluated the priority polycyclic aromatic hydrocarbons (PAHs) and heavy metals (Cu, Pb, Zn, Cd, Ni, and Cr) is soils and cryoconites on "St. Kliment Ohridski" Antarctic station territory and its vicinities, and their results suggested that there was no significant effect of anthropogenic activities on the environmental components of the landscapes.

Risk control and security utilization of the contaminated soils and sediments is crucial for ecological remediation. Some traditional methods including chemical leaching, vitrification, land farming, and soil covering are constrained by processing duration, geological problems, economical impracticality and negative impacts on soil properties (Gong et al., 2018; Purkis et al., 2021; Rajendran et al., 2021). Chemical stabilization is widely used in farmlands contaminated with heavy metals because of its low cost and high efficiency for reducing the migration and bioavailability (Lin et al., 2019; Shen et al., 2019). Based on the Superfund Remedy Report in USA, the stabilization/solidification is still the most popular *in-situ* remediation technology, which accounted for nine out of 35 total decision documents between 2015 and 2017 (US EPA, 2020). However, the long-term sustainability of the technology and the potential impact factors weaken the remediation effect are still not fully known, which limited the large-scale utilization of the technology (Wang et al., 2021). Phytoremediation is an environmental-friendly and economical strategy, but it is time-consuming and strong dependence on contaminant types, plant species, and soil types (Marques et al., 2009; Cui et al., 2016; Ashraf et al., 2019). Particularly, most hyperaccumulator is low biomass and the total removal of heavy metals is in low level (Marques et al., 2009). Therefore, some metal-tolerant plants with large biomass are recommended for phytoremediation (Cui et al., 2016). For example, Zhang et al. reviewed the application of giant reed in the field of phytoremediation of heavy metals and discussed the potential application of giant reed combined with advanced remediation technologies in ecological remediation.

Xu et al. reported the combination of lime immobilization and four Cu-tolerance plants can effectively decrease water-soluble can exchangeable Cu and Cd, which can significantly decrease the environmental risk of the contaminated area.

Future Research

This *Research Topic collection* advances our understanding on the spatial distribution of contaminants and their effects on plants and microbial community structure. Moreover, this Research Topic also highlights the phytoremediation with large biomass plants in heavy metals contaminated soils. Nevertheless, great challenges on the soil and sediment pollution, process and remediation needs more attentions. Therefore, the following aspects need further attention to support the environmental management and security utilization for soils and sediments: 1) Effectively identify the sources of the pollutants in the soils and sediments; 2) The mechanism of pollutant fate and biogeochemistry processes in the soils and sediments environment; 3) Efficient strategies of degrading and/or removing pollutants from soils; 4) More environmental-friendly bioremediation and combination of multiple measures; 5) Engineering technologies urgently needed in the field. 6) Sustainable green remediation materials and technologies; 7) Scientific assessment methods for the sites after remediation; 8) The influences of global climate change induced by human activities on the fate, transformation, and transportation of the pollutants.

AUTHOR CONTRIBUTIONS

All authors listed have made a substantial, direct, and intellectual contribution to the work and approved it for publication.

ACKNOWLEDGMENTS

Authors would like to acknowledge the Natural Science Foundation of Universities of Anhui Province (KJ2020ZD35), the National Nature Science Foundation of China (41601340).

REFERENCES

Ashraf, S., Ali, Q., Zahir, Z. A., Ashraf, S., and Asghar, H. N. (2019). Phytoremediation: Environmentally Sustainable Way for Reclamation of Heavy Metal Polluted Soils. *Ecotoxicology Environ. Saf.* 174, 714–727. doi:10.1016/j.ecoenv.2019.02.068

Boente, C., SierraRodríguez-Valdés., C., Rodríguez-Valdés, E., and Menéndez-Aguado, J. M. (2017). Soil Washing Optimization by Means of Attributive Analysis: Case Study for the Removal of Potentially Toxic Elements from Soil

Contaminated with Pyrite Ash. *J. Clean. Pro* 142, S0959652616318418. doi:10.1016/j.jclepro.2016.11.007

Cui, H., Fan, Y., Yang, J., Xu, L., Zhou, J., and Zhu, Z. (2016). *In Situ* phytoextraction of Copper and Cadmium and its Biological Impacts in Acidic Soil. *Chemosphere* 161 (oct), 233–241. doi:10.1016/j.chemosphere.2016.07.022

Gong, Y., Zhao, D., and Wang, Q. (2018). An Overview of Field-Scale Studies on Remediation of Soil Contaminated with Heavy Metals and Metalloids: Technical Progress over the Last Decade. *Water Res.* 147, 440–460. doi:10.1016/j.watres.2018.10.024

He, L., Zhong, H., Liu, G., Dai, Z., and Xu, J. (2019). Remediation of Heavy Metal Contaminated Soils by Biochar: Mechanisms, Potential Risks and Applications in china. *Environ. Pollut.* 252 (Pt A). doi:10.1016/j.envpol.2019.05.151

Khalid, S., Shahid, M., Niazi, N. K., Murtaza, B., Bibi, I., and Dumat, C. (2016). A Comparison of Technologies for Remediation of Heavy Metal Contaminated Soils. *J. Genchem Explor* 182, 247–268. doi:10.1016/j.gexplo.2016.11.021

Lin, J. J., Sun, M. Q., Su, B. L., Owens, G., and Chen, Z. L. (2019). Immobilization of Cadmium in Polluted Soils by Phytogenic Iron Oxide Nanoparticles. *Sci. Total Environ.* 659, 491–498. doi:10.1016/j.scitotenv.2018.12.391

Marques, A. P. G. C., Rangel, A. O. S. S., and Castro, P. M. L. (2009). Remediation of Heavy Metal Contaminated Soils: Phytoremediation as a Potentially Promising Clean-Up Technology. *Crit. Rev. Env Sci. Tec* 39, 622–654. doi:10.1080/10643380701798272

Purkis, J. M., Tucknott, A., Croudace, I. W., Warwick, P. E., and Cundy, A. B. (2021). Enhanced Electrokinetic Remediation of Nuclear Fission Products in Organic-Rich Soils. *Appl. Geochem.* 125, 104826. doi:10.1016/j.apgeochem.2020.104826

Rajendran, S., Priya, T. A. K., Khoo, K. S., Hoang, T. K. A., Ng, H. S., Munawaroh, H. S. H., et al. (2021). A Critical Review on Various Remediation Approaches for Heavy Metal Contaminants Removal from Contaminated Soils. *Chemosphere* 287, 132369. doi:10.1016/j.chemosphere.2021.132369

Shen, Z., Jin, F., O'Connor, D., and Hou, D. (2019). Solidification/Stabilization for Soil Remediation: an Old Technology with New Vitality[J]. *Environ. Sci. Technol.* 53, 11615–11617. doi:10.1021/acs.est.9b04990

Song, B., Zeng, G., Gong, J., Liang, J., Xu, P., Liu, Z., et al. (2017). Evaluation Methods for Assessing Effectiveness of *In Situ* Remediation of Soil and Sediment Contaminated with Organic Pollutants and Heavy Metals. *Environ. Int.* 105 (aug), 43–55. doi:10.1016/j.envint.2017.05.001

Sun, Z., Hu, Y., and Cheng, H. (2020). Public Health Risk of Toxic Metal(loid) Pollution to the Population Living Near an Abandoned Small-Scale Polymetallic Mine. *Sci. Total Environ.* 718. doi:10.1016/j.scitotenv.2020.137434

Tang, Z., Zhang, L., Huang, Q., Yang, Y., NieCheng, Z. J., Yang, Y., et al. (2015). Contamination and Risk of Heavy Metals in Soils and Sediments from a Typical Plastic Waste Recycling Area in north china. *Ecotox. Environ. Safe.* 122 (DEC.), 343–351. doi:10.1016/j.ecoenv.2015.08.006

US EPA (2020a). *EPA-542-R-20-001 Superfund Remedy Report*. 16th edition. US: United States Environmental Protection Agency.

Wang, J., Shi, L., Zhai, L., Zhang, H., Wang, S., Zou, J., et al. (2021). Analysis of the Long-Term Effectiveness of Biochar Immobilization Remediation on Heavy Metal Contaminated Soil and the Potential Environmental Factors Weakening the Remediation Effect: A Review. *Ecotox. Environ. Safe.* 207, 111261. doi:10.1016/j.ecoenv.2020.111261

Ye, S., Zeng, G., Wu, H., Zhang, C., Dai, J., Liang, J., et al. (20172017). Biological Technologies for the Remediation of Co-contaminated Soil. *Crit. Rev. Biotechnol.* 37 (8), 1–15. doi:10.1080/07388551.2017.1304357

Zhang, C., Wu, L., Luo, Y., Zhang, H., and Christie, P. (2008). Identifying Sources of Soil Inorganic Pollutants on a Regional Scale Using a Multivariate Statistical Approach: Role of Pollutant Migration and Soil Physicochemical Properties. *Environ. Pollut.* 151 (3), 470–476. doi:10.1016/j.envpol.2007.04.017

Zhang, Y., Labianca, C., Chen, L., Gisi, S. D., and Wang, L. (2021). Sustainable *Ex-Situ* Remediation of Contaminated Sediment: a Review. *Environ. Pollut.* 287, 117333. doi:10.1016/j.envpol.2021.117333

Zhao, F. J., Ma, Y., Zhu, Y. G., Zhong, T., and Mcgrath, S. P. (2015). Soil Contamination in china: Current Status and Mitigation Strategies. *Environ. Sci. Technol.* 49 (2), 750. doi:10.1021/es5047099

Conflict of Interest: The authors declare that the research was conducted in the absence of any commercial or financial relationships that could be construed as a potential conflict of interest.

Publisher's Note: All claims expressed in this article are solely those of the authors and do not necessarily represent those of their affiliated organizations, or those of the publisher, the editors and the reviewers. Any product that may be evaluated in this article, orclaim that may be made by its manufacturer, is not guaranteed or endorsed by the publisher.

frontiers in Environmental Science

ORIGINAL RESEARCH
published: 24 March 2021
doi: 10.3389/fenvs.2021.639460

Security Regional Division of Farmland Soil Heavy Metal Elements in North of the North China Plain

*Chenchen Kong and Shiwen Zhang**

School of Earth and Environment, Anhui University of Science and Technology, Huainan, China

A total of 94 soil samples from different soil depths (0~25 cm, 25~50 cm) were collected of farmland soil around the plain of Beijing, and the concentrations of five heavy metal elements (Cd, Cr, Pb, As, and Hg) were measured using standard methods. The safety utilization evaluation method of heavy metals was based on three different evaluation methods. Then, the governance principles and specific management control strategy were determined in detail according to the core pollution source analysis of each safety grade zone. The results show that there are four different comprehensive safe utilization areas: safe, low-risk, medium-risk, and high-risk utilization. Among them, the study area was dominated by low-risk utilization areas, and the risk trend was gradually weakening from the center of the city to the periphery. Based on the characteristics of different security zones, this study puts on the governance principles of priority protection, long-term monitoring and moderate optimization, strengthens early warning, and cooperates with effective repair and priority governance. And then it puts forward practical control strategies according to the core pollution sources of each safety utilization zone. Our findings may provide a clear direction for rational utilization of land resources and renovation in the future.

Keywords: farmland soil, heavy metals, core pollution sources, safety utilization, zoning, control strategy

OPEN ACCESS

Edited by:
Chunhao Gu,
University of Delaware, United States

Reviewed by:
Mingkai Qu,
Institute of Soil Science (CAS), China
Yingui Cao,
China University of Geosciences, China
Wenji Zhao,
Capital Normal University, China

****Correspondence:***
Shiwen Zhang
mamin1190@126.com

Specialty section:
This article was submitted to Toxicology, Pollution and the Environment, a section of the journal Frontiers in Environmental Science

Received: *09 December 2020*
Accepted: *25 January 2021*
Published: *24 March 2021*

Citation:
Kong C and Zhang S (2021) Security Regional Division of Farmland Soil Heavy Metal Elements in North of the North China Plain. Front. Environ. Sci. 9:639460. doi: 10.3389/fenvs.2021.639460

INTRODUCTION

Soil is an organic part of the ecological environment, a natural environment on which mankind depends and also a natural resource for agricultural production. As an important line of defense for the protection of human health and environmental quality, soil quality is directly related to economic development, social progress, and people's well-being (Ungureanu et al., 2017). With the rapid development of urbanization and industrialization in recent years, heavy metal contamination of soil has become more and more intense. Being ubiquitous, highly persistent, nonbiodegradable, and able to accumulate in soils at environmentally hazardous levels, heavy metal contamination directly causes serious harm to soil environment and indirectly damages human health through food intake and other related approaches (Mohammadi et al., 2018). According to a survey conducted by the Ministry of Agriculture of the People's Republic of China, 64.8% of the 1.4 million hm^2 sewage-irrigated area in China suffers from heavy metal pollution. In view of that, scientific research on the status of heavy metal pollution in farmland soil is of great significance for agricultural production and soil safety (Zhang et al., 2014; Zhang et al., 2017).

At present, the related fields of soil heavy metals have led researchers to carry out several relevant studies. Most of the previous studies focused on the spatial distribution characteristics of soil heavy

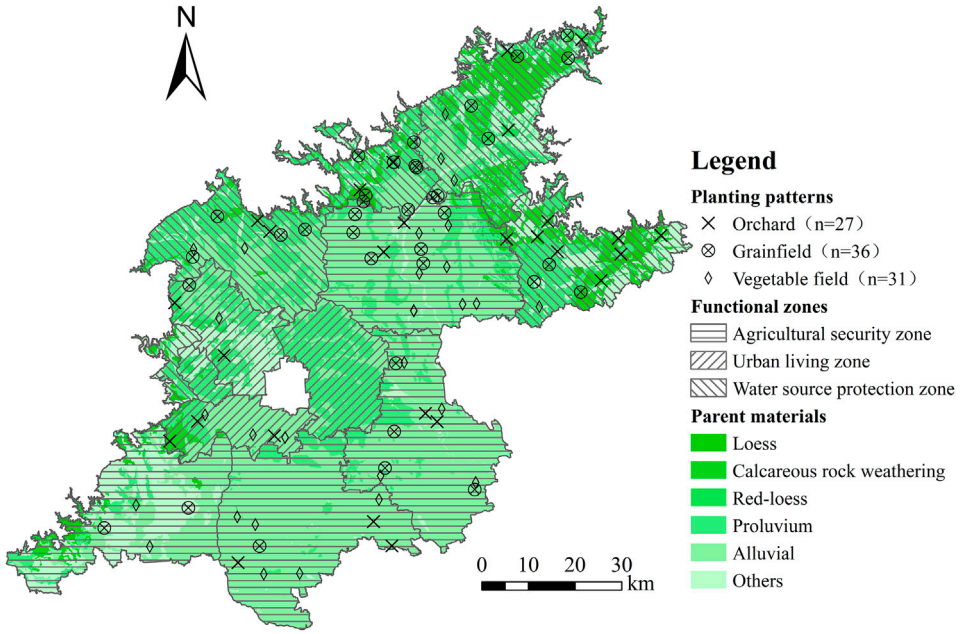

FIGURE 1 | Location of the study area and distribution of sampling points.

metals and the analysis of pollution sources (Manta et al., 2002; Da-wei and He-rong, 2017; Wang et al., 2019; Qu et al., 2020), the risk assessment of heavy metal pollution (Soå'Ek-Podwika et al., 2016; Yan et al., 2016; Huang et al., 2018; Yang et al., 2018), and evaluation methods (Luo et al., 2017). However, there were few studies on the safety utilization of heavy metals from different soil depths.

Based on the monitored data, basic physicochemical properties of the soil, and related environmental factors, this essay took farmland soil around the plain of Beijing as the research object; analyzed the horizontal and vertical distribution characteristics of heavy metals (Cd, Cr, Pb, As, and Hg) in the soil of the study area; and used the geoaccumulation index, the improved geoaccumulation comprehensive index, and the potential ecological risk index and carried out the assessment of soil heavy metals. Then it puts forward a scheme for the regional division of the security of soil heavy metals. Furthermore, the core pollution sources of areas with different safety utilization grades were analyzed, and the governance principles and specific management control strategies of different grades of comprehensive utilization areas were determined. The research findings of this essay will provide scientific reference for the control of pollution risk of soil heavy metals and contribute to the efficient and safe utilization of soil.

MATERIALS AND METHODS

Description of the Study Area

The study was conducted in an area of approximately 7779.12 km^2 located in the southeast of Beijing. According to the digital elevation of Beijing, with the 100 m contour line as the boundary, the area with elevation ≤100 m was considered as the study area. The research area from north to south includes the water source protection zone (namely, Miyun, Pinggu, Huairou, and Changping), the agricultural security zone (namely, Shunyi, Tongzhou, Daxing, and Fangshan), and the urban living zone (Haidian, Shijingshan, Mentougou, Fengtai, and Chaoyang), a total of three functional areas and 13 districts and counties. The agricultural land planting patterns in the research area include many types, mainly grainfield, orchard, and vegetable land. Besides, fluvoaquic soil, cinnamon soil, and a small amount of paddy soil are the main soil types. Moreover, soil parent materials mainly include alluvial, proluvium, calcareous rock weathering, loess, and red-loess.

Sampling and Analysis

According to the distribution of agricultural land (grainfield, orchard, and vegetable plot) in the study area, a total of 94 samples of different planting patterns by setting different soil depths (0–25 cm, 25–50 cm) were collected, and the global positioning system (GPS) locator was applied to record its accurate coordinates and the attributes of the functional areas of the sampling points, planting patterns, soil types, and other basic attributes. A map indicating the field sampling points in the studied areas (sample locations) was given in **Figure 1**. In order to ensure the representativeness of the sample, soil samples were collected at the center point and two adjacent corners for each sample point, and the samples at the same depth were mixed to form the sample to be tested. The contact part of the sample with the metal sampling apparatus was removed in the field. After picking out visible impurities (such as the roots of the plants and debris), samples were naturally air-dried, crushed, and sieved for further analysis. Finally, elements including Pb, Cr, and Cd were

TABLE 1 | The classification standard of evaluation index (Shi and Wang, 2013; Song et al., 2017).

Geoaccumulation index				Potential ecological risk index	
I_{geo}	Risk level	I	Risk level	RI	Risk level
<0	Pollution-free	<0	Risk-free	E_r^i <40 or *RI* <150	Slightly ecological harm
0~1	Slightly pollution	0~1	Low-risk	40≤ E_r^i <80 or 150≤ *RI* <300	Moderate ecological harm
1~2	Moderate pollution	1~2	Medium-risk	80≤ E_r^i <160 or 300≤ *RI* <600	Strong ecological harm
2~3	Medium to strong pollution	2~3	High-risk	160≤ E_r^i <320 or *RI* ≥600	Very strong ecological harm
3~4	Strong pollution			≥320	Extremely strong ecological harm
4~5	Strong to extremely strong pollution				
>5	Extremely strong pollution				

detected by atomic absorption spectrometry, whereas As and Hg were detected by atomic fluorescence spectrometry.

Descriptive statistics analysis, coefficient of variation, and principal components analysis were carried out by using IBM SPSS software (version 21.0). The Empirical Bayesian Kriging (EBK) interpolation method in the ArcGIS 10.2 geostatistics module was applied to predict soil heavy metal samples data.

EVALUATION METHODS

Geoaccumulation Index

The geoaccumulation index method was proposed by Muller, a scientist at the University of Hamburg in Germany in 1969. It was used to quantitatively assess the degree of heavy metal pollution in sediments (Muller, 1969; Li et al., 2014). The calculation is

$$I_{geo} = \log_2\left[\frac{C_n}{K \times B_n}\right],$$

where I_{geo} is the geoaccumulation index, C_n is the actual measured concentration of the element in the measured sample (mg·kg^{-1}), K is the correction coefficient (general K = 1.5) taken considering the variation of background values that may be caused by differences in the rocks around the area, and B_n is the environmental background value (mg·kg^{-1}) of the sample element.

The background value of Beijing soil was used as the reference value (the background values of Cd, Cr, Pb, As, and Hg were 0.119, 29.8, 24.6, 7.09, and 0.08 mg·kg^{-1}, respectively) (Jian, 1988; Chen et al., 2004). The classification standard of evaluation index was shown in **Table 1**.

In order to fully consider the different contribution ratios of each heavy metal element, to further compare the differences in the results of multifactor assessments, this study has made a certain degree of improvement based on the geoaccumulation index, has introduced the ecotoxicity of different heavy metals, and has calculated the weighted sum of the geoaccumulation index of different elements, so as to comprehensively analyze the environmental quality between elements or regions (Hakanson, 1980; Song et al., 2017). The calculation is

$$I = \sum_{i=1}^{n}\left(\frac{I_{geo} \times T_r^i}{T}\right)$$

where I is the improved geoaccumulation index, I_{geo} is the geoaccumulation index, T_r^i is the toxicity coefficient corresponding to each heavy metal element (the toxicity coefficients of Cd, Cr, Pb, As, and Hg were 30, 2, 5, 10, and 40, respectively) (Xu et al., 2008), and T is the sum of the toxicity coefficients of each heavy metal element.

The classification standard of evaluation index was shown in **Table 1**.

Potential Ecological Risk Index

The potential ecological risk index method was proposed by the Swedish scientist Hakanson according to the characteristics and different effects of heavy metal elements on the environment. This method combined the ecological effects of heavy metals, environmental effects, and toxicology while considering the content of heavy metals in soil. It is an indicator that comprehensively reflects the potential of heavy metals on the ecological environment and is of great significance for the precontrol of soil environmental pollution (Liu W. et al., 2016; Janadeleh et al., 2018). The potential ecological risk index (RI) is calculated as follows:

$$RI = \sum_{i=1}^{n} E_r^i = \sum_{i=1}^{n} T_r^i \times C_r^i = \sum_{i=1}^{n} \frac{T_r^i \times C_r^i}{C_n^i}$$

where RI is the variety of heavy metal potential ecological risk index, E_r^i is the potential ecological risk coefficient of a particular heavy metal, T_r^i is the toxicity coefficient of each heavy metal element, C_r^i is the pollution factor of heavy metal element I, C_i is the actual measured concentration of the element in the measured sample (mg·kg^{-1}), and C_n^i is the environmental background value of the sample element (mg·kg^{-1}).

The classification standard of evaluation index was shown in **Table 1**.

RESULTS AND DISCUSSION

Analysis on the Characteristics of Heavy Metal Content in Soil

The basic descriptive statistics of the heavy metal concentrations analyzed in soil samples around the plain of Beijing were listed in **Table 2** and **Figure 2**. In the soil depth of 0~25 cm, the mean concentrations of Cd, Cr, Pb, As, and Hg were 0.124 ± 0.111 mg·kg^{-1},

TABLE 2 | Statistical descriptive of the heavy metal concentrations analyzed in soil samples in the study area.

Soil depth	Heavy metal	Number of samples	Background/mg·kg^{-1}	Mean/mg·kg^{-1}	Max/mg·kg^{-1}	Min/mg·kg^{-1}	CV
0~25 cm	Cd	94	0.119	0.124 ± 0.111	1.070	0.034	0.895
	Cr	94	29.8	34.793 ± 16.300	103.000	6.890	0.468
	Pb	94	24.6	8.776 ± 22.213	211.000	0.532	2.531
	As	94	7.09	7.936 ± 2.651	20.400	2.180	0.334
	Hg	94	0.08	0.145 ± 0.165	0.890	0.016	1.137
25~50 cm	Cd	94	0.119	0.087 ± 0.055	0.357	0.021	0.633
	Cr	94	29.8	34.806 ± 16.385	108.000	9.540	0.471
	Pb	94	24.6	8.012 ± 8.866	65.000	0.643	1.107
	As	94	7.09	7.894 ± 2.296	15.100	2.220	0.291
	Hg	94	0.08	0.095 ± 0.094	0.672	0.007	0.983

Note: The rate of exceeding standard is the ratio of the standard sample points of each county and the total sample number of each county.

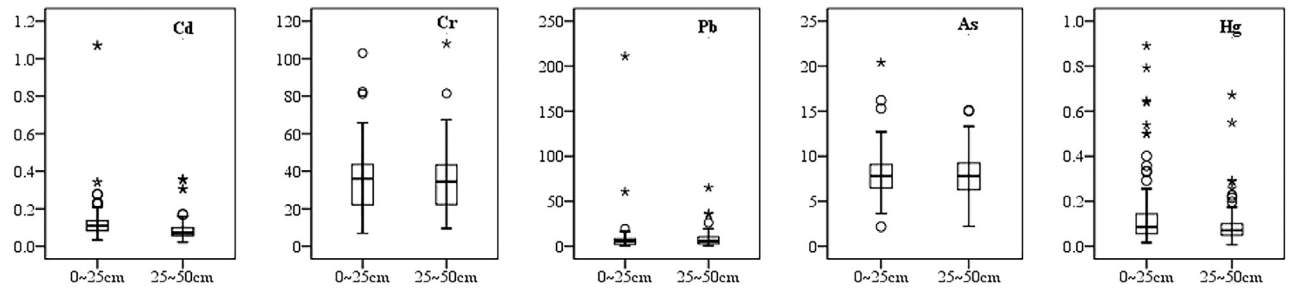

FIGURE 2 | Box plots of heavy metal concentrations (mg·kg^{-1}).

34.793 ± 16.300 mg·kg^{-1}, 8.776 ± 22.213 mg·kg^{-1}, 7.936 ± 2.651 mg·kg^{-1}, and 0.145 ± 0.165 mg·kg^{-1}, respectively. Concentration levels of the measured elements in the soil samples, except Pb, were higher than the corresponding soil background values in Beijing, while the element of Hg was 1.8 times the background value. It can be seen that the economic development was accompanied by human activities which have caused the accumulation of heavy metals. The lower concentration of Pb may be due to the continuous increase of urban green coverage, which has a certain barrier and filter effect on heavy metals emitted by motor vehicles. In recent years, Beijing has adopted a large number of measures (such as new cylinder production technology and improved gasoline and diesel quality) to reduce the pollution of automobile exhaust gas which, to a certain extent, reduced the enrichment of Pb. The coefficient of variation (CV) of the heavy metals decreased in the order of Pb (2.531) >Hg (1.137) >Cd (0.895) >Cr (0.468) >As (0.334). CV for metals, except for Cr and As, was obtained as relatively high values. Besides, as can be seen from **Figure 2** that the distribution of these three heavy metals was uneven and has great discreteness, the soil in this area was affected by exogenous Pb, Hg, and Cd, which was consistent with the research results of Chen Xiaolin et al. (Chen et al., 2012). In the soil depth of 25~50 cm, the mean contents of Cd, Cr, Pb, As, and Hg were 0.087 ± 0.055 mg·kg^{-1}, 34.806 ± 16.385 mg·kg^{-1}, 8.012 ± 8.866 mg·kg^{-1}, 7.894 ± 2.296 mg·kg^{-1}, and 0.095 ± 0.094 mg·kg^{-1}, respectively. Among them, Cr, As, and Hg were higher than the corresponding soil background values in Beijing; only the concentrations of Cr were higher than 0–25 cm, showing the double overlapping effect of man-made and natural geology. The CV of the heavy metals decreased in the order of Pb (1.107) >Hg (0.983) >Cd (0.633) >Cr (0.471) >As (0.291). The ranking of CV values was consistent with the soil depth of 0–25 cm.

Pearson correlation analysis was conducted to evaluate the relationships between the five heavy metals from different soil depths (**Figure 3**). The red lines in the upper triangle were fitted lines of the locally weighted scatterplot smoothing, the histograms in the diagonal indicated the data value distribution of the corresponding variables, and the correlation coefficients between different paired variables were shown in the lower triangles. The correlation coefficients among the five heavy metals (Cd, Cr, Pb, As, and Hg) from different soil depths (0~25 cm, 25~50 cm) were 0.674, 0.579, 0.290, 0.859, and 0.743, respectively, which showed that there were positive correlations among the five heavy metals from different soil depths. There had been a significantly ($p < 0.01$) positive correlation with Cr (0~25 cm)-Hg (0~25 cm, 25~50 cm), Hg (0~25 cm)-Pb(25~50 cm), and Cd (25~50 cm)-As (25~50 cm) and a significant ($p < 0.05$) correlation with Cr (0~25 cm, 25~50 cm)-Pb(25~50 cm), Pb(0~25 cm)- Hg (25~50 cm). These groups of heavy metals exhibited significant positive correlation, indicating that they generally had some homology or compound pollution, while negative correlation indicates that they may not had homology.

Classification of the Safety Utilization Zones of Heavy Metals in Soil

Based on the three evaluation methods of the geoaccumulation index, the improved geoaccumulation comprehensive index, and

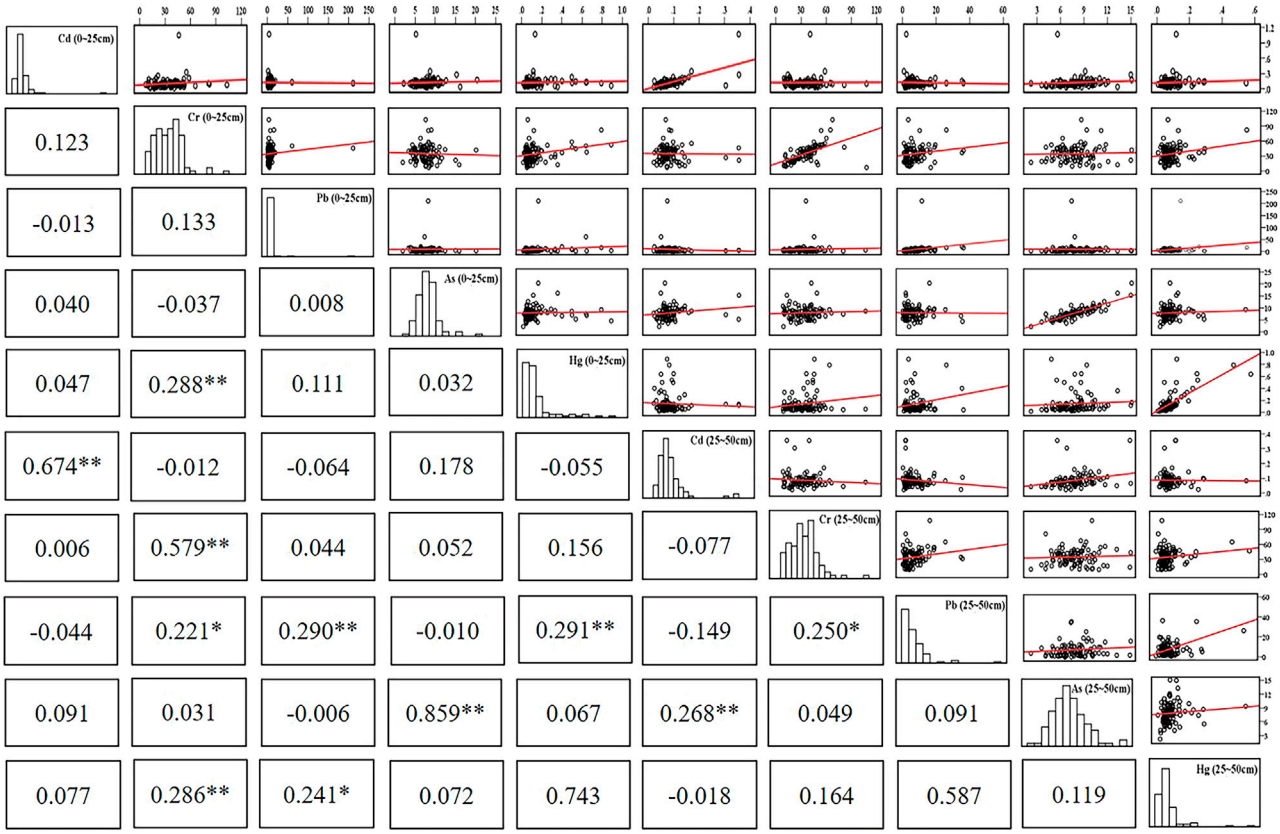

FIGURE 3 | The matrix of Pearson correlations for different heavy metals.

TABLE 3 | Security zone evaluation grades.

Zones	Index
Grade I: safe utilization zone	I_{geo}< 0; I < 0; RI < 150
Grade II: low-risk zone	0 ≤ I_{geo}<1; 0 ≤ I < 1; RI < 150
Grade III: medium-risk zone	1 ≤ I_{geo}<2; 1 ≤ I < 2; 150 ≤ RI < 300
Grade IV: high-risk zone	I_{geo}≥2; I ≥ 2; RI ≥ 300

the potential ecological risk index, we put forward a scheme for the regional division of the security of soil heavy metals. The division scheme and its expression were shown in **Table 3**. The land was divided into four grades: Grade I (safe utilization zone), where the heavy metal concentrations and other pollutants in the soil were low, and the environmental quality keeps a clean state. In Grade II (low-risk zone), there was a small amount of accumulation of heavy metals and other pollutants in the soil. The environmental quality was light pollution, and the soil and crops began to be contaminated. In Grade III (medium-risk zone), the heavy metals and other pollutants in the region have been enriched significantly, the surrounding environment has suffered moderate pollution, and the soil and crops have been threatened to a certain degree. In Grade IV (high-risk zone), the heavy metal concentrations and other pollutants in this area were high, which was much higher than the relevant environmental quality standards, and will cause serious damage to soil, crops, and even human life and health.

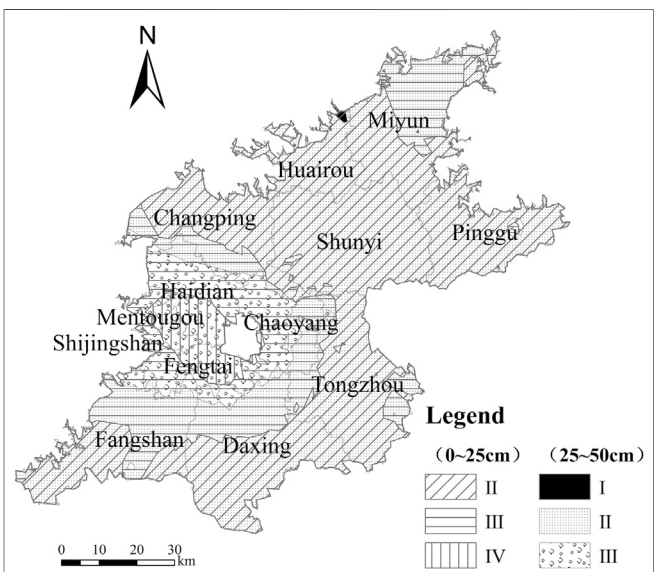

FIGURE 4 | Comprehensive zones of land safety utilization.

According to the qualitative division scheme in **Table 3**, the comprehensive zoning of farmland soil safety and utilization in Beijing plain area was shown in **Figure 4**. It divided the 0~25 cm

TABLE 4 | Principal component analysis of heavy metals in soil.

Heavy metals	0~25 cm						25~50 cm					
	Before rotation			After rotation			Before rotation			After rotation		
	PC1	PC2	PC3	PC1	PC2	PC3	PC1	PC2	PC3	PC1	PC2	PC3
Cd	0.311	0.668	−0.469	0.224	0.839	0.098	−0.170	0.806	0.011	−0.146	0.800	−0.128
Cr	0.764	−0.046	−0.184	0.759	0.163	−0.136	0.499	−0.090	0.849	0.119	−0.006	0.982
Pb	0.446	−0.368	0.469	0.498	−0.538	0.133	0.867	−0.064	−0.192	0.871	−0.065	0.175
As	0.026	0.671	0.715	−0.020	0.036	0.981	0.208	0.779	0.111	0.161	0.790	0.116
Hg	0.718	−0.036	0.081	0.720	−0.008	0.069	0.823	0.092	−0.338	0.891	0.077	0.011
Contribution rate/%	27.935	20.718	19.849	27.847	20.417	20.238	35.030	25.546	17.670	32.279	25.489	20.478
Cumulative contribution rate/%	27.935	48.653	68.502	27.847	48.264	68.502	35.030	60.576	78.246	32.279	57.768	78.246

farmland soil of the study area into three grades: low-risk zone (Grade II), medium-risk zone (Grade III), and high-risk zone (Grade IV). The low-risk area was about 4819.325 km^2, accounting for 61.952% of the total area of the study area. It is mainly distributed in most areas outside the city center perimeter. The medium-risk area was approximately 2583.294 km^2, accounting for 33.208% of the total area of the study area. It was mainly distributed around the urban area, the northern part of Miyun, the middle of Pinggu, and a small area in the southeast of Tongzhou. The high-risk area was about 376.500 km^2, accounting for 4.840% of the total area of the study area. It was concentrated in Mentougou, Shijingshan, and parts of their borders with Haidian and Fengtai. Meanwhile, the study area in the soil depth of 25~50 cm also can be divided into three grades: safe utilization area (Grade I), low-risk area (Grade II), and middle-risk area (Grade III). Among them, the safe utilization zone was about 6.563 km^2, accounting for only 0.084% of the total area of the study area, located in the northern part of Huairou. The low-risk area was about 6518.052 km^2, accounting for 83.789% of the total area of the study area. It was mainly distributed in most areas outside the city center perimeter. The medium-risk area was about 1255.399 km^2, accounting for 16.138% of the total area of the study area. It was distributed in the areas surrounding the city center perimeter such as Haidian, Fengtai, Chaoyang, Mentougou, Shijingshan, and the middle part of Pinggu.

On the whole, the safety classification of heavy metals in most parts of the study area was low-risk. Since plastic films in agricultural land in Beijing was very common, there will be large amounts of plastic residues in the soil. In plastics, heavy metals were often used as stabilizers (Zheng et al., 2005a). Moreover, agricultural activities such as pesticides and chemical fertilizers increased heavy metals in the soil; for example, livestock breeders will put additives containing heavy metals in their feedstuffs, after which dung of livestock and poultry will be widely used in agricultural lands (Chen et al., 2005). As a result, heavy metals in the area will create a wide range of low-risk areas.

Analysis of Core Pollution Sources in Different Security Utilization Zones

Feature extraction was performed according to principal component analysis to further analyze the source of heavy metals in the study area. The load of principal component factors was obtained as shown in **Table 4**. Furthermore, since the heavy metal concentrations of each soil sample only represented the soil environment of the sample itself (Liu P. et al., 2016), therefore it was necessary to interpolate the information of samples to obtain surface information and then evaluate the spatial distribution of the five heavy metals. At the same time, combined with the results of the principal component analysis for the purpose of determining the source that caused heavy metal enrichment in the end, normal quantile plot of geoaccumulation index of different heavy metals and after Gaussian transformation were shown in **Figure 5**. The numerical distribution was approximately normal. Therefore, the normal distribution index interpolation analysis can be performed without the need of normal distribution transformation. The results were shown in **Figure 6**.

It can be seen from **Table 4** that in 0~25 cm soil depth the contribution rate of principal component 1 (PC1) was 27.935%, and the positive load of Cr and Hg was greater. Therefore, PC1 mainly reflected the enrichment information of Cr and Hg. With reference to **Figure 6**, we can see that the two heavy metals were concentrated on Mentougou, Shijingshan, and parts of their borders with Haidian and Fengtai (**Figure 6b1**, **Figure 6b2**). Mining was one of the most polluting sources of heavy metals in the soil of Mentougou now, and the massive accumulation of Hg was closely related to mining and transportation processes (Xing et al., 2016). In addition, Hg was often regarded as a sign element of burning coal and garbage burning. Shougang Group was located in Shijingshan district; the production process was accompanied by a large amount of oil, burning of coal and other fossil fuels, and the consumption of transportation vehicles, which will cause soil pollution in the area and even affect the surrounding Haidian and Fengtai (Zheng, et al., 2005a). There was a landfill site in Nankou Town in the western part of Changping where a large number of heavy metals (mainly Hg) will enter the atmosphere and migrate in the surrounding area for a long distance around it (Zheng et al., 2005b). In addition, the large amount of dust generated by mining will affect the environment as a result of the wind power. Long-term leaching of large amounts of coal gangue and tailings slag caused heavy metal elements (such as Hg and Cr) in the ore body which can be moved to the surrounding soil environment (Xing et al., 2016). For the soil heavy metal Cr, Xiaoni Huo proposed that the enrichment of Cr mainly comes from mining

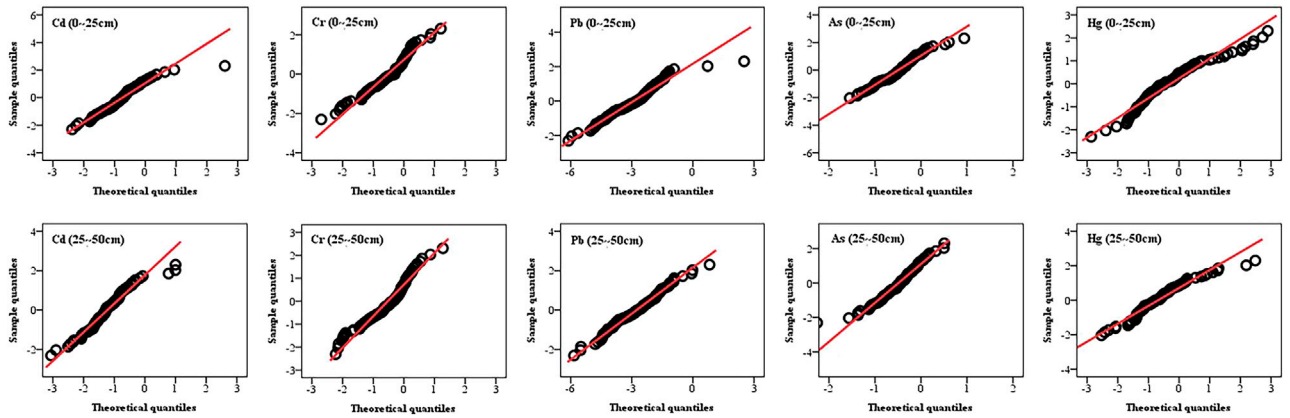

FIGURE 5 | Normal quantile plot of geoaccumulation index and after Gaussian transformation.

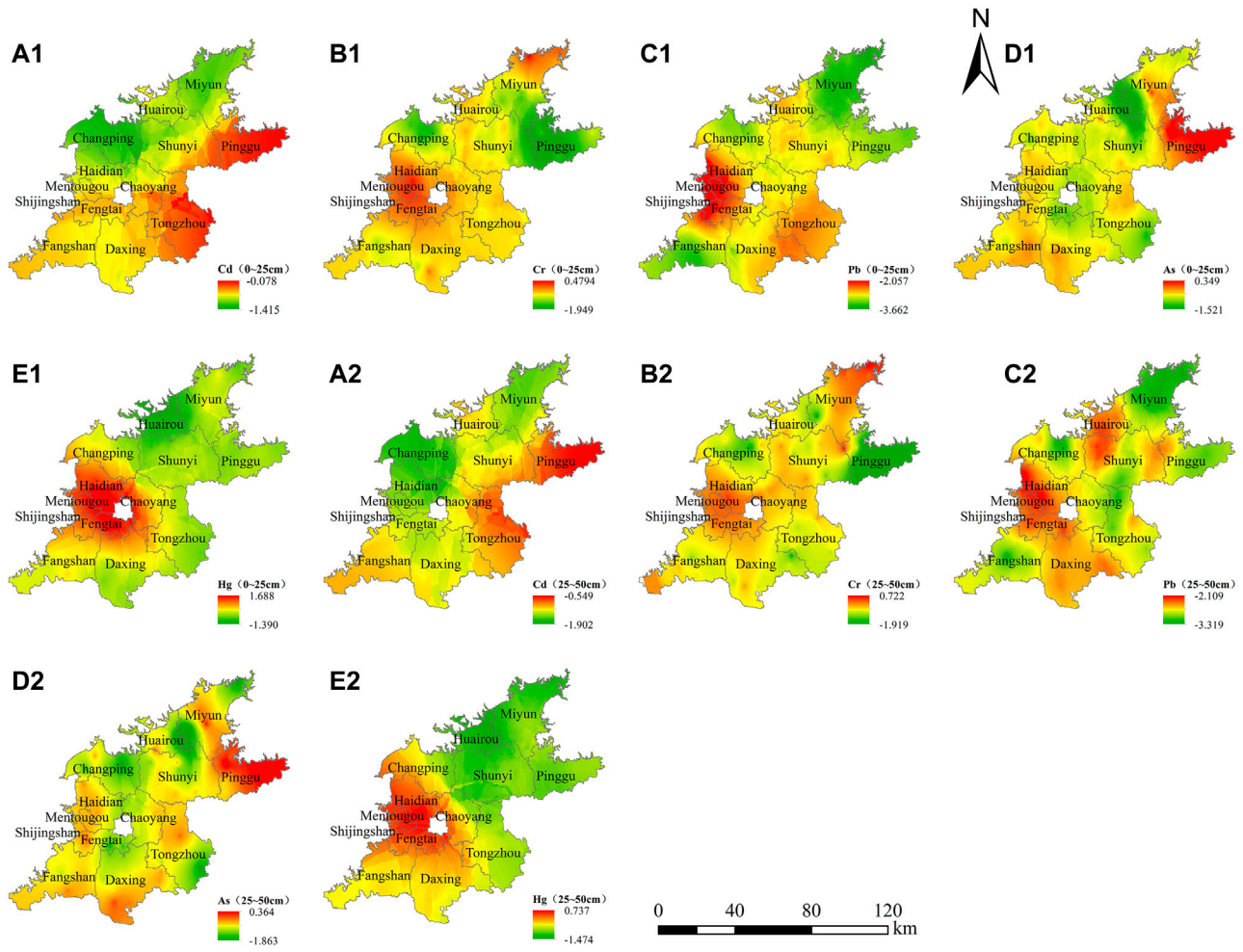

FIGURE 6 | Spatial distribution of heavy metal evaluation results in different soil depths. **(A1–E1)** correspond to the spatial distribution of heavy metal (Cd, Cr, Pb, As, and Hg) evaluation results in 0–25 cm soil depths, while **(A2–E2)** corresponding to the spatial distribution of heavy metal (Cd, Cr, Pb, As, and Hg) evaluation results in 25–50 cm soil depths.

and sewage irrigation in the study of soil heavy metals in Beijing (Huo, et al., 2009). Therefore, PC1 represented industrial sources such as mining and coal combustion. The contribution of principal component 2 (PC2) was 20.718% and its load at the Cd content was higher, and Pb and Hg were negative load. The Cd element filled the Pinggu and Tongzhou regions (**Figure 6a1**), but it did not pollute the study area. Considering that all the samples in this study came from farmland soil, to some extent, unreasonable application of pesticides and chemical fertilizers in the actual agricultural production process will lead to the accumulation of Cd in the soil, and the heavy metal Cd may be derived from the above agricultural production activities. Therefore, PC2 can be expressed as the pollution of agricultural production activities such as pesticides and chemical fertilizers. The contribution rate of principal component 3 (PC3) was 20.238%, in which As had a high positive load and was mainly concentrated in the Pinggu area. It is generally known that As was usually regarded as the accompanying element of Au. Since the Wanzhuang gold ore was located in Pinggu, mining of the gold ore will activate the originally stable As in the area and then cause damage to the soil through the river system (Hu et al., 2013), which will cause the enrichment of As element for a long time. So, PC3 can be interpreted as the mining of gold mines.

At 25~50 cm soil depth, the contribution rate of principal component 1 (PC1) accounted for 32.279% of the total variable, and heavy metals Hg and Pb had larger positive loads. Because they had a high coefficient of variation, and there were a few samples with high content and large degree of dispersion, it can be considered that it was mainly controlled by human factors. As can be seen from **Figure 6**, both Hg and Pb were concentrated around the urban area (**Figure 6e2**, **Figure 6c2**), in which heavy metal Pb did not cause pollution in the study area, while Hg elements caused a slight pollution risk in some areas near the urban area. As smelting of steel was the main industry in Shijingshan area, there was a large amount of vehicle transportation and fossil fuel combustion. In addition, the urban population was large and the density of motor vehicles was high; the emission of vehicle exhaust leads to the increase of Pb in the atmosphere and then atmospheric deposition causes its concentration to increase. Zheng Yuanming proposed that human activities such as atmospheric deposition, landfill, and pesticide application were the main factors leading to the accumulation of heavy metal Pb in Beijing (Zheng, et al., 2005b). Combined with the analysis of the pollution source of Hg element in 0~25 cm soil, PC1 can be interpreted as pollution from coal burning, combustion of refuse, and vehicle emission from mining transportation. The contribution rate of the main component 2 (PC2) was 25.489%. Among them, Cd and As were loaded heavily. In addition to the accumulation of Cd in soil by using nitrogen, phosphorus, and potassium fertilizers, the wastewater, tailings, and residues produced in activities such as mining, mineral processing, and smelting would aggravate this element pollution. The main accumulation areas of the two heavy metals were mainly concentrated in Pinggu mining area (**Figure 6a2**, **Figure 6d2**), in which As produces mild pollution in this area. Meanwhile, combined with the analysis of the pollution source of As in 0~25 cm soil, PC2 represented industrial activities such as mining. The contribution rate of the main component 3 (PC3) was 20.478%, and the load of only the heavy metal Cr was the highest. Studies have shown that it was less controlled by human activities, mainly affected by weathering and erosion of rocks (Zheng, et al., 2005c). The variation of Cr in 25~50 cm soil was relatively small, and the heavy metals of Pb, Hg, and Cd, which were mainly affected by external sources, had lower loading in PC3. In summary, PC3 can be regarded as a natural source of soil parent material and weathering products.

The total contributions of the three principal components from different soil depths were 68.502% (0–25 cm) and 78.246% (25–50 cm), respectively. In general, the main sources of heavy metals in soils can be divided into natural sources (parent materials) and human activities. Among them, the source of human activities was the main reason for the accumulation of heavy metals in the area, such as mining, vehicle transportation, coal burning, garbage burning, and pesticide and fertilizer application.

Management and Control Strategy of Land Safety Utilization

According to the characteristics of different security zones, combined with the source apportionment results of soil heavy metal pollution in the study area, we proposed the rationalization proposals for the land of zoning utilization and management based on the principles of safety utilization, targeted governance and adjust measures to local conditions. The specific content was depicted in **Table 5**.

It can be seen from **Table 5** that the safe utilization zone should be based on the principle of priority protection and strictly control the emergence of new sources of pollution in the surrounding areas so as to maintain the state of security in the region. Low-risk zone should be based on long-term monitoring and moderate optimization as the purpose of governance, reduce the intervention of known sources of pollution, and propose corresponding economically feasible measures. Ultimately, it makes the state of land in the region slowly transition to a safe state. Medium-risk zone should comply with the principle of strengthening early warning and cooperating with effective repair, focusing on the state of land in real time and strengthening early warning measures. At the same time, methods such as chemical leaching, phytoremediation, and biodegradation can be used to reduce the effectiveness of heavy metals in soil and crops. High-risk zone should take priority governance as the purpose of governance. At the same time, actively adopting restoration measures to protect human health from harm is needed. Ultimately, it was planned to increase the status of the land around the region by one grade after several repair cycles.

CONCLUSION

The three evaluation results of the geoaccumulation index, the improved geoaccumulation index, and the potential ecological risk

TABLE 5 | Management and control strategy of land safety utilization.

Grades	Core pollution source	Governance principles and specific management control strategy
Grade I: safe utilization	/	Priority protection: strictly controlling the emergence of new sources of pollution around the area, especially the risk of heavy metals due to mineral development and soil erosion in the northern part of Miyun, so as to maintain the long-term safety and stability of the land in this area.
Grade II: low-risk zone	Hg, Cr, As	Long-term monitoring and moderate optimization: a. In view of the wide scope and large area of this grade, it is mainly necessary to limit the use of plastic film in agricultural land throughout the entire study area. b. Promote advanced technologies and encourage farmers to rationally apply chemical inputs (such as fertilizers and pesticides). c. Strictly control the product quality of fertilizers.
Grade III: medium-risk zone	Hg, Cr, As	Strengthen early warning and cooperate with effective repair: a. The areas surrounding the city center should strictly control the enrichment of Hg and Cr. Real-time attention to the status of heavy metal accumulation in the soil of the landfill site in western Changping, the Shougang Group, and the Mentougou ore concentration area. Strengthen early warning measures and guard against increased risk grades. b. The middle part of Pinggu needs to optimize the gold mining process to prevent the continuous accumulation of As. c. The northern part of Miyun should strengthen its management and law enforcement efforts to prevent the phenomenon of illegal mining. At the same time, it should do a good job in the environmental monitoring of the upstream mining area of the water source protection areas and carry out timely repair and treatment of tailings. d. The southeast of Tongzhou should minimize sewage irrigation, optimize agronomic measures, and control the accumulation of As.
Grade IV: high-risk zone	Hg (moderate pollution), Cr	Priority governance: a. Tracking and evaluation of the heavy metals Hg and Cr produced by mining and iron and steel smelting in Mentougou and Shijingshan district, and systematic repair of the ecological hazards caused by heavy metals. b. Expand the coverage of greenery to block and filter the heavy metal elements produced by transport vehicles. If necessary, return the grain plots to forestry. Limiting the cultivation of edible agricultural products in agricultural land in urban areas to ensure the safety of animals, plants, agricultural products, and food within a certain range of that region and the periphery.

index showed that most of the study areas were within the slight risk; the city center perimeter was the main enrichment zone for heavy metals, and its distribution showed a trend of weakening from the center of the city to the periphery. Meanwhile, as the urban living zones of Haidian, Shijingshan, Mentougou, Fengtai, and Chaoyang districts, whether the ecological risks brought by the heavy metal enrichment will cause harm to the health of the surrounding environment and the residents in the area should be worthy of attention. The main sources of heavy metals in the soil can be divided into natural sources and human activities, among which the anthropogenic source was the main reason for the accumulation of heavy metals. According to the scheme for the regional division of the security of soil heavy metals which we put, the land was divided into four types of zones: safe, low-risk, medium-risk, high-risk utilization. The results showed that the low-risk states dominated in the study area. Furthermore, in the light of various grades of core pollution sources, we took priority protection, long-term monitoring and moderate optimization, strengthened early warning and cooperated with effective repair, priority governance as a governance purpose to put forward specific management and control strategies.

This study took farmland soil around the plain of Beijing as the research object, putting forward a scheme for the regional division of the security of soil heavy metals based on the different evaluation methods. Future studies will incorporate more indicators to propose a more comprehensive and systematic land regionalization scheme and aim at the pollution characteristics of each area to provide more accurate, economical, and feasible remediation measures, making the research of more practical significance.

DATA AVAILABILITY STATEMENT

The raw data supporting the conclusions of this article will be made available by the authors, without undue reservation.

AUTHOR CONTRIBUTIONS

CK focused on the implementation of the main work, and SZ focused on the supplement and improvement after the completion of this research.

FUNDING

This work was supported by the National Key Research and Development Program of China (2016YFD0300801) and the National Natural Science Foundation of China (41471186).

ACKNOWLEDGMENTS

The authors would like to thank the local people for their cooperation and all those who helped us with this research.

REFERENCES

Chen, T. B., Zheng, Y. M., Chen, H., Wu, H. T., Zhou, J. L., Luo, J. F., et al. (2005). Arsenic accumulation in soils for different land use types in Beijing. *Geog. Res.* 24 (2), 229–(235.) [in Chinese, with English summary]. doi:10.11821/yj2005020009

Chen, T. B., Zheng, Y. M., Chen, H., and Zheng, G. D. (2004). Background concentrations of soil heavy metals in Beijing. *Huan Jing Ke Xue* 25 (1), 117–(122.) [in Chinese, with English summary]. doi:10.13227/j.hjkx.2004.01.026

Chen, X. L., Yang, D., Hu, D. Q., Lian, D. Q., and Wang, X. D. (2012). Beijing city soil heavy metal distribution and evaluation: take inner 5th ring road area for an example. *Environ. Sci. Technol.* 35 (s2), 78–(81.) [in Chinese, with English summary].

Da-wei, H., and He-rong, G. (2017). Sources analysis and content characteristics of soil heavy metal in Sunan mining area, China. *Earth Environ.* 45 (5), 546–554. doi:10.14050/j.cnki.1672-9250.2017.05.008

Hakanson, L. (1980). An ecological risk index for aquatic pollution control. a sedimentological approach. *Water Res.* 14 (8), 975–1001. doi:10.1016/0043-1354(80)90143-8

Hu, Y., Zhou, L., and Wei, C. (2013). Study on spatial variability of soil heavy metals environments and its pollution characteristics in Beijing water protective area. *Chin. J. Soil Sci.* 44 (6), 1483–(1490.) [in Chinese, with English summary]. doi:10.1016/0043-1354(80)90143-8

Huang, D., Gui, H., Lin, M., and Peng, W. (2018). Chemical speciation distribution characteristics and ecological risk assessment of heavy metals in soil from Sunan mining area, Anhui province, China. *Hum. Ecol. Risk Assess.* 24 (6), 1694–1709. doi:10.1080/10807039.2017.1422973

Huo, X., Li, H., Zhang, W., Sun, D., Zhou, L., and Li, H. (2009). Multi-scale spatial structure of heavy metals in Beijing cultivated soils. *Trans. Chin. Soc. Agric. Eng.* 25 (3), 000223–(000229.) [in Chinese, with English summary].

Janadeleh, H., Jahangiri, S., and Kameli, M. A. (2018). Assessment of heavy metal pollution and ecological risk in marine sediments (a case study: Persian Gulf). *Hum. Ecol. Risk Assess.* 24 (8), 2265–2274. doi:10.1080/10807039.2018.1443792

Jian, L. (1988). *The handbook of the environmental background value[M]*: Beijing: China Environmental Science Press [in Chinese, with English summary].

Li, Z., Ma, Z., van der Kuijp, T. J., Yuan, Z., and Huang, L. (2014). A review of soil heavy metal pollution from mines in China: pollution and health risk assessment. *Sci. Total Environ.* 468–469, 843–853. doi:10.1016/j.scitotenv.2013.08.090

Liu, P., Wu, K., Luo, M., Li, C., Zhu, P., Zhang, Q., et al. (2016). Evaluation of agricultural land soil heavy metal elements exceed standards and safe utilization zones. *Trans. Chin. Soc. Agric. Eng.* 32 (23), 254–262. [in Chinese, with English summary]. doi:10.11975/j.issn.1002-6819.2016.23.035

Liu, W., Yang, J. J., Wang, J., Wang, G., and Cao, Y. E. (2016). Contamination assessment and sources analysis of soil heavy metals in opencast mine of East Junggar basin in Xinjiang. *Huan Jing Ke Xue* 37 (5), 1938–1945. [in Chinese, with English summary]. doi:10.13227/j.hjkx.2016.05.043

Luo, C., Bi, J., Xiao, G., and Zhang, F. (2017). Pollution characteristics and assessment of heavy metals in soil of different industry zones of Ningdong base in Ningxia, China. *Ecol. Environ. Sci.* 26 (7), 1221–1227. [in Chinese, with English summary]. doi:10.16258/j.cnki.1674-5906.2017.07.019

Manta, D. S., Angelone, M., Bellanca, A., Neri, R., and Sprovieri, M. (2002). Heavy metals in urban soils: a case study from the city of Palermo (Sicily), Italy. *Sci. Total Environ.* 300 (1), 229–243. doi:10.1016/s0048-9697(02)00273-5

Mohammadi, A., Hajizadeh, Y., Taghipour, H., Mosleh Arani, A., Mokhtari, M., and Fallahzadeh, H. (2018). Assessment of metals in agricultural soil of surrounding areas of Urmia Lake, Northwest Iran: a preliminary ecological risk assessment and source identification. *Hum. Ecol. Risk Assess.* 24 (8), 2070–2087. doi:10.1080/10807039.2018.1438173

Muller, G. (1969). Index of geoaccumulation in sediments of the Rhine river. *Geojournal* 2 (108), 108–118.

Qu, M., Chen, J., Huang, B., and Zhao, Y. (2020). Source apportionment of soil heavy metals using robust spatial receptor model with categorical land-use types and RGWR-corrected *in-situ* FPXRF data. *Environ. Pollut.* 270, 116220. doi:10.1016/j.envpol.2020.116220

Shi, Z. F., and Wang, L. (2013). Contents of soil heavy metals and evaluation on the potential pollution risk in Shenmu mining area. *J. Agro-Environ. Sci.* 32 (6), 1150–1158. [in Chinese, with English summary]. doi:10.11654/jaes.2013.06.010

Soå'Ek-Podwika, K., Ciarkowska, K., and Kaleta, D. (2016). Assessment of the risk of pollution by sulfur compounds and heavy metals in soils located in the proximity of a disused for 20 years sulfur mine (SE Poland). *J. Environ. Manage.* 180, 450–458. doi:10.1016/j.jenvman.2016.05.074

Song, J. X., Zhu, Q., Jiang, X. S., Zhao, H. Y., Liang, Y. H., Luo, Y. X., et al. (2017). GIS-based heavy metals risk assessment of agricultural soils-a case study of Baguazhou, Nanjing. *Acta Pedol. Sin.* 54 (1), 81–91. [in Chinese, with English summary]. doi:10.11766/trxb201603100033

Ungureanu, T., Iancu, G. O., Pintilei, M., and Chico□, M. M. (2017). Spatial distribution and geochemistry of heavy metals in soils: a case study from the NE area of Vaslui county, Romania. *J. Geochem. Explor.* 176, 20–32. doi:10.1016/j.gexplo.2016.08.012

Wang, S., Cai, L.-M., Wen, H.-H., Luo, J., Wang, Q.-S., and Liu, X. (2019). Spatial distribution and source apportionment of heavy metals in soil from a typical county-level city of Guangdong province, China. *Sci. Total Environ.* 655 (MAR.10), 92–101. doi:10.1016/j.scitotenv.2018.11.244

Xing, Y., Yan, G., Hou, Q., Sun, N., and Pan, X. (2016). Spatial distribution and pollution characteristics of heavy metals in soil of Mentougou mining area of Beijing city, China. *J. Agric. Resour. Environ.* 33 (6), 499–507. [in Chinese, with English summary]. doi:10.13254/j.jare.2016.0088

Xu, Z. Q., Ni, S., Tuo, X. G., and Zhang, C. J. (2008). Calculation of heavy metals' toxicity coefficient in the evaluation of potential ecological risk index. *Environ. Sci. Technol.* 31 (2), 112–115. [in Chinese, with English summary]. doi:10.3969/j.issn.1003-6504.2008.02.030

Yan, W., Liu, D., Peng, D., Mahmood, Q., Chen, T., Wang, Y., et al. (2016). Spatial distribution and risk assessment of heavy metals in the farmland along mineral product transportation routes in Zhejiang, China. *Soil Use Manage.* 32 (3), 338–349. doi:10.1111/sum.12268

Yang, Q., Li, Z., Lu, X., Duan, Q., Huang, L., and Bi, J. (2018). A review of soil heavy metal pollution from industrial and agricultural regions in China: pollution and risk assessment. *Sci. Total Environ.* 642 (nov.15), 690–700. doi:10.1016/j.scitotenv.2018.06.068

Zhang, J., Ma, C., Kuang, H., and Zhou, A. (2017). Assessment of heavy metals pollution in soil of Qingdao based on matter-element extension model. *China Environ. Sci.* 37 (2), 661–668. [in Chinese, with English summary]. doi:10.3969/j.issn.1000-6923.2017.02.037

Zhang, X. M., Zhang, X. Y., Zhong, T. Y., and Jiang, H. (2014). Spatial distribution and accumulation of heavy metal in arable land soil of China. *Huan Jing Ke Xue* 35 (2), 692–703. [in Chinese, with English summary]. doi:10.13227/j.hjkx.2014.02.047

Zheng, Y., Chen, T., Chen, H., Zheng, G., and Luo, J. (2005b). Lead accumulation in soils under different land use types in Beijing city. *Acta Geog. Sin.* 60 (5), 791. doi:10.3321/j.issn:0375-5444.2005.05.010

Zheng, Y. M., Chen, T., Zheng, G. D., Huange, Z., and Lou, J. (2005c). Chromium and nickel accumulations in soils under different land uses in Beijing municipality. *Resour. Sci.* 27 (6), 162–166. [in Chinese, with English summary]. doi:10.3321/j.issn:1007-7588.2005.06.026

Zheng, Y. M., Luo, J. F., Chen, T. B., Chen, H., Zheng, G. D., Wu, H. T., et al. (2005a). Cadmium accumulation in soils for different land uses in Beijing. *Geog. Res.* 24 (4), 542–(548.) [in Chinese, with English summary]. doi:10.11821/yj2005040008

Conflict of Interest: The authors declare that the research was conducted in the absence of any commercial or financial relationships that could be construed as a potential conflict of interest.

frontiers in Environmental Science

ORIGINAL RESEARCH
published: 29 March 2021
doi: 10.3389/fenvs.2021.641497

Spatial Variation in Cadmium and Mercury and Factors Influencing Their Potential Ecological Risks in Farmland Soil in Poyang Lake Plain, China

Xinyi Huang[1], *Huimin Yu*[1,2], *Xiaomin Zhao*[1]*, *Xi Guo*[1], *Yingcong Ye*[1] *and Zhe Xu*[1]

[1]*Jiangxi Agricultural University, Jiangxi, China,* [2]*Institute of Territorial Spatial Survey and Planning of Jiangxi Province, Jiangxi, China*

Due to the irreversibility of heavy metal pollution, the presence of heavy metals in farmland soil is associated with severe ecological risks that endanger both the environment and human health. Cadmium (Cd) and mercury (Hg) are two toxic heavy metals found widely in polluted soil. Cd is not readily fixed in the soil and is therefore easily accumulated by plants, while Hg has a wide range of pollution sources. The aims of this study were to explore the spatial variation in Cd and Hg concentrations in farmland soil in Poyang Lake Plain, China, and to assess their potential ecological risks as influenced by natural and human factors. A total of 283 soil samples were obtained from Fengcheng city, central Jiangxi Province. Data were then analyzed using geostatistics, the potential ecological risk index, Pearson's correlation analysis, and Geodetector. The results showed moderate variation in soil Cd and Hg concentrations, with a remarkable difference in their spatial distribution. Cd concentrations in the northwest and northeast of Fengcheng were below the regional background level in Jiangxi; in most remaining areas, Cd concentrations were between the regional background level and national risk screening value. Areas with Hg concentrations lower than the regional background level were largely concentrated in the south, east and north of Fengcheng, and gradually increased towards the central, where they exceeded the regional background level but were below the national risk screening value. Overall, the potential ecological risk level of Cd was predominantly low, while that of Hg was moderate. The comprehensive potential ecological risk was low in most areas for both Cd and Hg, with some scattered areas of moderate risk. Moreover, the comprehensive potential ecological risk index of both Cd and Hg was significantly correlated with soil pH, total phosphorous, elevation, distance from a river ($p < 0.01$), and distance from a road ($p < 0.05$). The most significant factor influencing the comprehensive potential ecological risk index of these two heavy metals was soil pH of 5.2–5.6, followed by total $p \leq 0.52$ mg kg^{-1}. In conclusion, moderate pollution of Cd and Hg occurred in farmland soil in Poyang Lake Plain where their comprehensive potential ecological risk level was generally low and mainly influenced by soil pH and total phosphorous.

Keywords: farmland, soil heavy metal, spatial variation, potential risk, impacting factors

OPEN ACCESS

Edited by:
Jun Zhou,
University of Massachusetts Lowell, United States

Reviewed by:
Xuchao Zhu,
Institute of Soil Science (CAS), China
Hong-Yi Li,
Jiangxi University of Finance and Economics, China

***Correspondence:**
Xiaomin Zhao
zhaoxm889@126.com

Specialty section:
This article was submitted to Toxicology, Pollution and the Environment, a section of the journal Frontiers in Environmental Science

Received: *14 December 2020*
Accepted: *18 February 2021*
Published: *29 March 2021*

Citation:
Huang X, Yu H, Zhao X, Guo X, Ye Y and Xu Z (2021) Spatial Variation in Cadmium and Mercury and Factors Influencing Their Potential Ecological Risks in Farmland Soil in Poyang Lake Plain, China. Front. Environ. Sci. 9:641497. doi: 10.3389/fenvs.2021.641497

INTRODUCTION

Heavy metals are an inherent component of soil, and there are more or less heavy metals in soils with different parent materials. However, human factors such as industrial development and the application of pesticides and fertilizers have led to the accumulation of heavy metals in farmland soil and subsequent heavy metal pollution (Aelion et al., 2008; Chabukdhara and Nema, 2013; Kelepertzis, 2014). Sources of heavy metal pollution in farmland soils are diverse, possibly from industry, sewage irrigation, urban activities or general agricultural practices (Jiang et al., 2018). The level of heavy metal pollution in farmland soil is closely associated with the quality and safety of agricultural products as well as severe ecological risks related to the toxicity, persistence, and bioaccumulation characteristics of heavy metals (Barlas et al., 2005; Ihedioha et al., 2016; Zhou et al., 2020). By entering the food chain, heavy metal pollutants also have an eventual effect on human health (Mazej et al., 2010; Hu et al., 2017; Liu et al., 2019). Research on the sources, spatial distribution and risk assessment of heavy metals in soil has attracted wide attention from governments and scientists (Yuan et al., 2015; Zhao and Luo, 2015).

The spatial distribution and distribution characteristics of heavy metal content in farmland soil are not only related to soil texture, physicochemical properties and structural conditions in the region, but also closely related to human activities (An et al., 2016; Lü et al., 2018), and by studying the spatial distribution and characteristics of heavy metals in farmland, it is helpful to find the causes and future development trends of their characteristics. There are many methods to study the spatial distribution of heavy metals in soil (Loredo et al., 2003; Cai et al., 2019). In some studies, assessment of spatial distribution of heavy metals in soils using multiple linear regression and neural network genetic algorithm based on satellite images (Arman et al., 2017). In more studies, spatial interpolation methods (such as ordinary Kriging and inverse distance weight method) are used to describe the spatial distribution characteristics of heavy metals in soil. By drawing contour maps to describe the spatial distribution of metals, for example, it was found that heavy metals in urban and industrial soils were significantly higher than in residential and private areas (Imperato et al., 2003); Spatial analysis of heavy metal concentration in soil by spatial interpolation in order to further study the influencing factors of spatial distribution characteristics of heavy metals (Ding et al., 2016; Wang et al., 2019).

Risk is fuzzy, grey and uncertain. Many studies on the risk of heavy metal pollution have been carried out in different countries and regions to assess the degree of pollution in sediments by using geoaccumulation index methods (Raj and Jayaprakash, 2008); for the polluted environment, especially urban soil, the impact of soil heavy metal pollution on urban population is analyzed by health risk assessment method (Tepanosyan et al., 2017); soils in industrial cities are most vulnerable to heavy metal pollution. Single pollution index and Nemerow comprehensive pollution index are used to evaluate the degree of heavy metal pollution (Hu et al., 2018). Potential ecological risk index method is proposed by Hakanson (1980) to evaluate the ecological risk of heavy metals in aquatic sediments. It can effectively combine the ecological, environmental and toxicological effects, and consider the biological toxicity of heavy metals (Hakanson, 1980; Chen et al., 2017). It is a widely used and reliable method in heavy metal pollution assessment. Principal component analysis is often used in the study of risk factors (Facchinelli et al., 2001; Lv et al., 2015). Geodetectors are a set of statistical methods to detect spatial variability and reveal the driving forces behind them, and they also can detect both numerical data and qualitative data, and are ideal methods to explore risk factors. Geodetectors have two advantages. One is that they can detect both numerical data and qualitative data without linear assumption. The other is that they can detect the interaction of two factors with dependent variables. This method has a clear physical meaning (Wang and Xu, 2017; Qiao et al., 2019).

Poyang Lake Plain is an important area of food production in China, with the quality of farmland soil in the region closely related to the environmental quality of the lake (Jiang et al., 2018), and Fengcheng is one of the important grain production bases. With the increasing demand for food products, the rapid economic development of Poyang Lake Urban Agglomeration, the excessive use of pesticides and a large number of heavy metal sewage irrigation tillage soil have aggravated the pollution load in some regions of the region (Zhang et al., 2017; Dai et al., 2018). Heavy metal pollution in farmland is a serious threat to the sustainability and safety of food crop production in the Poyang Lake Plain, which is a potential obstacle to food trade in the region (Jiang et al., 2018). However, despite these findings, the research scope of existing studies remains extensive. Poyang Lake Plain includes Fengcheng and an additional 24 counties, all of which vary in natural conditions and artificial factors that could potentially affect the spatial variation in heavy metals in farmland soil. The ecological risk of heavy metals in these areas has also yet to be revealed, with factors influencing the potential ecological risk again varying between regions. Thus, existing research on the spatial variation in heavy metals, their potential ecological risks and associated influencing factors in farmland soil in Poyang Lake Plain is insufficient. Further research into the spatial distribution of heavy metals and identification of the factors influencing their potential ecological risks is therefore important in terms of management and control, agricultural sustainability and eco-environmental safety, as well as protection of human health on a regional scale.

In this study, we investigated the distribution and spatial differentiation characteristics of Cd and Hg in farmland soil of Fengcheng City in the Poyang Lake Plain, and simulated the spatial structure and change of heavy metals in farmland soil by geostatistics combined with semi-variogram (such as ordinary Kriging estimation), which has the advantage of visualization for the spatial distribution and uncertainty analysis of heavy metals (Ha et al., 2014). Potential ecological risk assessment of heavy metals based on biotoxicological and environmental effects using potential ecological risk index method. Compared with the general study on the factors affecting the spatial distribution of heavy metals, this study used correlation analysis and Geodetector principle to explore the risk factors and their influence degree of potential ecological risks of heavy metals,

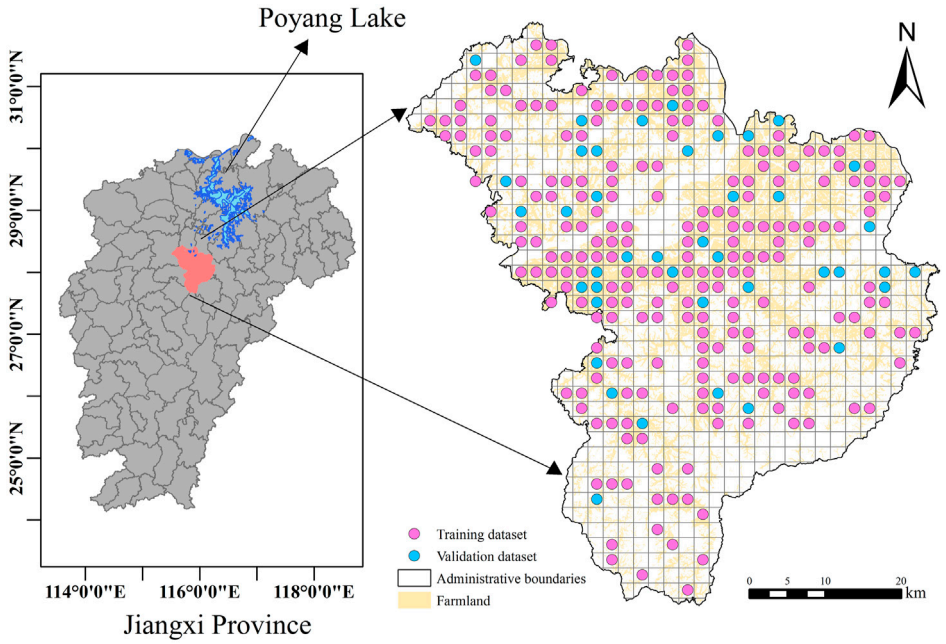

FIGURE 1 | Geographical location of the study region in Poyang Lake Plain and the distribution of sampling points in Fengcheng, Jiangxi Province, China.

and comprehensively considered the influencing factors of natural background of farmland soil and human activities, so as to provide insight into heavy metal pollution in Poyang Lake Plain, which will aid the prevention and control of farmland soil pollution as well as the utilization and protection of agricultural resources on a regional scale.

MATERIALS AND METHODS

Site Description

The study was conducted in Fengcheng city, central Jiangxi Province, China, in the middle and lower reaches of Ganjiang River, at the southern margin of Poyang Lake Basin (between 115°25′–116°27′ E and 27°42′–28°27′ N). Fengcheng, a pilot city directly under provincial government control, is the main food production base in China and one of the first National Pilot Demonstration Zones under the Sustainable Agricultural Development Plan. The total area of cultivated land is about 10.87 million hm^2, which is a population-intensive agricultural area. Fengcheng belongs to the subtropical humid monsoon climate, the annual average precipitation is about 1552.1 mm, the annual average temperature is 15.3–17.7°C, frost-free period is about 274 days. The terrain is high in the south and low in the north, gradually tilting from southwest to northeast. Low mountainous areas are distributed in the south, while the central part is relatively low and flat, where Ganjiang River forms a valley floodplain. Meanwhile, undulating hills dominate the northwest and southeast. The total land area of Fengcheng is 284,500 hm^2. The geographic location of the study region is shown in **Figure 1**.

Data Collection and Processing

Soil sampling was conducted in October 2018 according to the principle of uniform distribution and increased sampling point density in typical areas, with additional consideration given to both economic efficiency and feasibility. A total of 283 sampling points were distributed among regular 1 × 1 km grids throughout the region, with surface soil samples collected at depths of 0–20 cm. Three to five replicate samples were taken from each grid and mixed to form a composite sample. A handheld global positioning system (HD8200X-GPS, Zhonghaida, Guangzhou, China) was used to record the latitude and longitude of each sampling point. The distribution of the sampling points is also shown in **Figure 1**.

The soil samples were air-dried, with impurities removed by hand, then ground and sieved before heavy metal analysis. Cd concentrations were measured by graphite furnace atomic absorption spectrophotometry (GFAAS-AA800, Perkin Elmer Inc., Waltham, MA, United States) and Hg concentrations were measured by cold atomic absorption spectrophotometry (AFS-9530, Haiguang Instrument Co., Ltd., Beijing, China).

Eleven outliers over three standard deviations were eliminated, giving a final 271 samples for data analysis. The Kolmogorov-Smirnov test for normality was conducted using SPSS 22.0 (IBM SPSS, Somers, NY, United States); data that did not conform to the normal distribution were transformed into normal distribution using the logarithm. Correlation analyses between heavy metal concentrations and associated influencing factors were also performed using SPSS 22.0.

Semi-variogram analysis and model fitting were performed with GS + version 7.0 (Gamma Design Software, LLC., Plainwell, United States). Optimal model parameters were obtained based

on the maximum coefficient of determination (R^2) and the minimum residual sum of squares (RSS). Ordinary Kriging interpolation was then performed according to the optimal model parameters, Ordinary Kriging is the most commonly used geostatistical interpolation method, which provides the parameters required for spatial interpolation, and uses the semi-variogram to quantify the spatial variation of regional variables and the spatial distribution of heavy metals in the study region was mapped using ArcGIS 10.2 (ESRI Inc., Redlands, CA, United States).

Analytical methods

Geostatistics

Geostatistics was used to determine the spatial variation of Cd and Hg concentrations. Geostatistics is a tool that describes the spatial correlation of regionalized variables using semi-variograms (Ha et al., 2014). The semivariogram, also known as the semivariance, represents the spatial variation and correlation with regionalized variables. It is a key parameter in studies of the spatial variation in soil properties, forming the basis for accurate ordinary Kriging interpolation (Xie et al., 2010). The formula is as follows:

$$r(h) = \frac{1}{2N(h)} \sum_{i=1}^{N(h)} [Z(x) - Z(x+h)]^2 \quad (1)$$

where $r(h)$ is the semivariogram, h is the separation distance, $N(h)$ is the pairwise number of data points separated by distance h, Z(x) is the value of a regionalized variable at spatial position x, and Z (x + h) is the value of a regionalized variable at position x + h.

In the spatial structure of regionalized variables, the coefficient of variation (CV) represents dispersion between data, reflecting spatial variation in a set of samples (Kasel et al., 2017). In general, CV < 10% indicates low variation, CV = 10–100% indicates moderate variation, and CV ≥ 100% indicates high variation (Zhong et al., 2007). The nugget/sill ratio C0/(C0 + C) represents the ratio of random variation to total spatial variation, reflecting the spatial autocorrelation between variables. C0/(C0 + C) < 25% represents high spatial correlation, in which non-human structural factors play a major role; C0/(C0 + C) = 25–75% represents moderate spatial correlation affected by both natural and human factors; and C0/(C0 + C) > 75% indicates low spatial correlation, in which random factors play a major role (Lei et al., 1985; Tang, 2007).

Potential Ecological Risk Index Method

The ecological risk of heavy metal pollution was assessed using the potential ecological risk index proposed by Hakanson (1980), which is based on the background value of heavy metals in the soil (China National Environmental Monitoring Center (CNEMC), 1990; He and Xu, 2006). The risk index value is then calculated from the biotoxicity (toxicity coefficients) and environmental effect (pollution index) of the heavy metal in question as follow:

$$RI = \sum_{i}^{n} E_r^i = \sum_{i}^{n} \left(T_r^i \times C_f^i \right) = \sum_{i}^{n} \left(T_r^i \times \frac{C_D^i}{C_R^i} \right) \quad (2)$$

where C_D^i is the measured concentration of heavy metal i in soil, C_R^i is the regional background level of heavy metal i in soil, T_r^i is the toxicity coefficients of heavy metal i, C_f^i is the pollution index of heavy metal i, E_r^i is the potential ecological risk index of heavy metal i [according to the E_r^i, the potential ecological risk level of soils can be classified into five grades: low ($E_r^i < 40$), moderate ($40 \le E_r^i < 80$), high ($80 \le E_r^i < 160$), very high ($160 \le E_r^i < 320$), and extremely high ($320 \le E_r^i$)], and RI is the comprehensive potential ecological risk index of heavy metals in the soil environment [according to the RI, the potential ecological risk level of soils can be divided into four grades: low ($RI < 150$), moderate ($150 \le RI < 300$), high, ($300 \le RI < 600$), and very high ($RI \ge 600$)] (Hakanson, 1980; Lv et al., 2013).

In this study, the toxicity coefficients of Cd and Hg were 30 and 40 (Xu et al., 2008), regional background levels of soil Cd and Hg in Jiangxi were 0.108 and 0.084 (China National Environmental Monitoring Center (CNEMC), 1990), and the risk screening values of Cd and Hg for soil pollution of agricultural land in China were 0.3 and 0.5 (National Standard of the People's Republic of China, 2018), respectively.

The Principle of Geodetector

Spatial variation is one of the basic characteristics of geographical phenomena. Geodetector refers to a series of statistical methods for detecting spatial differentiation and revealing the driving forces behind them (Wang and Xu, 2017). First, we adopted the factor detector to quantify the relative importance of particular factors in explaining spatial variation in the potential ecological risks of heavy metals, as measured by the q statistic:

$$q = 1 - \frac{\sum_{h=1}^{L} N_h \sigma_h^2}{N\sigma^2} = 1 - \frac{SSW}{SST} \quad (3)$$

$$SSW = \sum_{h=1}^{L} N_h \sigma_h^2, SST = N\sigma^2 \quad (4)$$

where q is the relative influence of a particular factor on the spatial distribution of heavy metal concentrations in soil (q = 0–1), $h = 1,\ldots, L$ is the class of influencing factors, N_h and N are the number of units in class h and the study area, respectively, σ_k^2 and σ^2 are the variance in heavy metal concentrations in class h and the study area, respectively, and SSW and SST are the within sum of squares and the total sum of squares, respectively.

The q value satisfies the non-central F~(L-1, N-L; λ) distribution as follows:

$$F = \frac{N-L}{L-1} \frac{q}{1-q} \sim F(L-1, N-L; \lambda) \quad (5)$$

$$\lambda = \frac{1}{\sigma^2} \left[\sum_{h=1}^{L} \overline{Y}_h^2 - \frac{1}{N} \left(\sum_{h=1}^{L} \sqrt{N_h}\, \overline{Y}_h \right)^2 \right] \quad (6)$$

The risk detector was then used to determine whether there were significant differences between the attribute means of two sub-areas, as measured by the t statistic:

TABLE 1 | Descriptive statistics of Cd and Hg concentrations in farmland soil in the study region.

Metal	Sampling point	Minimum (mg/kg)	Maximum (mg/kg)	Mean (mg/kg)	Standard deviation (mg/kg)	Skewness	Kurtosis	Coefficient of variance (%)	Significance value of the K–S test	Distribution pattern
Cd	271	0.050	0.580	0.150	0.067	0.384[a]	1.699[a]	44.67	0.001[a]	Approximate lognormal distribution
Hg	271	0.029	0.557	0.130	0.057	−0.169[a]	0.352[a]	43.85	0.2[a]	Lognormal distribution

[a]*Skewness, kurtosis, and significance in the K-S test after logarithmic conversion.*

$$t_{\overline{y}_{h=1}-\overline{y}_{h=2}} = \frac{\overline{Y}_{h=1} - \overline{Y}_{h=2}}{\left[\frac{Var\left(\overline{Y}_{h=1}\right)}{n_{h=1}} + \frac{Var\left(\overline{Y}_{h=2}\right)}{n_{h=2}}\right]^{1/2}} \quad (7)$$

where $\overline{Y}_h$ represents the attribute mean in sub-area h (in this study, this represents the concentration of a particular heavy metal), n_h represents the number of samples in sub-area h, and Var represents the variance in heavy metal concentrations. The t statistic approximately complies with the Student's t distribution, wherein the degree of freedom is calculated as:

$$df = \frac{\frac{Var\left(\overline{Y}_{h=1}\right)}{n_{h=1}} + \frac{Var\left(\overline{Y}_{h=2}\right)}{n_{h=2}}}{\frac{1}{n_{h=1}-1}\left[\frac{Var\left(\overline{Y}_{h=1}\right)}{n_{h=1}}\right]^2 + \frac{1}{n_{h=2}-1}\left[\frac{Var\left(\overline{Y}_{h=2}\right)}{n_{h=2}}\right]^2} \quad (8)$$

The null hypothesis was H_0: $\overline{Y}_{h=1} = \overline{Y}_{h=2}$, whereby H_0 is rejected at confidence level α, representing a significant difference between the attribute means of two sub-areas.

According to existing research, and taking into account data availability and accessibility, 14 factors that could influence the potential ecological risks of Cd and Hg in farmland soil in the study region were selected. These were soil properties: soil type, texture, pH, organic matter, total nitrogen (N), total phosphorous (P), and total potassium (K); topographical factors: slope and elevation; and distance factors: distance of sampling points from rivers, residents, roads, railways, and mining lands. All factors were extracted from vector data based on existing studies.

RESULTS

Statistical characteristics of Cd and Hg Concentrations

The descriptive statistics of Cd and Hg concentrations in farmland soil in Fengcheng are listed in **Table 1**. There was a remarkable difference between the maximum and minimum concentrations of the two heavy metals. The original Cd and Hg concentrations did not follow a normal distribution, but after processing, had an approximate lognormal and a lognormal distribution, respectively. According to their CV values, Cd and Hg concentrations in the study area show moderate variation.

The spatial Structure and Distribution of Cd and Hg

Spatial Structure of Cd and Hg

The optimal models and fitting parameters of Cd and Hg concentrations in the study region are summarized in **Table 2**. The optimal models for both heavy metals were exponential. Nugget/sill ratios for both Between 25 and 75%, indicating that their concentrations were moderate spatial autocorrelation, and are affected by random factors such as human activities and structural factors. The range of Cd was larger than that of Hg, suggesting that Cd has greater spatial correlation than Hg. The R^2 values of Hg and Cd were 0.766 and 0.609 respectively, indicating that the goodness-of-fit of the semi-variagram was better for Cd than H.

Spatial Distribution of Cd and Hg

The semivariogram can be used to explain the spatial structure of heavy metal concentrations, thereby reflecting spatial variation; however, the information provided by this function has limitations (Wang et al., 2014). To further characterize the spatial distribution of Cd and Hg concentrations in the study region, we therefore conducted ordinary Kriging interpolation according to the optimal semivariogram models. The spatial distributions of the two heavy metal concentrations are shown in **Figure 2**, revealing remarkable differences between Cd and Hg in farmland soil throughout the study region.

In ArcGIS-Geostatistical Analyst tool, the training set and validation set of sampling points are selected by subset tool, which are used to represent the cross-validation results of ordinary Kriging interpolation (**Table 3**). The root mean square errors of the two are 0.02, 0.03, and the interpretation coefficients are 0.76, 0.85, respectively. The test shows that the prediction accuracy is high and the interpolation results are reliable (Jiang and Guo, 2019).

It can be found from **Figure 2** that the distribution differences of Cd and Hg in the whole city are obvious. A small part of Cd content less than the background value of soil elements in Jiangxi Province is mainly concentrated in the northwest and northeast of the city, and the distribution is more dispersed. The main distribution of Cd content exceeding the soil pollution risk screening value of agricultural land in China is in the central and southeast regions of the study area,it can also be seen from the map that Cd content in most areas of the city exceeded the background value of soil elements in Jiangxi Province but did not reach the level of risk screening value, mainly concentrated in the

TABLE 2 | Optimal models and fitting parameters for Cd and Hg concentrations in farmland soil in the study region.

Metal	Theoretical model	Nugget (C_0)	Sill (C_0 + C)	Nugget/sill (C_0/C_0 + C, %)	Range (A_0, km)	R^2	Residual sum of squares
Cd	Exponential	0.0702	0.1582	44.41	8.61	0.766	4.197E–06
Hg	Exponential	0.0582	0.1992	29.21	6.24	0.609	3.83E–07

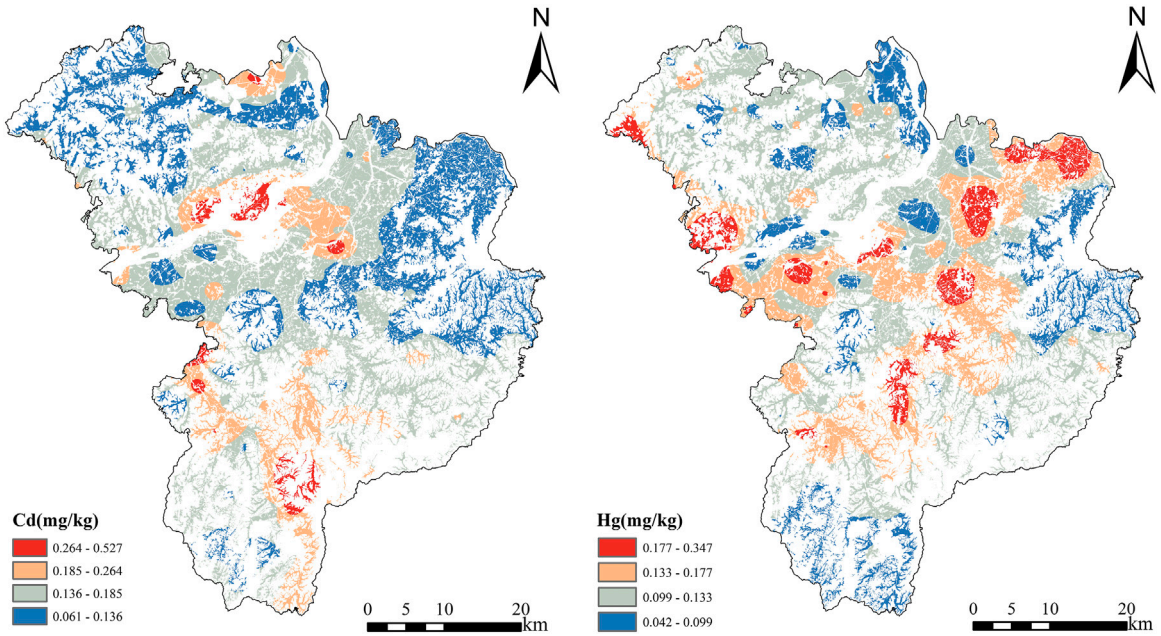

FIGURE 2 | Spatial distribution of Cd and Hg concentrations in farmland soil in the study region.

TABLE 3 | Cross validation of ordinary Kriging interpolation results

Index	RMSE	R2	RPD
Cd	0.02	0.76	1.91
Hg	0.03	0.85	2.22

0.136–0.185 range. Hg in Fengcheng City did not exceed the national screening value of soil pollution risk of agricultural land, but most exceeded the background value of Hg in Jiangxi Province. The high value areas were mainly distributed in the central part of Fengcheng City, mainly concentrated in the range of 0.099–0.133. Distribution of Hg within background values of soil in Jiangxi Province in southern, eastern and northern parts of the study area, most of the rest exceed the background value of Jiangxi Province, but are still in the range of risk screening values. From the spatial distribution of Cd and Hg, it can be seen that the high value area of Cd is close to the city center, which is closely related to human activities, and its influence range may pose a threat to farmland grain production and ecological environment safety around the city, however, the distribution of Hg is relatively dispersed, and it does not have a certain concentration as Cd, which is related to its main source of pesticide and fertilizer application.

Potential Ecological Risk Levels of Cd and Hg

Using the potential ecological risk index results, the sampling points were classified into different risk levels (**Figure 3**), with the number of sampling points associated with different risk levels shown in **Figure 4**. The risk index of both Cd and Hg was categorized into four levels each. The risk level of Cd was generally low (level 1) at 141 sampling points, accounting for 52.03% of total sampling points, with only one point showing a high level of risk (level 4). Meanwhile, the potential ecological risk level of Hg was moderate (level 2) at 161 sampling points, accounting for 59.41% of total sampling points, with only 0.74% of points represented by a high risk level (level 4).

Based on the potential ecological risk index of heavy metals Cd and Hg, the comprehensive potential ecological risk index of each sample point was calculated. The zoning map of soil comprehensive potential ecological risk index in the study area was made by ArcGIS 10.2 (ESRI Inc., Redlands, CA, United States) software (**Figure 4**). It is not difficult to see that the comprehensive potential ecological risk index of soil in the study area is between 32.38 and 217.36. From the spatial distribution, moderate (150 ≤ RI < 300) and intensity (300 ≤ RI < 600) potential ecological risk areas are mainly distributed in the central region of the city. According to the grid reclassification statistics, the regions with slight potential ecological harm (150 ≤

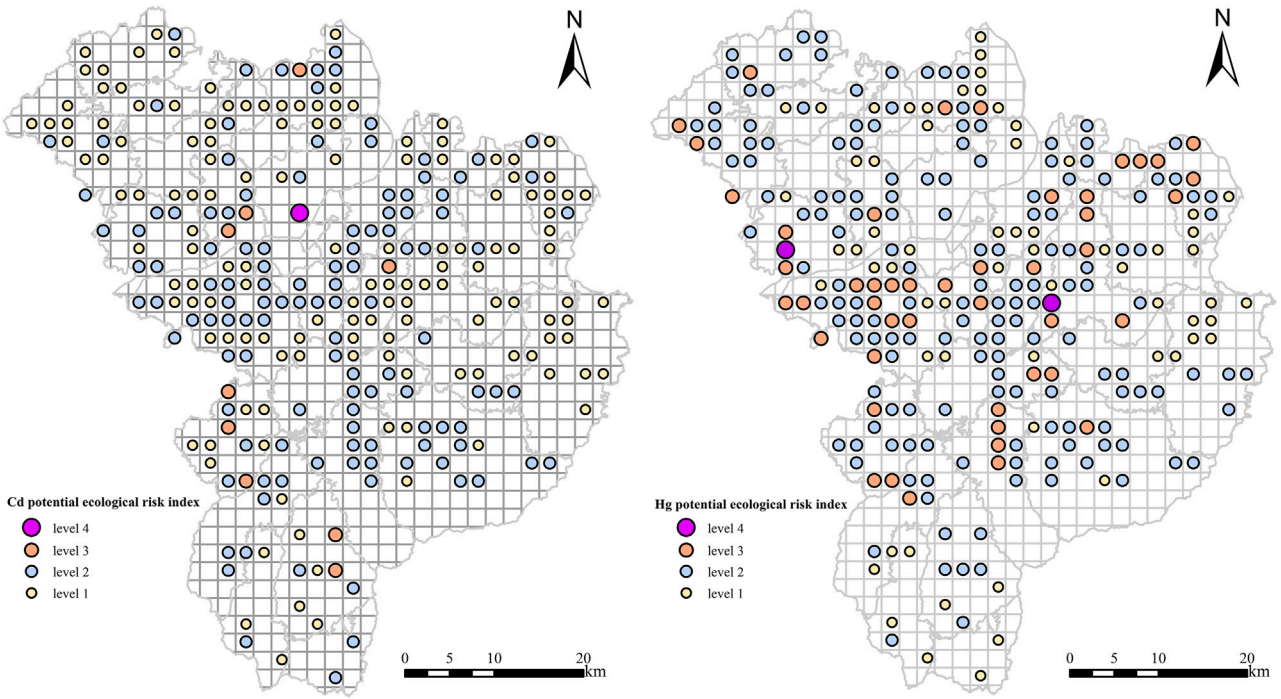

FIGURE 3 | Classification of sampling points associated with different potential ecological.

RI < 300) were the majority, accounting for 86.19%. The lowest potential ecological risk index showed a relatively dispersed block distribution in spatial distribution, and the moderate (150 ≤ RI < 300) and intensity (300 ≤ RI < 600) potential ecological risk areas were also dispersed. The overall potential ecological risk of heavy metals in the soil of the study area was relatively low.

Factors Influencing the Potential Ecological Risks of Cd and Hg

Correlation Analysis

Spatial variation analysis revealed that the distribution of Cd and Hg concentrations in farmland soil in the study region was influenced by external factors; however, these associated factors are complex and diverse. Land use patterns and vegetation cover types are important factors controlling spatial distribution and accumulation of heavy metals in soils at site, county and watershed scales. To identify the different factors influencing the potential ecological risks, we first conducted correlation analysis between the risk index of Cd and Hg, the comprehensive risk index, and the 14 associated factors (**Table 4**). Four factors (soil texture, soil type, total N, and distance from residential areas) had no significant correlation with the risk index of Cd and Hg or the comprehensive risk index; however, the remaining 10 factors were all significantly correlated with at least one index.

The potential ecological risk coefficient of Cd was significantly correlated with pH and negatively correlated with Total K (p-values < 0.01), and the distance from the road showed a significant negative correlation (p-values < 0.05). Meanwhile, the potential ecological risk coefficient of Hg element was negatively correlated with total phosphorus, slope, elevation and distance to the river (p-values < 0.01), as well as with organic matter distance from a railway and distance from a mining area (p-values < 0.05). The comprehensive potential ecological risk index of soil showed a significant positive correlation with pH, while negative correlation were found with Total P, elevation and distance to river (p-values < 0.01), and a significant negative correlation with distance to road (p-values < 0.05).

Geodetector Analysis

The factor detector of Geodetector was subsequently used to measure the relative influence of the selected factors on the potential ecological risks of Cd and Hg (**Table 5**). The explanatory power of the top six factors influencing the potential ecological risk of Cd was ranked as follows: pH > distance from a road > distance from a river > soil texture > slope > total K; however, only the effects of pH were significant (p < 0.05). Meanwhile, the explanatory power of the top six factors influencing the potential ecological risk of Hg was as follows: distance from a railway > total P > slope > distance from a river > elevation > organic matter, but only the effect of total P and distance from a railway was significant (p < 0.05). In terms of the comprehensive potential ecological risk index of heavy metals, total P and total P had the greatest explanatory power (p < 0.05).

The results obtained using the risk detector showed that the most significant factor influencing the potential ecological risk of Cd was a soil pH of 5.2–5.6. The most significant factor influencing the potential ecological risk of Hg was distance from a railway >6004.02 mm, while the second was total $p \leq 0.52$ mg kg^{-1}. The most significant factor influencing the comprehensive potential ecological risk was soil pH of 5.2–5.6 followed by $p \leq 0.52$ mg kg^{-1}.

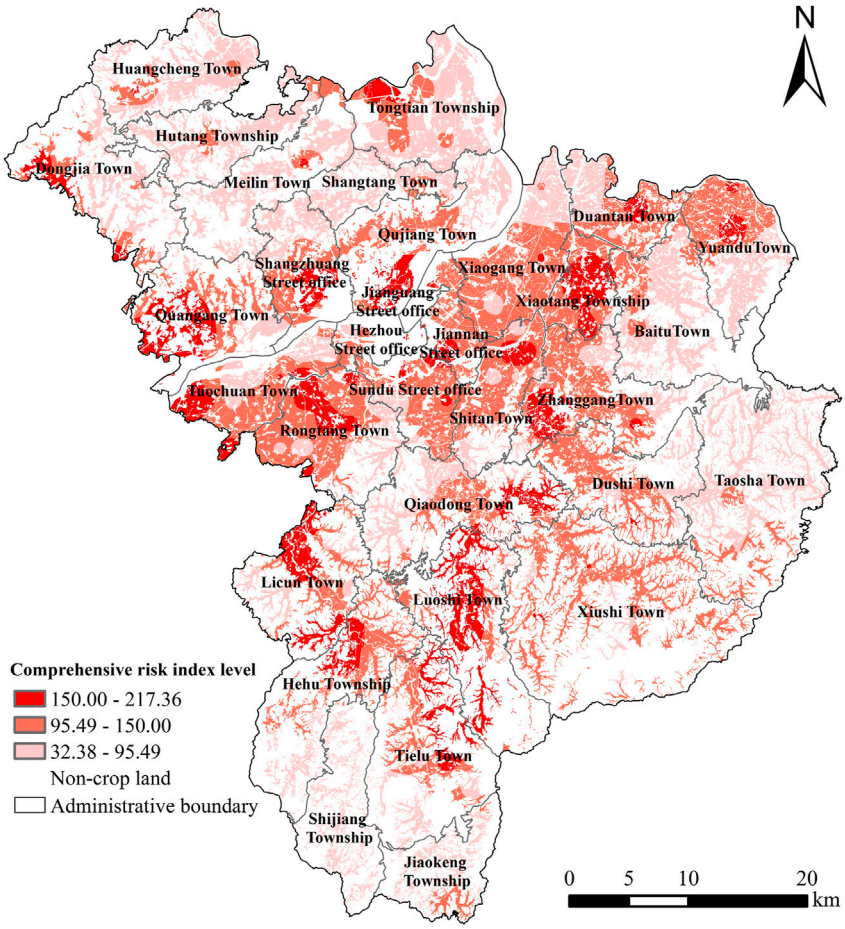

FIGURE 4 | Zonation of comprehensive potential ecological risk levels of Cd and Hg in farmland soil across the study region.

TABLE 4 | Correlations between the potential ecological risk of Cd and Hg and associated influencing factors in farmland soil in the study region.

Factor	Cd	Hg	RI
Soil texture	−0.019	−0.032	−0.049
Soil type	0.056	0.068	0.090
pH	0.246**	0.069	0.162**
Organic matter	−0.002	−0.134*	−0.097
Total N	0.049	−0.059	−0.025
Total P	−0.075	−0.196**	−0.167**
Total K	−0.227**	−0.008	−0.106
Slope	0.061	−0.160**	−0.099
Elevation	−0.098	−0.168**	−0.180**
Distance from a river	−0.092	−0.177**	−0.184**
Distance from a residential area	−0.035	−0.118	−0.104
Distance from a road	−0.133*	−0.081	−0.124*
Distance from a railway	0.112	−0.140*	−0.065
Distance from a mining area	0.035	−0.112*	−0.081

*$p < 0.05$; **$p < 0.01$.

DISCUSSION

Potential ecological risk index method introduces the toxic coefficient and links the ecological and environmental effects of heavy metals with their toxicology. This index can therefore be used to comprehensively reflect the potential impacts of Cd and Hg on the ecological environment of farmland soil, providing useful information for the management and protection of soil environments as well as human health. Remarkable differences in the spatial distribution of Cd and Hg concentrations were observed throughout the study region. The results show that a handful of areas with Cd concentrations below the regional background level were found in the northwest and northeast; however, most other areas had a soil Cd concentration above this background level, with only a few areas in the central and southeast possessing a soil Cd concentration higher than the national risk screening value. Meanwhile, those with a Hg concentration lower than the regional background level distributed in the southern, eastern and northern parts of the country, and remaining areas with concentrations between the regional background level and national risk screening value, gradually increasing toward the central.

According to the land-use map of Fengcheng (**Figure 5**), urban road traffic networks are mainly concentrated in central and northern areas, while emerging industrial parks, mainly featuring new energy, photovoltaic electronics, and machinery industries, are located in the center of the city. Cd and Hg have

TABLE 5 | The explanatory power and statistical significance of the top six major factors influencing the potential ecological risks of Cd and Hg in farmland soil in the study region.

Metal	Explanatory power and significance	1	2	3	4	5	6
Cd	*q* statistic	pH	Distance from a road	Distance from a river	Soil texture	Slope	Total K
	p value (0.05)	4.11% 0.03	2.97% 0.62	2.67% 0.58	2.53% 0.15	1.61% 0.34	1.47% 0.18
Hg	*q* statistic	Distance from a railway	Total P	Slope	Distance from a river	Elevation	Organic matter
	p value (0.05)	5.57% 0.00	4.86% 0.02	2.42% 0.23	2.37% 0.12	1.94% 0.10	1.90% 0.19
RI	*q* statistic	pH	Elevation	Soil type	Total P	Distance from a river	Distance from a road
	p value (0.05)	5.46% 0.00	3.83% 0.12	3.72% 0.47	3.13% 0.03	2.50% 0.11	1.49% 0.43

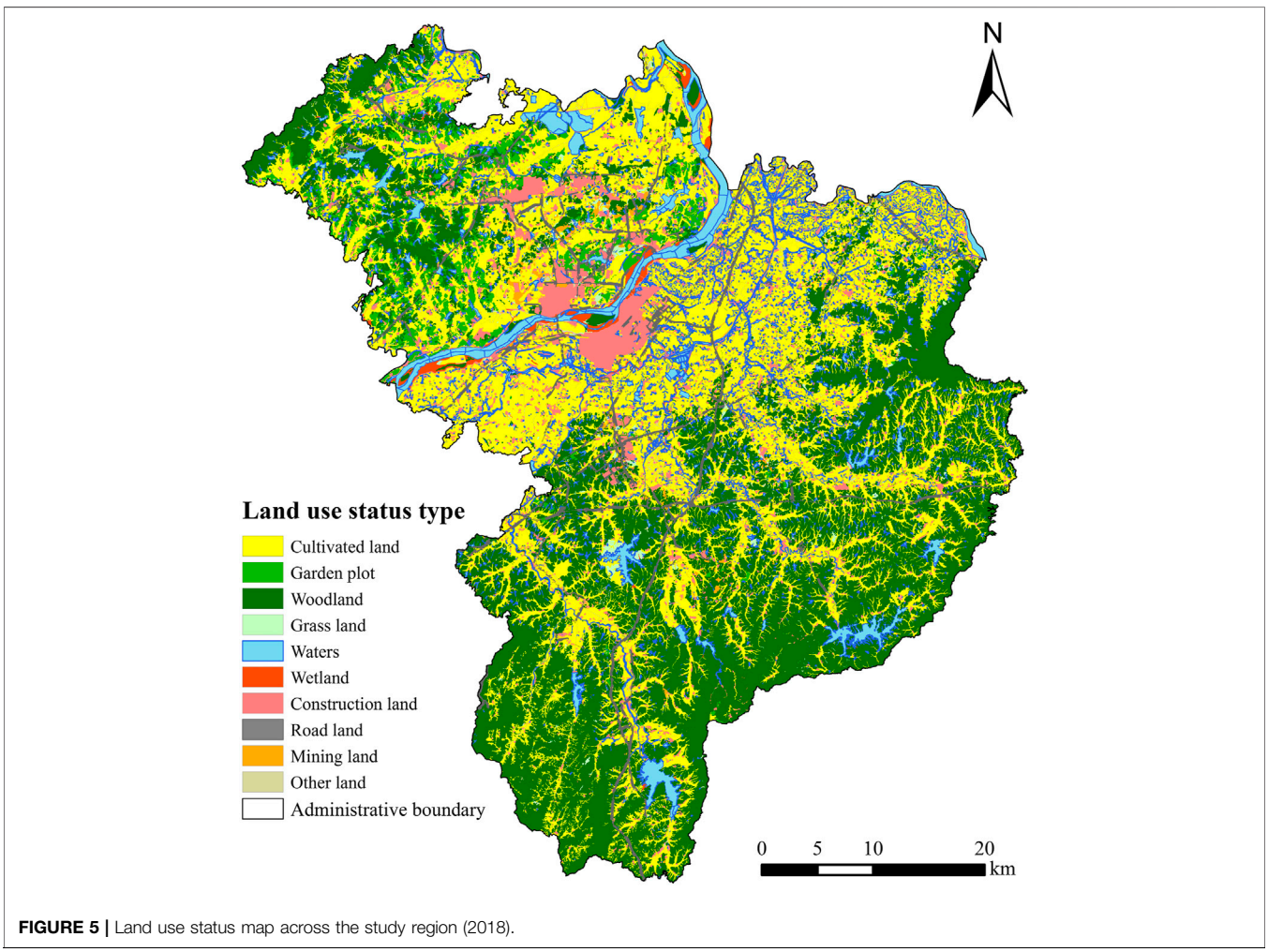

FIGURE 5 | Land use status map across the study region (2018).

therefore accumulated in this region as a result of human factors, and that is consistent with Zhou's conclusion that compared with natural factors, human activities release more partition content into soil, which is more likely to affect crop growth retardation (Zhou et al., 2020; Boussen et al., 2013). The area with the highest Cd concentration was located near the dense urban roads, close to mining land. In addition to soil parent material, this Cd was therefore deemed to have originated from vehicle exhaust

emissions and smelting, this is consistent with Yang's findings that major sources of cadmium and mercury come from human activities and from transport and industrial activities (Yang et al., 2020). A small amount of Cd was thought to be related to a combination of accidental factors such as field sampling, laboratory test errors. Low Hg concentrations were found in the south and east of Fengcheng, far from industrial parks and road traffic, were there is less of an effect from human factors. These results suggest that Cd and Hg detected in farmland soil in the study region are derived from external sources, notably human activities such as industrial production, agricultural fertilization, and residential areas. Over time, these heavy metal concentrations could therefore exceed their respective regional background levels, resulting in heavy metal pollution (Shi et al., 2019).

The potential ecological risks of Cd and Hg at sampling points across the study region were categorized into four levels. For Cd, the number of sampling points with a high risk level (level 4) was low, the majority being associated with a low risk level (level 1). For Hg, the majority of sampling points were associated with a moderate risk level (level 2). The potential ecological risks of Cd and Hg in humans are well known. For example, Cd is known to enter the human body through the food chain, causing damage to the kidneys, brain, bones and nervous system, and resulting in acute or chronic poisoning and even cancer (Sriramachari and Jain, 1997; Bandara et al., 2008). Meanwhile, Hg is easily absorbed by human skin, as well as *via* the respiratory tract and digestive system, with bioaccumulation causing damage to the brain and liver, again posing serious health risks (Zhang et al., 2018). The Hg concentrations of farmland soil in the study region were lower than those of Cd; however, the potential ecological risk of Hg was higher. Reasonable precautions should therefore be taken to prevent Hg input and decrease the potential ecological risk level. The comprehensive potential ecological risk of both Cd and Hg was generally low in farmland soil throughout the study region; however, the comprehensive risk level in central parts was higher than in the south and north, mainly because this area is more heavily influenced by human activities such as industry and transportation.

The potential ecological risk of Cd and Hg in farmland soil in the study region was found to be influenced by both natural and human factors. Human activities can change soil pH and fertility, thereby affecting the migration and transformation of heavy metals in the soil, and ultimately influencing the potential ecological risk. Based on a long-term field experiment, Chen et al. revealed that the application of P fertilizer was the main factor leading to an increase in Cd and Hg concentrations in farmland soil (Chen and Dong, 2005). In addition, topographic factors such as slope were also found to have a direct effect on the distribution and redistribution of water and thermal resources (Wei and Shao, 2009), in turn affecting the conversion and sequestration, and potential ecological risk, of heavy metals in soil. Heavy metals emitted from automobile exhausts and those present in vehicle tires are also deposited in farmland, driven by climatic factors such as rainfall, further affecting the accumulation of Cd and Hg. In line with this, our results are similar to a previous study (Liu et al., 2016; Turkyilmaz et al., 2018), whereby distance from a road was considered one of the most important factors influencing the potential ecological risks of Cd and Hg in farmland soil. Moreover, industrial wastewater and domestic sewage discharge into rivers used for agricultural irrigation was also found to be another important reason for increasing concentrations and potential ecological risk levels of heavy metals in farmland soil. Furthermore, the occurrence of heavy metals varies across soil types and textures; thus, the potential ecological risk of Cd and Hg in farmland soil is also affected, to a certain extent, by soil texture. Explanatory power q of the selected factors varied little in terms of the potential ecological risk of Cd and Hg, suggesting that both heavy metals are jointly affected by multiple factors. Using Geodetector, the two most significant factors influencing the potential ecological risk of Cd were a pH of 5.2–5.6 and Distance from a road, while for Hg, distance from a railway >6004.02 m and total $p \leq 0.52$ mg kg^{-1} were most significant. These results highlight the need for future management and control of heavy metal pollution in farmland soil in this and similar regions.

CONCLUSION

In this study, the concentrations of Cd and Hg in farmland soil in Fengcheng both showed moderate variation, influenced by both natural and human factors. Both human and natural factors have a comprehensive effect on the spatial distribution of the two heavy metals. Moreover, while concentrations of Cd and Hg in most areas exceeded the regional background level in Jiangxi, they did not reach the national risk screening value for soil pollution of agricultural land in China. The most significant factor influencing the potential ecological risk of Cd was a pH of 5.2–5.6. Meanwhile, the most significant factor affecting Hg was distance from a railway >6004.02 m, followed by total $p \leq 0.52$ mg kg^{-1}. The most significant factor affecting the comprehensive potential ecological risk index was soil pH of 5.2–5.6 followed by total $p \leq 0.52$ mg kg^{-1}. Overall, the potential ecological risk of heavy metals in the study region was low. These results provide insight into heavy metal pollution in Poyang Lake Plain, which will aid the prevention and control of farmland soil pollution as well as the utilization and protection of agricultural resources on a regional scale.

DATA AVAILABILITY STATEMENT

The raw data supporting the conclusion of this article will be made available by the authors, without undue reservation.

AUTHOR CONTRIBUTIONS

All authors listed have made a substantial, direct, and intellectual contribution to the work and approved it for publication. XH and HY contributed equally to this work.

FUNDING

This research was supported by the National Key R and D Program of China (No. 2017YFD0301603).

REFERENCES

Aelion, C., Davis, H. T., McDermott, S., and Lawson, A. (2008). Metal concentrations in rural topsoil in South Carolina: potential for human health impact. *Sci. Total Environ.* 402, 149–156. doi:10.1016/j.scitotenv.2008.04.043

An, J., Gong, X., Chen, H., and Wei, S. (2016). Temporal and spatial characteristics and health risk assessments of heavy metal pollution in soils of Shenfu irrigation area. *J. Agro-Environ. Sci.* 35 (1), 37–44. doi:10.11654/jaes.2016.01.005

Arman, N., Mohammad, A., Babak, K., and Mohammad, S. (2017). Assessment of spatial distribution of soil heavy metals using ANN-GA, MSLR and satellite imagery. *Environ. Monit. Assess. Int. J.* 185 (5), 214

Bandara, J., Senevirathna, D., Dasanayake, D., Herath, V., Bandara, J., Abeysekara, T., et al. (2008). Chronic renal failure among farm families in cascade irrigation systems in Sri Lanka associated with elevated dietary cadmium levels in rice and freshwater fish (Tilapia). *Environ. Geochem. Health* 30 (5), 465–478. doi:10.1007/s10653-007-9129-6

Barlas, N., Akbulut, N., and Aydoğan, M. (2005). Assessment of heavy metal residues in the sediment and water samples of Uluabat Lake, Turkey. *Bull. Environ. Contam. Toxicol.* 74 (2), 286–293. doi:10.1007/s00128-004-0582-y

Boussen, S., Soubrand, M., Bril, H., Ouerfelli, K., and Abdeljaouad, S. (2013). Transfer of lead, zinc and cadmium from mine tailings to wheat (*Triticum aestivum*) in carbonated mediterranean (Northern Tunisia) soils. *Geoderma* 192, 227–236. doi:10.1016/j.geoderma.2012.08.029

Cai, L., Wang, Q., Wen, H., Luo, J., and Wang, S. (2019). Heavy metals in agricultural soils from a typical township in Guangdong province, China: occurrences and spatial distribution. *Ecotoxicol. Environ. Saf.* 168, 184–191. doi:10.1016/j.ecoenv.2018.10.092

Chabukdhara, M., and Nema, A. (2013). Heavy metals assessment in urban soil around industrial clusters in Ghaziabad, India: probabilistic health risk approach. *Ecotoxicol. Environ. Saf.* 87, 57–64. doi:10.1016/j.ecoenv.2012.08.032

Chen, F., and Dong, Y. (2005). Variation of soil heavy metal contents in a long-term fertilization experiment. *Soil* 37 (3), 308–311. doi:10.13758/j.cnki.tr.2005.03.015

Chen, M., Ding, S., Zhang, L., Li, Y., Sun, Q., and Zhang, C. (2017). An investigation of the effects of elevated phosphorus in water on the release of heavy metals in sediments at a high resolution. *Sci. Total Environ.* 575, 330–337. doi:10.1016/j.scitotenv.2016.10.063

China National Environmental Monitoring Centre (CNEMC) (1990). *The background values of Chinese soils*. Beijing: Environmental Science Press of China, 101–501.

Dai, L., Wang, L., Li, L., Liang, T., Zhang, Y., Ma, C., et al. (2018). Multivariate geostatistical analysis and source identification of heavy metals in the sediment of Poyang lake in China. *Sci. Total Environ.* 621, 1433–1444. doi:10.1016/j.scitotenv.2017.10.085

Ding, Q., Cheng, G., Wang, Y., and Zhuang, D. (2016). Effects of natural factors on the spatial distribution of heavy metals in soils surrounding mining regions. *Sci. Total Environ.* 578, 577–585. doi:10.1016/j.scitotenv.2016.11.001

Facchinelli, A., Sacchi, E., and Mallen, L. (2001). Multivariate statistical and gis-based approach to identify heavy metal sources in soils. *Environ. Pollut.* 114 (3), 313–324. doi:10.1016/S0269-7491(00)00243-8

Ha, H., Olson, J., Bian, L., and Rogerson, P. (2014). Analysis of heavy metal sources in soil using kriging interpolation on principal components. *Environ. Sci. Technol.* 48 (9), 4999–5007. doi:10.1021/es405083f

Hakanson, L. (1980). An ecological risk index for aquatic pollution control.a sedimentological approach. *Water Res.* 14, 975–1001. doi:10.1016/0043-1354(80)90143-8

He, J., and Xu, G. (2006). *Study on background value of soil environment in Jiangxi province*. Beijing, China: China Environmental Science Press, 314.

Hu, B., Jia, X., Hu, J., Xu, D., Xia, F., and Li, Y. (2017). Assessment of heavy metal pollution and health risks in the soil-plant-human system in the Yangtze river delta, China. *Int. J. Environ. Res. Public Health* 14 (14), 1–18. doi:10.3390/ijerph14091042

Hu, B., Zhao, R., Chen, S., Zhou, Y., Jin, B., Li, Y., et al. (2018). Heavy metal pollution delineation based on uncertainty in a coastal industrial city in the Yangtze river delta, China. *Int. J. Environ. Res. Public Health* 15 (4), 710. doi:10.3390/ijerph15040710

Ihedioha, J. N., Ukoha, P., and Ekere, N. (2016). Ecological and human health risk assessment of heavy metal contamination in soil of a municipal solid waste dump in uyo, nigeria. *Environ. Geochem. Health* 39 (3), 497–515. doi:10.1007/s10653-016-9830-4

Imperato, M., Adamo, P., Naimo, D., Arienzo, M., Stanzione, D., and Violante, P. (2003). Spatial distribution of heavy metals in urban soils of Naples city (Italy). *Environ. Pollut.* 124 (2), 247–256. doi:10.1016/S0269-7491(02)00478-5

Jiang, Y., Rao, L., Sun, K., Han, Y., and Guo, X. (2018). Spatio-temporal distribution of soil nitrogen in Poyang lake ecological economic zone (South-China). *Sci. Total Environ.* 626, 235–243. doi:10.1016/j.scitotenv.2018.01.087

Jiang, Y., and Guo, X. (2019). Multivariate and geostatistical analyses of heavy metal pollution from different sources among farmlands in the Poyang lake region, China. *J. Soil. Sediment.* 19, 2472–2484. doi:10.1007/s11368-018-2222-x

Kasel, S., Bennett, L. T., Aponte, C., Fedrigo, M., and Nitschke, C. R. (2017). Environmental heterogeneity promotes floristic turnover in temperate forests of south-eastern Australia more than dispersal limitation and disturbance. *Landsc. Ecol.* 32, 1613–1629. doi:10.1007/s10980-017-0526-7

Kelepertzis, E. (2014). Accumulation of heavy metals in agricultural soils of Mediterranean: insights from Argolida basin, Peloponnese, Greece. *Geoderma* 221–222 (27), 82–90. doi:10.1016/j.geoderma.2014.01.007

Lei, Z., Yang, S., Xu, Z., and Vachaud, G. (1985). Preliminary investigaion of the spatial variability of soil properties. *J. Hydraulic Eng.* (09), 10–21. doi:10.13243/j.cnki.slxb.1985.09.002

Liu, H. L., Zhou, J., Li, M., Hu, Y. M., Liu, X., and Zhou, J. (2019). Study of the bioavailability of heavy metals from atmospheric deposition on the soil-pakchoi (*Brassica chinensis* l.) system. *J. Hazard. Mater.* 362, 9–16. doi:10.1016/j.jhazmat.2018.09.032

Liu, Y., Ma, Z., Lv, J., and Bi, J. (2016). Identifying sources and hazardous risks of heavy metals in topsoils of rapidly urbanizing East China. *J. Geogr. Sci.* 26 (6), 735–749. doi:10.1007/s11442-016-1296-x

Loredo, J., Pereira, A., and Ordonez, A. (2003). Untreated abandoned mercury mining works in a scenic area of asturias (Spain). *Environ. Int.* 29 (4), 481–491. doi:10.1016/S0160-4120(03)00007-2

Lü, J., Jiao, W.-B., Qiu, H.-Y., Chen, B., Huang, X.-X., and Kang, B. (2018). Origin and spatial distribution of heavy metals and carcinogenic risk assessment in mining areas at You'xi county Southeast China. *Geoderma* 310, 99–106. doi:10.1016/j.geoderma.2017.09.016

Lv, J., Liu, Y., Zhang, Z., Dai, J., Dai, B., and Zhu, Y. (2015). Identifying the origins and spatial distributions of heavy metals in soils of Ju country (Eastern China) using multivariate and geostatistical approach. *J. Soil. Sediment.* 15 (1), 163–178. doi:10.1007/s11368-014-0937-x

Lv, J., Zhang, Z., Li, S., Liu, Y., Sun, Y., and Dai, B. (2013). Assessing spatial distribution, sources, and potential ecological risk of heavy metals in surface sediments of the Nansi lake, Eastern China. *J. Radioanal. Nucl. Chem.* 299 (3), 1671–1681. doi:10.1007/s10967-013-2883-2

Mazej, Z., Al Sayegh-Petkovsek, S., and Pokorny, B. (2010). Heavy metal concentrations in food chain of lake velenjsko jezero, slovenia: an artificial lake from mining. *Arch. Environ. Contam. Toxicol.* 58 (4), 998–1007. doi:10.1007/s00244-009-9417-5

National Standard of the People's Republic of China (2018). *Soil environmental quality. Risk control standard for soil contamination agricultural land (trial) GB15618-2018*, 2–3.

Qiao, P., Yang, S., Lei, M., Chen, T., and Dong, N. (2019). Quantitative analysis of the factors influencing spatial distribution of soil heavy metals based on geographical detector. *Sci. Total Environ.* 664, 392–413. doi:10.1016/j.scitotenv.2019.01.310

Raj, S. M., and Jayaprakash, M. (2008). Distribution and enrichment of trace metals in marine sediments of bay of bengal, off ennore, south-east coast of india. *Environ. Geol.* 56 (1), 207–217. doi:10.1007/s00254-007-1156-1

Shi, R., Zhang, Y., Xu, M., Zhang, X., and Zhao, Z. (2019). Pollution evaluation and source apportionment of heavy metals in soils from tianjin suburbs, China. *J. Agro-Environ. Sci.* 38 (5), 1069–1078. doi:10.11654/jaes.2018-1152

Sriramachari, S., and Jain, A. K. (1997). Trace elements in human nutrition and health. *Indian J. Med. Res.* 105 (5), 246–247. doi:10.1177/026010609601100206

Tang, L. (2007). Effects of soil properties on crop cd uptake and prediction of cd concentration in grains. *J. Agro-Environ. Sci.* 26 (2), 699–703.

Tepanosyan, G., Maghakyan, N., Sahakyan, L., and Saghatelyan, A. (2017). Heavy metals pollution levels and children health risk assessment of yerevan

kindergartens soils. *Ecotoxicol. Environ. Saf.* 142, 257–265. doi:10.1016/j.ecoenv.2017.04.013

Turkyilmaz, A., Cetin, M., Sevik, H., Isinkaralar, K., and Saleh, E. A. A. (2018). Variation of heavy metal accumulation in certain landscaping plants due to traffic density. *Environ. Dev. Sustain.* 22 (3), 2385. doi:10.1007/s10668-018-0296-7

Wang, J., and Xu, C. (2017). Geodetector: principle and prospective. *Acta Geogr. Sin.* 72 (01), 116–134. doi:10.11821/dlxb201701010

Wang, S., Cai, L. M., Wen, H. H., Luo, J., Wang, Q. S., and Liu, X. (2019). Spatial distribution and source apportionment of heavy metals in soil from a typical county-level city of guangdong province, China. *Sci. Total Environ.* 655, 92–101. doi:10.1016/j.scitotenv.2018.11.244

Wang, Y., Bai, Y., and Wang, J. (2014). Distribution of soil heavy metal and pollution evaluation on the different sampling scales in farmland on Yellow River irrigation area of Ningxia: a case study in Xingqing County of Yinchuan City. *Huan Jing Ke Xue* 35 (7), 2714. doi:10.13227/j.hjkx.2014.07.039

Wei, X., and Shao, M. (2009). Distribution of micronutrients in soils as affected by landforms in a Loessial Gully Watershed. *Environ. Sci. Tech.* 30 (9), 2741–2746. doi:10.13227/j.hjkx.2009.09.009

Xie, X. J., Kang, J. C., Yan, G. D., Zhang, J. P., and Zhu, W. W. (2010). Heavy metal concentration in agricultural soils around the upper-middle reaches of Huangpu river. *China Environ Sci.* 30 (8), 1110–1117. doi:10.3724/SP.J.1088.2010.00432

Xu, Z. Q., Ni, S. J., Tuo, X. G., and Zhang, C. J. (2008). Calculation of heavy metals' toxicity coefficient in the evaluation of potential ecological risk index. *Environ. Sci. Tech.* 31 (2), 112–115. doi:10.19672/j.cnki.1003-6504.2008.02.030

Yang, A., Wang, Y. H., Hu, J., Liu, X. L., and Li, J. (2020). Evaluation and source of heavy metal pollution in surface soil of Qinghai-Tibet plateau. *Huan Jing Ke Xue* 41 (2), 886–894. doi:10.13227/j.hjkx.201907195

Yuan, R., Yu, G., Qiu, X., Zong, L., and Zheng, L. (2015). Regionally spatial variation of soil heavy metals and their influences on vegetable quality: a case study of Baguazhou and Jiangxinzhou, Nanjing, China. *J. Agro-Environment Sci.* 34 (8), 1498–1507. doi:10.11654/jaes.2015.08.010

Zhang, H., Jiang, Y., Ding, M., and Xie, Z. (2017). Level, source identification, and risk analysis of heavy metal in surface sediments from river-lake ecosystems in the Poyang lake, China. *Environ. Sci. Pollut. Res. Int.* 24, 21902–21916. doi:10.1007/s11356-017-9855-y

Zhang, P., Qin, C., Hong, X., Kang, G., Qin, M., Yang, D., et al. (2018). Risk assessment and source analysis of soil heavy metal pollution from lower reaches of yellow river irrigation in China. *Sci. Total Environ.* 633, 1136–1147. doi:10.1016/j.scitotenv.2018.03.228

Zhao, Q., and Luo, Y. (2015). The macro strategy of soil protection in China. *Bull. Chin. Acad. Sci.* 30 (4), 452–458. doi:10.16418/j.issn.1000-3045.2015.04.003

Zhong, X. L., Zhou, S. L., Li, J. T., and Zhao, Q. G. (2007). Spatial variability of soil heavy metals contamination in the Yangtze river delta–a case study of Taicang city in Jiangsu Province. *Acta. Pedol. Sin.* 44 (1), 33–40. doi:10.11766/trxb200508260106

Zhou, J., Zhang, C., Du, B., Cui, H., Fan, X., Zhou, D., et al. (2020). Effects of zinc application on cadmium (cd) accumulation and plant growth through modulation of the antioxidant system and translocation of cd in low- and high-cd wheat cultivars. *Environ. Pollut.* 265 (Pt A), 115045. doi:10.1016/j.envpol.2020.115045

Conflict of Interest: The authors declare that the research was conducted in the absence of any commercial or financial relationships that could be construed as a potential conflict of interest.

frontiers in Environmental Science

ORIGINAL RESEARCH
published: 20 April 2021
doi: 10.3389/fenvs.2021.661148

Spatial Distribution Characteristic of Antimony in Typical Paddy Soil of Eastern Hunan Province, China

ChenRan Wang[1], DaJuan Wan[1], XueYing Cao[2], Huan Wang[1], JiaQi Chen[1], NingXiang Ouyang[3], YangZhu Zhang[3] and ChangYin Tan[1]*

[1] College of Geographic Science, Hunan Normal University, Changsha, China, [2] Rural Vitalization Research Institute, Changsha University, Changsha, China, [3] College of Resources & Environment, Hunan Agricultural University, Changsha, China

Considering the eastern part of Hunan Province as the research area, 34 sampling sites were set up, 198 samples were collected from representative paddy soil, the distribution characteristics of antimony (Sb) were studied. The results showed that: (1) The content of Sb on the surface of paddy soil ranging from 0.07 to 11.00 mg/kg and the geometric mean was 1.56 mg/kg. (2) The distribution of contents of Sb in paddy soil in different areas was shown as Yueyang > Changsha > Zhuzhou > Xiangtan. (3) Sb showed a strong migration in paddy soil in the research area and its content increased initially and then decreased or gradually decreased with the increase of profile depth. (4) The content of Sb in the substratum was significantly affected by parent materials.

Keywords: eastern Hunan Province, paddy soil, antimony, distribution characteristics, parent material

OPEN ACCESS

Edited by:
Hongbiao Cui,
Anhui University of Science and Technology, China

Reviewed by:
Changfeng Ding,
Institute of Soil Science (CAS), China
Xuebo Zheng,
Tobacco Research Institute (CAAS), China

***Correspondence:**
DaJuan Wan
dajuanwan@163.com

Specialty section:
This article was submitted to Soil Processes, a section of the journal Frontiers in Environmental Science

Received: *01 February 2021*
Accepted: *17 March 2021*
Published: *20 April 2021*

Citation:
Wang C, Wan D, Cao X, Wang H, Chen J, Ouyang N, Zhang Y and Tan C (2021) Spatial Distribution Characteristic of Antimony in Typical Paddy Soil of Eastern Hunan Province, China. Front. Environ. Sci. 9:661148. doi: 10.3389/fenvs.2021.661148

INTRODUCTION

The heavy metal elements in soils have shown the characteristics of low degradability, intensive perniciousness, high crypticity, and complicated ecological effects, which brought adverse effects to ecological environment and human health. The Bulletin of National Soil Pollution Survey (Ministry of Ecology Environment of the People's Republic of China, 2014) reported that the soil sites exceeding the rate of farmland in China were as high as 19.4%, with mainly inorganic pollutants. Agricultural soils form the basis of all agricultural production activities. As a consequence, these research studies on the distribution characteristics of heavy metals and potential ecological hazards in agricultural soils are of great importance to ensure normal agricultural production activities. As a toxic and harmful heavy metal element, antimony (Sb) has been classified as a priority pollutant by the US Environmental Protection Agency (Callahan, 1980). It has been reported that a long-distance migration of Sb can be met by atmospheric circulation and river transport (Reimann et al., 2010). In addition, the content of Sb in the Arctic Circle has increased significantly in recent years (Krachler et al., 2005), which confirmed the possibility of transboundary pollution. The content of Sb in soil crept up gradually owing to the mining and mineral utilization in recent years, which threatened human health and the safety of the ecological system, and thus gradually drawing our attention.

Being the hometown of non-ferrous metals, there were many kinds of non-ferrous metals with large reserves in Hunan Province. Compared with the other heavy metals, Sb reserves were at the forefront of the world. As one of the advantage mineral resources in Hunan Province, it occupied an important position in China and the world (Tang and Tang, 2010). At present, there were 117 Sb ores in Hunan Province (Ding et al., 2013), among them, the tin mine in Lengshuijiang enjoyed the title of "*Antimony capital of the world*" because of its highest

Sb reserves in the world. However, its mining and utilization may not only lead to severe pollution to surrounding soil, but also increase the content of Sb in soils far away from mining areas by a long-distance migration. As a major Sb-producing province, the background value of Sb in soils in Hunan Province was 1.87 mg/kg, which was higher than the national average (Qi and Cao, 1991). In recent years, most research reports of Hunan Province about soil Sb focused on the mining areas (Wang et al., 2010; Li et al., 2017), while only a few reports on the content of Sb in soils far away from mining areas. According to the distribution of mineral resources in Hunan Province, the spatial distribution of Sb in an agricultural soil of eastern Hunan Province, which localized east to a line of Tongdao County-Huaihua City-Yuanling County-Yingfengqiao Town in Yiyang City-Chenglingji in Yueyang City, showed strong heterogeneity (Jia et al., 2013). According to the report by Xiang et al. (2011), paddy soil showed the highest content of Sb among the different land-use types. And the intake of Sb in rice accounted for one-third of the total intake of the human body (Wu et al., 2011). Considering that the area of paddy soil in eastern Hunan Province was the largest among the total area of paddy soil in Hunan Province (Yang, 1987) and rice was the main foodstuff product in Hunan Province, eastern Hunan Province was elected. So, the research on the distribution characteristics and migration of Sb in paddy soil of eastern Hunan Province is of great importance, it can offer basic information about the safe utilization of paddy soil and food security.

MATERIALS AND METHODS

General Situation of the Research Area

The research area is localized to eastern Hunan Province with longitude and latitude coordinates of 111°53′−114°15′E and 26°03′−29°51′N. This area is high in the southeast and low in the northwest, with various types of landforms. The climate in this research area belongs to a middle subtropical monsoon climate, which is hot and rainy in summer and warm and rainy in winter. In this research, the annual mean temperature is 18.2°C and the annual average precipitation is 1,510.15 mm. This research area includes Changsha City, Zhuzhou City, Xiangtan City, and Yueyang City, which is one of the most suitable areas for agricultural development.

Sample Collection

All sampling sites were determined by using an integrated geographical unit. The administrative map, the present land-use map, and the soil map of Hunan Province were overlapped, and the results were corrected by the second general survey of Hunan Province. Firstly, the most representative parent materials in the area were found, and then sampling was carried out in the place where the paddy field was most concentrated. These sampling sites were determined by using a simple random distribution method as shown in **Figure 1**, and 34 sampling sites were set up and 198 samples were collected. The sampling procedure followed the requirement of "*Field soil description and sampling manual.*" The depth of a profile was 140 cm with stratified sampling. Each soil sample was composed of at least five sites by using an S-shaped sampling method. About 1 kg of soil sample was prepared by a quarter method and then labeled with serial numbers and global positioning system (GPS) coordinates.

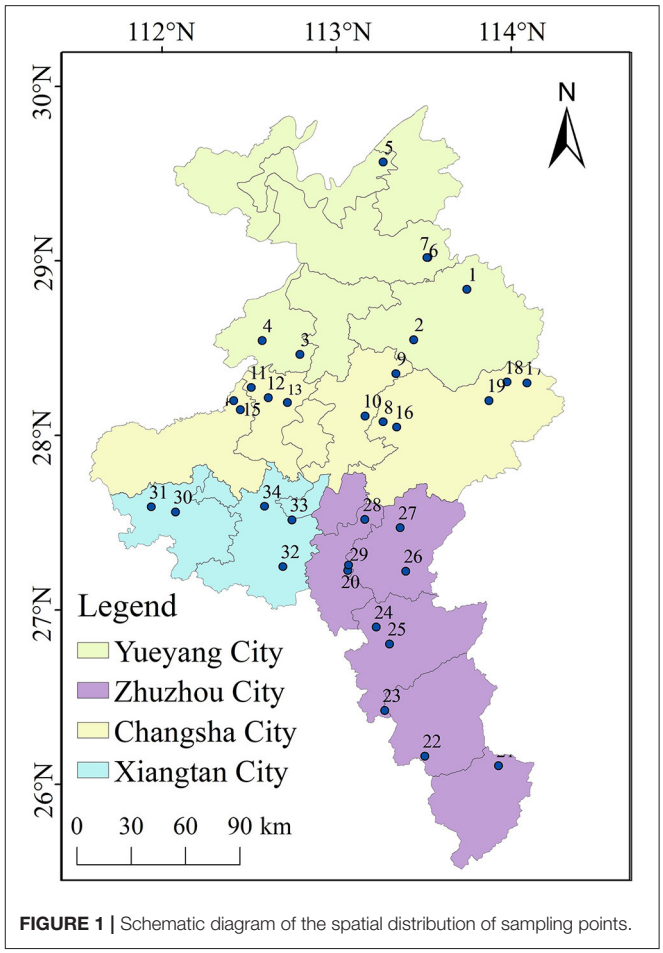

FIGURE 1 | Schematic diagram of the spatial distribution of sampling points.

Sample Treatment and Determination

After removing plant roots and gravel, soil samples were dried in the lab and then grounded for further analysis (10, 60, and 100 mesh). The total content of Sb was determined by "*Solid and sediment—Determination of aqua regia extracts of 12 metal elements—Inductively coupled plasma mass spectrometry*" (HJ 803-2016). The quality of samples passed the standards for the National reference material soil sample, GBW07404 (GSS-4), GBW07405 (GSS-5), and GBW07407 (GSS-7). The determination of physiochemical properties of soils followed "*The analysis method of soil agricultural chemistry*" (Lu, 2000).

Research Method

Water washing coefficient (WWC) (Nan and Li, 2000) is used to present a vertical migration of heavy metal, as described in Formula (1):

$$WWC_{ij} = \frac{M_{(i-1)j}}{M_{ij}} \quad (1)$$

TABLE 1 | Concentrations of antimony (Sb) on the surface layer of paddy soil.

Max	Min	Arithmetic mean	Geometric mean	CV	Coefficient of skewness	Coefficient of kurtosis	pH	K-S test
mg.kg^{-1}								
11.00	0.07	3.10	1.56	1.13	1.294	0.109	4.70–8.10	logarithmic normal distribution

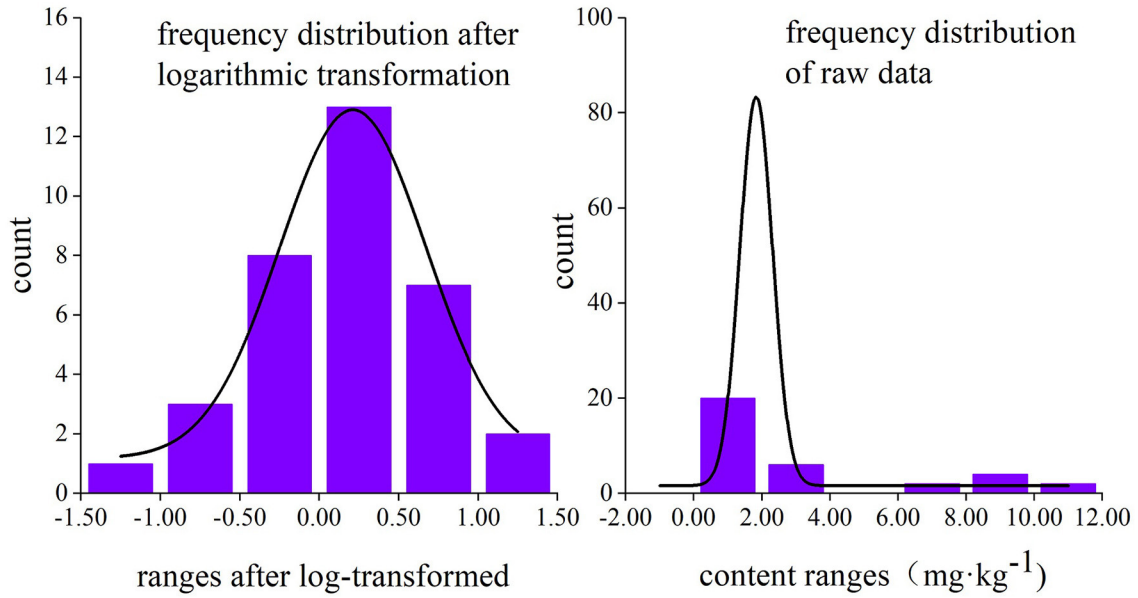

FIGURE 2 | Frequency distribution of antimony (Sb) on the surface layer of paddy soil.

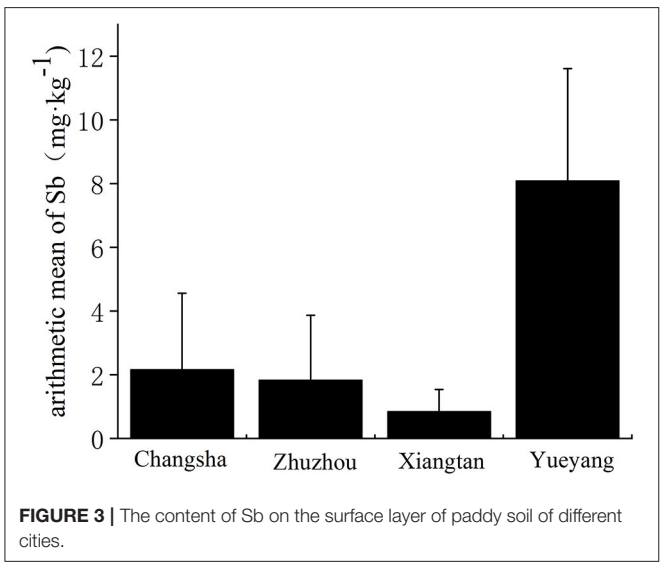

FIGURE 3 | The content of Sb on the surface layer of paddy soil of different cities.

Formula (1): $M_{(i\text{-}1)j}$ is the mean content of heavy metal j in layer $(i-1)$, M_{ij} is the mean content of heavy metal j in layer i. A higher WWC ratio means a stronger vertical migration of heavy metal.

RESULTS AND ANALYSIS

The Horizontal Distribution Characteristics of Sb

The statistics summary of the content of Sb in the topsoil of paddy soil in eastern Hunan Province was analyzed by using SPSS22 and listed in **Table 1**. An approximate logarithmic normal distribution was observed for the data of the surface layer, and the frequency distribution was shown in **Figure 2**. The coefficient of variation was 1.13, this high value shall be caused by multiple sampling sites with high contents of Sb. If the mean content of Sb is presented as arithmetic mean, the content of Sb of paddy soil in the research area will be artificially increased. Since the content of Sb followed a normal distribution after a logarithmic transformation, it would be more reasonable to use the geometric mean value to express the average content of Sb on the surface of paddy soil (Chen et al., 1991). From **Table 1**, it was observed that the content of Sb of the surface of paddy soil in eastern Hunan Province fell in a region of 0.07–11.00 mg/kg, and the geometric mean was 1.56 mg/kg, which was close to the background value of the content of Sb in soils in Hunan Province (1.87 mg/kg). This result suggested that the mean content of Sb on the surface of paddy soil in eastern Hunan Province stayed in a clean condition, and the impact of human activities was small. The pH value fell in a region of

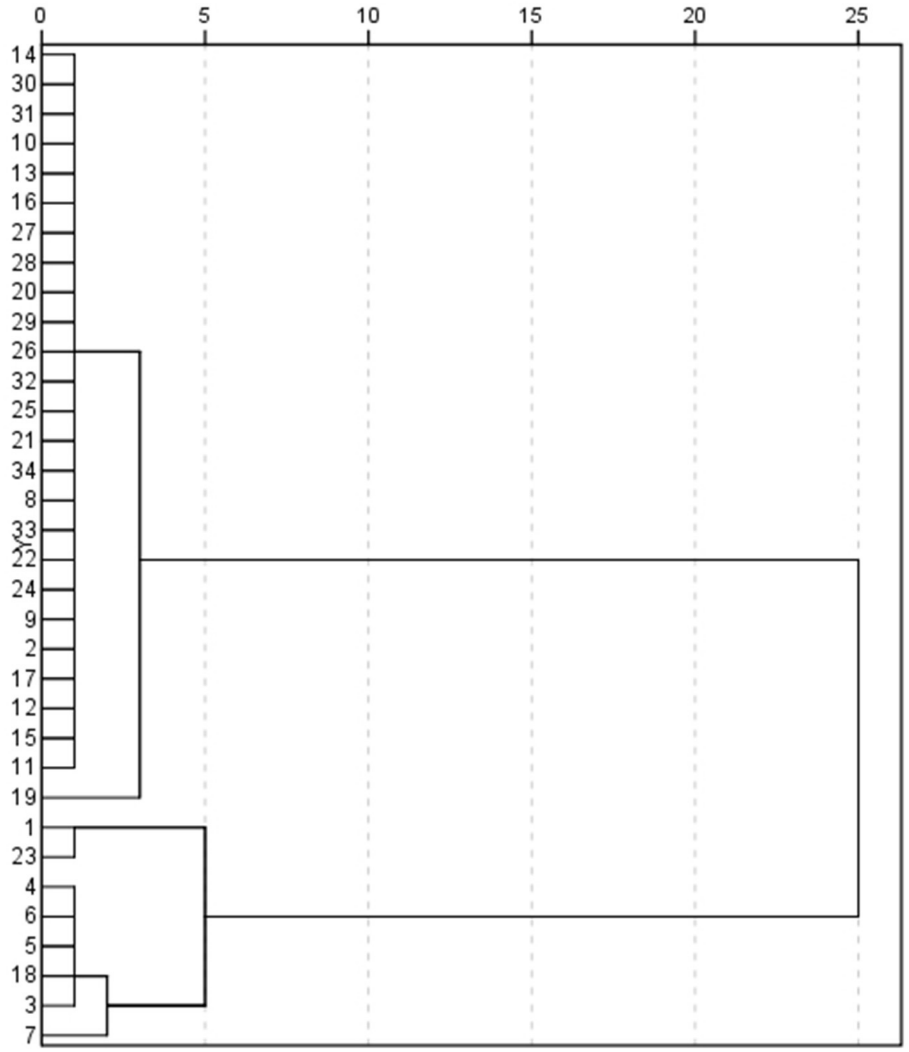

FIGURE 4 | Clustering tree of the sampling point.

4.70–8.10 with a mean value of 5.67, the soil environment was slightly acidic.

The content of Sb in different cities were showed in **Figure 3**. The contents of Sb on the surface of paddy soil in Changsha City, Zhuzhou City, Xiangtan City, and Yueyang City were 0.67–9.32, 0.07–6.93, 0.14–1.60, 0.91–11.00 mg/kg, respectively. The contents of Sb in some sampling sites were higher than the background value of the content of Sb in soils in China (0.38–2.98 mg/kg) (Qi and Cao, 1991). The distribution of the contents of Sb followed an order of Yueyang City > Changsha City > Zhuzhou Sity > Xiangtan City. The highest value was found in the southeast of Xiangyin County in Yueyang City, and the lowest value was found in the middle and western of You County in Zhuzhou City, the difference of the content of Sb between them was 10.93 mg/kg. According to the Nielsen grading standard, the content of Sb on the surface of paddy soil in the research area was classified as a medium to strong variation. In Zhuzhou City, the variation coefficient of the content of Sb on the surface of paddy soil showed the highest value of 1.12. Such a high coefficient of variation indicated that some sample sites have shown higher contents of Sb on the surface of paddy soil in this area, which shall have a high possibility of correlation with human activities, this observation is consistent with the feature that Zhuzhou City is the biggest industrial city in Hunan Province. The variation coefficient of the content of Sb on the surface of paddy soil in Yueyang City showed the lowest value of 0.44. However, the average content of Sb was much higher than the background value in Hunan Province, indicating a high cumulativeness of the content of Sb on the surface of paddy soil in this area. This result shall be attributed to the terrain reason of "low in north and high in south" in eastern Hunan Province, which made a long-distance migration of Sb easy to deposit. To find out if there was a significant difference between the content of Sb of various areas, the contents of Sb of the surface layer of paddy soil in different

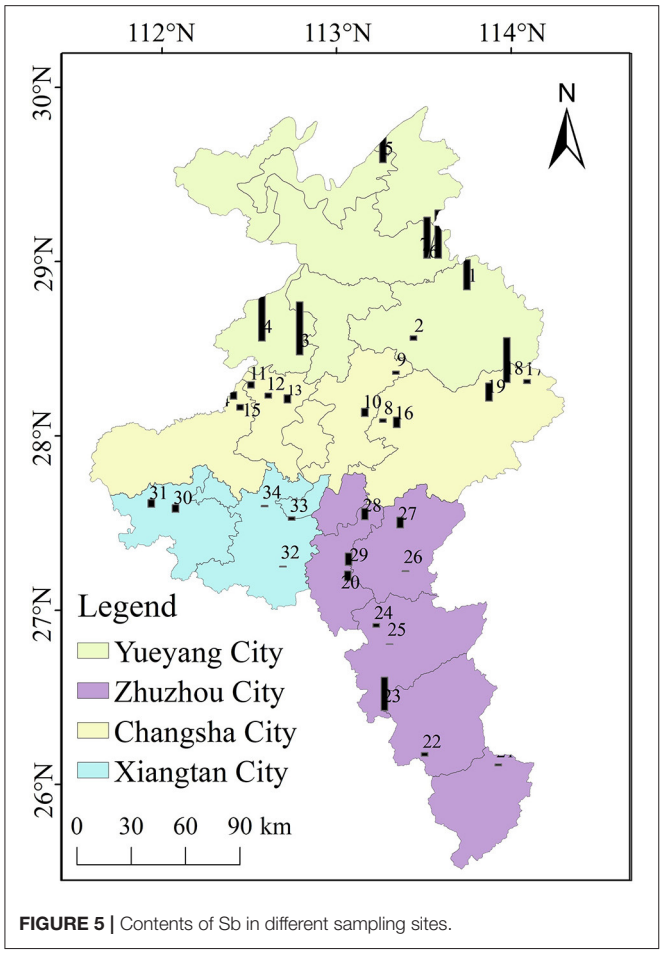

FIGURE 5 | Contents of Sb in different sampling sites.

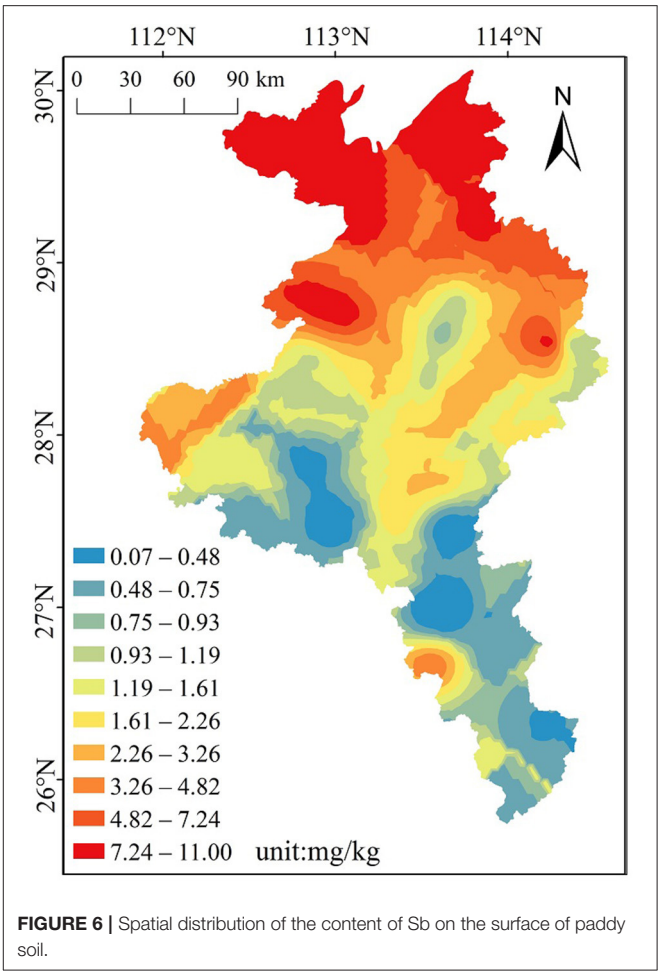

FIGURE 6 | Spatial distribution of the content of Sb on the surface of paddy soil.

areas were analyzed by using the ANOVA method. According to the inspection results, there was no significant difference between the contents of Sb on the surface of paddy soil in Changsha City, Zhuzhou City, and Xiangtan City, but the content of Sb on the surface of paddy soil in Yueyang City was obviously higher than those in other areas ($p < 0.05$).

After classifying all sampling sites from different areas with a hierarchical cluster method, those with high correlation shall be classified together and their content of Sb had similar characteristics. A clustering method was the link between the different groups, the hierarchical clustering result was shown in **Figure 4**. All sampling sites have been classified into three groups with an interclass distance of five. The first group included sampling sites of 2, 8–10, 13–14, 16, 20–22, 25–34, which were mainly localized in the middle and south of the research area. Their contents of Sb were nearly the same as the background value of Sb in Hunan Province. The second group included sampling sites of 1, 23, and the third group included sampling sites of 3–7, 18, which were mainly localized in the north of the research area. The average content of Sb in the second and third sampling points was 6.59 and 9.80 mg/kg, respectively. Their contents of Sb were higher than the background value of Sb in Hunan Province. This result suggested that the content of Sb in the north of the research area was relatively high, showing a decreasing tendency from north to south. The spatial distribution of the content of Sb in north Hunan Province was shown in **Figures 5**, **6**. In the south, sampling sites with a high content of Sb were located in Liling County and Zhuzhou City, which were related to the local industrial activities.

The difference in the content of Sb among various areas can be reflected by comparing the content of Sb in the soils. The background value of Sb in various areas is different owing to the influence from soil parent materials, soil-forming processes, human activities, etc. during the soil formation. If we only compare the content of Sb in different areas, we will artificially magnify the impacts of Sb on the environment in high background value areas and ignore the impacts of Sb on the environment in low background value areas. As a consequence, this work used a relative content (measured value: background value) to compare the content of Sb in soils in various areas. It was observed from **Table 2** that the contents of Sb in soils in different landforms and different areas were different. The relative contents of Sb in mine soils and agricultural soils around the mining areas were much higher than those of other areas, showing a high accumulation of Sb. As for those soils far away from the mining areas, the relative content of Sb of paddy soil in Yueyang City showed the highest value of 4.33, which was

TABLE 2 | Comparison of Sb in topsoil from different regions.

Region		Max	Min	Mean	Background	Relative content (measured value/background value)	References
mg·kg^{-1}							
Measured in	Changsha	6.40	0.61	2.16	1.87	1.16	–
this study	Zhuzhou	8.19	0.05	1.83	1.87	0.98	–
	Xiangtan	1.86	0.67	0.85	1.87	0.45	–
	Yueyang	11.19	0.91	8.09	1.87	4.33	–
Honghe Farm, Sanjiang Plain		–	–	2.89	0.91	3.17	Liu et al., 2019
Farmland in downstream region of Yuxi River		34.4	41.03	12.26	1.87	6.56	Fei et al., 2017
Xikuangshan in Hunan Province		5,045	100	695	1.87	371.66	He, 2007
Guizhou dushan county antimony smelter		98.52	5.02	26.65	2.24	11.90	Xiong et al., 2020
Dalian		1.79	0.24	1.01	0.84	1.20	MEMSC, 1990
Wenzhou		2.82	0.46	0.74	1.53	0.48	
Ningbo		1.48	0.61	0.92	1.53	0.60	
Xiamen		0.81	0.22	0.45	0.65	0.69	
Shenzhen		2.72	0.21	0.76	0.54	1.41	

similar to the relative content of Sb of agricultural soil in Honghe Farm of Sanjiang Plain. The relative content of Sb of paddy soil in Xiangtan City showed the lowest value of 0.45. According to the comparison of the relative content of Sb between different areas, it was found that the accumulation of Sb in paddy soil in Yueyang City was relatively high, while that of Changsha City, Zhuzhou City, and Xiangtan City was relatively low.

The Vertical Distribution Characteristics of Sb

After a long cultivating history, the distribution characteristics of content of Sb have changed in profiles, rendering a comprehensive influence of multiple factors. The distribution characteristics of Sb under the influence of multiple factors cannot be clearly explained by simply analyzing the content of Sb on the surface of paddy soil. The analysis of the vertical distribution of Sb in a profile was helpful to have a precise understanding of the distribution characteristics and migration of Sb. In conclusion, the content of Sb in the research area showed a complicated correlation with the increase of soil depth, its content mainly increased firstly and then decreased or gradually decreased. The detailed distribution characteristics in a profile were shown in **Figure 7**.

It was observed from **Figure 7** that, as for the first type of profile, the content of Sb firstly increased and then decreased. It showed that the migration of Sb in the plow layer and the accumulation of Sb in the plow pan were greatly affected by external sources. More specifically, the content of Sb varied in a wide range of 0–40 cm, which firstly increased and then decreased, and the maximum value was observed at 20 cm. The content of Sb below 40 cm varied in a narrow range and showed a decreasing tendency. The maximum content of Sb in this profile was obviously higher than that in other profiles. This tendency was mainly observed from the sampling sites in Liling County of Zhuzhou City and Yueyang City. Yueyang City is rich in mineral resources, and Liling County is rich in coal resources. As a common trace element in metal sulfide ore and coal (Qi et al., 2008), Sb can be released into soil *via* various paths, including mining, smelting, transportation, and utilization, and then it finally accumulated in the plow pan by leaching migration during tillage.

As for the second type of profile, the content of Sb gradually decreased, indicating a decreased migration with an increase of this profile. This result was consistent with the report by Cai et al. (2020) on the vertical migration characteristics of Sb in farmland soil contaminated by dam break of Huashan tailings pond in Anhui Province. In agricultural activities, the use of pesticides and chemical fertilizers increased the content of organic matter in the surface soil, which enhanced the adsorption of organic matter for Sb, leading to a decreased vertical migration in this profile. As for the first situation, the content of Sb decreased smoothly, and as for the second situation, the content of Sb decreased dramatically in 15–35 cm and then smoothly decreased below 35 cm. There was a common feature for the second situation, which was the high content of Sb in the top of soils.

As for the third type of profile, the content of Sb firstly decreased and then increased. The lowest contents of Sb of some profiles were observed at 30 cm, while those of other profiles were observed at 70 cm. The content of Sb of sampling site number two varied in a wide range, showing an obvious decreasing tendency in the surface soil and an obvious increasing tendency in the deep soil. The content of Sb of other sampling sites fell in a narrow region. The different varying tendencies were related with the parent materials and physiochemical properties of soils. If the soil clay content was low in the middle soil and high in the deep soil, a decreasing tendency would be firstly observed and then followed by an increasing tendency (Shi et al., 2016). Under the influence of parent materials, their content may increase gradually with the depth of a profile (Yang et al., 2020).

As for the fourth type of profile, the content of Sb showed a fluctuational tendency with increasing depth. It is assumed that paddy soil is water saturated in the plowing season but

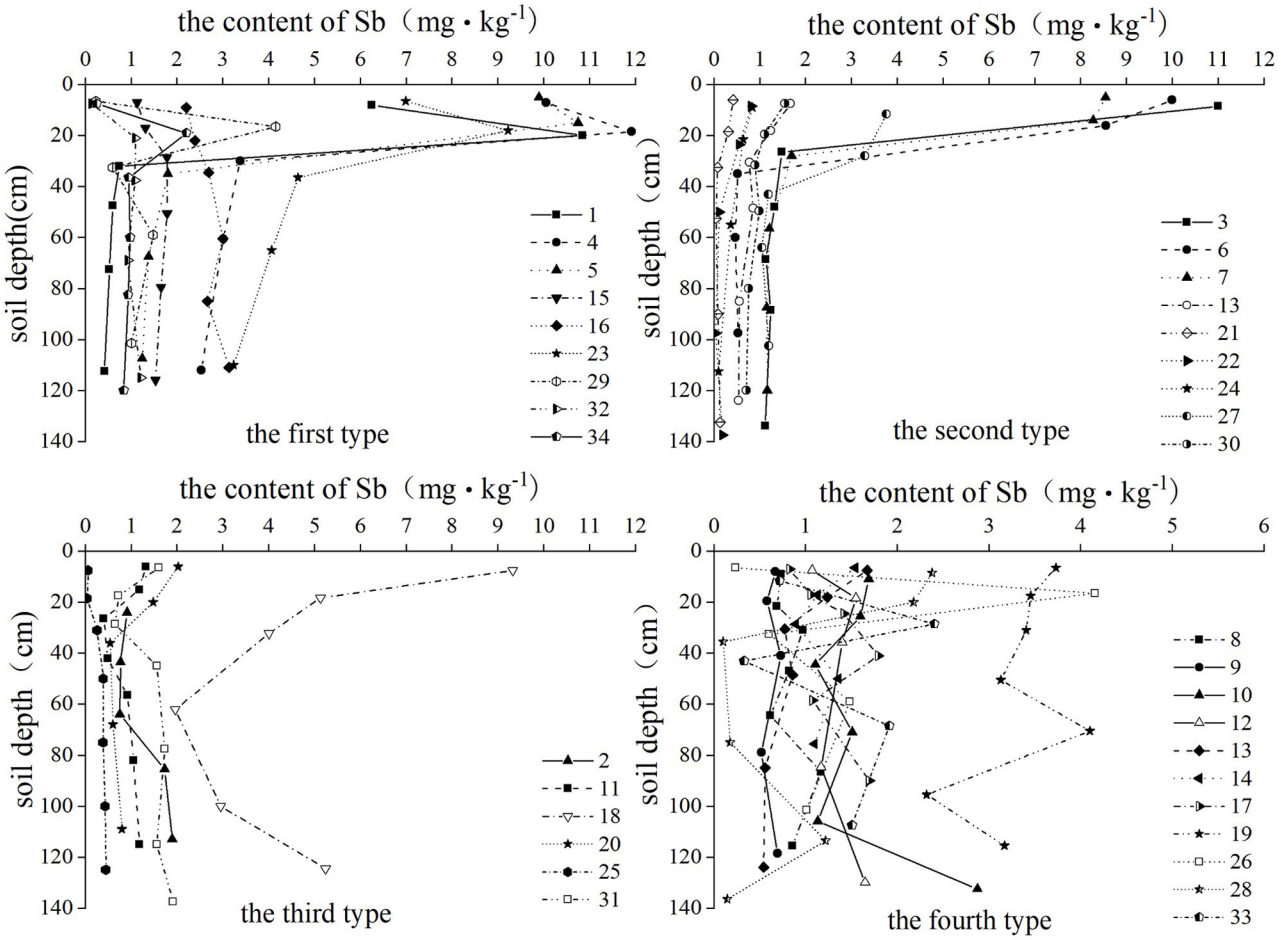

FIGURE 7 | The profile distribution characteristics of Sb in paddy soil.

water deficient in the non-plowing season, which leads to a periodic oxidation–reduction reaction of paddy soil. As a consequence, a vertical migration of Sb occurred in profiles in the research area. The difference of contents of Sb of all profiles with the same depth varied in a wide range. The biggest difference of 4.00 mg/kg showed at 70 cm, while the smallest difference of 0.09 mg/kg showed at 5 cm. Although there was no obvious correlation between the contents of Sb of different profiles with increasing depth, a similarity was observed as the fact that the sampling sites with a high content of Sb in the surface soil had a high content of Sb in the bottom soil.

For a clear understanding of leaching migration characteristics in the vertical profile of Sb, WWC was used. The formula introduced in the research method was used for calculation. The WWC values of Sb in the plow layer and plow pan were calculated as 1.08 and 0.32, respectively, indicating a stronger migration of Sb in the plow layer than in the plow pan. Although the WWC value of the plow pan was relatively low, the downward migration of Sb in paddy soil of the research area was relatively high in the whole profiles. This result was consistent with the migration characteristics of soil Sb near Xikuangshan mining areas (Yang et al., 2015). Such Sb migration characteristics were related to the acidic soil in the research area. The low WWC value of the plow pan was due to the higher content of Sb in the plow pan, which decreased the relative downward leaching loss.

Characteristics of the Content of Sb in Different Soil Parent Materials

The heavy metals in soil parent materials are the original sources of soil heavy metals. Different soil parent materials have different heavy metal contents, which are responsible for the initial difference in heavy metal contents between different areas (de Souza et al., 2015). By analyzing the difference of contents of Sb between the paddy soils originated from various soil parent materials, it is helpful to understand the reasons for a relatively high heavy metal content in the research area. The content characteristics of Sb in paddy soils developed on various soil parent materials were listed in **Table 3**.

TABLE 3 | The content of Sb in paddy soil formed by different parent soils.

Parent materials (numbers of sampling sites)		Granite weathering ($n = 9$)	Plate shale weathering ($n = 7$)	Quaternary red clay ($n = 9$)	Fluvial sediment ($n = 3$)	Purple sandy shale weathering ($n = 5$)	The combination of purple sand weathering and Quaternary red clay ($n = 1$)
mg·kg^{-1}							
Plow layer	Range	0.42–9.99	0.14–9.90	0.07–11.00	0.72–10.05	0.23–3.73	0.82
($n = 34$)	Mean	2.73	4.49	3.31	3.95	1.40	–
Plow pan	Range	0.32–10.86	0.73–10.75	0.05–8.27	1.55–11.92	0.69–4.16	0.56
($n = 34$)	Mean	2.94	5.25	2.52	5.29	2.40	–
Substratum	Range	0.09–1.87	1.08–3.77	0.40–2.96	1.30–2.83	0.67–3.12	0.10
($n = 34$)	Mean	0.62	2.10	1.32	1.85	1.33	–

It was observed from **Table 3** that the highest content of Sb was observed from the plow pan of paddy soil originated from a fluviolacustrine sedimentary deposit, while the lowest content of Sb was observed from the substratum of paddy soil originated from the combination of purple sand weathering and quaternary red clay. The contents of Sb s of paddy soil in the plow layer originated from various parent materials followed an order from high to low of plate shale weathering > fluviolacustrine sedimentary deposit > quaternary red clay > granite weathering > purple sand shale weathering > the combination of purple sand weathering and quaternary red earth. The content of Sb of paddy soil originated from quaternary red earth varied in the widest region, while that from purple sand shale weathering varied in the narrowest region. The contents of Sb of paddy soil in the plow pan originated from various parent materials followed an order from high to low of fluviolacustrine sedimentary deposit > plate shale weathering > granite weathering > quaternary red clay > purple sand shale weathering > the combination of purple sand weathering and quaternary red earth. The content of Sb of paddy soil originated from granite weathering varied in the widest region, while that from purple sand shale weathering varied in the narrowest region. The contents of Sb of paddy soil in the substratum originated from various parent materials followed an order from high to low of plate shale weathering > fluviolacustrine sedimentary deposit > purple sand shale weathering > quaternary red clay > granite weathering. The content of Sb of paddy soil originated from plate shale weathering varied in the widest region, while that from a fluviolacustrine sedimentary deposit varied in the narrowest region.

It has been reported (Wu, 2014) that the heavy metal contents of surface soil were affected by both soil parent materials and human activities, representing the second environment of soil. While the deep soil suffered from minor human activities, representing the features of soil primary layers, so the heavy metal contents were mainly controlled by soil parent materials. The variation coefficients of paddy soils originated from different parent materials in the plow layer, plow pan, and substratum were determined as 0.41, 0.58, and 0.61, respectively. The highest variation coefficients of the substratum suggested that the content of Sb in this layer was most affected by parent materials. For a further understanding of the effect of parent materials on the content of Sb in different soil layers, ANOVA was performed by using the soil parent material as the only factor. No significant difference was observed for the content of Sb of paddy soil in the plow layer and plow pan between the different soil parent materials. This result suggested that the soil parent materials had no obvious effects ($p > 0.05$) on the content of Sb on the surface of paddy soil. A high content of Sb in a sampling site was caused by human factors, geographical positions, climate conditions, and biological effects. There were significant differences between the content of Sb of paddy soil in the substratum originated from granite weathering and those from other soil parent materials ($p < 0.05$), which meant that soil parent materials had an obvious effect on the content of Sb of paddy soil in the substratum.

CONCLUSIONS

(1) The content of Sb on the surface of paddy soil fell in a region of 0.07–11.00 mg/kg with a geometric mean of 1.56 mg/kg, indicating a clean condition with minor effects from human activities.
(2) The distribution of contents of Sb in paddy soil of various areas followed an order of Yueyang City > Changsha City > Zhuzhou City > Xiangtan City. The highest value was found in the southeast of Xiangyin County in Yueyang City, and the lowest value was found in the central and western of You County in Zhuzhou City.
(3) The content of Sb showed a strong migration with the increase of profile depth in the research area, and its content increased firstly and then decreased or gradually decreased.
(4) ANOVA was performed on the content of Sb of paddy soil in different soil layers by using soil parent materials as a factor. It was found that soil parent materials had obvious effects on the content of Sb of the substratum, but minor effects on the content of Sb of the plow layer and plow pan.

DATA AVAILABILITY STATEMENT

The raw data supporting the conclusions of this article will be made available by the authors, without undue reservation.

AUTHOR CONTRIBUTIONS

CW, HW, JC, and NO carried out the determination of the content of Sb and the physical and chemical properties. CW, DW, XC, YZ, and CT participated in discussing the results. CW prepared the draft of the manuscript. DW and CW revised the manuscript. All authors contributed to the article and approved the submitted version.

FUNDING

This research was supported by Hunan Innovative Province Construction Special Fund (2020NK2001) and the Natural Science Foundation of Changsha (kq2007082).

REFERENCES

Cai, Y., Shao, L., Fan, X., Li, Y., Meng, F., and Zhang, H. (2020). Release and vertical migration characteristics of As and Sb in farmland soil polluted by dam break of Huashan tailing reservoir in Anhui province environmental chemistry. *Environ. Chem.* 39, 2479–2489. doi: 10.7524/j.issn.0254-6108.2020041303

Callahan, M. A. (1980). *Water-Related Environmental Fate of 129 Priority Pollutants*. Office of Water Planning and Standards, Office of Water and Waste Management, US Environmental Protection Agency.

Chen, J., Wei, F., Zheng, C., Wu, Y., and Adriano, D. C. (1991). Background concentrations of elements in soils of China. *Water Air Soil Pollut*. 57, 699–712. doi: 10.1007/BF00282934

de Souza, J., Abrahão, W., de Mello, J., da Silva, J., da Costa, M., and de Oliveira, T. (2015). Geochemistry and spatial variability of metal (loid) concentrations in soils of the state of Minas Gerais, Brazil. *Sci. Tot. Environ.* 505, 338–349. doi: 10.1016/j.scitotenv.2014.09.098

Ding, J., Yang, Y., and Deng, F. (2013). Resource potential and metallogenic prediction of antimony ore in China. *Geol. China* 40, 846–858.

Fei, J., Min, X., Wang, Z., Pang, Z., Liang, Y., and Ke, Y. (2017). Health and ecological risk assessment of heavy metals pollution in an antimony mining region: a case study from South China. *Environ. Sci. Pollut. Res*. 24, 27573–27586. doi: 10.1007/s11356-017-0310-x

He, M. (2007). Distribution and phytoavailability of antimony at an antimony mining and smelting area, Hunan, China. *Environ. Geochem. Health* 29, 209–219. doi: 10.1007/s10653-006-9066-9

Jia, B., Huang, G., and Sun, H. (2013). *Report on the Evaluation Results of Mineral Resources Potential in Hunan Province*. Changsha: Hunan Provincial Geological Survey Institute.

Krachler, M., Zheng, J., Koerner, R., Zdanowicz, C., Fisher, D., and Shotyk, W. (2005). Increasing atmospheric antimony contamination in the northern hemisphere:Snow and ice evidence from Devon Island, Arctic Canada. *J. Environ. Monit*. 7, 1169–1176. doi: 10.1039/b509373b

Li, X., Yang, H., Zhang, C., Zeng, G., Liu, Y., Xu, W., et al. (2017). Spatial distribution and transport characteristics of heavy metals around an antimony mine area in central China. *Chemosphere* 170, 17–24. doi: 10.1016/j.chemosphere.2016.12.011

Liu, Z., Wang, G., Fang, Y., Jiang, M., Liu, C., Yao, X., et al. (2019). Contents of 55 elements in natural swamp, returning farmland to wetlands and farmland surface soil of Honghe farm in Sanjiang plain wetland. *Science* 17, 713–717. doi: 10.13248/j.cnki.wetlandsci.2019.06.015

Lu, R. (2000). *Methods for Agricultural Chemical Analysis of Soil*. Beijing: China Agricultural Science and Technology press.

MEMSC (1990). *The Background Values of Soil Elements in China*. Beijing: Meterological Press.

Ministry of Ecology and Environment of the People's Republic of China (2014). *Ministry of Natural Resources of the People's Republic of China*. *Bulletin of the National Survey on Soil Pollution*. Beijing.

Nan, Z., and Li, J. (2000). Profile distribution and behavior of heavy metals cadmium, lead and nickel in cultivated soil in arid area—taking calcareous soil in Baiyin city as an example. *Arid Zone Res*. 17, 39–45.

Qi, C., Liu, G., Chou, C. L., and Zheng, L. (2008). Environmental geochemistry of antimony in Chinese coals. *Sci. Tot. Environ*. 389, 225–234. doi: 10.1016/j.scitotenv.2007.09.007

Qi, W., and Cao, J. (1991). Study on soil environmental background value of antimony. *Chin. J. Soil Sci*. 22, 209–210.

Reimann, C., Matschullat, J., Birke, M., and Salminen, R. (2010). Antimony in the environment: lessons from geochemical mapping. *Appl. Geochem*. 25, 175–198. doi: 10.1016/j.apgeochem.2009.11.011

Shi, Y., Yue, R., and Zhang, H. (2016). Study on vertical stratification of heavy metals in soil around nonferrous metals mining and smelting base. *Chin. J. Soil Sci*. 47, 186–191. doi: 10.19336/j.cnki.trtb.2016.01.029

Tang, W., and Tang, X. (2010). Select the strategic reserve variety of superiority mineral resources in Hunan. *Non Ferrous Mining Metallurgy* 26, 57–59.

Wang, X., He, M., Xie, J., Xi, J., and Lu, X. (2010). Heavy metal pollution of the world largest antimony mine-affected agricultural soils in Hunan province (China). *J. Soils Sediments* 10, 827–837. doi: 10.1007/s11368-010-0196-4

Wu, F., Fu, Z., Liu, B. J., Mo, C., Chen, B., Corns, W., et al. (2011). Health risk associated with dietary co-exposure to high levels of antimony and arsenic in the world's largest antimony mine area. *Sci. Tot. Environ.* 409:3344. doi: 10.1016/j.scitotenv.2011.05.033

Wu, H. (2014). *Distribution Characteristics of Heavy Metal Elements and Influence of Parent Materials in Soils of Hainan Province*. Beijing: China University of Geosciences.

Xiang, M., Zhang, G., Li, L., Wei, X., and Cai, Y. (2011). Distribution of heavy metal pollution in surface soil of lead-antimony smelting area in Guangxi. *Acta Mineral. Sin*. 31, 250–255. doi: 10.16461/j.cnki.1000-4734.2011.02.004

Xiong, J., Han, Z., Wu, P., Zeng, Y., Luo, G., and Yang, W. (2020). Spatial distribution, pollution assessment and health risk assessment of antimony and arsenic in soils around Dushan antimony smelter. *Acta Sci. Circumstantiae* 40, 655–664. doi: 10.13671/j.hjkxxb.2019.0387

Yang, F. (1987). *Hunan Soil[M]*. Beijing: China Agriculture Press.

Yang, H., He, M., and Wang, X. (2015). Concentration and speciation of antimony and arsenic in soil profiles around the world's largest antimony metallurgical area in China. *Environ. Geochem. Health* 37, 21–33. doi: 10.1007/s10653-014-9627-2

Yang, S., Jin, G., Fang, Q., Liao, S., Luo, W., Jia, J., et al. (2020). Review on analysis of soil heavy metal pollution sources in China in recent ten years (2009-2018). *Jiangsu Agric. Sci*. 48, 17–24. doi: 10.15889/j.issn.1002-1302.2020.20.003

Conflict of Interest: The authors declare that the research was conducted in the absence of any commercial or financial relationships that could be construed as a potential conflict of interest.

frontiers in Environmental Science

ORIGINAL RESEARCH
published: 28 April 2021
doi: 10.3389/fenvs.2021.630668

Spatial Variation in Microbial Community in Response to As and Pb Contamination in Paddy Soils Near a Pb-Zn Mining Site

Lina Zou[1], Yanhong Lu[2], Yuxia Dai[1], Muhammad Imran Khan[3], Williamson Gustave[4], Jun Nie[2], Yulin Liao[2], Xianjin Tang[1]*, Jiyan Shi[1] and Jianming Xu[1]*

[1]Institute of Soil and Water Resources and Environmental Science, College of Environmental and Resource Sciences, Zhejiang Provincial Key Laboratory of Agricultural Resources and Environment, Zhejiang University, Hangzhou, China, [2]Soil and Fertilizer Institute of Hunan Province, Hunan Academy of Agricultural Sciences, Changsha, China, [3]Institute of Soil and Environmental Sciences, University of Agriculture, Faisalabad, Pakistan, [4]School of Chemistry, Environmental and Life Sciences, University of The Bahamas, Nassau, The Bahamas

OPEN ACCESS

Edited by:
Jian Chen,
Florida International University, United States

Reviewed by:
Xiaomin Li,
South China Normal University, China
Baogang Zhang,
China University of Geosciences, China

***Correspondence:**
Jun Nie
niejun197@163.com
Xianjin Tang
xianjin@zju.edu.cn

Specialty section:
This article was submitted to Toxicology, Pollution and the Environment, a section of the journal Frontiers in Environmental Science

Received: *18 November 2020*
Accepted: *15 April 2021*
Published: *28 April 2021*

Citation:
Zou L, Lu Y, Dai Y, Khan MI, Gustave W, Nie J, Liao Y, Tang X, Shi J and Xu J (2021) Spatial Variation in Microbial Community in Response to As and Pb Contamination in Paddy Soils Near a Pb-Zn Mining Site. Front. Environ. Sci. 9:630668. doi: 10.3389/fenvs.2021.630668

Mining activity is a growing environmental concern as it contributes to heavy metals (HMs) pollution in agricultural soils. Microbial communities play an important role in the biogeochemical cycling of HMs and have the potential to be used as bioindicators. Arsenic (As) and lead (Pb) are the most hazardous HMs and are mainly originated from mining activities. However, spatial variation in microbial community in response to As and Pb contamination in paddy soils remains overlooked. In this study, the biological and chemical properties of sixteen soil samples from four sites (N01, N02, N03, and N04) near a Pb-Zn mining site at different As and Pb levels were examined. The results showed that soil pH, total As and Pb, bioavailable As and Pb, nitrate-nitrogen (NO_3^--N) and ammonia-nitrogen (NH_4^+-N) were the most important factors in shaping the bacterial community structure. In addition, significant correlations between various bacterial genera and As and Pb concentrations were observed, indicating their potential roles in As and Pb biogeochemical cycling. These findings provide insights into the variation of paddy soil bacterial community in soils co-contaminated with different levels of As and Pb.

Keywords: Pb-Zn mining site, arsenic, lead, microbial community, paddy soil

INTRODUCTION

Mining mineral ore has both significant positive and negative impacts on mining areas. Mining resources have been endorsed as a mean to stimulate socioeconomic development and reduce poverty (Li et al., 2014). However, mining activities generate waste, such as mine tailings, acid mine drainages and fly ashes that contain harmful trace heavy metals (HMs) (Chen et al., 2018; Liu et al., 2019). HMs can be transported from mining sites to neighboring agricultural soils through surface runoff and atmospheric dust deposition (Mu et al., 2020). Consequently, most neighboring agricultural soils are contaminated with HMs, and the soil thereafter serves as a long-term sink for HMs (Hahn et al., 2019; Cheng et al., 2020).

In China, mining activities are prevalent and this has led to serious soil HMs contamination nationwide (Zhong et al., 2020). According to the Chinese National Soil Contamination Survey Report, approximately 33.4% of soil around mining sites were contaminated with HMs

(Mee and Mnr, 2014). Among them, arsenic (As) and lead (Pd) commonly co-exist in high concentrations due to mining and smelting of mineral ores (Wang et al., 2020a; Fernandez-Macias et al., 2020), and threaten soil, plant and human health. In paddy soil, excess As and Pb can reduce soil quality, stunt plant growth, and ultimately affect human health through the food chain (Du et al., 2018; Rai et al., 2019). For example, Wang et al. (2018) reported that the concentrations of As and Pb (up to 2749 and 624 $\mu g\,kg^{-1}$, respectively) in rice grains grown in fields neighboring mining sites were significantly higher than the threshold value of 200 $\mu g\,kg^{-1}$ (GB2762–2017). Therefore, the investigation of the HMs pollution in paddy soils surrounding mining areas can assess the risk of HMs to human health and provide the scientific basis for the remediation of HMs contaminated soils.

HMs accumulation in soils affects both the soil physiochemical properties and the microbial community structure over short- and long-term periods (Zhu et al., 2019). Zhang et al. (2015) reported that HMs in paddy soil may have adverse effects on the microbial activities and nutrients bioavailability. Pb contaminations have been shown to inhibit soil respiration and reduce microbial biomass (Liu et al., 2017). Similarly, dynamic changes were observed in the soil microbial community as a result of As contamination (Wang et al., 2016). Furthermore, in the soil-rice system, As contamination can markedly influence the iron (Fe) plaque-associated microbial community structure and metabolic potential (Hu et al., 2019). Although many attempts were tried to remediate As and Pb pollution in soils neighboring mining sites, few have reported the combined effect of As and Pb contamination on the soil microbial community (Tian et al., 2020; She et al., 2021).

Molecular techniques such as high-throughput sequencing techniques have been used to evaluate the changes in microbial community due to HMs pollution (Ros et al., 2009; Gołębiewski et al., 2014). Changes in soil microbial community structure and diversity could serve as biomarkers to study the effect of HMs on soil health (Vinhal-Freitas et al., 2017; Li et al., 2020b; Di Cesare et al., 2020). However, it should be noted that some studies have reported that HMs contamination had limited effect on the microbial community structure (Lorenz et al., 2006). Other soil factors such as pH, organic matter (OM), moisture, clay content and nutrient content can have a profound influence on the microbial activities, which might play more important role in reshaping microbial communities than the HMs concentrations (Jiang et al., 2019). However, studies on the difference between microbial communities in paddy soils with different distances from the mining site and the responses of microorganisms to HMs and soil properties are limited. HMs polluted paddy soil with various distances from the mining site may present different soil characteristics and HMs concentration gradients, then the most important factor in shaping the microbial communities remains unknown.

For this purpose, this present study was conducted with soil samples from four sites along a Pb-Zn mining site to 1) explore the influence of the different distance from the mining site on the physiochemical properties of As and Pb polluted paddy soils; 2) evaluate the combined effects of As and Pb pollution on soil bacterial community structure; 3) examine the correlativity between soil physiochemical properties and bacterial communities. Chemical analysis coupled with Miseq sequencing techniques were applied to achieve the goals. The observations and findings in this study could be used to develop more effective bioremediation strategies for the polluted paddy soil in mining area.

MATERIALS AND METHODS

Study Area and Sampling

The study area is located near a Pb-Zn mining site (29°59′35.00″ N, 120°45′55.20″ E) in Shangyu city, Zhejiang province, China (**Figure 1**). The study area has a typical subtropical climate, densely surrounded by paddy field. A total of 16 top-soil samples (0–20 cm) were collected from the four sites referred to as N01, N02, N03, and N04. The four sites are all paddy fields and one growth cycle is performed over one year. Soil samples (four in total, approximately 300 g each) were collected from random points at each site and were mixed uniformly to form a composite sample. Four replicate composite samples were collected from each site (denoted as samples N01–1, N01–2, N01–3, N01–4, and so on). Soil samples were properly sealed and transported to the laboratory on ice. The collected soil samples were divided into two parts; one part was stored at −80°C for molecular analyses, and the other part was used for the physicochemical analysis.

Chemical Analysis

Soil samples from N01, N02, N03, and N04 site were analyzed for different physicochemical parameters including soil pH, OM, moisture content, dissolved organic carbon (DOC), available nitrate-nitrogen (NO_3^--N) and ammonia-nitrogen (NH_4^+-N) concentrations, total As, Pb and other HMs concentrations, total sulfur (S) and SO_4^{2-}. Soil pH and OM were measured following methods described in our pervious study (Zou et al., 2018). Moisture content was measured by drying fresh soil samples overnight in an oven at 105°C (O'Kelly, 2004). DOC was extracted with ultrapure water from fresh soil at a ratio of 1:2 (soil: water) and the concentration was analyzed with an automated N/C analyzer (Multi N/C 2100, Analytik Jena, Germany) (Xu et al., 2015). Available NH_4^+-N and NO_3^--N concentrations were determined in 1 M KCl extracts (1:5, w/v) using the colorimetric methods (Stock, 1983). Soil SO_4^{2-} was extracted by shaking freeze-dried soils with ultrapure water at a ratio 1:25 (soil:water) and analyzed by ion chromatography (Dionex, United States) (Xu et al., 2015). In order to determine the total Fe, S and other HMs, 0.2 g soil was digested using a concentrated acid mixture (5 ml of HNO_3, 3 ml of $HClO_4$, and 5 ml of HF) and was analyzed by inductively coupled plasma-optical emission spectrometry (ICP-OES, iCAP 6300, Thermo, United States). For total As analysis, 0.2 g air-dried soil was digested with 10 ml diluted aqua regia (aqua regia: water = 1:1, v/v) at 100°C for 2 h, and As concentration in digested samples were determined by atomic fluorescence spectrometry (AFS-9130, Beijing Jitian Instrument Company, China) (Zou et al., 2018). In order to determine the

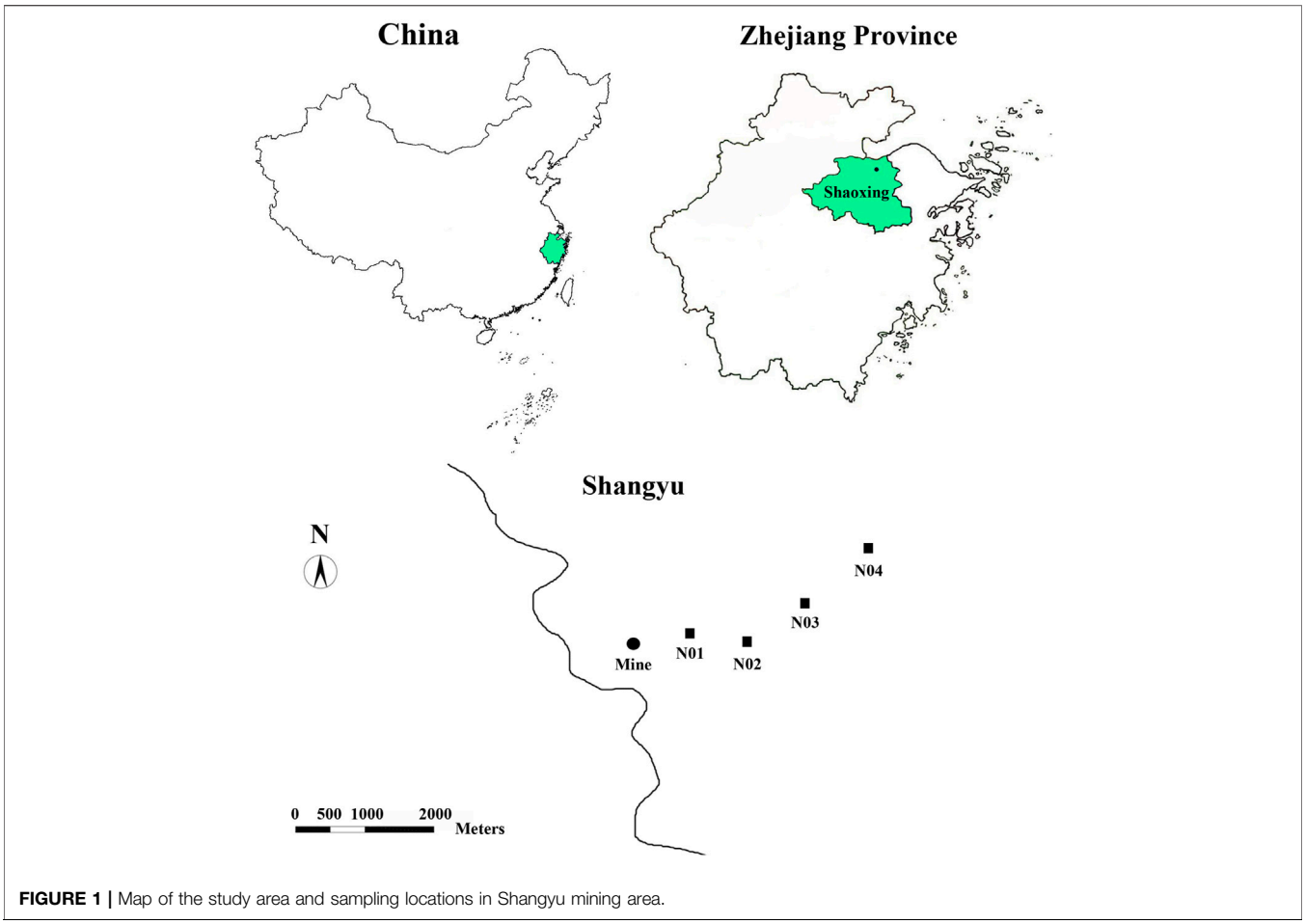

FIGURE 1 | Map of the study area and sampling locations in Shangyu mining area.

accuracy of the total metal analysis, a reference soil (GBW 07429, the National Research Center for standards in China) was used. The extract efficiencies ranged from 97.8 to 104.6% of the target values.

Bioavailable As and Pb Fraction in Soil

As and Pb were fractionated according to a 4-step modified European Community Bureau of Reference (BCR) sequential extraction procedure including F1: extracted with 0.11 M acetic acid (exchangeable fraction); F2: extracted with 0.5 M hydroxylammonium chloride (reducible fraction); F3: extracted with 8.8 M hydrogen peroxide followed by 1.0 M ammonium acetate (oxidizable fraction); F4: extracted with hydrofluoric acid followed by Aqua Regia (nitric acid + hydrochloric acid; 1:3 *v*/*v*) (residual fraction) (Rauret et al., 1999). The sum of exchangeable and reducible fractions was defined as bioavailable fractions according to a previous study (Roosa et al., 2014). The extracted solutions were analyzed by ICP-OES for different As and Pb fractions. The difference between the sum of each phase concentration and the total concentrations of As and Pb were compared to verify the accuracy of the sequential extraction procedure.

Microbial Biomass Carbon

Microbial biomass carbon (MBC) in soils was estimated by chloroform fumigation-extraction method (Vance et al., 1987; Brookes, 1995). Briefly, 6 subsamples of 5 g moist soil were weighed into different glass centrifuge tubes and three of them were fumigated with ethanol-free chloroform. Both fumigated and non-fumigated samples were incubated for 24 h at 25°C in the dark. After incubation, all the samples were extracted with 25 ml of 0.5 M K_2SO_4 and filtered. Then, the fumigated samples were heated in a 100°C water bath for 60 min and lost moisture was replenished. Total dissolved carbon in the extracts was determined by an automated N/C analyzer (Multi N/C 2100, Analytik Jena, Germany). MBC was calculated according to **Eq. 1** (Jaenicke et al., 2011):

$$\mathrm{MBC} = \frac{\left(C_f - C_{nf}\right)}{k_{EC}}. \quad (1)$$

where C_f = total dissolved carbon extracted from fumigated soil, C_{nf} = total dissolved carbon extracted from nonfumigated soil and k_{EC} = 0.45.

Soil DNA Extraction, PCR Amplification and Sequencing Analysis

Total DNA was extracted (four replicate samples) for each site using Fast DNA® Spin Kit for Soil (MP Biomedicals, Santa Ana, United States) according to the manufacturer's protocol. Total genomic DNA was amplified using primers 926 F (5' - AAA CTY AAA KGA ATT GAC GG - 3′) and 1392 R (5' -ACG GGC GGTGTG TRC- 3′) that amplifies the V6-V8 region of the 16 S rRNA gene (Luo et al., 2016). The 16 S rRNA tag-encoded high-throughput sequencing was carried out on Illumina Miseq platform at the Tianke Technology Co., Ltd (Hangzhou, China). Sequencing reads were assigned to each sample according to the individual unique barcode and filtered to remove ambiguous reads. Operational taxonomic units (OTUs) were clustered with 97% similarity cutoff using UPARSE (V8.1.1861) (Wang et al., 2007). For each OTU, a representative sequence was selected and used to assign taxonomic composition by using the RDP classifier (V11.4) against the SILVA database (www.arb-silva.de). The 16S rRNA gene sequences reported in this paper have been deposited in the NCBI SRA under the accession No. PRJNA678872.

Statistical Analysis

Statistical analyses for the experimental data were performed using the SPSS® 19.0 (SPSS, United States) software. The significance of the treatment effects was assessed by analysis of variance (ANOVA), followed by comparisons between treatment means using the least significant difference (LSD) at $p < 0.05$. Alpha diversity index including Chao1, Shannon, Simpson, ACE and Coverage were calculated using QIIME software (V1.9.1) (Caporaso et al., 2010). The similarity among microbial communities in different soil samples was determined using UniFrac analysis by QIIME software. Principal coordinate analysis (PCoA) plots of the OTU-based weighed UniFrac distances between all samples and heatmap of Spearman's rank correlations coefficients between geochemical parameters and the top 35 bacterial genera were generated by R software (V3.5.1) (http://www.r-project.org/). Redundancy analysis (RDA) was performed based on abundant bacteria genera (relative abundance top 35) and selected physicochemical parameters by Canoco 5 (Biometrics Wageningen, The Netherlands) (Aazami et al., 2015).

RESULTS AND DISCUSSION

Physicochemical Characterization of Soil Samples

The long term and continuous use of As and Pb contaminated paddy soil poses a serious health risks, since rice have a high tendency to accumulate As and Pb in its grains (Biswas et al., 2020). Paddy soil contaminated by As and Pb in mining areas has been widely documented (Kashyap et al., 2019; Zheng et al., 2020). However, the impact of mining activities on paddy soil physicochemical and microbial properties at various distances away from the mine is not well understood. HMs contamination and physicochemical properties of paddy soil play an important role in microbial metabolism (Zhao et al., 2013). Physicochemical characteristics of collected soils from the four sites were presented in **Table 1**. For all four sites, the soil pH was close to neutral (6.56–7.33), and the maximum pH was observed in site N01. The NO_3^--N and NH_4^+-N concentrations were significantly higher in site N01 as compared to the other studied sites ($p < 0.05$).

As and Pb were found to be the dominant HMs in the selected sites (**Table 1** and **Table 2**). The high As and Pb concentrations can be ascribed to intensive mining activities in the area. Previous studies have shown that As and Pb can easily be translocated from the mining site to neighboring farmlands via surface runoff and/or dust particles deposition (Wang et al., 2011; Guo et al., 2017; Li et al., 2020c). The total As and Pb concentrations in the studied area ranged between 44.4–388 mg kg^{-1} and 0.20–2.12 g kg^{-1}, respectively. The results also showed that the As and Pb concentrations in all the sites exceeded the soil environmental quality risk control standard for soil contamination of agricultural land in China (GB15618–2018) ($6.5 < pH \leq 7.5$, As 25 mg kg^{-1}, Pb 120 mg kg^{-1}) (Mee, 2018). For example, the As and Pb concentrations in N01 were 15 and 17 times of the soil environmental quality risk control standard (GB15618–2018), respectively. These results were consistent with the previous studies that suggested agricultural soils near mining sites were seriously polluted (Leung et al., 2017; Zhen et al., 2019).

A clear As and Pb gradient was observed at all four sites. The As and Pb concentrations decreased with increasing distance from the mining site and vice versa (**Table 2**). Previous studies have reported that the HMs concentrations in the topsoil usually decrease with the increase in the distance away from the mine (Li et al., 2015; Shen et al., 2017; Li et al., 2020c). A significant correlation was observed between total As and total Pb ($r = 0.970$, $p < 0.001$) (**Supplementary Table S1**), which indicated that these metal (loid)s had similar pollution sources (Sun et al., 2010). Furthermore, HMs bioavailable concentrations in soils have been reported to have better correlation with their accumulation in plants, which would directly threaten human health via food chain (Zhang et al., 2018). The bioavailable As concentration in N01 was significantly higher than other sites ($p < 0.05$). However, bioavailable As concentrations in N02, N03, and N04 were much lower compared to their total As concentrations. On the contrary, the bioavailable Pb concentrations were about half of the total concentrations for all four sites. Bioavailable As ($r = 0.715$, $p < 0.01$) and Pb ($r = 0.667$, $p < 0.01$) were positively corrected with soil pH, while bioavailable As ($r = -0.656$, $p < 0.01$) and Pb ($r = -0.585$, $p < 0.05$) were negatively corrected with soil OM (**Supplementary Table S1**). This indicates that pH and OM might be the main factors influencing As and Pb bioavailability in our study. pH may affect the bioavailability of As and Pb by influencing the adsorption of As and Pb on soil minerals. For example, the decreasing positive surface charge of soil minerals with increasing pH facilitated the desorption of As (Masscheleyn et al., 1991). With the increase of OM, the toxicity of HMs could be reduced through chelation and sequestration of metal cations onto OM (Macoustra et al., 2019).

TABLE 1 | Physicochemical characteristics of the paddy soil samples from each site. Different letters indicate significant differences among the different sites ($p < 0.05$).

Samples	pH	OM (%)	Moisture (%)	Total Fe	DOC	NO_3^--N	NH_4^+-N	SO_4^{2-}	Total S	Cd	Cr	Cu	Zn	Ni
				mmol g^{-1} dry soil	mg kg^{-1} dry soil				g kg^{-1} dry soil	mg kg^{-1} dry soil				
N01	7.33 ± 0.08a	4.95 ± 0.81ab	28.2 ± 2.03c	586 ± 27.2b	28.0 ± 5.22c	39.2 ± 9.38a	45.8 ± 11.1a	3.41 ± 0.55a	0.39 ± 0.03a	1.11 ± 0.11a	42.0 ± 7.63a	58.1 ± 9.07a	168 ± 6.25a	31.6 ± 0.90b
N02	6.56 ± 0.27b	3.81 ± 0.54b	35.6 ± 1.72bc	456 ± 28.0c	41.4 ± 7.25b	0.95 ± 0.56b	3.21 ± 0.38b	1.56 ± 0.19b	0.21 ± 0.03b	0.50 ± 0.08c	24.3 ± 6.99b	13.3 ± 0.37b	122 ± 17.9b	22.2 ± 1.14c
N03	6.16 ± 0.14c	6.03 ± 0.22a	42.0 ± 8.73b	574 ± 3.85b	37.7 ± 10.3bc	2.15 ± 0.90b	2.16 ± 0.72b	3.27 ± 0.46a	0.33 ± 0.04a	0.74 ± 0.05 b	31.4 ± 9.19b	15.3 ± 0.93b	133 ± 10.7ab	31.4 ± 0.41b
N04	6.40 ± 0.02bc	6.11 ± 1.17a	55.5 ± 4.90a	661 ± 25.1a	67.7 ± 12.3a	2.73 ± 0.59b	3.45 ± 1.29b	1.43 ± 0.30b	0.41 ± 0.16a	0.47 ± 0.16c	44.8 ± 10.2a	15.1 ± 0.81b	173 ± 38.7a	36.9 ± 0.48a

Abbreviations: DOC, dissolved organic carbon; OM, organic matter; Total S, Total sulfur.

TABLE 2 | Total and bioavailability concentrations of As and Pb in soil samples collected from four sites. Different letters indicate significant differences among the different sites ($p < 0.05$).

Samples	As (mg kg^{-1})		Pb (g kg^{-1})	
	Bioavailable Conc.	Total Conc.	Bioavailable Conc.	Total Conc.
N01	113 ± 10.8a	388 ± 10.6a	1.24 ± 0.06a	2.12 ± 0.03a
N02	13.7 ± 1.23b	124 ± 10.4b	0.36 ± 0.01 b	0.54 ± 0.02b
N03	7.17 ± 2.96b	74.8 ± 2.75c	0.24 ± 0.01c	0.34 ± 0.01c
N04	6.34 ± 2.13b	44.4 ± 3.74d	0.15 ± 0.01 d	0.20 ± 0.02d

Abbreviations: Conc., concentration.

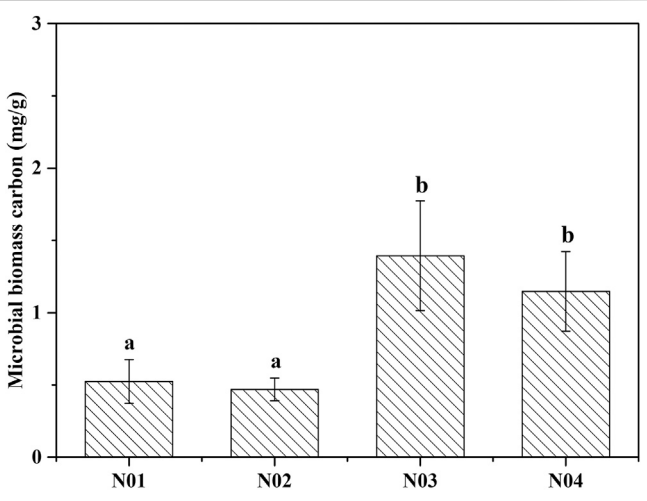

FIGURE 2 | Microbial biomass carbon (MBC) collected from four different sites near a Pb-Zn mining site. Different letters indicate significant differences among the different sites ($p < 0.05$).

Changes in Soil Microbial Biomass Carbon

Soil microbial biomass carbon (MBC) has been widely used as a bioindicator to evaluate soil quality since the soil microbial community is more sensitive to changes in soil composition compared to soil physiochemical properties (Feyzi et al., 2020). The MBC concentrations in N03 (1.39 mg g^{-1}) and N04 (1.15 mg g^{-1}) were significantly ($p < 0.05$) higher compared to those in N01 (0.52 mg g^{-1}) and N02 (0.47 mg g^{-1}) (**Figure 2**). The MBC concentrations increased with decreasing As and Pb concentrations. Moreover, significant negative correlations between MBC and As and Pb concentrations were observed (**Supplementary Table S1**). Our results are consistent with those of a previous study (Zhen et al., 2019) reporting that MBC was significantly reduced in soils collected near a mining site in Shaoguan city, China, particularly due to the presence of high HMs concentration. Other studies also noticed that MBC decreased significantly with the increasing metal concentrations (Khan et al., 2010; Xu et al., 2019). This indicated that due to the presence of excess metals in the contaminated soils, the MBC was suppressed and the microbial population was impeded to multiply (Xu et al., 2019). This may have occurred because soil MBC is sensitive to HMs, since microorganisms require additional energy to deal with stress caused by HMs (Yang et al., 2006). This additional energy requirement may result in a reduction in the amount of substrate used for microbial growth (Xiao et al., 2017).

Changes in Microbial Community Structure

Soil microbial community structure and diversity have also been used as an index for soil HMs pollution due to their sensitivity to soil physiochemical changes (Song et al., 2018). A total of 882,322 valid reads were obtained from the sixteen paddy

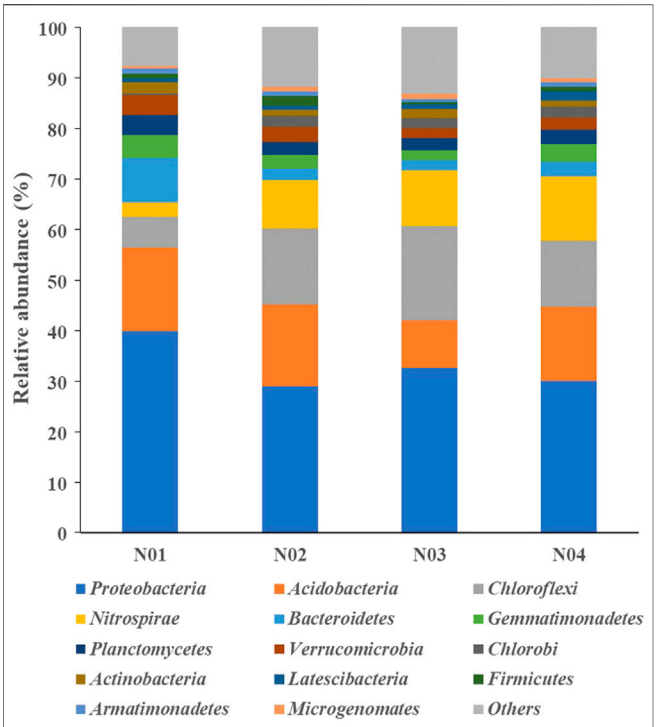

FIGURE 3 | Relative abundances (>1%) of dominant microbial taxa across different samples at the phylum levels.

soil samples through Illumina MiSeq platform and the average sequence length was 463 bp. A total of 642,574 operational taxonomic units (OTUs) was revealed. The number of OTUs from N01 was significantly lower than those from N02, N03 and N04 ($p < 0.05$) (**Supplementary Table S2**). The alpha diversity indexes including ACE and Chao1 from N03 and N04 were significantly higher than the samples from N01 and N02 ($p < 0.05$) (**Supplementary Table S2**). Soil microbial diversity in moderately and heavily contaminated soil were observed to be reduced compared to those of healthy soil (Golebiewski et al., 2014). Similar to our study, Shen et al. (2019) also observed that As and Pb contamination could decrease microbial diversity. Furthermore, the PCoA [PC1 vs PC2 (explaining 86.74%)] analysis suggested an obvious separation of the bacterial communities in N01, N02 and N03 while the bacterial communities in N04 was close to N02 and N03 (**Supplementary Figure S1**).

The microbial community structures differed among the four sampled sites. The relative abundance of the sequences obtained from the different sites at the phylum level are shown in **Figure 3**. The top 10 dominant phyla in all samples were, *Proteobacteria* (28.9–39.8%), *Acidobacteria* (9.3–16.6%), *Chloroflexi* (6.2–18.7%), *Nitrospirae* (2.8–12.7%), *Bacteroidetes* (2.0–8.9%), *Gemmatimonadetes* (1.9–4.4%), *Planctomycetes* (2.5–4.0%), *Verrucomicrobia* (1.9–3.9%), *Chlorobi* (1.9–3.9%) and *Actinobacteria* (1.2–2.2%). These phyla have also been reported in previous studies as dominant bacterial groups in paddy soil (Li et al., 2017; Zhen et al., 2019; Li et al., 2020a). Pollution-related changes in the relative abundance of the phyla were observed. The relative abundances of *Proteobacteria, Bacteroidetes*, *Planctomycetes*, and *Verrucomicrobia* were significantly higher in N01 than those in N02, N03 and N04 ($p < 0.05$), while the relative abundances of *Chloroflexi*, *Nitrospirae,* and *Chlorobi* were significantly lower in N01 ($p < 0.05$). These results indicate that soil HMs pollution may suppress some microbial phyla while promote the growth of HMs resistant microbes (Xu et al., 2018). Thus, we can deduce from our results that the phyla *Proteobacteria* and *Bacteroidetes* are able to endure high As and Pb stresses. Previous studies have reported that the members of the phylum *Proteobacteria* are able to tolerate high HMs stress (Schneider et al., 2017; Li et al., 2020c), which was consistent with the results of our study. Moreover, other studies have shown that *Proteobacteria* dominate in the metal-tolerant cultures, because many species belonging to this phyla can reduce Fe and facilitate soil-adsorbed metals release which inadvertently increase metal stress (Francis and Dodge, 1990; Jiang et al., 2017). *Proteobacteria* and *Bacteroidetes* have also been reported to harbor the majority of HMs resistance genes base on

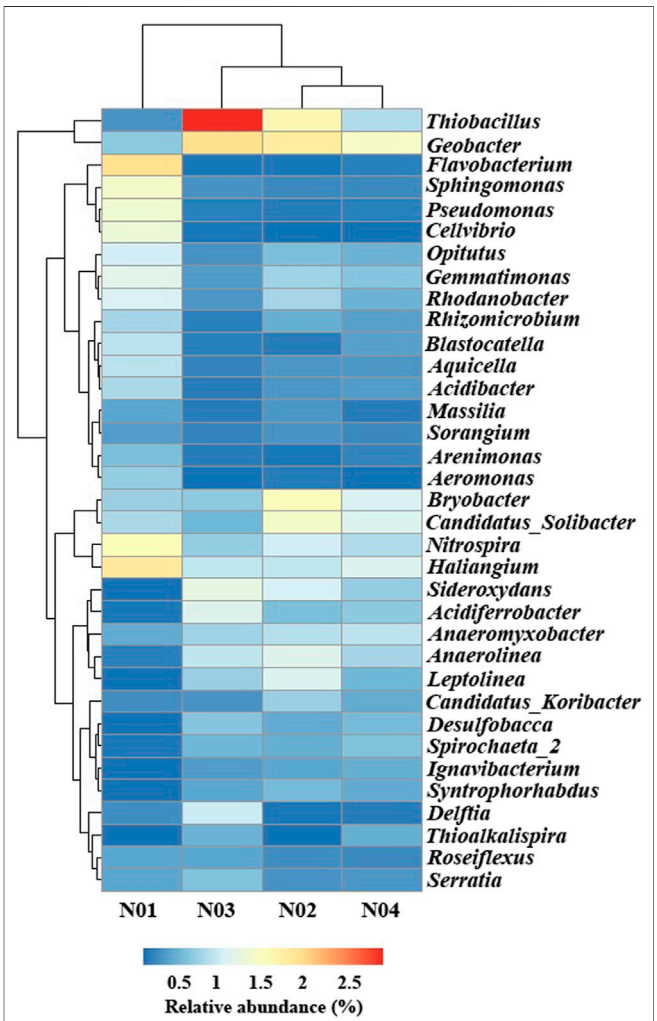

FIGURE 4 | Relative abundances of top 35 microbial genrea aross different samples at four sites.

metagenome sequencing (Yan et al., 2020). Furthermore, an increase in *Bacteroidetes* relative abundance have been observed in Pb spiked soils compared to the unspiked soils (Hou et al., 2020).

In order to further understand the microbial community response to geochemical conditions and HMs, the OTUs were further classified to the genus level (**Figure 4**). The four sampled sites were clustered into two distinct groups (one group included N01 and the other group included N02, N03, and N04) which was consistent with the results shown in the PCoA plot (**Figure 4** and **Supplementary Figure S1**). *Flavobacterium* (2.0%), *Haliangium* (1.8%), *Nitrospira* (1.5%), *Sphingomonas* (1.4%) and *Pseudomonas* (1.3%) were the most abundant genera in N01, while *Geobacter* (1.4–1.9%), *Thiobacillus* (0.8–3.0%), and *Bryobacter* (0.6–1.5%) were the most abundant genera in N02, N03 and N04. The relative abundance of *Haliangium*, *Nitrospira*, *Flavobacterium*, *Opitutus*, *Sphingomonas*, *Pseudomonas*, *Aquicella*, *Acidibacter*, *Blastocatella,* and *Sorangium* were significantly higher in N01 than those in N02, N03, and N04 ($p < 0.05$). Previous studied have shown that the most of the bacterial strains from these genera are commonly involved in As resistance (Guo et al., 2017; Titah et al., 2018; Li et al., 2020c). *Haliangium* was observed to flourish in HMs stressed environments (Marti et al., 2017). Similarly, the abundances of *Flavobacterium* were observed to increase under high Pb stress (Wang et al., 2020b). *Flavobacterium* was also isolated from As contaminated soil as an As-resistant genus and it was able to reduce arsenate (As(V)) under erobic conditions (Wang and Mulligan, 2006). Besides, *Flavobacterium* related groups are able to methylate As as a detoxification strategy (Honschopp et al., 1996). *Nitrospira* are nitrite-oxidizing bacteria that can provide nitrate which takes part in the oxidation of arsenite (As(III)) (Yu et al., 2020). Studies have found that in HMs polluted soil, *Sphingomonas* was the most abundant genus and had a potential to remove Pb from seawater (Chen, 2012; Guo et al., 2017). *Pseudomonas* has been reported to be involved in As redox processes (Cavalca et al., 2013). Moreover, the As(III) efflux pump protein gene *arsB* and As transporter protein gene *acr3*P was also detected within the genus of *Pseudomonas* (Sanyal et al., 2016). *Acidibacter* and *Blastocatella* increased in HMs polluted soil and their significant positive correlation with Pb or As was also observed by Guo et al. (2017). The relative abundance of *Geobacter*, *Thiobacillus*, *Sideroxydans*, *Anaerolinea*, *Anaeromyxobacter*, *Leptolinea*, *Spirochaeta_2, Desulfobacca*, *Syntrophorhabdus,* and *Ignavibacterium* were significantly higher in N02, N03, N04 than those in N01 ($p < 0.05$). These results indicated that these microorganisms were relatively sensitive to As and Pb toxicity and the abundances were abruptly declined with the increase of HMs concentrations (Giller et al., 1998). *Geobacter* populations were reported as Fe and sulfate reducing bacteria, while *Anaeromyxobacter* were Fe reducing bacteria and *Desulfobacca* were sulfate reducing bacteria (Sun et al., 2015a). Besides, *Thiobacillus* were found to be involved in Fe and S oxidation and *Thiobacillus* can oxidize elemental sulfur (Wang et al., 2021). *Sideroxydans* were involved in Fe oxidation (Blothe and Roden, 2009). Most of these sensitive microorganisms were Fe- and S-related bacteria indicating their important roles in lightly contaminated sites. We speculated that As and Pb contamination in paddy soil might have an inhibition effect on Fe and S cycling in paddy soil.

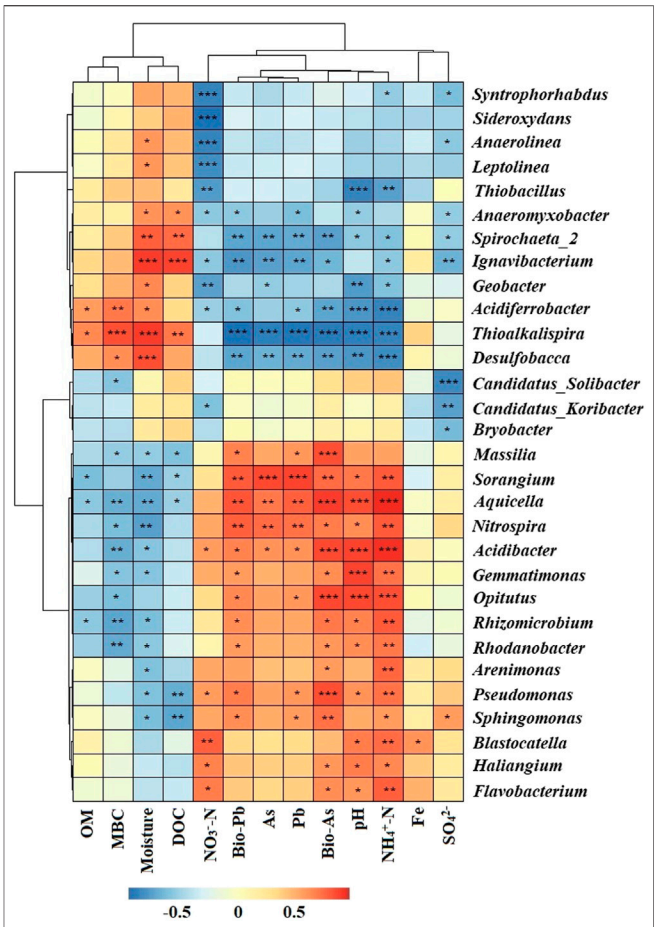

FIGURE 5 | Heatmap of Spearman's rank correlations coefficients between geochemical parameters and the relative abundance of top 35 bacterial genera. The corresponding value of heatmap is Spearman correlation coefficient where "r" value is between −1 and 1, r < 0 is negative correlation, r > 0 is positive correlation. The asterisk indicates significant differences. *$p < 0.05$, **$p < 0.01$, ***$p < 0.001$. Abbreviations: As, Pb, Fe (total As, Pb, Fe in soil); Bio-As, Pb (bioavailability As, Pb); MBC (microbial biomass carbon); OM (organic matter); DOC (dissolved organic carbon).

Correlation Between Environmental Parameters and Microbial Community

In microbial ecology, understanding the relationship between environmental variables and microbial community structure is a key goal (Liang et al., 2011). Spearman's rank correlations coefficients between geochemical parameters and bacterial abundances were determined (**Figure 5**). The relative abundance of *Acidibacter* positively correlated with total As, total Pb, bioavailable Pb ($p < 0.05$) and bioavailable As ($p < 0.001$) concentrations in soil. Similar results have also been reported by Guo et al. (2017). *Nitrospira*, *Aquicella* and

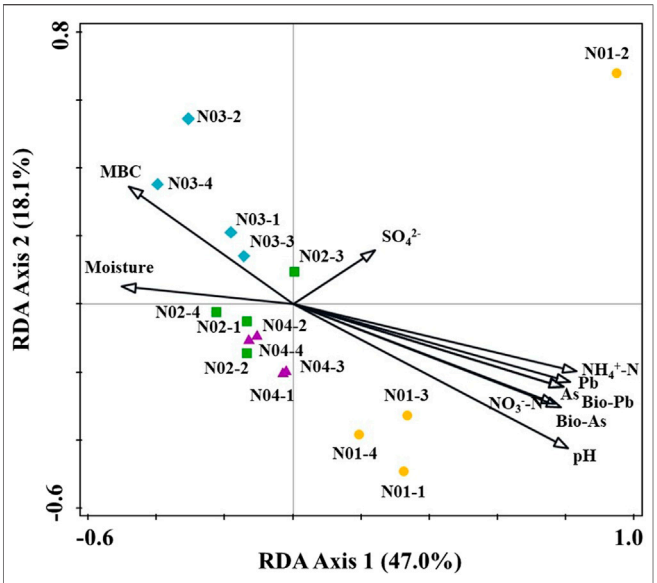

FIGURE 6 | Redundancy analysis (RDA) diagram of the geochemical parameters and the top 35 bacterial genera. Abbreviations: As, Pb, Fe (total As, Pb, Fe in soil); Bio-As, Pb (bioavailability As, Pb); MBC (microbial biomass carbon).

Sorangium were also positively correlated with total As, bioavailable As, total Pb and bioavailable Pb concentrations. Other genera like *Sphingomonas*, *Pseudomonas* and *Massilia* also had positive correlations with total or bioavailable As or Pb. These results suggested that As and Pb contamination may facilitate the growth of these bacterial groups. *Thioalkalispira* ($p < 0.001$), *Desulfobacca* ($p < 0.01$) and *Spirochaeta_2* ($p < 0.01$) were negatively correlated with total As, bioavailable As, total Pb and bioavailable Pb concentrations. Among them, *Nitrospira*, *Aquicella* and *Sorangium* were positively correlated with different forms of As and Pb, indicating their high HMs tolerance while *Thioalkalispira*, *Desulfobacca* and *Spirochaeta_2* were sensitive to As and Pb pollution. pH, moisture and NH_4^+-N had significant correlations with most of the genera. Redundancy analysis (RDA) was used to reveal the possible linkages between the microbial communities and geochemical parameters (**Figure 6**). Although the pollution source of the soil was from a Pb-Zn mining site, no significant correlation between the microbial communities and the Zn concentration could be found. It might be due to the low Zn concentrations in soil. Besides, it has been reported that high levels of Zn had no effect on the species diversity compared to unpolluted soil in mining areas (Xu et al., 2017). Total As, bioavailable As, total Pb and bioavailable Pb concentrations along with pH, NH_4^+-N, NO_3^--N, moisture, SO_4^{2-} and MBC were the main factors influencing bacterial community compositions (**Figure 6**). Total As, bioavailable As, total Pb and bioavailable Pb concentrations along with pH, NH_4^+-N and NO_3^--N positively correlated with microbial communities from N01 while negatively correlated with microbial communities from N02, N03, and N04. Soil moisture positively correlated with microbial communities from N02, N03, and N04. It is widely accepted that pH has a significant effect on the overall diversity and composition of microbial communities (Gu et al., 2017). Any significant deviation in pH could impose stress on single-celled organisms because the intracellular pH of most microorganisms are usually within 1 pH unit of neutral (Fierer and Jackson, 2006). Soil pH could also influence other environmental parameters (e.g. nutrient availability or cationic metal solubility), that plays an important role in microbial survival (Sun et al., 2015b). Previous studies also reported that pH had a greater impact on bacterial community composition in HMs contaminated agricultural soils when compared with HMs in soil (Cavani et al., 2016; Jiang et al., 2016). Two types of nitrogen (NH_4^+-N and NO_3^--N) were significantly correlated with soil genera in this study, suggesting their important role in shaping the soil microbial community (Deng et al., 2018). Anderson et al. (2009) reported that NH_4^+-N and NO_3^--N showed positive correlations with the shifts in microbial community structure, which was consistent with our results. Paddy soils could provide good habitats for nitrogen cycling, which in turn have the potential to shape the microbial communities (Sun et al., 2015a). Additionally, moisture is a major environmental factor that determines the redox conditions of soils and the metabolism of microbes (Honma et al., 2016). For example, wet-dry transition in soil would result in a microbial community shift of anaerobic to erobic microbes (Pett-Ridge and Firestone., 2005). This is especially true for paddy soil which are intermittently flooded during rice production.

CONCLUSION

In this study, we used the high throughput sequencing to examine the effects of physicochemical parameters on the microbial community variation in HMs contaminated soils along an As and Pb gradient. Our results showed that high amounts of HMs were presented near the mining site, and their concentrations decreased with increasing distance from the mining site. As and Pb contamination have a profound impact on the microbial community structure of paddy soils. Different forms of As and Pb (total and bioavailable) and soil physicochemical components (pH, NH_4^+-N, NO_3^--N, moisture, and MBC) had significant influences on the bacterial community compositions. Some genera including *Haliangium*, *Nitrospira,* and *Flavobacterium* were positively correlated with different forms of As and Pb, indicating their high tolerance and their important role in As and Pb cycling while other genera including *Geobacter*, *Thiobacillus,* and *Sideroxydans* were sensitive to HMs contamination. Our finding provided important information that should be taken into consideration when developing bioremediation strategies for the polluted paddy soil in mining area.

DATA AVAILABILITY STATEMENT

The datasets presented in this study can be found in online repositories. The names of the repository/repositories and accession number(s) can be found in the article/ **Supplementary Material**.

AUTHOR CONTRIBUTIONS

XT and JN performed the study conceptualization and supervision. LZ performed the literature search and wrote the original draft. YL, YD, MK, WG, and LY carried out the writing, reviewing and JS and JX performed the study supervision and validation editing. All authors read and approved the final manuscript.

ACKNOWLEDGMENTS

The National Key Technology R&D Program (2018YFD0800202) supported this study.

SUPPLEMENTARY MATERIAL

The Supplementary Material for this article can be found online at: https://www.frontiersin.org/articles/10.3389/fenvs.2021.630668/full#supplementary-material

REFERENCES

Aazami, J., Esmaili-Sari, A., AbdoliSohrabi, A. H., and Van den Brink, P. J. (2015). Monitoring and Assessment of Water Health Quality in the Tajan River, Iran Using Physicochemical, Fish and Macroinvertebrates Indices. *J. Environ. Health Sci. Engineer.* 13, 29. doi:10.1186/s40201-015-0186-y

Anderson, J. A. H., Hooper, M. J., Zak, J. C., and Cox, S. B. (2009). Characterization of the Structural and Functional Diversity of Indigenous Soil Microbial Communities in Smelter-Impacted and Nonimpacted Soils. *Environ. Toxicol. Chem.* 28, 534–541. doi:10.1897/08-281.1

Biswas, J. K., Warke, M., Datta, R., and Sarkar, D. (2020). Is Arsenic in Rice a Major Human Health Concern? *Curr. Pollut. Rep.* 6, 37–42. doi:10.1007/s40726-020-00148-2

Blothe, M., and Roden, E. E. (2009). Composition and Activity of an Autotrophic Fe(II)-oxidizing, Nitrate-Reducing Enrichment Culture. *Appl. Environ. Microbiol.* 75, 6937–6940. doi:10.1128/AEM.01742-09

Brookes, P. C. (1995). The Use of Microbial Parameters in Monitoring Soil Pollution by Heavy Metals. *Biol. Fertil. Soils.* 19, 269–279. doi:10.1007/bf00336094

Caporaso, J. G., Kuczynski, J., Stombaugh, J., Bittinger, K., Bushman, F. D., Costello, E. K., et al. (2010). QIIME Allows Analysis of High-Throughput Community Sequencing Data. *Nat. Methods* 7, 335–336. doi:10.1038/nmeth.f.303

Cavalca, L., Corsini, A., Zaccheo, P., Andreoni, V., and Muyzer, G. (2013). Microbial Transformations of Arsenic: Perspectives for Biological Removal of Arsenic from Water. *Future Microbiol.* 8, 753–768. doi:10.2217/fmb.13.38

Cavani, L., Manici, L. M., Caputo, F., Peruzzi, E., and Ciavatta, C. (2016). Ecological Restoration of a Copper Polluted Vineyard: Long-Term Impact of Farmland Abandonment on Soil Bio-Chemical Properties and Microbial Communities. *J. Environ. Manage.* 182, 37–47. doi:10.1016/j.jenvman.2016.07.050

Cesare, A. D., Pjevac, P., Eckert, E., Curkow, N., Šparica, M. M., Corno, G., et al. (2020). The Role of Metal Contamination in Shaping Microbial Communities in Heavily Polluted Marine Sediments. *Environ. Pollut.* 265, 114823. doi:10.1016/j.envpol.2020.114823

Chen, M., Lu, G., Wu, J., Yang, C., Niu, X., Tao, X., et al. (2018). Migration and Fate of Metallic Elements in a Waste Mud Impoundment and Affected River Downstream: A Case Study in Dabaoshan Mine, South China. *Ecotoxicology Environ. Saf.* 164, 474–483. doi:10.1016/j.ecoenv.2018.08.063

Cheng, W., Lei, S., Bian, Z., Zhao, Y., Li, Y., and Gan, Y. (2020). Geographic Distribution of Heavy Metals and Identification of Their Sources in Soils Near Large, Open-Pit Coal Mines Using Positive Matrix Factorization. *J. Hazard. Mater.* 387, 121666. doi:10.1016/j.jhazmat.2019.121666

Deng, S., Ke, T., Li, L., Cai, S., Zhou, Y., Liu, Y., et al. (2018). Impacts of Environmental Factors on the Whole Microbial Communities in the Rhizosphere of a Metal-Tolerant Plant: *Elsholtzia Haichowensis* Sun. *Environ. Pollut.* 237, 1088–1097. doi:10.1016/j.envpol.2017.11.037

Du, F., Yang, Z., Liu, P., and Wang, L. (2018). Accumulation, Translocation, and Assessment of Heavy Metals in the Soil-Rice Systems Near a Mine-Impacted Region. *Environ. Sci. Pollut. Res.* 25, 32221–32230. doi:10.1007/s11356-018-3184-7

Fernandez-Macias, J. C., Gonzalez-Mille, D. J., Garcia-Arreola, M. E., Cruz-Santiago, O., Rivero-Perez, N. E., Perez-Vazquez, F., et al. (2020). Integrated Probabilistic Risk Assessment in Sites Contaminated with Arsenic and Lead by Long-Term Mining Liabilities in San Luis Potosi, Mexico. *Ecotox. Environ. Safe.* 197, 8. doi:10.1016/j.ecoenv.2020.110568

Feyzi, H., Chorom, M., and Bagheri, G. (2020). Urease Activity and Microbial Biomass of Carbon in Hydrocarbon Contaminated Soils. A Case Study of Cheshmeh-Khosh Oil Field. *Iran.* Ecotox. Environ. Safe. 199, 11. doi:10.1016/j.ecoenv.2020.110664

Fierer, N., and Jackson, R. B. (2006). The Diversity and Biogeography of Soil Bacterial Communities. *Proc. Natl. Acad. Sci.* 103, 626–631. doi:10.1073/pnas.0507535103

Francis, A. J., and Dodge, C. J. (1990). Anaerobic Microbial Remobilization of Toxic Metals Coprecipitated with Iron Oxide. *Environ. Sci. Technol.* 24, 373–378. doi:10.1021/es00073a013

Giller, K. E., Witter, E., and Mcgrath, S. P. (1998). Toxicity of Heavy Metals to Microorganisms and Microbial Processes in Agricultural Soils: A Review. *Soil Biol. Biochem.* 30, 1389–1414. doi:10.1016/s0038-0717(97)00270-8

Gołębiewski, M., Deja-Sikora, E., Cichosz, M., Tretyn, A., and Wróbel, B. (2014). 16S rDNA Pyrosequencing Analysis of Bacterial Community in Heavy Metals Polluted Soils. *Microb. Ecol.* 67, 635–647. doi:10.1007/s00248-013-0344-7

Gu, Y., Van Nostrand, J. D., Wu, L., He, Z., Qin, Y., Zhao, F. J., et al. (2017). Bacterial Community and Arsenic Functional Genes Diversity in Arsenic Contaminated Soils from Different Geographic Locations. *Plos. One.* 12. e0189656. doi:10.1371/journal.pone.0189656

Guo, H., Nasir, M., Lv, J., Dai, Y., and Gao, J. (2017). Understanding the Variation of Microbial Community in Heavy Metals Contaminated Soil Using High Throughput Sequencing. *Ecotoxicology Environ. Saf.* 144, 300–306. doi:10.1016/j.ecoenv.2017.06.048

Hahn, J., Mann, B., Bange, U., and Kimmel, M. (2019). Horizon-specific Effects of Heavy Metal Mobility on Nitrogen Binding Forms in Forest Soils Near a Historic Smelter (Germany). *Geoderma* 355, 8. doi:10.1016/j.geoderma.2019.113895

Honma, T., Ohba, H., Kaneko-Kadokura, A., Makino, T., Nakamura, K., and Katou, H. (2016). Optimal Soil Eh, pH, and Water Management for Simultaneously Minimizing Arsenic and Cadmium Concentrations in Rice Grains. *Environ. Sci. Technol.* 50, 4178–4185. doi:10.1021/acs.est.5b05424

Honschopp, S., Brunken, N., Nehrkorn, A., and Breunig, H. J. (1996). Isolation and Characterization of a New Arsenic Methylating Bacterium from Soil. *Microbiol. Res.* 151, 37–41. doi:10.1016/s0944-5013(96)80053-x

Hou, X. L., Han, H., Tigabu, M., Li, Q. Y., Li, Z. X., Zhu, C. L., et al. (2020). Lead Contamination Alters Enzyme Activities and Microbial Composition in the Rhizosphere Soil of the Hyperaccumulator *Pogonatherum Crinitum*. *Ecotoxicol Environ. Saf.* 207, 111308. doi:10.1016/j.ecoenv.2020.111308

Hu, M., Sun, W., Krumins, V., and Li, F. (2019). Arsenic Contamination Influences Microbial Community Structure and Putative Arsenic Metabolism Gene

Abundance in Iron Plaque on Paddy Rice Root. *Sci. Total Environ.* 649, 405–412. doi:10.1016/j.scitotenv.2018.08.388

Jaenicke, S., Ander, C., Bekel, T., Bisdorf, R., Dröge, M., Gartemann, K. H., et al. (2011). Comparative and Joint Analysis of Two Metagenomic Datasets from a Biogas Fermenter Obtained by 454-pyrosequencing. *Plos. One.* 6. e14519. doi:10.1371/journal.pone.0014519

Jiang, B., Adebayo, A., Jia, J., Xing, Y., Deng, S., Guo, L., et al. (2019). Impacts of Heavy Metals and Soil Properties at a Nigerian E-Waste Site on Soil Microbial Community. *J. Hazard. Mater.* 362, 187–195. doi:10.1016/j.jhazmat.2018.08.060

Jiang, J., Pan, C. H., Xiao, A. P., Yang, X. A., and Zhang, G. M. (2017). Isolation, Identification, and Environmental Adaptability of Heavy-Metal-Resistant Bacteria from Ramie Rhizosphere Soil Around Mine Refinery. *3 Biotech.* 7, 6. doi:10.1007/s13205-017-0603-2

Jiang, L. F., Song, M. K., Yang, L., Zhang, D. Y., Sun, Y. T., Shen, Z. G., et al. (2016). Exploring the Influence of Environmental Factors on Bacterial Communities within the Rhizosphere of the Cu-Tolerant Plant. *Elsholtzia Splendens. Sci. Rep.* 6, 10. doi:10.1038/srep36302

Kashyap, R., Ahmad, M., Uniyal, S. K., and Verma, K. S. (2019). Dietary Consumption of Metal(loid)s-Contaminated Rice Grown in Croplands Around Industrial Sectors: a Human Health Risk Perspective. *Int. J. Environ. Sci. Technol.* 16, 8505–8516. doi:10.1007/s13762-019-02258-x

Khan, S., El-Latif Hesham, A., Qiao, M., Rehman, S., and He, J.-Z. (2010). Effects of Cd and Pb on Soil Microbial Community Structure and Activities. *Environ. Sci. Pollut. Res.* 17, 288–296. doi:10.1007/s11356-009-0134-4

Leung, H. M., Duzgoren-Aydin, N. S., Au, C. K., Krupanidhi, S., Fung, K. Y., Cheung, K. C., et al. (2017). Monitoring and Assessment of Heavy Metal Contamination in a Constructed Wetland in Shaoguan (Guangdong Province, China): Bioaccumulation of Pb, Zn, Cu and Cd in Aquatic and Terrestrial Components. *Environ. Sci. Pollut. Res.* 24, 9079–9088. doi:10.1007/s11356-016-6756-4

Li, P. F., Liu, M., Ma, X. Y., Wu, M., Jiang, C. Y., Liu, K., et al. (2020a). Responses of Microbial Communities to a Gradient of Pig Manure Amendment in Red Paddy Soils. *Sci. Total. Environ.* 705, 8. doi:10.1016/j.scitotenv.2019.135884

Li, P., Lin, C., Cheng, H., Duan, X., and Lei, K. (2015). Contamination and Health Risks of Soil Heavy Metals Around a Lead/zinc Smelter in Southwestern China. *Ecotoxicology Environ. Saf.* 113, 391–399. doi:10.1016/j.ecoenv.2014.12.025

Li, S., Wu, J., Huo, Y., Zhao, X., and Xue, L. (2020b). Profiling Multiple Heavy Metal Contamination and Bacterial Communities Surrounding an Iron Tailing Pond in Northwest China. *Sci. Total. Environ.* 752, 141827. doi:10.1016/j.scitotenv.2020.141827

Li, S., Zhao, B., Jin, M., Hu, L., Zhong, H., and He, Z. (2020c). A Comprehensive Survey on the Horizontal and Vertical Distribution of Heavy Metals and Microorganisms in Soils of a Pb/Zn Smelter. *J. Hazard. Mater.* 400. 123255. doi:10.1016/j.jhazmat.2020.123255

Li, X., Meng, D., Li, J., Yin, H., Liu, H., Liu, X., et al. (2017). Response of Soil Microbial Communities and Microbial Interactions to Long-Term Heavy Metal Contamination. *Environ. Pollut.* 231, 908–917. doi:10.1016/j.envpol.2017.08.057

Li, Z., Ma, Z., Van Der Kuijp, T. J., Yuan, Z., and Huang, L. (2014). A Review of Soil Heavy Metal Pollution from Mines in China: Pollution and Health Risk Assessment. *Sci. Total Environ.* 468-469, 843–853. doi:10.1016/j.scitotenv.2013.08.090

Liang, Y., Van Nostrand, J. D., Deng, Y., He, Z., Wu, L., Zhang, X., et al. (2011). Functional Gene Diversity of Soil Microbial Communities from Five Oil-Contaminated Fields in China. *Isme. J.* 5, 403–413. doi:10.1038/ismej.2010.142

Liu, G., Ling, S., Zhan, X., Lin, Z., Zhang, W., and Lin, K. (2017). Interaction Effects and Mechanism of Pb Pollution and Soil Microorganism in the Presence of Earthworm. *Chemosphere* 173, 227–234. doi:10.1016/j.chemosphere.2017.01.022

Liu, J., Yin, M., Zhang, W., Tsang, D. C. W., Wei, X., Zhou, Y., et al. (2019). Response of Microbial Communities and Interactions to Thallium in Contaminated Sediments Near a Pyrite Mining Area. *Environ. Pollut.* 248, 916–928. doi:10.1016/j.envpol.2019.02.089

Lorenz, N., Hintemann, T., Kramarewa, T., Katayama, A., Yasuta, T., Marschner, P., et al. (2006). Response of Microbial Activity and Microbial Community Composition in Soils to Long-Term Arsenic and Cadmium Exposure. *Soil Biol. Biochem.* 38, 1430–1437. doi:10.1016/j.soilbio.2005.10.020

Luo, F., Devine, C. E., and Edwards, E. A. (2016). Cultivating Microbial Dark Matter in Benzene-Degrading Methanogenic Consortia. *Environ. Microbiol.* 18, 2923–2936. doi:10.1111/1462-2920.13121

Macoustra, G., Holland, A., Stauber, J., and Jolley, D. F. (2019). Effect of Various Natural Dissolved Organic Carbon on Copper Lability and Toxicity to the Tropical Freshwater Microalga *Chlorella Sp. Environ. Sci. Technol.* 53, 2768–2777. doi:10.1021/acs.est.8b04737

Marti, R., Becouze-Lareure, C., Ribun, S., Marjolet, L., Souibgui, C. B., Aubin, J. B., et al. (2017). Bacteriome Genetic Structures of Urban Deposits Are Indicative of Their Origin and Impacted by Chemical Pollutants. *Sci. Rep.* 7, 14. doi:10.1038/s41598-017-13594-8

Masscheleyn, P. H., Delaune, R. D., and Patrick, W. H. (1991). Effect of Redox Potential and pH on Arsenic Speciation and Solubility in a Contaminated Soil. *Environ. Sci. Technol.* 25, 1414–1419. doi:10.1021/es00020a008

Mee, C. (2018). *Soil Environmental Quality Risk Control Standard for Soil Contamination of Agricultural Land.*

Mee, C., and Mnr, C. (2014). *The Report on the National Soil Contamination Survey.*

Mu, X., Wang, Z., Liu, L., Guo, X., Gu, C., Xu, H., et al. (2020). Multiple Exposure Pathways of First-Year University Students to Heavy Metals in China: Serum Sampling and Atmospheric Modeling. *Sci. Total Environ.* 746, 141405. doi:10.1016/j.scitotenv.2020.141405

O'Kelly, B. C. (2004). Accurate Determination of Moisture Content of Organic Soils Using the Oven Drying Method. *Dry. Technol.* 22, 1767–1776. doi:10.1081/DRT-200025642

Pett-Ridge, J., and Firestone, M. K. (2005). Redox Fluctuation Structures Microbial Communities in a Wet Tropical Soil. *Aem* 71, 6998–7007. doi:10.1128/aem.71.11.6998-7007.2005

Rai, P. K., Lee, S. S., Zhang, M., Tsang, Y. F., and Kim, K.-H. (2019). Heavy Metals in Food Crops: Health Risks, Fate, Mechanisms, and Management. *Environ. Int.* 125, 365–385. doi:10.1016/j.envint.2019.01.067

Rauret, G., López-Sánchez, J. F., Sahuquillo, A., Rubio, R., Davidson, C., Ure, A., et al. (1999). Improvement of the BCR Three Step Sequential Extraction Procedure Prior to the Certification of New Sediment and Soil Reference Materials. *J. Environ. Monitor.* 1, 57–61. doi:10.1039/a807854h

Roosa, S., Wattiez, R., Prygiel, E., Lesven, L., Billon, G., and Gillan, D. C. (2014). Bacterial Metal Resistance Genes and Metal Bioavailability in Contaminated Sediments. *Environ. Pollut.* 189, 143–151. doi:10.1016/j.envpol.2014.02.031

Ros, M., Pascual, J. A., Moreno, J. L., Hernandez, M. T., and Garcia, C. (2009). Evaluation of Microbial Community Activity, Abundance and Structure in a Semiarid Soil under Cadmium Pollution at Laboratory Level. *Water Air Soil Pollut.* 203, 229–242. doi:10.1007/s11270-009-0006-z

Sanyal, S. K., Mou, T. J., Chakrabarty, R. P., Hoque, S., Hossain, M. A., and Sultana, M. (2016). Diversity of Arsenite Oxidase Gene and Arsenotrophic Bacteria in Arsenic Affected Bangladesh Soils. *Amb. Express.* 6, 11. doi:10.1186/s13568-016-0193-0

Schneider, A. R., Gommeaux, M., Duclercq, J., Fanin, N., Conreux, A., Alahmad, A., et al. (2017). Response of Bacterial Communities to Pb Smelter Pollution in Contrasting Soils. *Sci. Total Environ.* 605-606, 436–444. doi:10.1016/j.scitotenv.2017.06.159

She, J. Y., Wang, J., Wei, X. D., Zhang, Q., Xie, Z. Y., Beiyuan, J. Z., et al. (2021). Survival Strategies and Dominant Phylotypes of Maize-Rhizosphere Microorganisms under Metal(loid)s Contamination. *Sci. Total. Environ.* 774, 145143. doi:10.1016/j.scitotenv.2021.145143

Shen, F., Liao, R., Ali, A., Mahar, A., Guo, D., Li, R., et al. (2017). Spatial Distribution and Risk Assessment of Heavy Metals in Soil Near a Pb/Zn Smelter in Feng County, China. *Ecotoxicology Environ. Saf.* 139, 254–262. doi:10.1016/j.ecoenv.2017.01.044

Shen, T., Liu, L., Li, Y., Wang, Q., Dai, J., and Wang, R. (2019). Long-term Effects of Untreated Wastewater on Soil Bacterial Communities. *Sci. Total Environ.* 646, 940–950. doi:10.1016/j.scitotenv.2018.07.223

Song, J., Shen, Q., Wang, L., Qiu, G., Shi, J., Xu, J., et al. (2018). Effects of Cd, Cu, Zn and Their Combined Action on Microbial Biomass and Bacterial Community Structure. *Environ. Pollut.* 243, 510–518. doi:10.1016/j.envpol.2018.09.011

Stock, W. D. (1983). An Evaluation of Some Manual Colorimetric Methods for the Determination of Inorganic Nitrogen in Soil Extracts. *Commun. Soil Sci. Plant Anal.* 14, 925–936. doi:10.1080/00103628309367420

Sun, M., Xiao, T., Ning, Z., Xiao, E., and Sun, W. (2015a). Microbial Community Analysis in Rice Paddy Soils Irrigated by Acid Mine Drainage Contaminated Water. *Appl. Microbiol. Biotechnol.* 99, 2911–2922. doi:10.1007/s00253-014-6194-5

Sun, W., Xiao, T., Sun, M., Dong, Y., Ning, Z., Xiao, E., et al. (2015b). Diversity of the Sediment Microbial Community in the Aha Watershed (Southwest China) in Response to Acid Mine Drainage Pollution Gradients. *Appl. Environ. Microbiol.* 81, 4874–4884. doi:10.1128/aem.00935-15

Sun, Y., Zhou, Q., Xie, X., and Liu, R. (2010). Spatial, Sources and Risk Assessment of Heavy Metal Contamination of Urban Soils in Typical Regions of Shenyang, China. *J. Hazard. Mater.* 174, 455–462. doi:10.1016/j.jhazmat.2009.09.074

Tian, H. J., Feng, J., Zhang, L. M., He, J. Z., and Liu, R. Y. (2020). Ecological Drivers of Methanotrophic Communities in Paddy Soils Around Mercury Mining Areas. *Sci. Total. Environ.* 721. 137760. doi:10.1016/j.scitotenv.2020.137760

Titah, H. S., Abdullah, S. R. S., Idris, M., Anuar, N., Basri, H., Mukhlisin, M., et al. (2018). Arsenic Resistance and Biosorption by Isolated Rhizobacteria from the Roots of *Ludwigia Octovalvis*. *Int. J. Microbiol.* 2018, 1–10. doi:10.1155/2018/3101498

Vance, E. D., Brookes, P. C., and Jenkinson, D. S. (1987). An Extraction Method for Measuring Soil Microbial Biomass C. *Soil Biol. Biochem.* 19, 703–707. doi:10.1016/0038-0717(87)90052-6

Vinhal-Freitas, I. C., Corrêa, G. F., Wendling, B., Bobuľská, L., and Ferreira, A. S. (2017). Soil Textural Class Plays a Major Role in Evaluating the Effects of Land Use on Soil Quality Indicators. *Ecol. Indicators.* 74, 182–190. doi:10.1016/j.ecolind.2016.11.020

Wang, L., Chen, L., Guo, B., Tsang, D. C. W., Huang, L., Ok, Y. S., et al. (2020a). Red Mud-Enhanced Magnesium Phosphate Cement for Remediation of Pb and as Contaminated Soil. *J. Hazard. Mater.* 400. doi:10.1016/j.jhazmat.2020.123317

Wang, L., Ma, L., and Yang, Z. (2018). Spatial Variation and Risk Assessment of Heavy Metals in Paddy Rice from Hunan Province, Southern China. *Int. J. Environ. Sci. Technol.* 15, 1561–1572. doi:10.1007/s13762-017-1504-y

Wang, Q., Garrity, G. M., Tiedje, J. M., and Cole, J. R. (2007). Naïve Bayesian Classifier for Rapid Assignment of rRNA Sequences into the New Bacterial Taxonomy. *AEM* 73, 5261–5267. doi:10.1128/aem.00062-07

Wang, R., Hou, D., Chen, J., Li, J., Fu, Y., Wang, S., et al. (2020b). Distinct Rhizobacterial Functional Assemblies Assist Two *Sedum Alfredii* Ecotypes to Adopt Different Survival Strategies under Lead Stress. *Environ. Int.* 143, 105912. doi:10.1016/j.envint.2020.105912

Wang, S., and Mulligan, C. N. (2006). Natural Attenuation Processes for Remediation of Arsenic Contaminated Soils and Groundwater. *J. Hazard. Mater.* 138, 459–470. doi:10.1016/j.jhazmat.2006.09.048

Wang, Y.-J., Chen, Z., Liu, P.-P., Sun, G.-X., Ding, L.-J., and Zhu, Y.-G. (2016). Arsenic Modulates the Composition of Anode-Respiring Bacterial Community during Dry-Wet Cycles in Paddy Soils. *J. Soils Sediments.* 16, 1745–1753. doi:10.1007/s11368-016-1369-6

Wang, Y., Zhao, Q. L., Hu, Y., Du, X., Ge, Wei., and Liu, W. J. (2011). Survey and Contamination Assessment of Heavy Metals in Soil and Plants Around the Pb/Zn Mine in Shangyu, Zhejiang Province (In Chinese). *Environ. Chem.* 30, 1354–1360.

Wang, Z., Zhang, B., He, C., Shi, J., Wu, M., and Guo, J. (2021). Sulfur-based Mixotrophic Vanadium (V) Bio-Reduction towards Lower Organic Requirement and Sulfate Accumulation. *Water Res.* 189, 116655. doi:10.1016/j.watres.2020.116655

Xiao, X.-Y., Wang, M.-W., Zhu, H.-W., Guo, Z.-H., Han, X.-Q., and Zeng, P. (2017). Response of Soil Microbial Activities and Microbial Community Structure to Vanadium Stress. *Ecotoxicology Environ. Saf.* 142, 200–206. doi:10.1016/j.ecoenv.2017.03.047

Xu, X., Zhang, Z., Hu, S., Ruan, Z., Jiang, J., Chen, C., et al. (2017). Response of Soil Bacterial Communities to Lead and Zinc Pollution Revealed by Illumina MiSeq Sequencing Investigation. *Environ. Sci. Pollut. Res.* 24, 666–675. doi:10.1007/s11356-016-7826-3

Xu, Y., He, Y., Zhang, Q., Xu, J., and Crowley, D. (2015). Coupling between Pentachlorophenol Dechlorination and Soil Redox as Revealed by Stable Carbon Isotope, Microbial Community Structure, and Biogeochemical Data. *Environ. Sci. Technol.* 49, 5425–5433. doi:10.1021/es505040c

Xu, Y., Seshadri, B., Bolan, N., Sarkar, B., Ok, Y. S., Zhang, W., et al. (2019). Microbial Functional Diversity and Carbon Use Feedback in Soils as Affected by Heavy Metals. *Environ. Int.* 125, 478–488. doi:10.1016/j.envint.2019.01.071

Xu, Y., Seshadri, B., Sarkar, B., Wang, H., Rumpel, C., Sparks, D., et al. (2018). Biochar Modulates Heavy Metal Toxicity and Improves Microbial Carbon Use Efficiency in Soil. *Sci. Total Environ.* 621, 148–159. doi:10.1016/j.scitotenv.2017.11.214

Yan, C. C., Wang, F., Geng, H. H., Liu, H. J., Pu, S. Y., Tian, Z. J., et al. (2020). Integrating High-Throughput Sequencing and Metagenome Analysis to Reveal the Characteristic and Resistance Mechanism of Microbial Community in Metal Contaminated Sediments. *Sci. Total. Environ.* 707, 11. doi:10.1016/j.scitotenv.2019.136116

Yang, Y., Campbell, C. D., Clark, L., Cameron, C. M., and Paterson, E. (2006). Microbial Indicators of Heavy Metal Contamination in Urban and Rural Soils. *Chemosphere* 63, 1942–1952. doi:10.1016/j.chemosphere.2005.10.009

Yu, Z. J., Liu, X. D., Zeng, X. B., Yin, H. Q., and Zeng, W. M. (2020). Effect of Arsenic Pollution Extent on Microbial Community in Shimen Long-Term Arsenic-Contaminated Soil. *Water Air Soil Poll.* 231 (7), 340. doi:10.1007/s11270-020-04716-6

Zhang, J., Li, H., Zhou, Y., Dou, L., Cai, L., Mo, L., et al. (2018). Bioavailability and Soil-To-Crop Transfer of Heavy Metals in Farmland Soils: A Case Study in the Pearl River Delta, South China. *Environ. Pollut.* 235, 710–719. doi:10.1016/j.envpol.2017.12.106

Zhang, X. Y., Zhong, T. Y., Liu, L., and Ouyang, X. Y. (2015). Impact of Soil Heavy Metal Pollution on Food Safety in China. *Plos. One.* 10, 14. doi:10.1371/journal.pone.0135182

Zhao, F.-J., Harris, E., Yan, J., Ma, J., Wu, L., Liu, W., et al. (2013). Arsenic Methylation in Soils and its Relationship with MicrobialarsMAbundance and Diversity, and as Speciation in Rice. *Environ. Sci. Technol.* 47, 7147–7154. doi:10.1021/es304977m

Zhen, Z., Wang, S. B., Luo, S. W., Ren, L., Liang, Y. Q., Yang, R. C., et al. (2019). Significant Impacts of Both Total Amount and Availability of Heavy Metals on the Functions and Assembly of Soil Microbial Communities in Different Land Use Patterns. *Front. Microbiol.* 10, 14. doi:10.3389/fmicb.2019.02293

Zheng, S. N., Wang, Q., Yu, H. Y., Huang, X. Z., and Li, F. B. (2020). Interactive Effects of Multiple Heavy Metal(loid)s on Their Bioavailability in Cocontaminated Paddy Soils in a Large Region. *Sci. Total. Environ.* 708, 8. doi:10.1016/j.scitotenv.2019.135126

Zhong, X., Chen, Z. W., Li, Y. Y., Ding, K. B., Liu, W. S., Liu, Y., et al. (2020). Factors Influencing Heavy Metal Availability and Risk Assessment of Soils at Typical Metal Mines in Eastern China. *J. Hazard. Mater.* 400. 123289. doi:10.1016/j.jhazmat.2020.123289

Zhu, N., Qiao, J., and Yan, T. (2019). Arsenic Immobilization through Regulated Ferrolysis in Paddy Field Amendment with Bismuth Impregnated Biochar. *Sci. Total Environ.* 648, 993–1001. doi:10.1016/j.scitotenv.2018.08.200

Zou, L., Zhang, S., Duan, D., Liang, X., Shi, J., Xu, J., et al. (2018). Effects of Ferrous Sulfate Amendment and Water Management on Rice Growth and Metal(loid) Accumulation in Arsenic and Lead Co-contaminated Soil. *Environ. Sci. Pollut. Res.* 25, 8888–8902. doi:10.1007/s11356-017-1175-8

Conflict of Interest: The authors declare that the research was conducted in the absence of any commercial or financial relationships that could be construed as a potential conflict of interest.

frontiers in Environmental Science

ORIGINAL RESEARCH
published: 29 April 2021
doi: 10.3389/fenvs.2021.656271

Polycyclic Aromatic Hydrocarbons and Potentially Toxic Elements in Soils of the Vicinity of the Bulgarian Antarctic Station "St. Kliment Ohridski" (Antarctic Peninsula)

Evgeny Abakumov[1]*, *Timur Nizamutdinov*[1], *Rossitsa Yaneva*[2] and *Miglena Zhiyanski*[2]

[1]Department of Applied Ecology, Biological Faculty, Saint Petersburg State University, Saint-Petersburg, Russia, [2]Forest Research Institute–Bulgarian Academy of Sciences, Sofia, Bulgaria

The investigation conducted was dialed to quantitative and qualitative evaluation of 15 priority polycyclic aromatic hydrocarbons (PAHs) and Potentially Toxic Elements (Cu, Pb, Zn, Cd, Ni, and Cr) is soils and cryoconites on "St. Kliment Ohridski" Antarctic station territory and its vicinities. Estimation of benzo(a)pyrene (BaP)–equivalents, PAHs and different PAHs isomer pair ratios were used for identification of general toxicity, nature and origin of individual PAHs and their groups. Total concentrations of PAHs in BaP–equivalents showed, that $\sum_{15}$PAH of all selected points was higher than the threshold concentration (20 μg × kg^{-1}–Russian environmental legislation) for benzo(a) pyrene. Different PAHs isomer ratios showed the natural (petrogenic) source of PAHs at all soils examples (except Cryosol Toxic Transportic). The maximum content among potentially toxic elements was recorded for Zn (75.7 mg × kg^{-}1 at L26), the minimum for Cd (0.201 mg × kg^{-1} at L1A). Average concentrations of potentially toxic elements are generally lower compared to the results of previous studies. Application of I_{geo} index, characterizes the majority of the studied soils as unpolluted or practically unpolluted. Data obtained indicates that there is no current critical anthropogenic load on the environmental components of the landscapes investigated.

Keywords: livingston island, isomer ratios, trace metals, pollution assessment, geoaccumulation index, sources

OPEN ACCESS

Edited by:
Zhu Li,
Institute of Soil Science (CAS), China

Reviewed by:
Omar Richard Harvey, Texas Christian University, United States
Tatiana Minkina, Southern Federal University, Russia

***Correspondence:**
Evgeny Abakumov
e_abakumov@mail.ru

Specialty section:
This article was submitted to Soil Processes, a section of the journal Frontiers in Environmental Science

Received: *20 January 2021*
Accepted: *12 April 2021*
Published: *29 April 2021*

Citation:
Abakumov E, Nizamutdinov T, Yaneva R and Zhiyanski M (2021) Polycyclic Aromatic Hydrocarbons and Potentially Toxic Elements in Soils of the Vicinity of the Bulgarian Antarctic Station "St. Kliment Ohridski" (Antarctic Peninsula). Front. Environ. Sci. 9:656271. doi: 10.3389/fenvs.2021.656271

INTRODUCTION

Nowadays the Antarctica is one of the most interesting and informative environmental model for evaluation of possible contaminants accumulation in pristine ecosystems. This territory was not intensively affected by human and therefore it can be used as reference area for adaptation and harmonization of threshold concentrations and evaluation of current contamination rates (Tin et al., 2009).

The challenges of nature conservation in Antarctica indicated in the Protocol on Environmental Protection (Madrid Protocol, 1998), faced with the necessity of regulation and implementation of environmental management in vicinities of the Antarctic stations with aim to decrease of hydrocarbons combustion effects and further accumulation of polycyclic aromatic compounds in the components of cryogenic ecosystems of Antarctica. In order to understand the amount of combusted fuel at the stations, data of the expedition of the Bulgarian Antarctic Institute in

2012–2013 can be exampled and taken into account for further evaluation. With aim to support the expedition, 5000 L of diesel liquid fuel were brought to the «St. Kliment Ohridski » station (December 14, 2012–February 25, 2013) (BAI, 2013). Other authors noted that the stations of the year-round stay (station Bellingshausen) can spend up to 150 000 L of diesel fuel per year (Abakumov et al., 2015).

The use of fossil fuels with current techniques leads to regular spilling of oil products that contaminate the surface and soils of terrestrial environments, inland and oceanic waters (Kennicutt et al., 1991; Waterhouse, 2001; Aislabie et al., 2004; Frenot et al., 2005). Numerous logistic aspects in Antarctic region result in waste disposal management, which often leads to the sporadic transportation of the untreated sewage into the ocean and on the territory around the stations (Connor, 2008; Tin et al., 2009; Martins et al., 2010).

Data obtained in previous researches showed that the large fuel spills from transport and tourist vessels have been occurring since the 80s of the 20th century. For example, in 1987 there was a spilling effect of 600,000 L diesel fuel near United States Palmer Station, Antarctic Peninsula (Aronson et al., 2011). The spills of hydrocarbon compounds and exhaust gases are the cause of chemical contamination the terrestrial Antarctic ecosystems, which is the most characteristic environmental impact of human activities in Antartica Chen and Blume (1997), Aislabie et al. (2004), Bargagli (2006) Several chemical and biological studies conducted recently have shown the presence of atypical chemical contaminants such as Potentially Toxic Elements (PTEs), Polychlorinated Biphenyl (PCB) Polycyclic Aromatic Hydrocarbons (PAHs) and Polychlorinated Dibenzodioxins (PCDDs) in soils, coastal waters, micro and macroorganisms (Snape et al., 2001; Negri et al., 2006; Hale et al., 2008; Martins et al., 2010; Abakumov et al., 2014; Abakumov et al., 2015; Pourret and Hursthouse, 2019).

Human and animal activities played an important role in PAHs distribution in the soil (Na et al., 2020). Among chemical pollutants, polycyclic aromatic hydrocarbons (PAHs) and trace metals have a special place, as they can enter the Antarctic not only through local discharges and emissions, but also through transboundary transfer from tropical and temperate regions of the southern hemisphere (Aislabie et al., 1999; Bargagli, 2006; Bargagli, 2008; Abakumov et al., 2014). Polycyclic aromatic hydrocarbons represent organic compounds of benzene series differing in the number and position of benzene rings showed mutagenic and carcinogenic effects. The higher molecular weight PAHs (MW > 202) with 4–6 benzene rings are frequently related to burning processes and are highly toxic to organisms due to their carcinogenic and mutagenic potential (Yunker et al., 2002; Yang et al., 2008; Martins et al., 2010). PAHs are known as mobile compounds that tend to be dispersed in the biosphere. There are PAHs of natural and anthropogenic origin that are included in the permanent monitoring list by the EU and United States Environmental Protection Agency (Baek et al., 1991; Nisbet and Lagoy, 1992; Howsam and Jones, 1998). In the Polar Regions with low temperatures, PAHs are less subjected to microbial degradation; therefore, they are deposited and preserved in soils and cryoconite (Lodygin et al., 2008; Hodson, 2014; Abakumov et al., 2015; Cook et al., 2016).

The proportion (isomer pair ratios) between concentrations of natural and anthropogenic PAHs can serve as an index of the anthropogenic influences of soil and can used as tracers to identify possible sources of PAH (Pandey et al., 1999; Yunker et al., 2002; Li et al., 2017).

Potentially Toxic Elements can be transported over long distances through the atmospheric circulation, and eventually deposited through dry and wet deposition to the Antarctic regions (Bargagli, 2006, 2008; Trevizani et al., 2018; Liu et al., 2021). They were determined in fossil fuels contaminated soils in different regions of Antarctica (Padeiro et al., 2016; Smykla et al., 2018; Alekseev and Abakumov, 2020; Gran-Scheuch et al., 2020). Also these elements have carcinogenic and mutagenic effects and can damage cellular membranes, proteins, enzymes, and DNA (Beyersmann and Hartwig, 2008; Ali et al., 2013; Padeiro et al., 2016).

The main goal of this work is to estimate the level of pollution of soils and cryoconites with potentially toxic elements and polycyclic aromatic hydrocarbons on the territory of the Bulgarian Antarctic Station "St. Kliment Ohridski" and its vicinity (Livingstone Island, South Shetland Islands, Antarctic Peninsula). In abovementioned context this research was aimed: 1) to estimate the concentrations of 15 PAHs and 6 potentially toxic elements, 2) to assess the contamination of soils with PAHs, their benzapyrene equivalents were calculated, as well as to calculate various isomeric ratios of PAHs, in order to identify their possible source of origin and 3) to assess the nature of soil contamination by potentially toxic elements, we calculated a geoaccumulation index (*Igeo*).

MATERIALS AND METHODS

The study was performed on 11 soil and cryoconite samples taken at the Bulgarian Antarctic Station "St. Kliment Ohridski" on Livingston Island (region of Antarctic Peninsula, Western Antarctica) during the Bulgarian Antarctic expedition realized form December 21, 2019 till January 6, 2020. The precise coordinates of the sampling points and geographic description of the area are presented in **Table 1**.

The soils were collected from the 0–10 cm depth and cryconites from cryoconite holes, all samples were saved in polyethylene bags, then was transported to the station laboratory air dried, after what the artificial remnants and roots have been removed, soils have been sieved through 2 mm and transported to Saint-Petersburg State University laboratories in polyethylene bags.

The Livingston Island is locating at 62°38′29″S and 60°21′53″W (**Figure 1**). The "St. Kliment Ohridski" station situated 88 km southwest of station Bellingshausen (King George Island), 796 km southeast of Diego Ramirez Islands (the southernmost land of South America), 2,96 km of Spanish summer station "Juan Carlos I", 28, 55 km from Chilean–United States station "Shirreff Base" (Ivanov, 2015).

TABLE 1 | Sampling points coordinates, geographic description and soil type of the study area (WRB, 2015).

No of point	Name	Coordinates	Sea altitude, m	Sampling site description. Soil name.
1	L1E	S 62° 38' 49.4" W 60° 22' 17.2"	35	Sea Lion Hill. Under the skua nest, close to the lake Sea Lion. No presence of sulfur is identified, folic, ornitic.
2	L1A			Soil name: Cryosoils, not gleyic, Leptic Stagnic
3	L1C			
4	L21	S 62° 38.468'	–	Playa Bulgaria
		W 60° 22.852'		Volcanic black colored material from the cryoconite hole
5	L28	S 62° 39.245'	4	Hanna Point. 2 soil pits: under Deschampsia (*Deschampsia antarctica*) and under Praciola crispa (*Colobanthus quitensis*).
		W 60° 36.442'		Soil name: Cryosol Leptic Ornitic Hypersceletic
6	L10	S 62°38.872'	458	Krumov Kamak.
		W 60°20.701'		Rock formation surrounded by glacier.
				Soil name: Cryosols Turbic Regolith without any additional indicators
7	L6	S 62°38.180'	5	Española Hill. Location on recently formed ornitogenic environment on the seacoast mall, parent materials composed by sandy textured fine earth and oval stones of marine genesis.
		W 60°21.493'		Soil name: Cryosols ornitic
8	L26	S 62°38'29"	–	Main House.
		W 60°21'53"		Soil name: Cryosol Toxic Transportic
9	L2	S 62°38'06.9"	1	Sinemorets Hill. NW part of Playa Bulgara top of the hill ridge, no vegetation, sporadic distribution of the lichens, flat areas, surrounded by big remnants of weathering of rocky parent materials, close to the lake; surface, covered by angular stones of irregular form.
		W 60°21'14.7"		Soil name: Cryosol Turbic Gleyic
10	L22	S 62° 39.251'		Hanna point
		W 60° 36.531'		Volcanic black colored material from the cryoconite hole
11	L9	S 62°38.073'	4	End of the Bay. First marine terrace covered by mosses, Deschampsia (*Deschampsia antarctica*). The terrace is composed by debris, many fine sediments and tephra, mixed with angular and oval stones. Indication of complicated genesis.
		W 60°20.962′		Soil name: Cryosols Leptic Folic (Umbric)

The first permanent (no wintering) station on Livingston Island was the Spanish one "Juan Carlos I" (62°39'46"S, 60°23'20"W), built from 7 to January 11, 1988 (Ivanov, 2015). Another scientific base on Livingston Island is the Chilean–United States facility Shirreff Base (62°28'12"S, 60°46'17"W), with its two sections named Guillermo Mann Base and Shirreff Field Station, and opened in 1990/91 and 1996/97, respectively, (CEP, 2011). The Bulgarian station appeared a few years later than the Spanish one. The "St. Kliment Ohridski" base was opened during the 1993/94-summer season on the Livingston Island. Infrastructure of station includes kitchen, messroom, living rooms, food storage, toilets and bathrooms.

All three bases are permanent settlements, although inhabited only during the summer season, with accommodation capacity for a total of 54 persons. In particular, most of the solid waste is shipped for dumping outside Antarctica, with incineration gradually phased out. As elsewhere in Antarctica, the island's bases use electricity produced mostly by diesel generators (Ivanov, 2015).

The Geoaccumulation Index (I_{geo}) allows us to classify seven levels (**Table 2**) of soil contamination, from Practically unpolluted ($I_{geo} \leq 0$) to Extremely polluted ($I_{geo} > 5$) (Muller, 1979; Jiang et al., 2019). The generic calculation formula is as follows:

$$I_{geo} = \log_2\left(\frac{C_n}{1.5B_n}\right) \quad (1)$$

where C_n–the measured concentration of the element in soil, B_n–the geochemical background value.

The content of Potentially Toxic Elements was determined following the standard ISO 11047–1998 "Soil Quality-Determination of Cadmium (Cd), Cobalt (Co), Copper (Cu), Lead (Pb), Manganese (Mg), Nickel (Ni), and Zinc (Zn) in Aqua Regia Extracts of Soil - Flame and Electrothermal Atomic Absorption Spectrometric" method at Atomic absorption spectrophotometer Kvant 2M (Moscow, Russia) (ISO, 1998).

The concentrations of 15 PAHs–naphthalene (NAP), acenaphthene (ANA), fluorene (FLU), phenanthrene (PHE), anthracene (ANT), fluoranthene (FLT), pyrene (PYR), benzo(a)anthracene (BaA), chrysene (CHR), benzo(b) fluoranthene (BbF), benzo(k)fluoranthene (BkF), 3,4-benzo(a) pyrene (BaP), dibenzo (a,h)anthracene (DBA), dibenzo (g,h,i) perylene (BPE), and indeno (1,2,3-c,d) pyrene (IPY) in soils and cryoconites on the territory of Bulgarian Antarctic base and its vicinities were determined on the basis of State Standard (GOST R 8.563–96), which is based on method Flyuorat-02-Panorama, Russia (GOST, 1996).

Extraction of PAHs was carried out at room temperature with a mixture of hexane-acetone (1:1) with ultrasonic treatment of the extraction system in an ultrasonic bath Branson 5510 (United States) (EPA, 2007). PAHs fraction was cleaned by using column chromatography on silica gel (SW, EPA, 1996). Qualitative and quantitative determination of PAHs in soils was carried out by the method of reversed-phase high-efficiency liquid chromatography in the gradient mode and

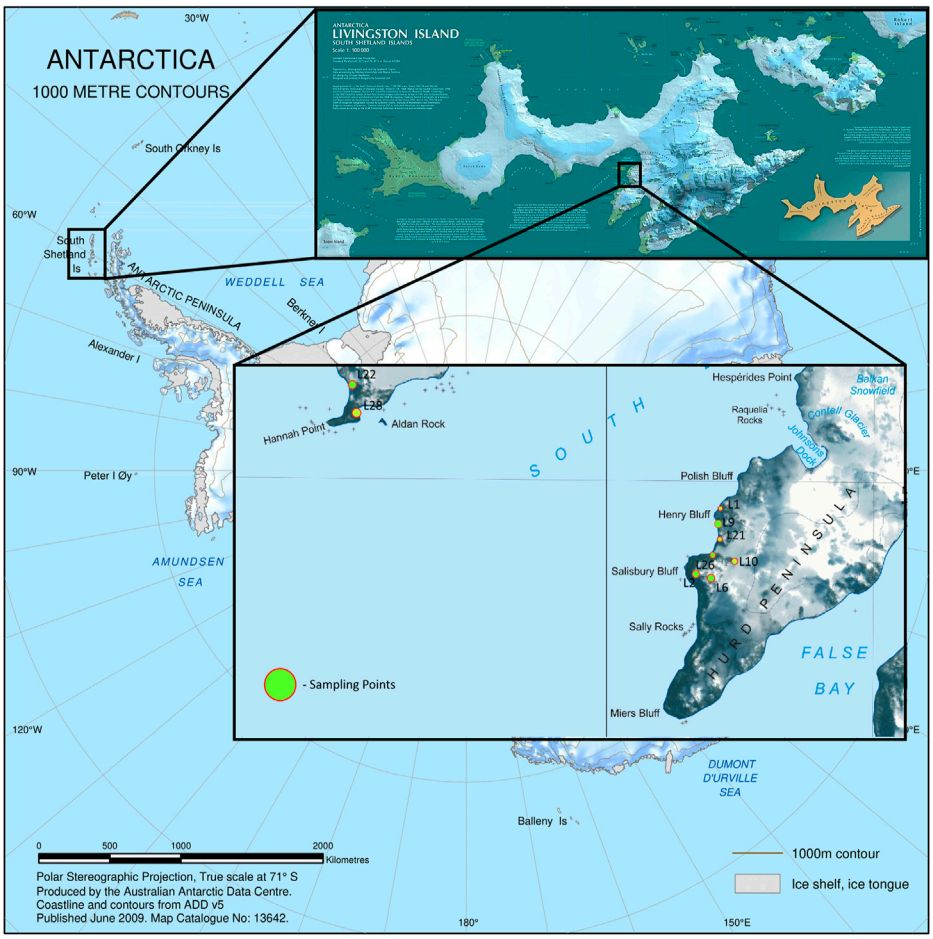

FIGURE 1 | Location map of St. Kliment Ohridski station (AAD, 2009; Ivanov, 2015).

TABLE 2 | Classification of I_{geo} value

			References
Classification	$I_{geo} \leq 0$	Practically unpolluted	Muller (1979), Jiang et al. (2019)
	$0 < I_{geo} \leq 1$	Uncontaminated to slightly polluted	
	$1 < I_{geo} \leq 2$	Moderately polluted	
	$2 < I_{geo} \leq 3$	Moderately to highly polluted	
	$3 < I_{geo} \leq 4$	Highly polluted	
	$4 < I_{geo} \leq 5$	Highly to extremely polluted	
	$I_{geo} > 5$	Extremely polluted	

spectrofluorometric detection on the chromatograph "Lumahrom" ("Lumex", Russia). Chromatography was performed at a temperature of 30°C on a column of Supelco Supelcosil ™ LC-PAH 5 μm (25 cm × 2.1 mm). The acetonitrile–water gradient was used as a mobile phase. Sample volume of 10 μl was introduced with the help of a dosing crane. Individual PAHs were identified with chromatography mass spectrometry (spectrograph model: Shimadzu QP 5050A, Japan) (Gilichinsky et al., 2010). The detection limits of the studied PAHs are: NAP–16 μg × kg^{-1}; ANA–1.5 μg × kg^{-1}; FLU–1.4 μg × kg^{-1}; PHE–2.0 μg × kg^{-1}; ANT–0.3 μg × kg^{-1}; FLT–6.7 μg × kg^{-1}; PYR–6.7 μg × kg^{-1}; BaA–1.5 μg × kg^{-1}; CHR–0.8 μg × kg^{-1}; BbF–1.4 μg × kg^{-1}; BkF–0.3 μg × kg^{-1}; BaP–0.3 μg × kg^{-1}; DBA–1.8 μg × kg^{-1}; BPE–1.6 μg × kg^{-1}; IPY–6.7 μg × kg^{-1}. Identification of PAHs was carried out by retention times and comparison of fluorescence spectra of components released the column with standard PAHs spectra. The quantitative analysis of PAHs was carried out using the external standard method. To assess the accuracy of the method, the above-described analytical procedure

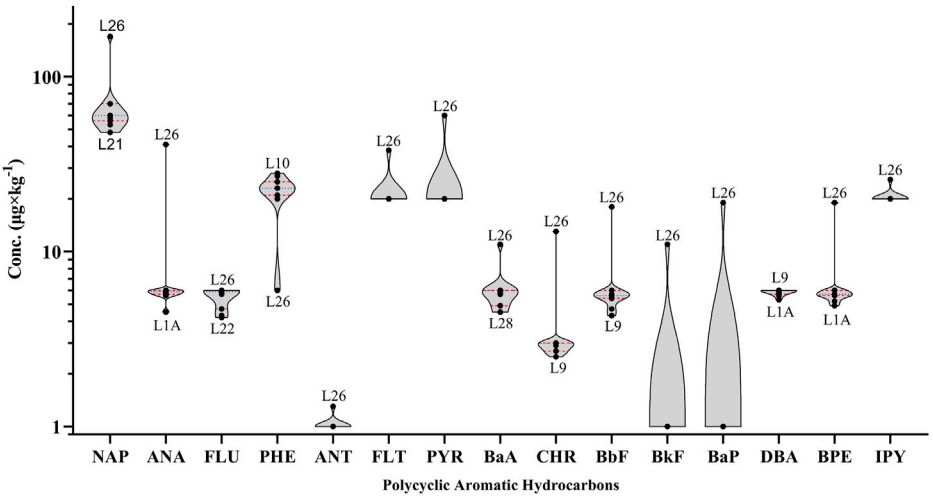

FIGURE 2 | PAHs concentrations in soils, μg × kg^{-1}.

was subjected to the standard of bottom sediments containing surfactants (Standard Reference Material® 1944 New York/New Jersey Waterway Sediment -NIST, United States) (Agency, 1986; PND, 2003; Gabov et al., 2007; Gabov et al., 2008).

Statistical data processing and visualization was performed using Statsoft Statistica 12, GraphPad Prizm 9.0.0 and QGIS 3.16.

RESULTS AND DISCUSSION

Concentration and Origin of PAHs

Some data on detected PAHs concentrations in soils of Livingstone Island (Bulgarian Antarctic Station "St. Kliment Ohridski" and its vicinity) are given in the **Figure 2**. It should be noted that at all sampling points (except L26) the differences in concentrations are minor. For example, naphthalene content in non-toxic soils types varies from 48 to 70 μg × kg^{-1}, phenanthrene (PHE) from 20 to 28 μg × kg^{-1} (**Figure 2**). Concentrations of other PAHs in all natural soils are almost the same. Calculated index $\sum_{15}$PAHs for all selected samples of natural soil ranged from 170 to 200 μg × kg^{-1}. $\sum 7_{carcinogenic}$PAHs (CHR, BbF, BkF, BaP, DBA, BPE, IPY) is 37 μg × kg^{-1}.

The following concentrations of PAHs in soils which are not subject to anthropogenic influence were noted in the earlier research in different regions of Antarctica. McMurdo Dry Valley (control site): NAP <30 μg × kg^{-1}, ANA <30 μg × kg^{-1}, PHE <30 μg × kg^{-1}, FLU <30 μg × kg^{-1}, ANT <30 μg × kg^{-1}, FLT <30 μg × kg^{-1}, PYR <30 μg × kg^{-1}, BaA <30 μg × kg^{-1} (Aislabie et al., 1999). Admiralty Bay, King George Island: Ulmann Point ∑PAHs <10 μg × kg^{-1}, Botany Point ∑PAHs <30 μg × kg^{-1}, Monsimet Cove ∑PAHs <15 μg × kg^{-1} for some higher molecular PAHs (FLU, PYR, BaA, CHR, BkF, BbF, BaP, IPY, DBA, BPE) (Martins et al., 2010).

The content of PAHs in the vicinity of Russian Antarctic stations was studied by Abakumov et al. (2015); in these works, the list of identified PAHs is similar to our work. Haswell Archipelago: $\sum_{15}$PAHs = 22.8 μg × kg^{-1}. Hudson Mountains: $\sum_{15}$PAHs = 33.9 μg × kg^{-1}. Vicinity of Leningradskaya station $\sum_{15}$PAHs = 21.7 μg × kg^{-1}. The vicinities of Mirny station $\sum_{15}$PAHs = 90.9 μg × kg^{-1} (Abakumov et al., 2015).

PAHs concentrations in Antarctica are often from soils and sediments located in highly contaminated areas where accidental spills have occurred, or close to research stations (Cabrerizo et al., 2012). On the Admiralty Bay, King George Island, Antarctica the maximum PAHs (high molecular PAHs (FLU, PYR, BaA, CHR, BkF, BbF, BaP, IPY, DBA, BPE)) concentration at Ferraz station occurred at 3.5 cm soil layer (454.9 μg × kg^{-1}). The PAHs isomer pair ratio analysis showed that the major sources of PAHs are fossil fuels/petroleum (gasoline and diesel). The authors suggested that this may be related to activities at British station "G" in 1960s (established at the location of the Ferraz station). In areas of Admiralty Bay with less anthropogenic impact PAHs content is significantly lower (from 11.8 to 270.5 μg × kg^{-1}) (Martins et al., 2004; Martins et al., 2010).

In the McMurdo Dry Valley region around Scott Base, Marble Point and the Wright Valley near Lake Vanda, $\sum_{15}$PAHs (same with our PAHs list) content of fuel oil-contaminated soils ranged from 41 to 8105 μg × kg^{-1} of dried soil. At the Scott Base PAHs levels of 362 μg × kg^{-1} in drum storage site were detected in the 0–2 cm surface soil layer compared with 8105 μg×kg^{-1} in the 2–10 cm depth and 2543 μg × kg^{-1} in the deeper 20–30 cm layer. At McMurdo Dry Valley reference points PAHs concentrations ranged from 15 to 45 μg × kg^{-1} dry weight (Aislabie et al., 2004).

Previous investigations in anthropogenic loaded areas in Antarctica have reported PAHs levels in soils in the vicinity of stations Bellingshausen and Henryk Artstowski (King George Island, South Shetland Islands) and station Academician Vernadsky (Galindez Island, Argentinian Islands). At some points around the station Academician Vernadsky, the content of $\sum_{15}$PAHs (same with our PAHs list) reaches 94771.2 μg × kg^{-1}. The maximum level of contamination is observed near the aerology building and diesel station, the contribution of HMW

PAHs exceeds 20%. At Bellingshausen station the maximum content of $\sum_{15}$PAHs in soil at the diesel station is up to 911 μg × kg^{-1}, with a higher contribution of HMW PAHs. In the vicinity of the Henryk Artstowski station $\sum_{15}$PAHs content ranges from 114 to 188.3 μg × kg^{-1} (Abakumov et al., 2014; Abakumov et al., 2015).

Previously, investigations of PAHs content in different regions and climatic conditions have already been conducted. The values of $\sum_{15}$PAHs (same with our list) ranged from 36.9 to 323 μg × kg^{-1} (dry weight) in soil (HMW PAHs prevailed), from 154 to 231 μg × kg^{-1} in moss, and from 48 to 333 μg × kg^{-1}in reindeer dung at Ny-Ålesund, Svalbard in the Arctic (Wang et al., 2009).

For a comparative assessment, it is important to cite the results of some studies of PAH content in soils of anthropogenic-loaded urbanized areas. Investigations of $\sum_{15}$PAHs (same with our PAHs list) content in soils of urbanized areas show the following results: Ljubljana 218–4,490 μg × kg^{-1}, Torino 148–3,410 μg × kg^{-1}, while soil samples from Glasgow show very high values 1490–5,1800 μg × kg^{-1}. Analyzed PAHs ratios indicated pyrogenic origin of chemicals as result of anthropogenic contribution (Morillo et al., 2007). The range concentrations of Σ_{16}PAHs [16 USEPA priority PAHs (identical to our list, but also includes Acenaphtylene)] in urban soils in Clay county, Ocala, Pensacola, and West Palm Beach were, respectively, 797–7909, 950–1,1451, 922–1,7698, and 1,133–3,0691 μg×kg^{-1}. PAHs sources in urban soils of Pensacola were dominated by vehicle emissions, those in Ocala and West Palm Beach were dominated by biomass combustion, and those in Clay county were dominated by petrogenic sources (Gao et al., 2019). In soils of Vasilievsky Island in St. Petersburg were detected extremely high concentrations of PAHs. The concentration of Σ_{15}PAHs (same with our PAHs list) is getting to the level 8,200 μg × kg^{-1}. The maximum PAH concentrations were detected in the soil along the highway with heavy traffic and considerable emission of combustion gases (Lodygin et al., 2008). It is well seen that the PAH content in soils subjected to permanent anthropogenic load is significantly higher compared to almost all the results obtained for the Antarctic territories.

In our investigation at the point with the highest anthropogenic load (L26, main house) $\sum_{15}$PAHs equals 445,1 μg × kg^{-1} (highest contribution: NAP 170 μg × kg^{-1}, PYR 60 μg × kg^{-1}, ANA 41 μg × kg^{-1}). At the other points $\sum_{15}$PAHs from 170 to 200 μg × kg^{-1} (Highest contribution: NAP 48–70 μg × kg^{-1}, PHE 20–28 μg × kg^{-1}). Compared with the studies mentioned above, it should be recognized that the anthropogenic load on the vicinities of Bulgarian Antarctic Station is not critical. It should be noted that station St. Kliment Ohridski is inhabited only in summer, unlike the other Antarctic stations (station Bellingshausen, station Academician Vernadsky, station Henryk Artstowski, station Scott Base, station Ferraz). This certainly has a positive effect on the anthropogenic impact on the vicinity of the station.

Based on the obtained data, it could be concluded that baseline sources for PAHs in Cryosols of Livingstone Island are found.

Particular attention should be paid to PAHs concentrations at the sampling point L26 (Hanna Point, Main House.) This point is located directly at the station "St. Kliment Ohridski". The soil type here is referred to Cryosol Toxic Transportic (WRB, 2015). $\sum_{15}$PAHs at this point is 455.1 μg × kg^{-1} (the main contribution is formed by: NAP 170 μg × kg^{-1}, PYR 60 μg × kg^{-1}, ANA 41 μg × kg^{-1}, FLT 38 μg × kg^{-1}, IPY 25.8 μg × kg^{-1}, BaP 19 μg × kg^{-1} (**Figure 2**). $\sum 7_{carcinogenic}$PAHs is 92.8 μg × kg^{-1}. Values of PAHs concentrations in the Toxic soil are much higher in comparison with the other studied natural soils.

Normally, PAHs can associate not only combustion processes but they are also found in sewage effluents, small oil spillages and natural sources including petroleum seeps (Martins et al., 2010). In order to identify the source of PAHs origin, different PAHs isomer pair ratios were calculated. This method of identification shows itself as a reliable and widely used in studies to identify the nature of the origin of PAHs (Yunker et al., 2002). Used PAH isomer pair ratios are shown in the **Table 3**.

Analyzing the results of PAHs isomer pair ratios calculations (**Table 4**) conclusions about the nature of PAHs origin in soils and cryoconites in the Bulgarian Antarctic Station "St. Kliment Ohridski" and its vicinity could be outlined.

The value of the ratio $\sum_{Pyr}$PAHs/$\sum_{15}$PAHs showed that all of the PAHs studied are results of petroleum spills, combustion processes or products of a baseline source. However, this indicator is too general and in order to better understand the processes of PAHs origin, it should rely on the results of previous ratio calculations. Also the ratio ∑ LMW PAHs/∑ HMW PAHs has shown that PAHs at all sampling points (except L21) have petrogenic origin.

The ANT/(ANT + PHE) value shows that all points except L26 have a natural origin (i.e. the Baseline source). At point L26 these PAHs are the result of the combustion processes. FLU/(FLU + PYR) ratio value characterize how as baseline source of this PAHs.

The results obtained by calculating the ratio BaA/(BaA + CHR) and IPY/(IPY + BPE) are of interest. Most often, the authors refer to PAHs as combustion products with results similar to ours (Yunker et al., 2002; Martins et al., 2010). However, Khaustov and Redina (2016) noted that the value of these ratios from 0,19 to 1,0 is typical for the background concentration of PAHs data in soils of northern and middle taiga (Khaustov and Redina, 2016). Since the climatic conditions of Livingstone Island are similar to those of the northern taiga, it should be recognized that the occurrence of these PAHs is linked more to natural than anthropogenic sources. Most sources use these two ratios to identify PAHs in locations with high anthropogenic load (Yan et al., 2006; Jiang et al., 2019; Gardes et al., 2020). Since there is no practice of burning wood fuel, coal and grass under Antarctic conditions, these two ratios have shown controversial results. Also, some researchers notes PAHs concentration in the particle phase was influenced significantly by temperature in the west Antarctic atmosphere (Na et al., 2020). The values of all other obtained isomeric ratios are well matched with the conditions of anthropogenic load and the possible influence of external factors on the nature of the origin of PAHs. The BaP/BPE value that all points except L26 have non-traffic source origin. From the PHE/ANT and FLU/PYR ratio value it can be seen that these PAHs at point L26 are formed as a result of pyrogenic processes, from other samples the

TABLE 3 | Possible PAHs isomer ratios.

PAHs isomer ratios	Range of values	Possible sources of PAH	References
ANT/(ANT + PHE)	<0.10	Petroleum/Baseline source	Yunker et al. (2002), Wang et al. (2009), Tobiszewski and Namieśnik (2012), Shamilishvili et al. (2016)
	>0.10	Indicates a dominance of combustion	
FLU/(FLU + PYR)	<0.40	Most petroleum/Baseline source	Mandalakis et al. (2002), Yunker et al. (2002), Fang et al. (2004), Ravindra et al. (2008), Shamilishvili et al. (2016)
	0.40–0.50	Liquid fossil fuel (vehicle and crude oil) combustion	
	>0.50	Characteristic of grass, wood or coal combustion	
BaA/(BaA + CHR)	<0.20	Petroleum/Baseline source	Yunker et al. (2002), Tobiszewski and Namieśnik (2012), Shamilishvili et al. (2016)
	0.20–0.35	Petroleum, combustion, baseline source	
	>0.35	Combustion	
IPY/(IPY + BPE)	<0.20	Petroleum/Baseline source	Yunker et al. (2002), Shamilishvili et al. (2016)
	0.20–0.50	Liquid fossil fuel (vehicle and crude oil) combustion	
	>0.50	Imply grass, wood and coal combustion	
PHE/ANT	>10	Petrogenic	Budzinski et al. (1997), Khairy et al. (2009)
	<10	Pyrolytic	
FLU/PYR	<1.0	Petrogenic	Budzinski et al. (1997), Khairy et al. (2009)
	>1.0	Pyrolytic	
BaP/BPE	<0.60	Non-traffic source	Pandey et al. (1999), Ravindra et al. (2008)
	>0.60	Traffic source	
∑ PyrPAHs[a]/∑ PAHs	<0.30	Petroleum/Baseline source	Hwang et al. (2004), Balmer et al. (2019)
	0.30–0.70	Petroleum, combustion, baseline source	
	>0.70	Mostly combustion	
∑ LMW PAHs[b]/∑ HMW PAHs[c]	<1	Pyrogenic	Soclo et al. (2000), Zhang et al. (2008), Chunhui et al. (2017)
	>1	Petrogenic	

[a]*pyrogenic PAHs–FLT, PYR, BaA, CHR, BbF, BkF, BaP, BPE, IPY.*
[b]*light molecular weight, 2-3 ring PAHs.*
[c]*heavy molecular weight HMW, 4-6 ring PAHs.*

TABLE 4 | PAHs isomer ratios in studied soils and cryoconites.

	L1E	L21	L28	L10	L6	L1A	L26	L2	L1C	L22	L9
ANT/(ANT + PHE)	0.05	0.05	0.04	0.03	0.04	0.04	0.18	0.04	0.04	0.04	0.04
FLU/(FLU + PYR)	0.23	0.23	0.18	0.19	0.23	0.23	0.09	0.22	0.22	0.17	0.23
BaA/(BaA + CHR)	0.69	0.67	0.63	0.62	0.67	0.67	0.46	0.66	0.60	0.69	0.70
IPY/(IPY + BPE)	0.78	0.77	0.78	0.78	0.77	0.80	0.58	0.77	0.78	0.78	0.79
BaP/BPE	0.18	0.17	0.18	0.18	0.17	0.20	1.00	0.17	0.18	0.18	0.19
PHE/ANT	21.00	20.00	27.00	28.00	23.00	23.00	4.62	23.00	23.00	25.00	23.00
FLU/PYR	0.30	0.30	0.22	0.24	0.30	0.30	0.10	0.29	0.29	0.21	0.30
∑ PyrPAHs[a]/∑ PAHs	0.38	0.41	0.37	0.35	0.39	0.37	0.41	0.35	0.38	0.38	0.37
∑ LMW PAHs[b]/∑ HMW PAHs[c]	0.97	1.10	0.89	0.80	1.00	0.93	0.98	0.84	0.97	0.95	0.93

[a]*pyrogenic PAHs - FLT, PYR, BaA, CHR, BbF, BkF, BaP, BPE, IPY.*
[b]*light molecular weight, 2-3 ring PAHs.*
[c]*heavy molecular weight HMW, 4-6 ring PAHs.*

values are characteristic for petrogenic processes of PAHs formation.

For cross-checking the nature of the origin of PAHs, bi-plots were constructed between some values of the obtained relations (**Figure 3**).

As can be seen in the figure above, the correlation values show high statistical correlation between each other ($r^2 > 0.66$). In all the plotted figures, the soil sample L26, which was sampled directly in the territory of the Antarctic station, stands apart. All PAHs for this soil, which are shown on the visualized ratios, are of pyrogenic (combustion) origin. The existence of PAHs of pyrogenic origin is caused by the incinerator using the diesel fuel used to eliminate waste, as well as by the diesel electric generator that supplies the station with electric power.

BaP-Equivalence of PAHs Concentrations

Taking into account that not all chemical contaminants have maximum permissible concentration (MPC) in soils, especially regional MPCs for Antarctic continent, BaP-equivalence of PAHs concentrations were calculated. Since in the EU and the

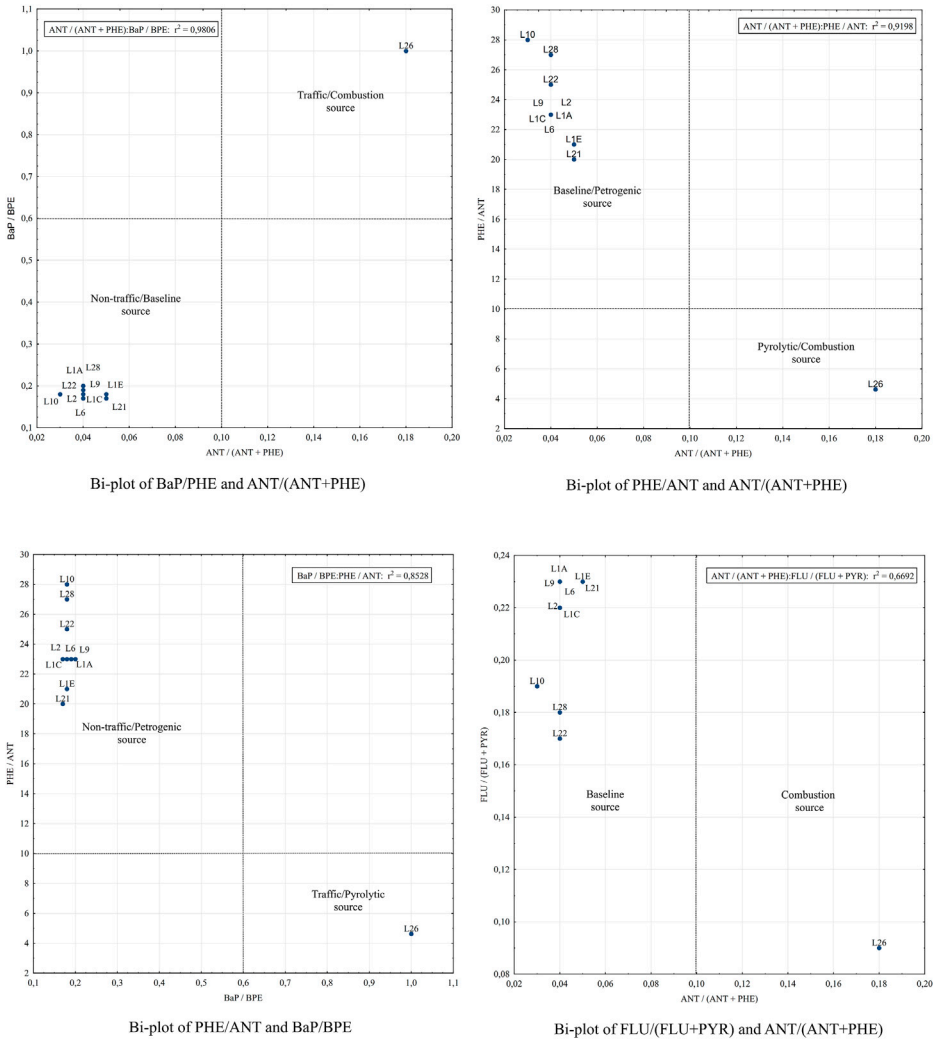

FIGURE 3 | Bi-plots of PAHs isomer ratios.

United States PAHs in various environments are controlled based on the calculation of human health risks, it was decided to use the standards adopted in Russian environmental legislation for convenience.

In Russia, the control of concentrations of various PAHs in the environment is based on monitoring 3-4 benzo(a)pyrene. According to the environmental protection laws, its maximum permissible concentration (MPC) in soil is 20 μg×kg^{-1} (Hygienic Norms, 2006). The methods of calculation of BaP-equivalents are well studied and have long been applied in studies of anthropogenic impact on natural territories (USEPA, 1993; Verbruggen et al., 2001; Jung et al., 2010). The method makes it possible to evaluate the effect of both the PAHs complex and each of them individually (Bari et al., 2010; Jennings, 2012).

BaP-equivalents values were calculated by simply multiplication of PAHs concentrations by Toxic Equivalent Factor (TEF) values (Nisbet and Lagoy, 1992). Benzo(a)pyrene was among the first chemical carcinogens identified more than 70°years ago. Many jurisdiction use TEFs applied to their BaP-equivalents to regulate other PAH (Loeb and Harris, 2008; Jennings, 2012; Shamilishvili et al., 2016).

The values of toxicity of investigated PAHs by 3-4 benzo(a) pyrene are presented on the **Figure 4**. As can be seen from the results obtained, for toxic soil (point L26) BaP-equivalents $\sum_{15}$PAHs is 56.2 μg × kg^{-1}, which is more than 2 times higher than the standards of Russian environmental legislation. The main contribution to BaP-equivalents $\sum_{15}$PAHs is formed by: DBA 30.0 μg × kg^{-1}, BaP 19.0 μg × kg^{-1}, IPY 2.58 μg × kg^{-1}. $\sum 7_{carcinogenic}$PAHs is 54.6 μg × kg^{-1}, which is also more than 2 times higher than the Russian standard. It should be noted that the share of carcinogenic PAHs in BaP-equivalents is more than 90 percent.

For natural Antarctic soils the proportion of different PAHs in BaP – equivalents are significantly different from toxic soil sample. For almost all samples of natural soil $\sum_{15}$PAHs in BaP-equivalents is close to 34 μg × kg^{-1}. The main

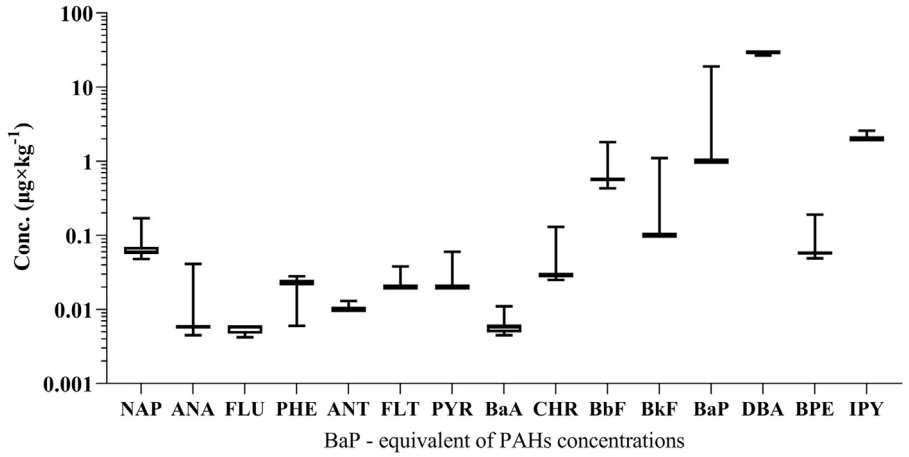

FIGURE 4 | PAHs concentrations in BaP–equivalent, μg × kg^{-1}.

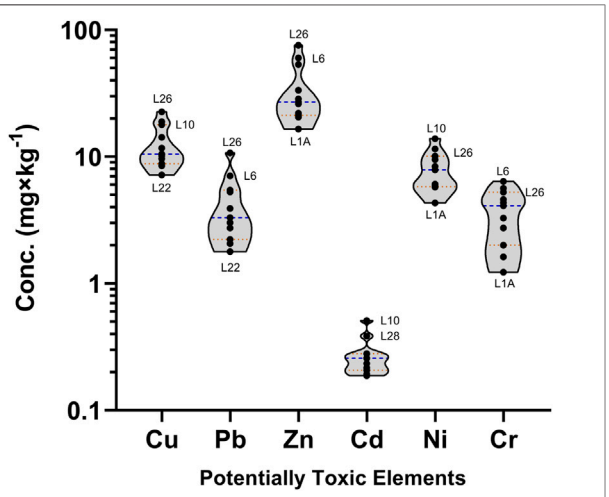

FIGURE 5 | Content of Potentially Toxic Elements in soil of Livingston Island, mg × kg^{-1}.

contribution in all cases is DBA 30 μg × kg^{-1}, IPY 2 μg × kg^{-1}, the remaining PAHs are significantly smaller. $\sum 7_{carcinogenic}$PAHs in BaP-equivalents for all natural soils is close to 33 μg × kg^{-1} with a DBA share of over 90%.

Taking into account that DBA concentrations in toxic and natural soils is a same (6 μg × kg^{-1}), one might say that baseline source of DBA in BaP-equivalents in soils and cryoconites more than Russian MPC of 3-4 benzo(a)pyrene.

Content of Potentially Toxic Elements

Figure 5 shows the content of Potentially Toxic Elements in soils and cryoconites. Zn has the highest content of all metals. In the soil sample from the anthropogenic-loaded area (L26) the Zn concentration is 75.7 mg × kg^{-1}. The lowest concentration was detected in sample L1A–16.5 mg × kg^{-1}. High concentrations of Zn were recorded at L6 and L10, although soils in these areas are not subjected to anthropogenic load. As can be seen in the diagram presented in **Figure 4**, the variability of concentrations of other metals is significantly lower compared to zinc. The content does not change significantly. The minimum content among all Potentially Toxic Elements is observed for Cd, the maximum concentration is fixed in point L10–0.509 mg × kg^{-1}.

Potential Toxic Elements in soils with anthropogenic load (Cryosol Toxic Transportic) following relation: Zn > Cu > Pb > Ni > Cr > Cd. Cryosol Ornitic: Zn > Ni > Cu > Pb > Cr > Cd. Typihical Cryosols and Cryoconites in most cases: Zn > Cu > Ni > Pb > Cr > Cd.

Previously, some results of studies of the content of potentially toxic elements in soils, cryoconites and ornithogenic sediments in the Antarctic Continent have already been published. In the cryoconites King George Island recorded the content of potentially toxic elements in the following order: Zn > Cu > Ni > Cr > Pb > Cd (Polyakov et al., 2020). In the anthropogenically loaded soils of Robert Island near The Chilean refuge Luis Risopatrón, the concentrations were in the following order Cr > Cu > Zn > Ni > Pb > Cd (Neto et al., 2017). Technosols from Hope Bay, Esperanza Station showed relation Pb > Zn > Cu > Ni > Cr > Cd. With an extremely high Pb content of 19381 mg × kg^{-1} and Cd content of 44 mg × kg^{-1} (Bueno Guerra et al., 2011). King George Island, Stranger Point, ornitoghenic soils near Gentoo penguin colonies, showed potentially toxic elements ratios: Cu > Zn > Pb > Cr > Ni > Cd, at a Cu concentration of 389.98 mg × kg^{-1} and a Cd concentration of 3.93 mg × kg^{-1} (Celis et al., 2015). Unfortunately, the soils of Livingston Island are poorly investigated in terms of heavy metals concentration, so below is a comparison with the results of few studies of soils of Livingston Island and King George Island, as it is similar in climate conditions and is a short distance to Livingston Island. Vlček et al. (2017) present data for pristine soils on Livingston Island (Hannah point area), which are similar to our results for undisturbed soils. The

TABLE 5 | Spearman Rank Order Correlations (r) between concentrations of potentially toxic elements (Bolded correlations are significant at $p < 0.05$).

	Cu	Pb	Zn	Cd	Ni	Cr
Cu	1.00	0.59	0.47	**0.82**	0.49	0.57
Pb		1.00	**0.70**	0.54	**0.74**	**0.61**
Zn			1.00	**0.61**	**0.91**	**0.85**
Cd				1.00	**0.62**	**0.71**
Ni					1.00	**0.82**
Cr						1.00

concentrations of 52 mg/kg are given (Santos et al., 2005). We also recorded the maximum concentrations of Zn, Cu and Pb among all the studied metals in a soil sample taken on the territory of the station "St. Kliment Ohridski" (point L26).

Statistical analysis of the obtained data matrix of trace elements concentrations showed that most elements are in close correlation relationship (**Table 5**).

Significant Spearman correlation coefficients ($r > 0.61$) were obtained practically for the elements. High correlation values

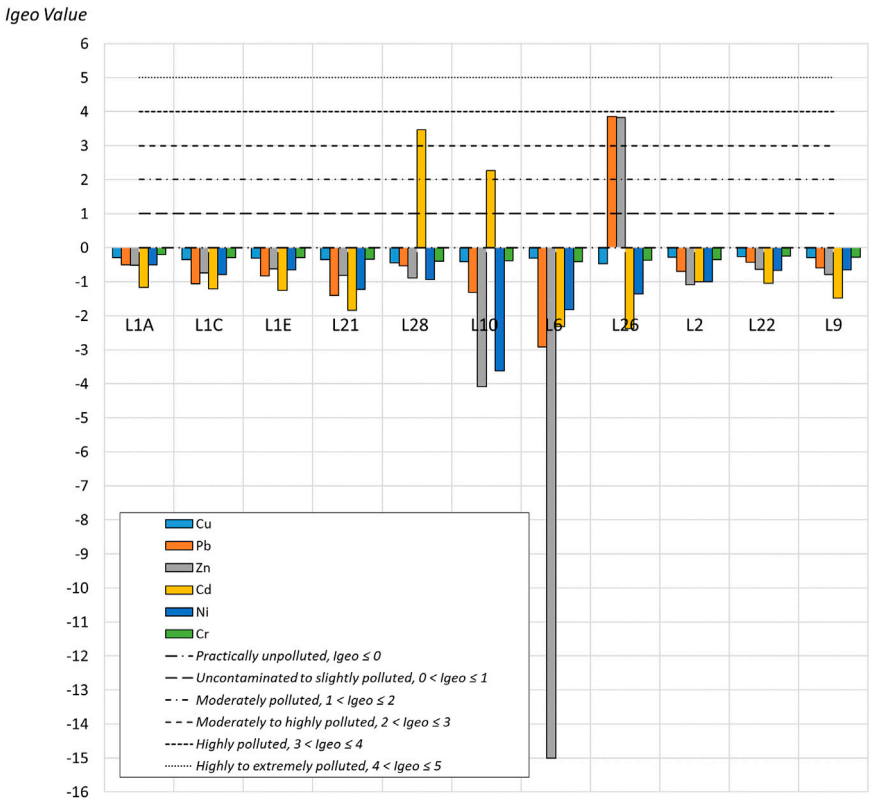

FIGURE 6 | I_{geo} values for the studied soils in the vicinity of "St. Kliment Ohridsky" station.

authors note the highest Zn concentration (55 mg × kg^{-1}) in undisturbed soils, which is identical to our data (Vlček et al., 2017). The results for the other heavy metals are also similar. The investigations Santos et al. (2005); Vlček et al. (2017); Bueno et al. (2018) provide data on the content of trace metals both in pristine soils of King George Island and for anthropogenically loaded areas near the Antarctic stations. The data given by these researchers for pristine soils are generally similar to ours. For anthropogenically loaded territories, there are similarities in the content of Cu, Zn, and Pb. The average Zn 63.1, Cu 52.2, and Pb 6.3 mg × kg^{-1} were found in the soils of Artigas Antarctic Scientific Base (Bueno et al., 2018). For soils of Brazilian Antarctic Station Comandante Ferraz (Ferraz), data on average Zn between Ni and Zn (r – 0.91), Cr and Zn (r – 0.85), and between Cd and Cu (r – 0.82) are especially significant.

Classification of Soil Contaminations

Livingston Island is not well surveyed in terms of background concentrations of trace metals in the soil, so we used concentrations of trace metals in King George Island soils to calculate the geoaccumulation index (I_{geo}). King George Island is the closest large island to Livingston Island, they are very similar in climatic conditions and are part of the South Shetland Islands. There are many publications on heavy metal content in the pristine soils of King George Island (Amaro et al., 2015; Dalfior et al., 2016; Alekseev and Abakumov, 2020; Polyakov et al., 2020). Based on these studies, we calculated average values of heavy metal concentrations in pristine soils of the South

Shetland Islands. The following values of the geochemical background value (B_n) were obtained: Cu–63, Pb–5.65, Zn–42.6, Cd–0.25, Ni–11.83, and Cr–22.95 mg × kg^{-1}.

In most of the studied soils, the values of the I_{geo} for all the studied potentially toxic elements are less than zero ($I_{geo} \leq 0$), which allows us to classify them as *Practically unpolluted* (**Figure 6**).

Values above zero are recorded at L28, L10, and L26 sampling points. At L28 point, the I_{geo} value for Cd is 3.46. This soil is characterized as *Highly polluted* ($3 < I_{geo} \leq 4$). Also a high level of Cd content compared with background values was recorded at point L10, the values of I_{geo} index equal to 2.26. Cd contamination is characterized as *Moderately to highly polluted* ($2 < I_{geo} \leq 3$). The highest values of the I_{geo} index are found at L26 point. Here Pb and Zn contamination is characterized as *Highly polluted* ($3 < I_{geo} \leq 4$). I_{geo} values for Pb and Zn at point L26 are 3.85 and 3.82, respectively. It should be noted that the study area near point L26, is anthropogenically loaded, soil samples were taken directly in the territory of the Bulgarian Antarctic station. Bueno et al. (2018) reports data on soil contamination of Ferraz station (King George Island) based on Igeo index calculations. The level of contamination of Zn (noderatlely to highly polluted) and Cr (Moderately polluted) is identified (Bueno et al., 2018). It can be noted a similarity with the character of soil contamination on the territory of the station "St. Kliment Ohridski".

Averaging the I_{geo} values for all points, the ratio of the pollution level is as follows Cr > Cu > Pb > Cd > Ni > Zn. With values for Cr and Zn equal to −0.32 and −1.94, respectively. The average values for all potentially toxic elements are characterized as Practically unpolluted ($I_{geo} \leq 0$).

DATA AVAILABILITY STATEMENT

The raw data supporting the conclusions of this article will be made available by the authors, without undue reservation.

AUTHOR CONTRIBUTIONS

EA–field work, conceptualization, TN–laboratory analyzes, data processing, MG–writing manuscript, RY–field work, data processing. All authors have read and agreed to the published version of the manuscript.

FUNDING

This work was supported by Russian Foundation for Basic Research, Projects No 18–04–00900, 19–54–18003 and 19–05–50107.

ACKNOWLEDGMENTS

The authors are very grateful to the participants and organizers of the Russian and Bulgarian Antarctic National Expeditions. And Research park of Saint-Petersburg State University, Chemical Analysis and Materials Research Centre for assistance with routine soil analyses.

REFERENCES

AAD (2009). *Antarctica: 1000 Metre Contours. 1: 45 000 000*. Australia: Australian Antarctic Division.

Abakumov, E., Lodygin, E., Gabov, D., and Krylenkov, V. (2014). [Polycyclic Aromatic Hydrocarbons Content in Antarctica Soils as Exemplified by the Russian Polar Stations]. *Gig Sanit* 1, 31–35.

Abakumov, E. V., Parnikoza, I. Y., Lupachev, A. V., Lodygin, E. D., Gabov, D. N., and Kunakh, V. A. (2015). [CONTENT OF POLYCYCLIC AROMATIC HYDROCARBONS IN SOILS OF ANTARCTIC STATIONS REGIONS]. *Gig Sanit* 94, 20–25.

Agency, U. S. E. P. (1986). *SW-846 Test Method 8310: Polynuclear Aromatic Hydrocarbons*. Washington, DC: US EPA.

Aislabie, J., Balks, M., Astori, N., Stevenson, G., and Symons, R. (1999). Polycyclic Aromatic Hydrocarbons in Fuel-Oil Contaminated Soils, Antarctica. *Chemosphere* 39 (13), 2201–2207. doi:10.1016/s0045-6535(99)00144-7

Aislabie, J. M., Balks, M. R., Foght, J. M., and Waterhouse, E. J. (2004). Hydrocarbon Spills on Antarctic Soils: Effects and Management. *Environ. Sci. Technol.* 38 (5), 1265–1274. doi:10.1021/es0305149

Alekseev, I., and Abakumov, E. (2020). The Content and Distribution of Trace Elements and Polycyclic Aromatic Hydrocarbons in Soils of Maritime Antarctica. *Environ. Monit. Assess.* 192 (11), 1–22. doi:10.1007/s10661-020-08618-2

Ali, H., Khan, E., and Sajad, M. A. (2013). Phytoremediation of Heavy Metals-Concepts and Applications. *Chemosphere* 91 (7), 869–881. doi:10.1016/j.chemosphere.2013.01.075

Amaro, E., Padeiro, A., de Ferro, A. M., Mota, A. M., Leppe, M., Verkulich, S., et al. (2015). Assessing Trace Element Contamination in Fildes Peninsula (King George Island) and Ardley Island, Antarctic. *Mar. Pollut. Bull.* 97 (1-2), 523–527. doi:10.1016/j.marpolbul.2015.05.018

Aronson, R. B., Thatje, S., McClintock, J. B., and Hughes, K. A. (2011). Anthropogenic Impacts on Marine Ecosystems in Antarctica. *Ann. New York Acad. Sci.* 1223 (1), 82–107. doi:10.1111/j.1749-6632.2010.05926.x

Baek, S., Field, R., Goldstone, M., Kirk, P., Lester, J., and Perry, R. (1991). A Review of Atmospheric Polycyclic Aromatic Hydrocarbons: Sources, Fate and Behavior. *Water Air Soil Pollut.* 60 (3-4), 279–300. doi:10.1007/bf00282628

BAI (2013). *Exchange of Information in Accordance with Article VII (5) Bulgarian Antarctic Activities 2012/2013 [Online]*. Sofia, Republica Bulgaria: Bulgarian Antarctic Institute. Available: http://www.ats.aq/devAS/..%5Cdocuments%5Cie%5Cbgann13e.doc [Accessed].

Balmer, J. E., Hung, H., Yu, Y., Letcher, R. J., and Muir, D. C. G. (2019). Sources and Environmental Fate of Pyrogenic Polycyclic Aromatic Hydrocarbons (PAHs) in the Arctic. *Emerging Contaminants* 5, 128–142. doi:10.1016/j.emcon.2019.04.002

Bargagli, R. (2006). *Antarctic Ecosystems: Environmental Contamination, Climate Change, and Human Impact*. Berlin, Germany: Springer Science & Business Media.

Bargagli, R. (2008). Environmental Contamination in Antarctic Ecosystems. *Sci. total Environ.* 400 (1-3), 212–226. doi:10.1016/j.scitotenv.2008.06.062

Bari, M. A., Baumbach, G., Kuch, B., and Scheffknecht, G. (2010). Particle-phase Concentrations of Polycyclic Aromatic Hydrocarbons in Ambient Air of Rural Residential Areas in Southern Germany. *Air Qual. Atmos. Health* 3 (2), 103–116. doi:10.1007/s11869-009-0057-8

Beyersmann, D., and Hartwig, A. (2008). Carcinogenic Metal Compounds: Recent Insight into Molecular and Cellular Mechanisms. *Arch. Toxicol.* 82 (8), 493–512. doi:10.1007/s00204-008-0313-y

Budzinski, H., Jones, I., Bellocq, J., Pierard, C., and Garrigues, P. (1997). Evaluation of Sediment Contamination by Polycyclic Aromatic Hydrocarbons in the Gironde Estuary. *Mar. Chem.* 58 (1-2), 85–97. doi:10.1016/s0304-4203(97)00028-5

Bueno, C., Kandratavicius, N., Venturini, N., Figueira, R., Pérez, L., Iglesias, K., et al. (2018). An Evaluation of Trace Metal Concentration in Terrestrial and Aquatic Environments Near Artigas Antarctic Scientific Base (King George Island, Maritime Antarctica). *Water Air Soil Pollut.* 229 (12), 1–11. doi:10.1007/s11270-018-4045-1

Bueno Guerra, M. B., Schaefer, C. E. G. R., Rosa, P. d. F., Simas, F. N. B., Pereira, T. T. C., and Pereira-Filho, E. R. (2011). Heavy Metals Contamination in Century-Old Manmade Technosols of Hope Bay, Antarctic Peninsula. *Water Air Soil Pollut.* 222 (1-4), 91–102. doi:10.1007/s11270-011-0811-z

Cabrerizo, A., Dachs, J., Barceló, D., and Jones, K. C. (2012). Influence of Organic Matter Content and Human Activities on the Occurrence of Organic Pollutants in Antarctic Soils, Lichens, Grass, and Mosses. *Environ. Sci. Technol.* 46 (3), 1396–1405. doi:10.1021/es203425b

Celis, J. E., Barra, R., Espejo, W., Gonzalez-Acuna, D., and Jara, S. (2015). Trace Element Concentrations in Biotic Matrices of Gentoo Penguins (Pygoscelis Papua) and Coastal Soils from Different Locations of the Antarctic Peninsula. *Water Air and Soil Pollution* 226(1). doi:10.1007/s11270-014-2266-5

CEP (2011). *Management Plan for Antarctic Specially Protected Area (ASPA) No. 149 CAPE SHIRREFF AND SAN TELMO ISLAND*. LIVINGSTON ISLAND, SOUTH SHETLAND ISLANDS. Buenos Aires, Argentina.

Chen, J., and Blume, H. (1997). Impact of Human Activities on the Terrestrial Ecosystem of Antarctica: a Review. *Polarforschung* 65 (2), 83–92.

Chunhui, W., Shaohua, W., Shenglu, Z., Yaxing, S., and Jing, S. (2017). Characteristics and Source Identification of Polycyclic Aromatic Hydrocarbons (PAHs) in Urban Soils: a Review. *Pedosphere* 27 (1), 17–26. doi:10.1016/S1002-0160(17)60293-5

Connor, M. A. (2008). Wastewater Treatment in Antarctica. *Polar Rec.* 44 (2), 165–171. doi:10.1017/s003224740700719x

Cook, J., Edwards, A., Takeuchi, N., and Irvine-Fynn, T. (2016). Cryoconite. *Prog. Phys. Geogr. Earth Environ.* 40 (1), 66–111. doi:10.1177/0309133315616574

Dalfior, B. M., Roriz, L. D., Junior, R. F., de Freitas, A. C., da Silva, H. E., Carneiro, M. T. W., et al. (2016). Evaluation of Pb, Cd, Sn, Co, Hg, Mo and as in Soil from Fildes Peninsula-Antarctica. *Quimica Nova* 39 (8), 893–900. doi:10.21577/0100-4042.20160134

EPA, U. (2007). Method 3550C–Ultrasonic Extraction. *Test. Methods Evaluating Solid Waste, Physical/chemical Methods* 3, 1–17.

Fang, G., Wu, Y.-S., Chen, M.-H., Ho, T.-T., Huang, S.-H., and Rau, J.-Y. (2004). Polycyclic Aromatic Hydrocarbons Study in Taichung, Taiwan, during 2002? 2003. *Atmos. Environ.* 38 (21), 3385–3391. doi:10.1016/j.atmosenv.2004.03.036

Frenot, Y., Chown, S. L., Whinam, J., Selkirk, P. M., Convey, P., Skotnicki, M., et al. (2005). Biological Invasions in the Antarctic: Extent, Impacts and Implications. *Biol. Rev.* 80 (1), 45–72. doi:10.1017/s1464793104006542

Gabov, D. N., Beznosikov, V. A., and Kondratenok, B. M. (2007). Polycyclic Aromatic Hydrocarbons in Background Podzolic and Gleyic Peat-Podzolic Soils. *Eurasian Soil Sc.* 40 (3), 256–264. doi:10.1134/s1064229307030039

Gabov, D. N., Beznosikov, V. A., Kondratenok, B. M., and Yakovleva, E. V. (2008). Formation of Polycyclic Aromatic Hydrocarbons in Northern and Middle Taiga Soils. *Eurasian Soil Sc.* 41, 1180–1188. doi:10.1134/s1064229308110069

Gao, P., Xu, M., Liu, Y., da Silva, E. B., Xiang, P., and Ma, L. Q. (2019). Emerging and Legacy PAHs in Urban Soils of Four Small Cities: Concentrations, Distribution, and Sources. *Sci. Total Environ.* 685, 463–470. doi:10.1016/j.scitotenv.2019.05.403

Gardes, T., Portet-Koltalo, F., Debret, M., Humbert, K., Levaillant, R., Simon, M., et al. (2020). Temporal Trends, Sources, and Relationships between Sediment Characteristics and Polycyclic Aromatic Hydrocarbons (PAHs) and Polychlorinated Biphenyls (PCBs) in Sediment Cores from the Major Seine Estuary Tributary, France. *Appl. Geochem.* 122, 104749. doi:10.1016/j.apgeochem.2020.104749

Gilichinsky, D., Abakumov, E., Abramov, A., Fyodorov-Davydov, D., Goryachkin, S., Lupachev, A., et al. (2010). *Soils of Mid and Low Antarctic: Diversity, Geography, Temperature Regime. World Congress of Soil Science, Soil Solutions Q20 for a Changing World*. Brisbane, Australia, 1–6.

GOST, R. (1996). R 8.563–96. *The State System of Measurements: Methods of Performing Measurements* (in Russian).

Gran-Scheuch, A., Ramos-Zuñiga, J., Fuentes, E., Bravo, D., and Pérez-Donoso, J. M. (2020). Effect of Co-contamination by PAHs and Heavy Metals on Bacterial Communities of Diesel Contaminated Soils of South Shetland Islands, Antarctica. *Microorganisms* 8 (11), 1749. doi:10.3390/microorganisms8111749

Hale, R. C., Kim, S. L., Harvey, E., La Guardia, M. J., Mainor, T. M., Bush, E. O., et al. (2008). Antarctic Research Bases: Local Sources of Polybrominated Diphenyl Ether (PBDE) Flame Retardants. *Environ. Sci. Technol.* 42 (5), 1452–1457. doi:10.1021/es702547a

Hodson, A. J. (2014). Understanding the Dynamics of Black Carbon and Associated Contaminants in Glacial Systems. *WIREs Water* 1 (2), 141–149. doi:10.1002/wat2.1016

Howsam, M., and Jones, K. C. (1998). Sources of PAHs in the Environment. in *PAHs and Related Compounds* (Berlin, Heidelberg: Springer), 137–174. doi:10.1007/978-3-540-49697-7_4

Hwang, H.-M., Wade, T. L., and Sericano, J. L. (2004). Destabilized Lysosomes and Elimination of Polycyclic Aromatic Hydrocarbons and Polychlorinated Biphenyls in Eastern Oysters (*Crassostrea virginica*). *Environ. Toxicol. Chem.* 23 (8), 1991–1995. doi:10.1897/03-467

Hygienic Norms, G. (2006). 2.1. 7.2041 06 "Maximum Permissi Ble Concentrations (MPC) of Chemical Substances in Soil. Approved by the Chief Sanitary Inspector of the Russian Federation on January 23.

ISO, S. Q. (1998). *Determination of Cadmium, Chromium, Cobalt, Copper, Lead, Manganese, Nickel and Zinc in Aqua Regia Extracts of Soil. Flame and Electrothermal Atomic Absorption Spectrometric Methods*. International Organization of Standardization. Geneva.

Ivanov, L. (2015). *General Geography and History of Livingston Island*. Sofia: Bulgarian Antarctic Research: a Synthesis. St. Kliment Ohridski University Press, 17–28.

Jennings, A. A. (2012). Worldwide Regulatory Guidance Values for Surface Soil Exposure to Carcinogenic or Mutagenic Polycyclic Aromatic Hydrocarbons. *J. Environ. Manag.* 110, 82–102. doi:10.1016/j.jenvman.2012.05.015

Jiang, F., Ren, B., Hursthouse, A., Deng, R., and Wang, Z. (2019). Distribution, Source Identification, and Ecological-Health Risks of Potentially Toxic Elements (PTEs) in Soil of Thallium Mine Area (Southwestern Guizhou, China). *Environ. Sci. Pollut. Res.* 26 (16), 16556–16567. doi:10.1007/s11356-019-04997-3

Jung, K. H., Yan, B., Chillrud, S. N., Perera, F. P., Whyatt, R., Camann, D., et al. (2010). Assessment of Benzo(a)pyrene-Equivalent Carcinogenicity and Mutagenicity of Residential Indoor versus Outdoor Polycyclic Aromatic Hydrocarbons Exposing Young Children in New York City. *Ijerph* 7 (5), 1889–1900. doi:10.3390/ijerph7051889

Kennicutt, M. C., Sweet, S. T., Fraser, W. R., Stockton, W. L., and Culver, M. (1991). Grounding of the Bahia Paraiso at Arthur Harbor, Antarctica. 1. Distribution and Fate of Oil Spill Related Hydrocarbons. *Environ. Sci. Technol.* 25 (3), 509–518. doi:10.1021/es00015a020

Khairy, M. A., Kolb, M., Mostafa, A. R., EL-Fiky, A., and Bahadir, M. (2009). Risk Assessment of Polycyclic Aromatic Hydrocarbons in a Mediterranean Semi-enclosed Basin Affected by Human Activities (Abu Qir Bay, Egypt). *J. Hazard. Mater.* 170 (1), 389–397. doi:10.1016/j.jhazmat.2009.04.084

Khaustov, A., and Redina, M. (2016). Indicator Ratio of Concentrations of Polycyclic Aromatic Hydrocarbons for Geoecological Studies of Environmental and Technical Objects. *Geoekologiya Inzhenernaya Geol. Gidrogeol. Geokriol.* 3, 220–233.

Li, Q., Kang, S., Wang, N., Li, Y., Li, X., Dong, Z., et al. (2017). Composition and Sources of Polycyclic Aromatic Hydrocarbons in Cryoconites of the Tibetan Plateau Glaciers. *Sci. Total Environ.* 574, 991–999. doi:10.1016/j.scitotenv.2016.09.159

Liu, K., Hou, S., Wu, S., Zhang, W., Zou, X., Yu, J., et al. (2021). Assessment of Heavy Metal Contamination in the Atmospheric Deposition during 1950-2016 A.D. From a Snow Pit at Dome A, East Antarctica. *Environ. Pollut.* 268 (Pt B), 115848. doi:10.1016/j.envpol.2020.115848

Lodygin, E. D., Chukov, S. N., Beznosikov, V. A., and Gabov, D. N. (2008). Polycyclic Aromatic Hydrocarbons in Soils of Vasilievsky Island (St. Petersburg). *Eurasian Soil Sc.* 41 (12), 1321–1326. doi:10.1134/s1064229308120107

Loeb, L. A., and Harris, C. C. (2008). Advances in Chemical Carcinogenesis: a Historical Review and Prospective. *Cancer Res.* 68 (17), 6863–6872. doi:10.1158/0008-5472.can-08-2852

Mandalakis, M., Tsapakis, M., Tsoga, A., and Stephanou, E. G. (2002). Gas-particle Concentrations and Distribution of Aliphatic Hydrocarbons, PAHs, PCBs and

PCDD/Fs in the Atmosphere of Athens (Greece). *Atmos. Environ.* 36 (25), 4023–4035. doi:10.1016/s1352-2310(02)00362-x

Madrid Protocol. (1998). Protocol on Environmental Protection to the Antarctic Treaty, Madrid, 4 October 1991, 30 ILM 1461 (Accessed January 14, 1998).

Martins, C. C., Bícego, M. C., Rose, N. L., Taniguchi, S., Lourenço, R. A., Figueira, R. C. L., et al. (2010). Historical Record of Polycyclic Aromatic Hydrocarbons (PAHs) and Spheroidal Carbonaceous Particles (SCPs) in Marine Sediment Cores from Admiralty Bay, King George Island, Antarctica. *Environ. Pollut.* 158 (1), 192–200. doi:10.1016/j.envpol.2009.07.025

Martins, C. C., Bícego, M. C., Taniguchi, S., and Montone, R. C. (2004). Aliphatic and Polycyclic Aromatic Hydrocarbons in Surface Sediments in Admiralty Bay, King George Island, Antarctica. *Antartic Sci.* 16 (2), 117–122. doi:10.1017/s0954102004001932

Morillo, E., Romero, A. S., Maqueda, C., Madrid, L., Ajmone-Marsan, F., Grcman, H., et al. (2007). Soil Pollution by PAHs in Urban Soils: a Comparison of Three European Cities. *J. Environ. Monit.* 9 (9), 1001–1008. doi:10.1039/b705955h

Muller, G. (1979). *Schwermetalle in den Sedimenten des Rheins: Veranderungen seit 1971* Umschau, 79, 778–783 (in German).

Na, G., Gao, Y., Li, R., Gao, H., Hou, C., Ye, J., et al. (2020). Occurrence and Sources of Polycyclic Aromatic Hydrocarbons in Atmosphere and Soil from 2013 to 2019 in the Fildes Peninsula, Antarctica. *Mar. Pollut. Bull.* 156, 111173. doi:10.1016/j.marpolbul.2020.111173

Negri, A., Burns, K., Boyle, S., Brinkman, D., and Webster, N. (2006). Contamination in Sediments, Bivalves and Sponges of McMurdo Sound, Antarctica. *Environ. Pollut.* 143 (3), 456–467. doi:10.1016/j.envpol.2005.12.005

Neto, E. D., Guerra, M. B. B., Thomazini, A., Daher, M., de Andrade, A. M., and Schaefer, C. (2017). Soil Contamination by Toxic Metals Near an Antarctic Refuge in Robert Island, Maritime Antarctica: A Monitoring Strategy. *Water Air Soil Pollut.* 228 (2). doi:10.1007/s11270-017-3245-4

Nisbet, I. C. T., and Lagoy, P. K. (1992). Toxic Equivalency Factors (TEFs) for Polycyclic Aromatic Hydrocarbons (PAHs). *Regul. Toxicol. Pharmacol.* 16 (3), 290–300. doi:10.1016/0273-2300(92)90009-x

Padeiro, A., Amaro, E., dos Santos, M. M. C., Araújo, M. F., Gomes, S. S., Leppe, M., et al. (2016). Trace Element Contamination and Availability in the Fildes Peninsula, King George Island, Antarctica. *Environ. Sci. Process. Impacts* 18 (6), 648–657. doi:10.1039/c6em00052e

Pandey, P. K., Patel, K. S., and Lenicek, J. (1999). Polycyclic Aromatic Hydrocarbons: Need for Assessment of Health Risks in India? Study of an Urban-Industrial Location in India. *Environ. Monit. Assess.* 59 (3), 287–319. doi:10.1023/a:1006169605672

PND, F. (2003). 16.1: 2: 2.2: 3.39-03. High Efficient Liquid Chro Matography Method to Determine the Mass Fraction of Benzo (A) Pyrene in Soils, Bottom Sediments, and Solid Wastes with a Lyumakhrom Liquid Chromatograph (in Russian).

Polyakov, V., Abakumov, E., and Mavlyudov, B. (2020). Black Carbon as a Source of Trace Elements and Nutrients in Ice Sheet of King George Island, Antarctica. *Geosciences* 10 (11). doi:10.3390/geosciences10110465

Pourret, O., and Hursthouse, A. (2019). It's Time to Replace the Term "Heavy Metals" with "Potentially Toxic Elements" when Reporting Environmental Research. *Ijerph* 16 (22), 4446. doi:10.3390/ijerph16224446

Ravindra, K., Wauters, E., and Van Grieken, R. (2008). Variation in Particulate PAHs Levels and Their Relation with the Transboundary Movement of the Air Masses. *Sci. Total Environ.* 396 (2-3), 100–110. doi:10.1016/j.scitotenv.2008.02.018

Santos, I. R., Silva-Filho, E. V., Schaefer, C. E. G. R., Albuquerque-Filho, M. R., and Campos, L. S. (2005). Heavy Metal Contamination in Coastal Sediments and Soils Near the Brazilian Antarctic Station, King George Island. *Mar. Pollut. Bull.* 50 (2), 185–194. doi:10.1016/j.marpolbul.2004.10.009

Shamilishvili, G., Abakumov, E., Gabov, D., and Alekseev, I. (2016). [Features of Fractional Composition of Polycyclic Aromatic Hydrocarbons and Multielement Contamination of Soils of Urban Territories and Their Hygienic Characteristics (On the Example of Soils of Functional Zones of Saint-Petersburg)]. *Gig Sanit* 95 (9), 827–837.

Smykla, J., Szarek-Gwiazda, E., Drewnik, M., Knap, W., and Emslie, S. D. (2018). Natural Variability of Major and Trace Elements in Non-ornithogenic Gelisoils at Edmonson Point, Northern Victoria Land, Antarctica. *Polish Polar Res.* 39 (1), 19–50. doi:10.24425/118737

Snape, I., Riddle, M. J., Stark, J. S., Cole, C. M., King, C. K., Duquesne, S., et al. (2001). Management and Remediation of Contaminated Sites at Casey Station, Antarctica. *Polar Rec.* 37 (202), 199–214. doi:10.1017/s0032247400027236

Soclo, H. H., Garrigues, P., and Ewald, M. (2000). Origin of Polycyclic Aromatic Hydrocarbons (PAHs) in Coastal Marine Sediments: Case Studies in Cotonou (Benin) and Aquitaine (France) Areas. *Mar. Pollut. Bull.* 40 (5), 387–396. doi:10.1016/s0025-326x(99)00200-3

SW, EPA (1996). "846 Test Method 3660C: Silica Gel Cleanup." *US Environmental Protection Agency*.

Tin, T., Fleming, Z. L., Hughes, K. A., Ainley, D. G., Convey, P., Moreno, C. A., et al. (2009). Impacts of Local Human Activities on the Antarctic Environment. *Antartic Sci.* 21 (1), 3–33. doi:10.1017/s0954102009001722

Tobiszewski, M., and Namieśnik, J. (2012). PAH Diagnostic Ratios for the Identification of Pollution Emission Sources. *Environ. Pollut.* 162, 110–119. doi:10.1016/j.envpol.2011.10.025

Trevizani, T. H., Petti, M. A. V., Ribeiro, A. P., Corbisier, T. N., and Figueira, R. C. L. (2018). Heavy Metal Concentrations in the Benthic Trophic Web of Martel Inlet, Admiralty Bay (King George Island, Antarctica). *Mar. Pollut. Bull.* 130, 198–205. doi:10.1016/j.marpolbul.2018.03.031

U.S. EPA. *Provisional Guidance for Quantitative Risk Assessment of Polycyclic Aromatic Hydrocarbons (PAH)*. Washington, DC: U.S. Environmental Protection Agency, Office of Research and Development, Office of Health and Environmental Assessment.

Verbruggen, E. M. J., Posthumus, R., and Van Wezel, A. (2001). Ecotoxicological Serious Risk Concentrations for Soil, Sediment and (Ground) Water: Updated Proposals for First Series of Compounds.doi:10.2118/68741-ms

Vlček, V., Juřička, D., and Míková, J. (2017). Heavy Metal Concentration in Selected Soils and Sediments of Livingston Island, Deception Island, King George Island, James Ross Island (Antarctica). *Czech Polar Rep.* 7 (1), 18–33.

Wang, Z., Ma, X., Na, G., Lin, Z., Ding, Q., and Yao, Z. (2009). Correlations between Physicochemical Properties of PAHs and Their Distribution in Soil, Moss and Reindeer Dung at Ny-Ålesund of the Arctic. *Environ. Pollut.* 157 (11), 3132–3136. doi:10.1016/j.envpol.2009.05.014

Waterhouse, E. J. (2001). Ross Sea region 2001: a state of the environment report for the Ross Sea region of Antarctica. Editor E. J. Waterhouse (Christchurch, NZ: New Zealand Antarctic Institute (Antarctica New Zealand)).

IUSS Working Group WRB (2015). World Reference Base for Soil Resources 2014, update 2015. International soil classification system for naming soils and creating legends for soil maps. World Soil Resources Reports No. 106. Rome: FAO.

Yan, B., Abrajano, T. A., Bopp, R. F., Benedict, L. A., Chaky, D. A., Perry, E., et al. (2006). Combined Application of δ13C and Molecular Ratios in Sediment Cores for PAH Source Apportionment in the New York/New Jersey Harbor Complex. *Org. Geochem.* 37 (6), 674–687. doi:10.1016/j.orggeochem.2006.01.013

Yang, Z., Feng, J., Niu, J., and Shen, Z. (2008). Release of Polycyclic Aromatic Hydrocarbons from Yangtze River Sediment Cores during Periods of Simulated Resuspension. *Environ. Pollut.* 155 (2), 366–374. doi:10.1016/j.envpol.2007.11.007

Yunker, M. B., Macdonald, R. W., Vingarzan, R., Mitchell, R. H., Goyette, D., and Sylvestre, S. (2002). PAHs in the Fraser River Basin: a Critical Appraisal of PAH Ratios as Indicators of PAH Source and Composition. *Org. Geochem.* 33 (4), 489–515. doi:10.1016/s0146-6380(02)00002-5

Zhang, W., Zhang, S., Wan, C., Yue, D., Ye, Y., and Wang, X. (2008). Source Diagnostics of Polycyclic Aromatic Hydrocarbons in Urban Road Runoff, Dust, Rain and Canopy Throughfall. *Environ. Pollut.* 153 (3), 594–601. doi:10.1016/j.envpol.2007.09.004

Conflict of Interest: The authors declare that the research was conducted in the absence of any commercial or financial relationships that could be construed as a potential conflict of interest.

frontiers in Environmental Science

ORIGINAL RESEARCH
published: 12 May 2021
doi: 10.3389/fenvs.2021.681934

Indirect Effects of Microplastic-Contaminated Soils on Adjacent Soil Layers: Vertical Changes in Soil Physical Structure and Water Flow

Shin Woong Kim[1,2]*, *Yun Liang*[1,2], *Tingting Zhao*[1,2] and *Matthias C. Rillig*[1,2]

[1]Institute of Biology, Freie Universität Berlin, Berlin, Germany, [2]Berlin-Brandenburg Institute of Advanced Biodiversity Research, Berlin, Germany

Previous microplastic research under laboratory conditions has focused on microplastics that are homogeneously mixed into test media, in order to maximize test reproducibility and uniform bio-accessibility. Here we specifically focused on testing the idea that microplastics in soil could affect adjacent soil layers not containing microplastic themselves. We included two different microplastics (low-density polyethylene films and polyacrylonitrile fibers) and carried out a soil column test consisting of three different vertical layers (0–3 cm, top, control soil; 3–6 cm, middle, microplastic-containing soil; 6–9 cm, bottom, control soil). Our study shows that microplastic-containing soil layers can act as an anthropogenic barrier in the soil column, interrupting the vertical water flow. These changes directly affected the water content of adjacent layers, and changes in the proportion of soil aggregate sizes occurred for each depth of the soil columns. We also observed that these physical changes trigger changes in soil respiration, but do not translate to effects on enzyme activities. These results imply that the soil environment in non-contaminated parts of the soil can be altered by microplastic contamination in adjacent layers, as might occur for example during ploughing on agricultural fields. More generally, our results highlight the need to further examine effects of microplastic in experiments that do not treat this kind of pollution as uniformly distributed.

Keywords: aggregates, fibers, films, heterogeneous pollution, water path

OPEN ACCESS

Edited by:
Hongbiao Cui,
Anhui University of Science and Technology, China

Reviewed by:
Xuetao Guo,
Northwest A and F University, China
Yuyi Yang,
Chinese Academy of Sciences, China

***Correspondence:**
Shin Woong Kim
swkim@zedat.fu-berlin.de

Specialty section:
This article was submitted to Toxicology, Pollution and the Environment, a section of the journal Frontiers in Environmental Science

Received: *17 March 2021*
Accepted: *26 April 2021*
Published: *12 May 2021*

Citation:
Kim SW, Liang Y, Zhao T and Rillig MC (2021) Indirect Effects of Microplastic-Contaminated Soils on Adjacent Soil Layers: Vertical Changes in Soil Physical Structure and Water Flow. Front. Environ. Sci. 9:681934. doi: 10.3389/fenvs.2021.681934

INTRODUCTION

Scientists estimate that less than 5% of plastic production is recycled (Sutherland et al., 2019), and a considerable amount of plastic waste is accumulating in the environment (Jambeck et al., 2015; Rillig and Lehmann, 2020). One of the main concerns about plastic pollution is that plastic waste can be slowly fragmented into smaller size under environmental conditions such as UV-radiation and mechanical weathering (Arthur et al., 2009). These tiny particles (<5 mm), defined as "microplastics," are ubiquitously observed in freshwater (Sarijan et al., 2021), oceans (Andrady, 2011), atmospheres (Chen et al., 2020), and soils (Rillig, 2012). An annual input rate of microplastics into European agricultural lands has been estimated to be 125–850 tons per million inhabitants, and

427 thousand˚tons of plastic mulch films are used every year in European farmlands (Nizzetto et al., 2016). Previous studies have reported that 300–67,500 mg kg^{-1} or 40–18,760 particles kg^{-1} of microplastics are observed in agricultural (Liu et al., 2018; Piehl et al., 2018; Zhang et al., 2018; Zhang and Liu, 2018; Ding et al., 2020), coastal (Zhou et al., 2018), floodplain (Scheurer and Bigalke, 2018), and industrial lands (Fuller and Gautam, 2016).

Research on microplastics effects has been mainly conducted under highly controlled laboratory conditions since this provides more accurate results, and many studies have mixed microplastic into test media as homogeneously as possible to keep variability of results low. In liquid media, homogenous dispersion of insoluble test substances (e.g., nanomaterials and microplastics) is an important requirement to reduce agglomeration or sedimentation, and the use of dispersants is often adopted as an efficient strategy (Potthoff et al., 2017). For soil, it is also recommended for target material to be mixed thoroughly and homogenized (Thomas et al., 2020). A recent study explained that the "homogeneity of exposure" is a crucial criterion to guarantee the reproducibility and uniform bio-accessibility during laboratory tests in microplastic research (de Ruijter et al., 2020).

Here, we were specifically interested in testing if microplastics in soil can affect adjacent soil layers not even containing microplastic themselves. Microplastics can induce changes in soil physicochemical and biological parameters, and these effects have been well-established in previous studies (Rillig and Lehmann, 2020). For instance, microplastic fibers can interfere with soil aggregate formation due to their linear shape (de Souza Machado et al., 2018; de Souza Machado et al., 2019; Zhang et al., 2019), and microplastic films influence soil tensile strength (Wan et al., 2019). It is likely that such physical changes in microplastic-containing soils would become more intense with time (de Souza Machado et al., 2018; de Souza Machado et al., 2019; Lehmann et al., 2020b), and that flows of water and nutrients into adjacent soil layers can be influenced. This would be important, because such indirect effects would suggest that previous work might have underestimated the extent of microplastic effects in soil. To capture this situation, we designed an experiment in which we added microplastic in a layer of a soil column, and this afforded us the opportunity to study effects on adjacent soil layers that are themselves not contaminated. We selected two different microplastics as target materials; low-density polyethylene (LDPE) films and polyacrylonitrile (PAN) fibers. The soil column was constructed with three layers (control soil; microplastic-containing soil; control soil), and two different levels of water addition (low and high) were included in the experimental design. To evaluate biophysical parameters at each depth of the soil columns, water content, water flow, soil aggregates sizes, soil respiration, and enzyme activities were measured after short- (1 day) and long-term (60 days) incubation periods.

MATERIALS AND METHODS

Preparation and Characterization of Microplastics

LDPE films and PAN fibers were prepared using commercial mulching films (thickness, 13.66 ± 2.32˚μm, Ihlshin Chemical Co., Ltd., Ansan, South Korea) and knitting wool (100% PAN, DIKTAS Sewing & Knitting Yarns Co., Turkey) (Kim et al., 2020). Each material was cut using sterilized scissors, and then passed through a 630 μm-sieve. Each microplastic was observed under a microscope, and close-up photographs were captured to determine average sizes using image analysis (ImageJ, 1.52a, National Institutes of Health, United States) (**Supplementary Figure S1**). The average area of LDPE films was calculated as 1.5 ± 0.8 mm^{-2} (n = 100), and the average length of PAN fibers was 2.4 ± 0.6 mm (n = 100). Target microplastics were stored at room temperature before main experiments. To characterize the actual nature of each material, a spectrophotometer (Jasco, model FT/IR-4100, ATR mode) was used, and each sample was scanned 32 times from 4000 to 600 cm^{-1}, with a resolution of 4 cm^{-1} (**Supplementary Figure S2**).

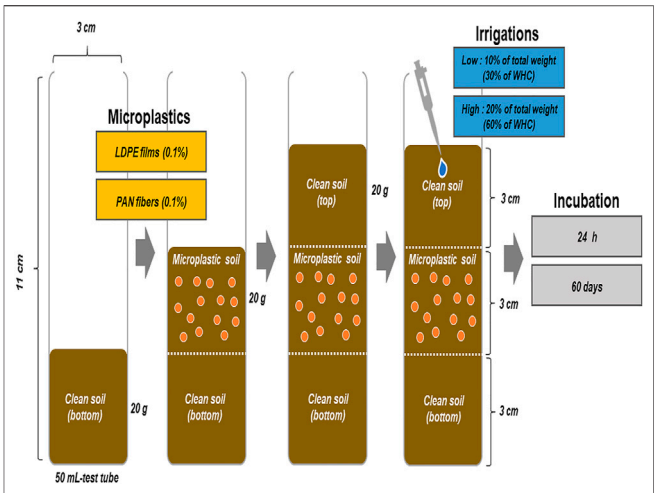

FIGURE 1 | The diagram of the soil column test in this study.

Soil Column Test

Test soil was collected from a grassland site of the Institute of Biology of Freie Universität, Berlin, Germany (52.45676N, 13.30240E) on January 20, 2020. The soil was passed through a 2 mm-sieve, and then dried at 60˚C for 24 h. The texture of test soil was a sand (sand 93.3%, silt 5.0%, and clay 1.7%), and pH and water holding capacity (WHC) were 6.7 ± 0.2 and 0.34 ± 0.10 ml g^{-1}, respectively (n = 3). In order to prepare microplastic soils (LDPE films and PAN fibers), 100 mg of each microplastic and 99.9 g of dry test soil were mixed using laboratory tweezers and a spatula, and each mixture was shaken using an overhead shaker (Reax 2, Heidolph, Germany) for 5 min (0.1% based on dry weight). The control soil was treated by an equivalent process (shaking), but not containing microplastics, and each soil was directly used for the soil column test. To prepare the soil column, 10 g of test soil was placed into 50 ml-test tubes (bottom layer), and 10 g of each microplastic-containing soil (LDPE films and PAN fibers, 0.1%) were added (microplastic-containing soil layer), after which additional test soil (10 g) was placed into the test tube (top layer) (n = 3). A control treatment was prepared with no microplastic-containing soil layer, but using an otherwise equivalent process (n = 3). The total soil

depth of the soil column was approximately 9 cm, and the depth of each layer (top, microplastic-containing soil, and bottom) was 3 cm (**Figure 1**). To moisten the soil columns, 3 ml (low level of irrigation) or 6 ml (high) of deionized water was carefully injected into surface soil (<1 cm) using a syringe needle, and these water levels were regarded as 10 and 20% of total soil weight. Each soil column was covered by a vented cap and incubated at 20°C-laboratory incubator (PP110plus, Memmert GmbH, Schwabach, Germany) in the dark for 1 day or 60 days, respectively. Changes in biological parameters are expected to be observed after long-term incubation, while the water infiltration occurs within 1–2 days (Schneider et al., 2018). We determined two test periods (1 and 60 days) to check both parameters in the soil columns. Since the different water content in soil can influence our measurement, parameters such as soil respiration and enzyme activities, water content was replenished every 3 days to keep uniform moisture during incubation periods.

At the end of each incubation period, soil samples of each depth (1 cm) were carefully collected using laboratorial spatula. The weights of each soil sample were recorded before and after drying at 60°C for 24 h to calculate water content (%). Soil structure of each depth were assessed as reported in previous study (de Souza Machado et al., 2019; Lehmann et al., 2020a). Shortly, the whole soil was gently passed through a set of stacked sieves (4,000, 2,000, 1,000, and 212 μm), and the weights of four separated fractions were recorded to determine the proportions (%) of each soil aggregate size class. Bulk density was computed by measuring the volume of soils within the plastic pot and soil dry weight (g cm^{-3}). We measured the soil respiration of three layers (top, microplastic-containing soil, and bottom), as CO_2 production rate (ppm h^{-1}) after 60 days of the experiment. Before the measurement, we flushed each of the tubes with CO_2-free air for five minutes to standardize among experimental units (Rillig et al., 2019). After 18 h, we sampled 1 ml of air from the headspace of each tube and injected this sample into an infrared gas analyzer (LiCOR 6400xt). Extracellular soil enzyme activities, acid phosphatase and β-D-glucosidase were measured after the 60 days incubation (Jackson et al., 2013). Briefly, 5 g of each soil sample (top, microplastic-containing soil, and bottom) was placed into a 50 ml test tube and mixed with 10 ml of 50 mM acetate buffer (pH 5.0–5.4), and 150 μl soil slurry was pipetted into each of six wells on a 96-well plate after vortexing. Then 150 μl acetate buffer was added into the last two wells of each samples (sample buffer control), and 150 μl substrate solutions (*p*-nitrophenyl-phosphate and *p*-nitrophenyl-β-glucopyranoside; Sigma, Germany) to the first four wells. Then the plates were kept in an incubator at 25°C for 2–4 h. After incubation, the microplates were centrifuged at 3000 x *g* for 5 min, and then 100 μl supernatant from each well was added into the new microplates with 10 μl 1 M NaOH and 190 μl distilled water in each well. Finally, the absorbance was recorded at 410 nm by a microplate reader (Benchmark Plus Microplate Spectrophotometer System, BioRad Laboratories, Hercules, CA, United States).

Dye Tracer Test

To observe the spatial patterns of water flow in the soil columns, dye tracer experiments were conducted with starting and 60 days incubated soil columns. The starting soil columns (0 days, before irrigation) were directly used for dye tracer test, and the 60 days incubated columns were dried at 60°C for 48 h. We employed Brilliant Blue dye as a tracer since it is highly visible (Schneider et al., 2018). Although dye transport is slower than the advance of infiltrating water, dye-stained soil patterns are generally considered to reasonable reflect flow patterns in soil experiments (Cey and Rudolph, 2009). We dissolved 100 mg of Brilliant Blue powder in 100 ml of deionized water, and 3 ml or 6 ml of dye solutions were applied to each soil column. After 24 h, the soil was carefully separated from the soil column, and vertically excavated to observe the soil profiles. To study the distribution of dye tracer in the soil profiles, photographs were captured. For each profile, the close-up photographs were adjusted for analyzing the relative pixel intensity of Brilliant Blue dyed path using ImageJ software (ImageJ, 1.52a, National Institutes of Health, United States).

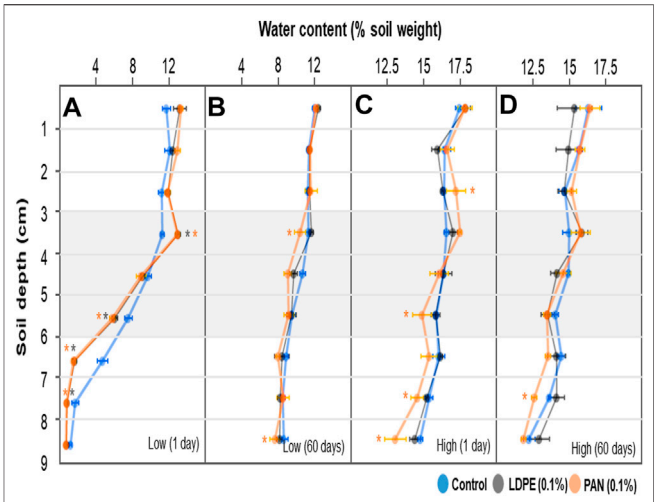

FIGURE 2 | Water contents (% soil dry weight) at each soil depth (0–9 cm) of each soil column (control and microplastic-containing soil layer treatments). Each soil column was irrigated either at a low level **(A,B)** or with higher water volume **(C,D)**, and incubated for 1 day **(A,C)** and 60 days **(B,D)**. Asterisk represents significance at the level of 5% (p = 0.05) between control and microplastic-containing soil layer treatments.

Statistical Analyses

Data were analyzed using the SPSS statistical software (Ver. 24.0, SPSS Inc., Chicago, IL, United States). One-way analysis for variance (ANOVA) and Turkey's tests were conducted to determine the significance ($p < 0.05$) of multiple comparisons.

RESULTS AND DISCUSSION

Effects on Water Contents and Flows

We observed each soil sample at each depth to examine the potential migration of microplastics during the soil column tests. As shown in **Supplementary Figures S3–S6**, microplastic-contaminated soil layers contained numerous LDPE films and PAN fibers, while only a few microplastic particles were found in top and bottom layers. We assume that the microplastics ended up in adjacent layers during the layer separation or soil analysis

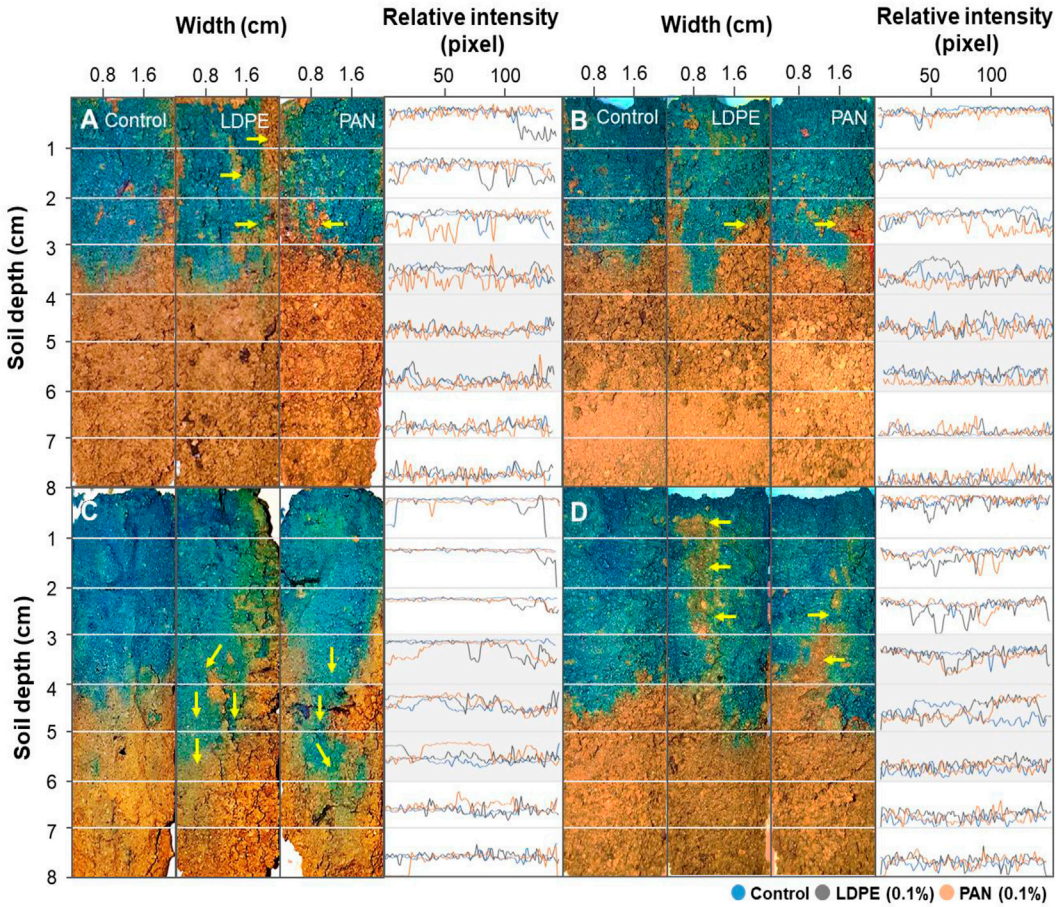

FIGURE 3 | Infiltrated dye stain patterns for vertical soil profiles. Each soil column was incubated for 0 days **(A,C)** and 60 days **(B,D)**, and irrigated either at a low level **(A,B)** or with higher water volume **(C,D)**.

steps. Although the microplastics may migrate to the adjacent soil layers with longer time or different conditions, we concluded here that the microplastics were not transported in our soil column tests. Water contents of each depth were considerably different already after the 1 day incubation. In the control treatment, after low-level irrigation, water content of the top layer (0–3 cm) was relatively higher than the bottom layer (6–9 cm), and this difference significantly increased in microplastic-containing soil layer treatments. Water contents increased to 13.03 ± 0.29 (LDPE films) and 12.98 ± 0.28 (PAN fibers) % in the top transition layer (3–4 cm), while the control treatment had a water content of 11.32 ± 0.19%. In the bottom transition layer (6–7 cm), water contents were 1.67 ± 0.19 (LDPE films) and 1.57 ± 0.23 (PAN fibers) %, while control treatment had 4.72 ± 0.57% (**Figure 2A**). The gaps of water contents between top and bottom layers were reduced after the 60 days of incubation, but significant differences among depths remained in the soil column containing PAN fiber layer (**Figure 2B**). In high-level irrigation treatments, only the soil layer with PAN fibers significantly influenced the vertical water distribution (**Figure 2C**), and the difference of water content in the top layer disappeared after the 60 days incubation, but remained in the bottom layer (**Figure 2D**).

The infiltrated dye stain patterns for vertical soil profiles are shown in **Figure 3**. In the control treatment after low-level irrigation, the dye tracer solution had uniformly infiltrated into soil depth 3–4 cm for both incubation periods (1 and 60 days), while uneven dye distributions and several discontinuities were observed in microplastic-containing soil layer treatments (yellow arrows in **Figures 3A,B**). After high-level irrigation, the maximum depth of dyed soil in the control treatment increased to 4–5 cm for both incubation periods (1 and 60 days) (**Figures 3C,D**). Paths of preferential flow appeared in microplastic-containing soil layer treatments (LDPE films and PAN fibers), and these patterns were observed below a soil depth of 6 cm (yellow arrows in **Figure 3C**). Although the dye transport does not exactly match the infiltrating water volume, the preferential flow indicates that the microplastic-containing soil layer might block and influence the water flow path in the soil column. These preferential flows were not observed after 60 days of incubation, and uneven dye distributions were observed in the top layers (yellow arrows in **Figure 3D**).

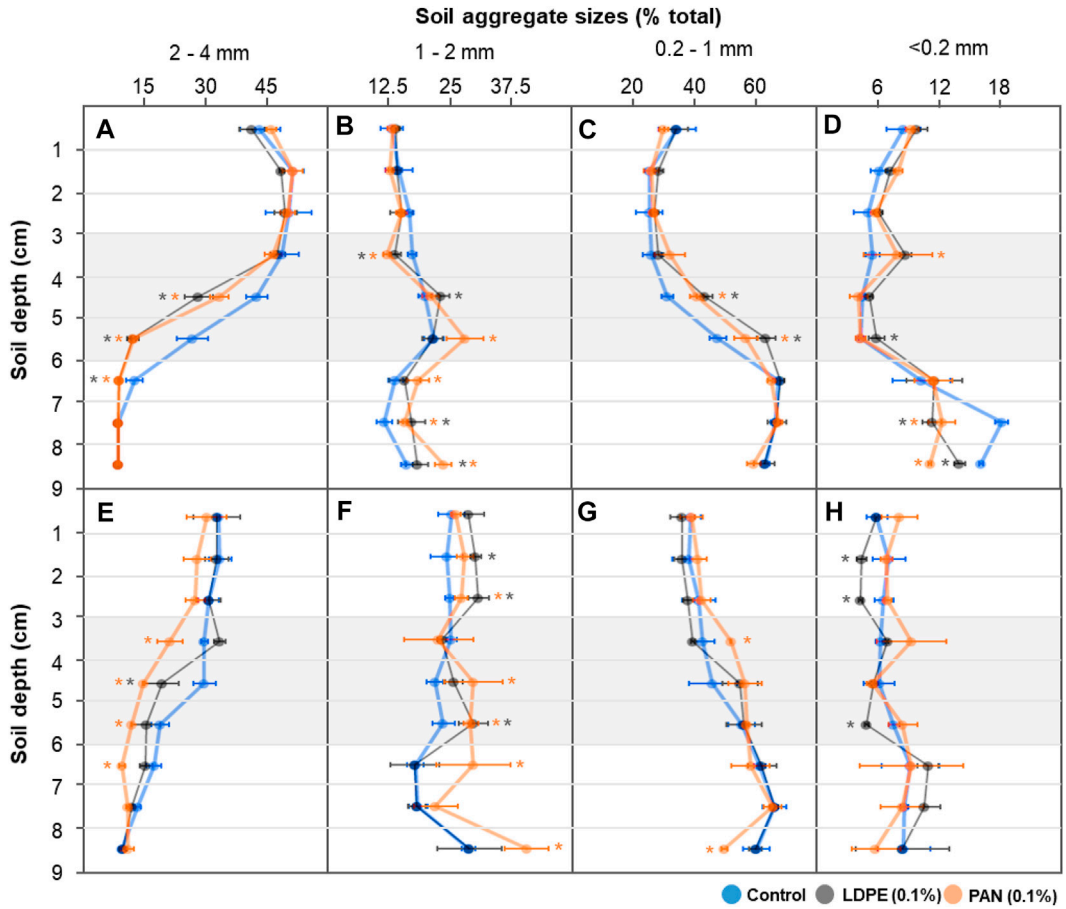

FIGURE 4 | Soil aggregate size fractions (2–4; 1–2; 0.2–1; <0.2 mm) at each depth (0–9 cm) after low-level irrigation. Each soil column was incubated for 1 day **(A–D)** and 60 days **(E–H)**. Asterisk represents significance at the level of 5% (p = 0.05) between control and microplastic-containing soil layer treatments.

Soil water content plays an important role in hydrological and biological processes, and spatial variability, both horizontally and vertically, is typically present in soil profiles (Wang and Liu, 2013). In anthropogenically modified soils, a high heterogeneity of substrates and unique patterns of water infiltration are often observed, such as in mine spoil soils, tilled soils, and biochar-containing soils (Andreini and Steenhuis, 1990; Badorreck et al., 2010; Schneider et al., 2018). A high spatial heterogeneity of pore volumes can be associated with anthropogenic (e.g., relict charcoal hearths) or natural fragments (e.g., organic matter and plant roots), and these can affect water flows in soil profiles (Schneider et al., 2018). There are several previous studies reporting that microplastics can influence water dynamics (de Souza Machado et al., 2018; de Souza Machado et al., 2019; Wan et al., 2019). Polyethylene films and polyester fibers induced changes in soil aggregation and pore sizes, and these phenomena can be directly or indirectly linked with water evaporation and soil cracking (Wan et al., 2019; Zhang et al., 2019). Alterations in soil structure can affect pore space in soils, which can simultaneously alter water holding capacity and water availability (de Souza Machado et al., 2019). Our study here shows that microplastic-containing soil layers can affect water contents and flows in adjacent soil layers, even if total water contents in the soil columns were kept the same in each treatment (control, LDPE films, and PAN fibers) (**Supplementary Figure S7**).

Effects on Soil Physical Structure

With low-level irrigation (1 day incubation) in the control treatment, large soil aggregate size fractions (2–4 mm) decreased with increasing soil depth, while intermediate sized fractions (1–2 and 0.1–1 mm) increased. This difference was more pronounced in microplastic-containing soil layer treatments, and mainly occurred in the microplastic-containing soil and bottom layers (<4 cm soil depth) (**Figures 4A–C**). After 60°days, the differences in soil aggregate size fractions between each soil depth were noticeably reduced in the control treatment, but significant differences among soil depths were still observed in the microplastic-containing soil layer treatments (**Figures 4E–G**). With high-level irrigation, large and intermediate sized soil aggregate fractions (2–4 and 1–2 mm) showed similar levels at each soil depth, but the PAN fiber layer influenced other size fractions (0.2–1 and <0.2 mm) (**Figures 5A–D**). After 60°days, the proportion of small soil aggregate size

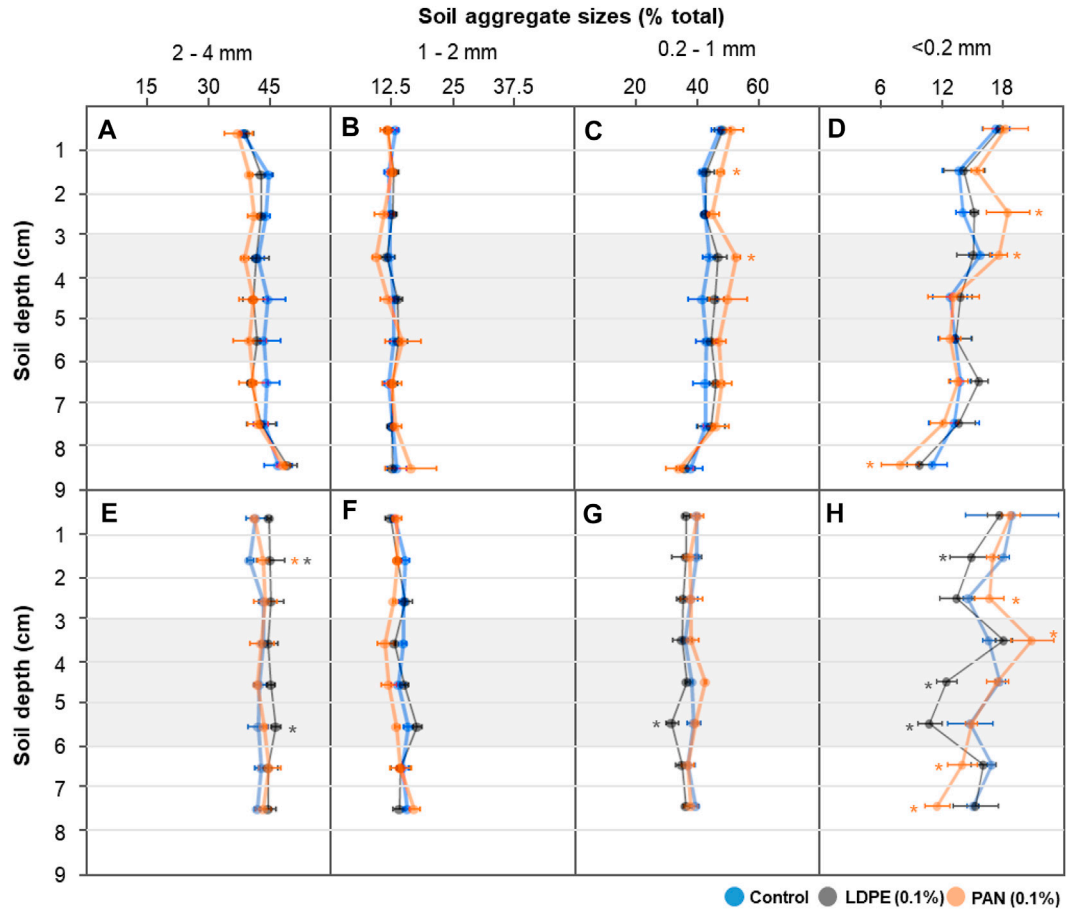

FIGURE 5 | The fractions of each soil aggregate size (2–4; 1–2; 0.2–1; <0.2 mm) in each depth (0–9 cm) after high-level irrigation. Each soil column was incubated for 1 day **(A–D)** and 60 days **(E–H)**. Asterisk represents significance at the level of 5% (p = 0.05) between control and microplastic-containing soil layer treatments.

fractions (<0.2 mm) was dramatically changed by LDPE films and PAN fiber layers. The proportion of the small size fraction significantly increased in the top layers and decreased in the bottom layers of PAN fiber treatment, and LDPE film layers had a significantly lower level than the control treatment (**Figure 5H**). Soil bulk density in the bottom layer seemed to be slightly influenced by microplastic-containing soil layers, but overall levels were similar in each treatment and depth (**Figure 6**).

The relative proportion of micro- (<0.2 mm) and larger macro-aggregates (2–4 mm) is crucial for pore size distribution (Horn and Smucker, 2005), and thus directly and indirectly influence the movement of water, gas, and nutrients (Jayarathne et al., 2021). We observed that the differences in size fractions between adjacent layers were less pronounced after the 60 days incubation since the water started to slowly infiltrate into the whole soil column from the soil surface (**Figures 2**, **4**). In microplastic-containing soil treatments with low-level irrigation, the significant differences in large and intermediate sized soil aggregate fractions (2–4, 1–2, and 0.2–1 mm) were still observed after 60 days of incubation (**Figures 4E–G**). With high-level irrigation, each size fraction in the soil columns after the 60 days incubation showed similar levels in control and microplastic treatments due to relatively homogenous water contents (**Figures 5E–G**), but fluctuations were observed in small soil aggregate size fractions (<0.2 mm) (**Figure 5H**). Since more intense irrigation can increase the dispersion of water and the mobility of clay particles (Horn and Dexter, 1989), the soil fraction in the size range of micro-aggregates seems to be influenced by both clay contents (Schweizer et al., 2019) and microplastics (Rillig and Lehmann, 2020).

The effects of microplastic fibers on soil aggregation have been well established in previous studies (de Souza Machado et al., 2019; Rillig and Lehmann, 2020). Aggregate water stability decreased by polyamide and polyester fibers in sandy loam soil (de Souza Machado et al., 2018; de Souza Machado et al., 2019; Lehmann et al., 2019), however, the contrary result that macro-aggregate fractions increased by polyester fibers addition in clayey soil (Zhang et al., 2019) was also observed. Films, which is one of the two microplastic shapes we use here, reduce tensile strength of soil, and desiccation shrinkage and cracking can be induced, depending on film particle size (Wan et al., 2019). In the present study, changes in each soil aggregate size fraction occurred in both microplastic-containing soil and bottom layers, and larger macro-aggregate fractions (2–4 mm)

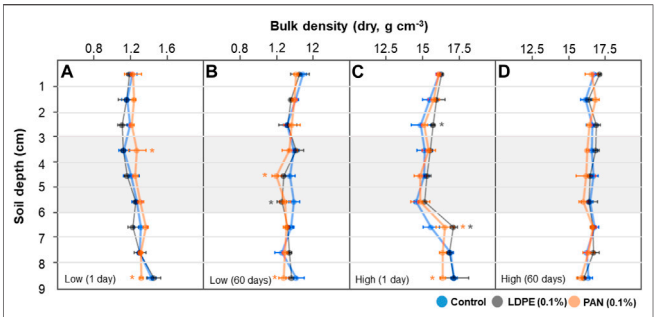

FIGURE 6 | Bulk density (dry, g cm^{-3}) at each soil depth (0–9 cm) of each soil column (control and microplastic-containing soil layer treatments). Each soil column was irrigated either at a low level **(A,B)** or with higher water volume **(C,D)**, and incubated for 1 day **(A,C)** and 60 days **(B,D)**. Asterisk represents significance at the level of 5% (p = 0.05) between control and microplastic-containing soil layer treatments.

decreased while micro-aggregates (<0.2 mm) were more variable. Our results here show that the microplastic-containing soil layer acts as an anthropogenic barrier, disrupting water flow paths into the bottom soil layer, and the different water contents in each layer seemed to be highly linked with the changes in the soil aggregate size fraction. Regarding microplastic target concentration, the changes in soil aggregate fractions by microplastic addition were induced in the ranges of 0.1–0.4% in previous reports (de Souza Machado et al., 2018; de Souza Machado et al., 2019; Lehmann et al., 2019). In our study, the soil aggregate size fractions were influenced not only in 0.1% of LDPE films or PAN fibers containing soil layers, but also in adjacent layers. Since many previous studies have focused on the homogeneous microplastic distribution in test soil and the effects in themselves, the observed changes in non-contaminated adjacent layers might mean that the effects of microplastics have been underestimated.

Effects on Biological Parameters

The results for soil respiration and enzyme activities are shown in **Supplementary Table S1**. A part of β-galactosidase data are missing due to experimental errors during measurements. With low-level irrigation, soil respiration rates (CO_2 production) in the top layers (0–3 cm) were 5.10–5.25 ppm h^{-1}, and those of the middle layers (3–6 cm) were 3.78–4.45 ppm h^{-1}. Significant changes were observed in the bottom layer (6–9 cm), as LDPE films and PAN fibers treatments had lower respiration (2.54 ± 0.12 (LDPE films), 2.75 ± 0.36 (PAN fibers) ppm h^{-1}) than control (3.27 ± 0.45 ppm h^{-1}). With high-level irrigation, soil respiration rates increased in the bottom layers with microplastic-containing soil layers, with 6.26 ± 0.80 (control), 7.64 ± 0.79 (LDPE films), and 7.86 ± 0.38 (PAN fibers) ppm h^{-1}, respectively. Enzyme activities in the bottom layers showed no significant differences between control and microplastic-containing soil layer treatments. Although acid phosphatase in soil columns containing PAN fibers tended to have higher activity (8.90 ± 5.02 and 8.32 ± 6.06 μmol mg^{-1} h^{-1} for low- and high-level irrigations, respectively), these values were not significantly different from the control (5.40 ± 3.05 and 4.09 ± 0.35 μmol mg^{-1} h^{-1}). The activities of β-D-glucosidase in each treatment were calculated as 1.92–3.68 (for low-level irrigation) and 2.10–3.08 (for high-level irrigation) μmol mg^{-1} h^{-1}, and there were no significant differences compared with control treatment.

Broad and extensive microbial responses to microplastic exposure have been reported in many previous studies (Liu et al., 2017; Yang et al., 2018; Huang et al., 2019). LDPE films and PAN fibers, the target microplastics in this study, can affect the rate of fluorescein diacetate hydrolysis (Huang et al., 2019; Liang et al., 2019). Microplastic fibers could provide more porosity, and their effects on soil respiration and enzyme activities can depend on soil water conditions (Lozano et al., 2021). Microplastic films can strongly influence soil respiration (Ng et al., 2020), and could reduce activity of aerobic microbes by affecting soil aeration due to their planar shape (Lehmann et al., 2020b). Previous studies have suggested that changes in soil structure can be a trigger for a series of events (de Souza Machado et al., 2018; de Souza Machado et al., 2019). Changes in soil structure can influence pore spaces, which can alter water dynamics and soil aeration, and this microplastic-driven physical change is particularly linked to biological or chemical processes. In our study, microplastic-containing soil layers interrupted water flow in soil and changed soil physical structure. These differences would be directly or indirectly linked with microbial activities: water content in soil has a linear relationship with soil respiration (Cook and Orchard, 2008), and soil aggregate size class is highly correlated with biological soil parameters since each size fraction has a different available organic matter content and C-N ratio (Ashman et al., 2003). We found evidence that microplastic-containing soil layers can affect a biological parameter (soil respiration) in the non-contaminated bottom layer. Despite the changes in soil respiration in the bottom layer, these changes did not translate to overall changes in the rate of enzyme activities.

CONCLUSION

Microplastics have unique properties compared with more traditional pollutants, such as heavy metals or organic chemicals, and many previous studies have reported effects of microplastic on soil properties. We here examined that microplastics-containing soil can affect adjacent soil layers not containing microplastic. We conducted a simple soil column test taking a phenomenological approach. Our results provide crucial evidence that microplastics-containing soil layers could act as an anthropogenic barrier, leading to vertically interrupted soil water flows and changes in physical structure. These effects occurred not only in microplastic-containing soil layers, but also in adjacent layers (top and bottom). Our results imply that the indirect effects on adjacent soils might be underestimated, and soil systems can be altered by microplastic contamination in unexpected ways. While our study was intended as a proof-of-concept, it also has relevance to real world situations, for example when plastic-containing soil surface layers are flipped during

certain ploughing operations in agricultural systems. Overall, we argue that future research should also consider heterogenous distribution of microplastic pollutants in ecosystems.

DATA AVAILABILITY STATEMENT

The original contributions presented in the study are included in the article/**Supplementary Material**, further inquiries can be directed to the corresponding author.

AUTHOR CONTRIBUTIONS

SK: conceptualization, design of the study, experiment set up, analysis of data, and writing. TZ and YL: analysis and writing. MR: review and editing. All authors contributed to the article and approved the submitted version.

ACKNOWLEDGMENTS

We acknowledge support by the Open Access Publication Initiative of Freie Universität Berlin. This work was supported by a post-doctoral grant from the National Research Foundation of Korea funded by the Ministry of Science, ICT, and Future Planning (2019R1A6A3A03031386). MR acknowledges support from an ERC Advanced Grant (grant no. 694368). YL acknowledges a scholarship from the China Scholarship Council. TZ acknowledges the China Scholarship Council for a scholarship (CSC No. 201608260012).

SUPPLEMENTARY MATERIAL

The Supplementary Material for this article can be found online at: https://www.frontiersin.org/articles/10.3389/fenvs.2021.681934/full#supplementary-material

REFERENCES

Andrady, A. L. (2011). Microplastics in the Marine Environment. *Mar. Pollut. Bull.* 62, 1596–1605. doi:10.1016/j.marpolbul.2011.05.030

Andreini, M. S., and Steenhuis, T. S. (1990). Preferential Paths of Flow under Conventional and Conservation Tillage. *Geoderma* 46, 85–102. doi:10.1016/0016-7061(90)90009-x

Arthur, C., Baker, J., and Bamford, H. (2009). *Proceedings of the International Research Workshop on the Occurrence, Effects, and Fate of Microplastic Marine Debris*, September 9–11 (Tacoma, WA, United States: University of Washington Tacoma).

Ashman, M. R., Hallett, P. D., and Brookes, P. C. (2003). Are the Links between Soil Aggregate Size Class, Soil Organic Matter and Respiration Rate Artefacts of the Fractionation Procedure? *Soil Biol. Biochem.* 35, 435–444. doi:10.1016/s0038-0717(02)00295-x

Badorreck, A., Gerke, H. H., and Vontobel, P. (2010). Noninvasive Observations of Flow Patterns in Locally Heterogeneous Mine Soils Using Neutron Radiation. *Vadose Zone J.* 9, 362–372. doi:10.2136/vzj2009.0100

Cey, E. E., and Rudolph, D. L. (2009). Field Study of Macropore Flow Processes Using Tension Infiltration of a Dye Tracer in Partially Saturated Soils. *Hydrol. Process* 23, 1768–1779. doi:10.1002/hyp.7302

Chen, G., Feng, Q., and Wang, J. (2020). Mini-review of Microplastics in the Atmosphere and Their Risks to Humans. *Sci. Total Environ.* 703, 135504. doi:10.1016/j.scitotenv.2019.135504

Cook, F. J., and Orchard, V. A. (2008). Relationships between Soil Respiration and Soil Moisture. *Soil Biol. Biochem.* 40, 1013–1018. doi:10.1016/j.soilbio.2007.12.012

de Ruijter, V. N., Redondo-Hasselerharm, P. E., Gouin, T., and Koelmans, A. A. (2020). Quality Criteria for Microplastic Effect Studies in the Context of Risk Assessment: A Critical Review. *Environ. Sci. Technol.* 54, 11692–11705. doi:10.1021/acs.est.0c03057

de Souza Machado, A. A., Lau, C. W., Kloas, W., Bergmann, J., Bachelier, J. B., Faltin, E., et al. (2019). Microplastics Can Change Soil Properties and Affect Plant Performance. *Environ. Sci. Technol.* 53, 6044–6052. doi:10.1021/acs.est.9b01339

de Souza Machado, A. A., Lau, C. W., Till, J., Kloas, W., Lehmann, A., Becker, R., et al. (2018). Impacts of Microplastics on the Soil Biophysical Environment. *Environ. Sci. Technol.* 52, 9656–9665. doi:10.1021/acs.est.8b02212

Ding, L., Zhang, S., Wang, X., Yang, X., Zhang, C., Qi, Y., et al. (2020). The Occurrence and Distribution Characteristics of Microplastics in the Agricultural Soils of Shaanxi Province, in North-Western China. *Sci. Total Environ.* 720, 137525. doi:10.1016/j.scitotenv.2020.137525

Fuller, S., and Gautam, A. (2016). A Procedure for Measuring Microplastics Using Pressurized Fluid Extraction. *Environ. Sci. Technol.* 50, 5774–5780. doi:10.1021/acs.est.6b00816

Horn, R., and Dexter, A. R. (1989). Dynamics of Soil Aggregation in an Irrigated Desert Loess. *Soil Tillage Res.* 13, 253–266. doi:10.1016/0167-1987(89)90002-0

Horn, R., and Smucker, A. (2005). Structure Formation and its Consequences for Gas and Water Transport in Unsaturated Arable and Forest Soils. *Soil Tillage Res.* 82, 5–14. doi:10.1016/j.still.2005.01.002

Huang, Y., Zhao, Y., Wang, J., Zhang, M., Jia, W., and Qin, X. (2019). LDPE Microplastic Films Alter Microbial Community Composition and Enzymatic Activities in Soil. *Environ. Pollut.* 254, 112983. doi:10.1016/j.envpol.2019.112983

Jackson, C. R., Tyler, H. L., and Millar, J. J. (2013). Determination of Microbial Extracellular Enzyme Activity in Waters, Soils, and Sediments Using High Throughput Microplate Assays. *JoVE* 80, 50399. doi:10.3791/50399

Jambeck, J. R., Geyer, R., Wilcox, C., Siegler, T. R., Perryman, M., Andrady, A., et al. (2015). Plastic Waste Inputs from Land into the Ocean. *Science* 347, 768–771. doi:10.1126/science.1260352

Jayarathne, J. R. R. N., Chamindu Deepagoda, T. K. K., Clough, T. J., Thomas, S., Elberling, B., and Smits, K. M. (2021). Effect of Aggregate Size Distribution on Soil Moisture, Soil-Gas Diffusivity, and N2O Emissions from a Pasture Soil. *Geoderma* 383, 114737. doi:10.1016/j.geoderma.2020.114737

Kim, S. W., Waldman, W. R., Kim, T.-Y., and Rillig, M. C. (2020). Effects of Different Microplastics on Nematodes in the Soil Environment: Tracking the Extractable Additives Using an Ecotoxicological Approach. *Environ. Sci. Technol.* 54, 13868–13878. doi:10.1021/acs.est.0c04641

Lehmann, A., Fitschen, K., and Rillig, M. (2019). Abiotic and Biotic Factors Influencing the Effect of Microplastic on Soil Aggregation. *Soil Syst.* 3, 21. doi:10.3390/soilsystems3010021

Lehmann, A., Leifheit, E. F., Feng, L., Bergmann, J., Wulf, A., and Rillig, M. C. (2020a). Microplastic Fiber and Drought Effects on Plants and Soil Are Only Slightly Modified by Arbuscular Mycorrhizal Fungi. *Soil Ecol. Lett.* doi:10.1007/s42832-020-0060-4

Lehmann, A., Leifheit, E. F., Gerdawischke, M., and Rillig, M. C. (2020b). Microplastics Have Shape-And Polymer-dependent Effects on Soil Processes. *bioRxiv*. doi:10.1101/2020.06.02.130054

Liang, Y., Lehmann, A., Ballhausen, M.-B., Muller, L., and Rillig, M. C. (2019). Increasing Temperature and Microplastic Fibers Jointly Influence Soil Aggregation by Saprobic Fungi. *Front. Microbiol.* 10, 2018. doi:10.3389/fmicb.2019.02018

Liu, H., Yang, X., Liu, G., Liang, C., Xue, S., Chen, H., et al. (2017). Response of Soil Dissolved Organic Matter to Microplastic Addition in Chinese Loess Soil. *Chemosphere* 185, 907–917. doi:10.1016/j.chemosphere.2017.07.064

Liu, M., Lu, S., Song, Y., Lei, L., Hu, J., Lv, W., et al. (2018). Microplastic and Mesoplastic Pollution in Farmland Soils in Suburbs of Shanghai, China. *Environ. Pollut.* 242, 855–862. doi:10.1016/j.envpol.2018.07.051

Lozano, Y. M., Aguilar-Trigueros, C. A., Onandia, G., Maaß, S., Zhao, T., and Rillig, M. C. (2021). Effects of Microplastics and Drought on Soil Ecosystem Functions and Multifunctionality. *J. Appl. Ecol.* doi:10.1111/1365-2664.13839

Ng, E. L., Lin, S. Y., Dungan, A. M., Colwell, J. M., Ede, S., Huerta Lwanga, E., et al. (2020). Microplastic Pollution Alters Forest Soil Microbiome. *J. Hazard. Mater.* 409, 124606. doi:10.1016/j.jhazmat.2020.124606

Nizzetto, L., Futter, M., and Langaas, S. (2016). Are Agricultural Soils Dumps for Microplastics of Urban Origin? *Environ. Sci. Technol.* 50, 10777–10779. doi:10.1021/acs.est.6b04140

Piehl, S., Leibner, A., Löder, M. G. J., Dris, R., Bogner, C., and Laforsch, C. (2018). Identification and Quantification of Macro- and Microplastics on an Agricultural Farmland. *Sci. Rep.* 8, 17950. doi:10.1038/s41598-018-36172-y

Potthoff, A., Oelschlägel, K., Schmitt-Jansen, M., Rummel, C. D., and Kühnel, D. (2017). From the Sea to the Laboratory: Characterization of Microplastic as Prerequisite for the Assessment of Ecotoxicological Impact. *Integr. Environ. Assess. Manag.* 13, 500–504. doi:10.1002/ieam.1902

Rillig, M. C., and Lehmann, A. (2020). Microplastic in Terrestrial Ecosystems. *Science* 368, 1430–1431. doi:10.1126/science.abb5979

Rillig, M. C. (2012). Microplastic in Terrestrial Ecosystems and the Soil?. *Environ. Sci. Technol.* 46, 6453–6454. doi:10.1021/es302011r

Rillig, M. C., Ryo, M., Lehmann, A., Aguilar-Trigueros, C. A., Buchert, S., Wulf, A., et al. (2019). The Role of Multiple Global Change Factors in Driving Soil Functions and Microbial Biodiversity. *Science* 366, 886–890. doi:10.1126/science.aay2832

Sarijan, S., Azman, S., Said, M. I. M., and Jamal, M. H. (2021). Microplastics in Freshwater Ecosystems: a Recent Review of Occurrence, Analysis, Potential Impacts, and Research Needs. *Environ. Sci. Pollut. Res.* 28, 1341–1356. doi:10.1007/s11356-020-11171-7

Scheurer, M., and Bigalke, M. (2018). Microplastics in Swiss Floodplain Soils. *Environ. Sci. Technol.* 52, 3591–3598. doi:10.1021/acs.est.7b06003

Schneider, A., Hirsch, F., Raab, A., and Raab, T. (2018). Dye Tracer Visualization of Infiltration Patterns in Soils on Relict Charcoal Hearths. *Front. Environ. Sci.* 6, 143. doi:10.10.3389/fenvs.2018.00143

Schweizer, S. A., Bucka, F. B., Graf-Rosenfellner, M., and Kögel-Knabner, I. (2019). Soil Microaggregate Size Composition and Organic Matter Distribution as Affected by Clay Content. *Geoderma* 355, 113901. doi:10.1016/j.geoderma.2019.113901

Sutherland, W. J., Fleishman, E., Clout, M., Gibbons, D. W., Lickorish, F., Peck, L. S., et al. (2019). Ten Years on: A Review of the First Global Conservation Horizon Scan. *Trends Ecol. Evol.* 34, 139–153. doi:10.1016/j.tree.2018.12.003

Thomas, D., Schütze, B., Heinze, W. M., and Steinmetz, Z. (2020). Sample Preparation Techniques for the Analysis of Microplastics in Soil-A Review. *Sustainability* 12, 9074. doi:10.3390/su12219074

Wan, Y., Wu, C., Xue, Q., and Hui, X. (2019). Effects of Plastic Contamination on Water Evaporation and Desiccation Cracking in Soil. *Sci. Total Environ.* 654, 576–582. doi:10.1016/j.scitotenv.2018.11.123

Wang, Y., Shao, M. a., and Liu, Z. (2013). Vertical Distribution and Influencing Factors of Soil Water Content within 21-m Profile on the Chinese Loess Plateau. *Geoderma* 193-194, 300–310. doi:10.1016/j.geoderma.2012.10.011

Yang, X., Bento, C. P. M., Chen, H., Zhang, H., Xue, S., Lwanga, E. H., et al. (2018). Influence of Microplastic Addition on Glyphosate Decay and Soil Microbial Activities in Chinese Loess Soil. *Environ. Pollut.* 242, 338–347. doi:10.1016/j.envpol.2018.07.006

Zhang, G. S., and Liu, Y. F. (2018). The Distribution of Microplastics in Soil Aggregate Fractions in Southwestern China. *Sci. Total Environ.* 642, 12–20. doi:10.1016/j.scitotenv.2018.06.004

Zhang, G. S., Zhang, F. X., and Li, X. T. (2019). Effects of Polyester Microfibers on Soil Physical Properties: Perception from a Field and a Pot Experiment. *Sci. Total Environ.* 670, 1–7. doi:10.1016/j.scitotenv.2019.03.149

Zhang, S., Yang, X., Gertsen, H., Peters, P., Salánki, T., and Geissen, V. (2018). A Simple Method for the Extraction and Identification of Light Density Microplastics from Soil. *Sci. Total Environ.* 616–617, 1056–1065. doi:10.1016/j.scitotenv.2017.10.213

Zhou, Q., Zhang, H., Fu, C., Zhou, Y., Dai, Z., Li, Y., et al. (2018). The Distribution and Morphology of Microplastics in Coastal Soils Adjacent to the Bohai Sea and the Yellow Sea. *Geoderma* 322, 201–208. doi:10.1016/j.geoderma.2018.02.015

Conflict of Interest: The authors declare that the research was conducted in the absence of any commercial or financial relationships that could be construed as a potential conflict of interest.

frontiers in Environmental Science

REVIEW
published: 13 May 2021
doi: 10.3389/fenvs.2021.652367

The Potential Application of Giant Reed (*Arundo donax*) in Ecological Remediation

Deng Zhang[1], *QianWen Jiang*[1], *DanYang Liang*[2], *Shixun Huang*[1]* *and Jianxiong Liao*[1]*

[1]*Guangxi Key Laboratory of Plant Conservation and Restoration Ecology in Karst Terrain, Guangxi Institute of Botany, Guangxi Zhuang Autonomous Region and Chinese Academy of Sciences, Guilin, China,* [2]*College of Tourism & Landscape Architecture (College of Plant and Ecological Engineering), Guilin University of Technology, Guilin, China*

Giant reed is known as one of the most important energy plants as a consequence of its huge dry biomass production. It can be used for bioenergy or biopolymer production. Thus, it can replace maize and reduce the production cost of biomass and electricity. Giant reed and its products have different uses in industry. The use of giant reed as a raw material to obtain cellulose past for the production of rayon viscose and paper. Thanks to the flexible and strong of the material, giant reed can be used in the manufacture of fishing rods, brass musical instruments, canes and construction supplies. One of the most important characteristics of giant reed is that it shows strong growth capability in different soils with wide ranges of pH, salinity and high heavy metal contents and can be used for ecological remediation. Giant reed was able not only to decontaminate polluted soils with heavy metals, but also to purify the wastewater and decrease the pH and make red mud safer. Here, we review the available evidence regarding the utilization of giant reed in the field of phytoremediation and discuss the potential application of giant reed combined with advanced remediation technologies in ecological remediation.

Keywords: ecological remediation, economic and ecological value, phytoremediation, heavy metal pollution, giant reed

OPEN ACCESS

Edited by:
Chunhao Gu,
University of Delaware, United States

Reviewed by:
Kuldeep Bauddh,
Central University of Jharkhand, India
Mihaly Czako,
University of South Carolina, United States

***Correspondence:**
Shixun Huang
hsx@gxib.cn
Jianxiong Liao
liaojianx@163.com

Specialty section:
This article was submitted to Toxicology, Pollution and the Environment, a section of the journal Frontiers in Environmental Science

Received: *12 January 2021*
Accepted: *16 April 2021*
Published: *13 May 2021*

Citation:
*Zhang D, Jiang Q, Liang D, Huang S and Liao J (2021) The Potential Application of Giant Reed (*Arundo donax*) in Ecological Remediation. Front. Environ. Sci. 9:652367. doi: 10.3389/fenvs.2021.652367*

INTRODUCTION

With the coming of the industrial revolution, humans were able to advance further into the 21st century. At present, the industry is a critical component of the world's economy. However, at the same time, the industrial processes also cause environmental pollution. It accounts for more than half of the total emissions of some key air pollutants and greenhouse gases, as well as other critical ecological impacts, including the release of pollutants to water and soil (Muradian and Martinez-Alier, 2001; Wang et al., 2019). Consequently, these pollutants can pose a health risk to humans and other organisms.

The discharge of excessive amount of heavy metals is one of the most severe environment pollutions. The toxicity of heavy metals is well documented for its impairment of plant growth and human health. Therefore, it is necessary to eliminate excessive amounts of heavy metals in soil and water to avoid negative consequences. Various conventional methods have been used to remove heavy metals, such as chemical precipitation, solvent extraction, membrane filtration, ion change, electrochemical removal and coagulation etc. (Burakov et al., 2018). However, questions have been raised to query these techniques in term of incomplete removal, low efficiency and costly disposal etc. Compared to conventional methods, phytoremediation has excellent potential to overcome those

drawbacks, improving the treatment efficiency and cut the expense. It has been reported that some hyperaccumulator plants can accumulate a large number of heavy metals. For example, *Alyssum bertolonii* can accumulate Ni up to about 10,000 $\mu g\, g^{-1}$ or 1% (Reeves et al., 2018). Soil salinization is another global environmental problem that could damage land quality and limit plant growth. It is estimated that over half of the irrigated farmlands are seriously impacted by soil salinization (Li et al., 2018). Although the use of chemical amendment, for example, use Ca to replace exchangeable Na, or apply organic amendments such as farm manure, poultry manure and plant ash to reduce the soil pH may be a practical strategy to improve soil remediation (Tejada et al., 2006; Dahlawi et al., 2018), the high cost and less efficiency of these methods were the main obstacles that limit their application (Nouri et al., 2017). Alternatively, halophytes are ideal plants for salt remediation of soil. For example, *Tecticornia indica* and *Suaeda fruticosa*, which can eliminate redundant salts from soil, and thus these plants are popularly used for the soil remediation (Rabhi et al., 2010). Water is essential for life on Earth. Any pollutants or contaminants which find their way into water will soon find their way into the bodies of plants and animals. Contaminated water is one of the most common forms of environmental pollution, not to mention one of the most damaging to the health of living organisms, entering bodies through drinking, contact, or uptake from roots. Water pollution can either be directly through the discharging of waste into a body of water such as a lake, river or the sea, or it can be indirect in that it is not deliberately disposed of into a watercourse but finds its way there. The most common cause of water pollution is human activity including industry, agriculture and livestock farming, rubbish and fecal water dumping. To abate water pollution, various treatments such as adsorption, biodegradation, coagulation, ion-exchange, and oxidation processes have been evaluated. However, the practice of these methods is very complexity (Jain et al., 2018; Shahid et al., 2019). Constructing wetlands to remediate wastewater is an efficient strategy because of its eco-friendly and low operational cost (Wang et al., 2018). This strategy mainly uses the plant-bacteria synergism to clean the organic matter, microorganisms, nitrogen, and phosphorus in the water.

Based on the above information, we can conclude that plants with excellent pollutant adsorption capacity have great potential in ecological remediation. In the following, we introduce the characterization of giant reed (*Arundo donax*) in the field of phytoremediation and discuss the potential application of giant reed combined with advanced remediation technologies in ecological remediation.

ORIGIN AND REPRODUCTION OF GIANT REED

Giant reed is a tall perennial rhizomatous grass that can reach 10 m in height (Barreca et al., 2019). Owing to its fast growth and great biomass, giant reed had been attracted the farmers and researchers attention to use for multi-purpose (Perdue, 1958; Bell, 1998). For a long time, the stem of the giant reed was used to make paper (Perdue, 1958). In Italy, giant reed has been used in industry since 1930, when a company registered a trademark to obtain cellulose for producing rayon viscose and paper (Facchini, 1941). The European "Giant reed Network" has been established since January 1997. The project, within the framework of the FAIR Program, has been designed to generate information about this plant's capacity to be brought into EU agriculture for energy and pulp production (Lewandowski et al., 2003). Due to its considerable growth capacity in different soils with wide ranges of pH, salinity, and trace metal contents, giant reed was used to absorb heavy metals and improve saline alkali soil in recent years (Herrera-Alamillo and Robert, 2012; Quinn et al., 2015). Giant reed is suitable for energy production because of the high biomass yield, which can reach to 37.7 t dry matter per ha and per year (Angelini et al., 2009). Among the different biomass crops for producing renewable energy to reduce greenhouse gas emissions due to fossil fuels, the giant reed is considered the best candidate (Di Mola et al., 2018). It is an ideal plant for dealing with extreme situations of soil conditions and water availability (**Figure 1**).

Because of its vast economic value, giant reed is widely planted in subtropical regions of the world, such as Southern Europe, North Africa, Australia, and America (Guo and Miao, 2010). Giant reed does not produce seed in many areas because the further development of the embryo is restricted (Balogh et al., 2012; Nikhade and Makde, 2014; Alshaal et al., 2015). The propagation of giant reed can be divided into rhizomes or stem cuttings and *in vitro* biotechnology methods.

Planting time on stem cuttings has a significant influence on the survival rate of the giant reed. Tang (2000) used the stem of the giant reed as propagules about February or March, and the survival rate reached 97%. However, the survival rate of cutting with the lateral branches of giant reed is not high. Luo et al. (2018) used different types and concentrations of plant hormones to treat the lateral branches of giant reed, and the highest survival rate was only 50%. Rhizomes are easy to generate roots in wet environments and produce new plant clones. The propagation of giant reed is more commonly used fragments of rhizomes.

Compared with rhizomes or stem cuttings, the efficiency of *in vitro* biotechnology methods is higher. Gubišová et al. (2016) report that stem segments containing an axillary bud of the giant reed can produce about 700 rooted and acclimatized plants in one year starting from one axillary bud on Murashige and Skoog medium supplemented with 0.5 $mg\, l^{-1}$ 6-benzyladenine or 0.2 $mg\, l^{-1}$ thidiazuron. Marton and Czako (2002) suggest that the immature inflorescences of giant reed are sterilized and then cultured *in vitro* to produce totipotent tissue from which mass propagation of plantlets is possible. Herrera-Alamillo and Robert (2012) use axillary buds from the lateral stems cultured in liquid medium supplemented with indole 3-acetic acid and kinetin to produce 900 plants from a single mother plant in 4 months Cavallaro et al. (2011) describe a protocol for the large-scale *in vitro* propagation of giant reed by adventitious bud formation. The technical system of callus induction, differentiation, and plant regeneration can significantly increase the reproduction coefficient of plants. Chen et al. (2016) report that Murashige and Skoog medium supplemented with 0.2 $mg\, l^{-1}$ naphthaleneacetic

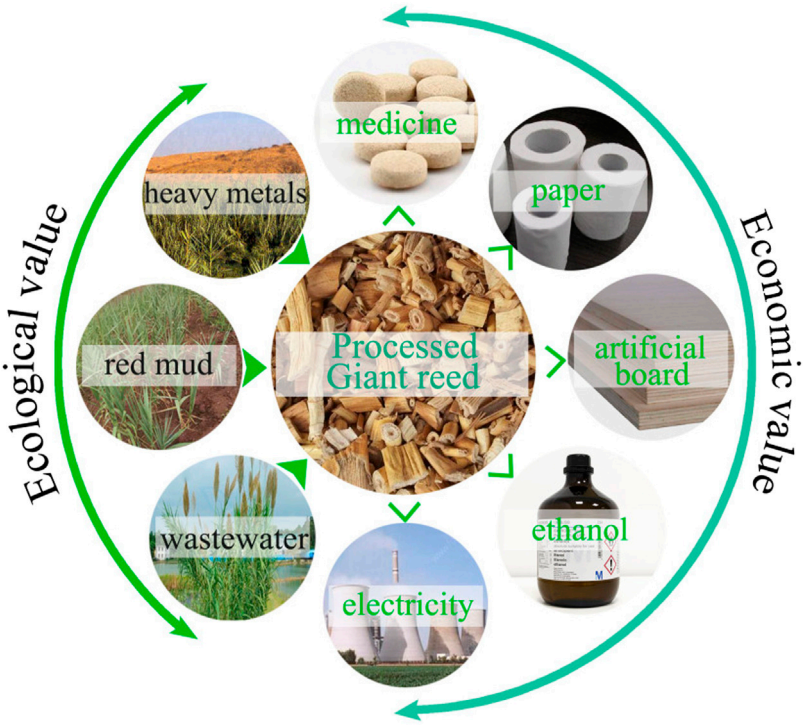

FIGURE 1 | Comprehensive application of giant reed.

acid and 2.0 mg l^{-1} 6-benzyladenine are used for the best callus differentiation medium in turn the bud differentiation stage reached 40.00%, while Yang et al. (2016) suggest that the callus (with an improved quality as well as an increased quantity) were transferred on the Murashige and Skoog medium with 0.5 mg l^{-1} kinetin and 1.0 mg l^{-1} 6-benzyladenine, on which both shoots and roots were simultaneously induced with a large quantity. The regenerated plants grow to more than 5.0 cm and transfer to Murashige and Skoog medium with 0.2 mg l^{-1} naphthaleneacetic acid and 1 g l^{-1} activated carbon. The rate of rooting was 100% for 7 days, and the average root number was four, and the length of the roots was 2–4 cm (Xian et al., 2018). The rooted seedings, which with roots 2–3 cm, were transplanted from culturing seedlings to fine river sand, yellow soil or humus soil after one week-day's treatment. The survival percent reaches 98% after a month.

THE ECONOMIC VALUE OF GIANT REED

Giant Reed Used as an Energy Crop

Giant reed has a wide range of adaptations and can be planted in marginal areas where crops cannot grow (Roberto, 2012). It grows very fast and can grow to 6 m or even higher (Liao et al., 2017). The mature crop shows average annual production rates of 3 kg dry matter m^{-2}, with maximum values acquired in fertilized plots and during winter harvest time (Angelini et al., 2005). Giant reed is a very suitable source of biomass because of its low cost and high productivity (Corno et al., 2014; Corno et al., 2015). Research shows that giant reed can replace maize and reduce the production cost of biomass and electricity (Corno et al., 2016). Giant reed stems can be transformed into useful, value-added reliable products through pyrolysis at appropriate conditions (Basso et al., 2005). Solid biofuels are conducive to preservation and transportation. Giant reed has good potential for biogas production through anaerobic digestion (AD). Among them, cellulose has the highest degradation rate and the most significant contribution to biogas production (Yang and Li, 2014).

Giant Reed Used as an Industrial Material

Its peculiar characteristics, such as its large diffusion on the territory, its stem's lightness combined with its adequate mechanical strength, and its high cellulose content, have allowed different industrial uses of giant reed (Perdue, 1958; Speck and Spatz, 2004; Barreca, 2012). Because of its advanced eco-friendly pulping and bleaching technology, giant reed has become an excellent substitute for wood fibers to meet pulp and paper products' rapid growth (Shatalov and Pereira, 2006). The fibers of giant reed possess high tensile strength and suitable raw material for particleboard production (Flores et al., 2011). The stem of the giant reed can be converted into activated carbon by various technologies, which shows excellent performance in wastewater treatment (Ahmed, 2016). In the Mediterranean region, giant reed has been traditionally employed to build fences and temporary shelters for men and animals, or as a prop for plants and as windbreak or shading barrier (Barreca and Fichera, 2013). Thanks to the lightness of the material, walls can

be erected even by farmers or breeders with modest tools (Barreca, 2012). Because of widespread and locally abundant, giant reed is widely used and has a greater diversity of uses in Cyprus's northwest. The culms are used to make baskets, tables, fishing equipment, musical instruments, candy bow, chandelier, distaff, heddle, knife, and fence (Barreca, 2012).

Giant Reed Used as Medicine

Modern pharmacological studies have proved the plants' role in treating diseases, reflected in current plant origin drug therapy. The use of medicinal plants to treat diseases has witnessed such treatments and increased awareness of the importance of using natural resources in the pharmaceutical industry (El Sheikha, 2017). Giant reed is considered as one of the medicinal plants. It was reported that aqueous extracts of the reed nodes, which contain the white hemicellulose membrane, and demonstrated a marked dose-dependent response for anti-biofilm activity, both in preventing MRSA biofilm formation and disrupting established biofilms (Quave et al., 2008). The antimicrobial effects of methanolic extracts of 14 medicinal plant species were examined comparing to conventional therapeutic antibiotics against standard bacterial strains (*Staphylococcus aureus*, *Micrococcus luteus, Klebsiella pneumoniae*, *Escherichia coli*, and *Pseudomonas eroginosa*). Among the four medicinal plants, the giant reed extract has the most significant effect on *Escherichia coli* and *Pseudomonas eruginosa* (Al-Snafi, 2015). Besides, the tender shoots can be used for the treatment of fever, wound suppuration, ear infection, typhoid, pneumonia and asthma (Sinha, 1996; Singh, 2003; Dhiren and Singh, 2015). Extractions of biologically active components from giant reed shoot is regarded as good anti-galactagogue, depurative, diaphoretic, emollient, hypertensive, hypotensive, and sudorific (Duke and Wain, 1981). In addition, the root of giant reed is also an alternative herbal medicine used as diaphoretic, emollient, diuretic, and cancer, dropsy, and headache (Mir et al., 2018).

PHYTOREMEDIATION POTENTIALS OF GIANT REED

Heavy Metal

With fast urbanization and industrialization, heavy metal pollution has become one of the utmost environmental severe issues that influence human health (Zhao et al., 2018). In the past 5 decades, more than 30,000 tons of Cr and 800,000 tons of Pb have been released into the environment around the world (Yang et al., 2018). Heavy metal pollution has an essential impact on crop yield and quality and affects the air and water environment and even human health. Many of them are toxic even at deficient concentrations, which are cytotoxic and carcinogenic, and mutagenic. Joint committee of World Health Organization (WHO) and Food and Agriculture Organization (FAO) on food additives (JCEFA) has set the maximum tolerable intake for As, Cd, Pb, and Cr as 2, 1, 6.03, and 3.32 μg/kg body weight/day, respectively (Dubey et al., 2018). Excessive levels of heavy metals can cause health risks, for instance, 1) the concentrations of Hg in whole blood reach 10 μg/L may lead to lung damage; kidney damage, proteinuria, allergy, and amalgam disease, 2) the dietary intake of Cd reach 0.01 mg/kg/day can affect kidney functioning, 3) intaking of Ni from contaminated food reach 5 mg/kg/day can affect renal functioning, and so on (Rai et al., 2019). Accumulation of heavy metals on soil can cause direct or indirect reduction of plant growth by adversely affecting various physiological and molecular activities of plants (Tiwari and Lata, 2018). The current research suggests that the maximum soil concentration for different heavy metal (loids) were as follows: As ranged from a maximum of 11–34 mg/kg, Cd from 0.15 to 21.84 mg/kg, Cu from 16 to 713 mg/kg, Ni from 25 to 740 mg/kg, Pb from 25 to 2025 mg/kg, and Zn from 25 to 3,925 mg/kg (O'Connor et al., 2018). However, the tolerance of most plants for safe limits of heavy metals is not high. Guideline for safe limits of some heavy metal as follow: Cd from 3 to 6 mg/kg, Cu from 135 to 270 mg/kg, Pb from 250 to 500 mg/kg, Zn from 300 to 600 mg/kg, Ni from 75 to 150 mg/kg (Nagajyoti et al., 2010). In high concentrations, heavy metals negatively impact the growth, biomass, and photosynthesis of plants and compromise sustainable food production (Etesami, 2018). As a result of heavy metals have detrimental effects on plants and humans. Recently, the remediation of heavy metal pollution has aroused people's concern. So far, several efficient methods have been reviewed for the removal of heavy metals such as chemical precipitation, adsorption, ion exchange, reverse osmosis, phytoremediation, bioremediation, membrane technology, and electrochemical treatment, etc. (Dixit et al., 2015). They can be classified into two main groups, including physicochemical and biological techniques. Key factors influencing the applicability and selection of such technologies are capital investment and operational cost, plant flexibility, and reliability and environmental impact, etc. (Fu and Wang, 2011). Physicochemical approaches include chemical precipitation, adsorption, ion exchange, reverse osmosis, membrane technology, and electrochemical treatment. These techniques are rapid but inadequate, high cost, intensive labor, altered soil properties, and disturbance of soil native microflora (Ali et al., 2013). Moreover, most of these techniques are ineffective when the concentration of heavy metals is below 100 mg/L (Ahluwalia and Goyal, 2007). Compared with physicochemical, biological remediation has many advantages, such as natural process, environmentally friendly, low cost, and high public acceptance (Ullah et al., 2015). Biological remediation use microorganisms and plants to remove toxic contaminants from the environment (Singh et al., 2009). Living or dead microorganisms can be used for the remediation of heavy metals. Among these microorganisms, bacteria, fungi, and algae are most widely used, for example, bacteria can remediate Hg, Pb, Cr, Cu, Zn, and Cd, fungi can remediate Pb, Cr, Cu, Co, and Cd, algae can remediate Pb, Cr, Cu, and Cd (Yin et al., 2019). Phytoremediation is an emerging green technology used of metallophytes and related soil microorganisms to reduce the concentration or toxic effects of heavy metals in the environment. Remediation of a metal-contaminated climate by phytoremediation has received extensive attention because it is cost-effective, efficient, resource-conserving, and eco-friendly (Baker et al.,

1994; Sumiahadi and Acar, 2018). Heavy metal removal from contaminated sites using different phytoremediation methods has been initiated worldwide since the last decade, including phytoremediation of organic, inorganic and radionuclides. This sustainable and cheap process is rapidly evolving into a viable alternative to traditional remedies and most suitable for developing countries (Ghosh and Singh, 2005).

Recently, the accumulation of heavy metals by giant reed attracted more and more attention from various fields of science and engineering and became a hot researching spot (Borso et al., 2018; Coppa et al., 2020; Delplace et al., 2020). Giant reed has promising ability to uptake wide variety of metals viz. Pb, Cd, Mo, As, Zn, Cu, Ni, Co, Fe, Mn, Cr, Hg, Al etc. from the environment (Miao et al., 2012; Delplace et al., 2020; Danelli et al., 2021). It is a promising candidate for the phytoremediation of Zn-/Cr-contaminated soil (Li et al., 2014). Biomass obtained in Zn and Cr contaminated soils presented higher ash content and higher Zn/Cr content than biomass from non-contaminated soils (Barbosa et al., 2013; Barbosa et al., 2015). Pu et al. (2017) reported that despite the oxidative stress involved in the mechanism of Cd toxicity associated with the high transport of Cd in giant reed, its photosynthetic system was not harmed. When giant reed grown on surface soil and irrigated with mixed heavy metal solutions of Cd(II) and Ni(II), the examined parameters, namely, stem height and diameter, number of nodes, fresh and dry weight of leaves, and net photosynthesis (Pn) were not affected (Papazoglou et al., 2005). Mahmood (2010) report that giant reed can extract arsenic (As) and mercury (Hg) in sufficient amounts, and Cano-Ruiz et al. (2020) report that giant reed showed a broad tolerance to cadmium (0.5 mM), chromium (0.2 mM), cooper (2 mM), nickel (0.5 mM) and lead (1 mM). Guarino et al. (2020) reported that giant reed can remove As through high and efficient volatilization. Biomass obtained in Pb contaminated soils presented higher ash content and lead content than biomass from non-contaminated soils (Sidella et al., 2013). Based on the findings of Domokos-Szabolcsy et al. (2018), giant reed can be identified as the first monocot hyperaccumulator of selenium. Some researchers find that the presence of chelating agent, organic fertilizer and mycorrhizal fungi have an impact on the ability to accumulate metals for giant reed. Atma et al. (2017) investigate that the addition of EDTA to the treatment increased plant uptake of arsenic. Other researchers also aimed at finding that compost fertilization and mycorrhizal fungi inoculations increase the metal uptake of giant reed (Fiorentino et al., 2013; Liu et al., 2017; Sarathambal et al., 2017).

The remediation mechanism from plants is distinct. According to growth potential in HM-contaminated sites, they can be classified into five main groups including plant extraction, plant degradation, plant stabilization, plant volatilization and rhizosphere filtration (Mukhopadhyay and Maiti, 2010; Ali et al., 2013; Thakur et al., 2016; Saxena et al., 2019). Recent studies show that giant reed shows good phytostabilization capability in the short-term while long-term can be used in phytoextraction processes (Cristaldi et al., 2020). The pH of the soil and the presence of chelating agents like mugineic acid family phytosiderophores (MAs) can mobilize metal ions into the soil solution. Metal ions can be taken up by the root of giant reed and come in contact with the cell wall. Giant reed can translocate the heavy metals to above-ground shoots or leaves and produce a large quantity of plant biomass that can be easily harvested (**Figure 2**). Various kinds of heavy metals can be extracted and accumulated in various organs (e.g., root, stem, leaf) by giant reed. Numerous studies have shown that the root is

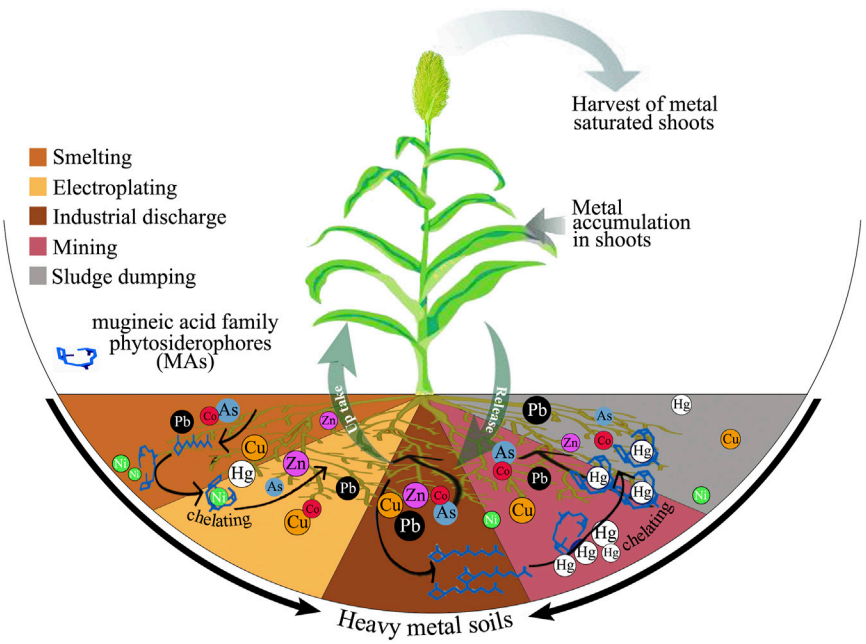

FIGURE 2 | The process of heavy metals accumulation in giant reed.

the highest concentration organ, and the stem is the lowest concentration organ (**Table 1**). However, the most inferior concentration organ is still a matter of debate that leaf can be the most deficient concentration organ when heavy metals in soil are out of threshold limit value (Cristaldi et al., 2020). It can become hyperaccumulator plants and absorb metal contaminants from the ground and translocate them to erial plant parts (Baker et al., 2000). In general, heavy metals exert multiple inhibitory effects on photosynthesis at several structural and metabolic levels (Clijsters and Van Assche, 1985). However, giant reed does not die after exposure to metal and show no visible signs of stress, and the photosynthetic rate of giant reed is not affected by heavy metals (Papazoglou et al., 2005). The phytoextraction process has a significant advantage for giant reed because most heavy metals are accumulated in the roots. In this way, the use of the upper parts (e.g., shoots and leaves) of giant reed is not affected, and the concentration of heavy metals in the soil can be reduced by collecting the roots of giant reed.

Previous research reported the mechanized harvest of the upper parts of giant reed. Curt et al. (2013) report that the strategy of two-step harvesting: stalk cutting and crushing and biomass collection and baling with this specific machinery is feasible. Assirelli et al. (2019) provide good results using a shredding machine for giant reed harvesting. Comparing to the mechanized harvest of the upper parts of giant reed, the roots of giant reed collecting are still a difficult task. Assirelli et al. (2013) use a modified stump grinder for *in situ* rhizome extraction. However, this method obtains most of the rhizomes with variable length, ranging between 4.4 and 6.4 cm, and most of the rhizomes were not excavated in the soil. It is an excellent way to digging rhizomes with a Noble sweep plow to a 0.30 m depth (San Martín et al., 2019). Because the rhizome depth of giant reed is 5–30 cm under the soil surface, this method can obtain almost entirely of rhizomes. Due to the low volatility of heavy metals, pyrolysis is an excellent way to extract heavy metals from the roots of giant reed. Grottola et al. (2019) report that the metals recovery is in the temperature range 653–873 K under steam assisted slow pyrolysis conditions.

Water Treatment

Water is one of the major issues humanity must tackle to achieve human society's sustainable development (Zhang et al., 2018). Although the total amount of water is enough on the Earth, the amount of drinkable water is limited. Surface and groundwater in many parts of the world are contaminated and not suitable for drinking (Gupta et al., 2012). The primary sources of water

TABLE 1 | Types and locations of giant reed accumulating heavy metals.

Metal type	Concentration organs	Highest concentration organ	Lowest concentration organ	References
Hg	Root, stem, leaf	Root	Leaf	Cristaldi et al. (2020)
Cd	Root, stem, leaf	Root	Stem	Guo and Miao (2010)
Cu	Root, stem, leaf	Root	Stem	Han and Wang (2007)
Pb	Root, stem, leaf	Root	Stem	Guo and Miao (2010)
Fe	Root, stem, leaf	Root	Stem	Castaldi et al. (2018)
Ni	Root, stem, leaf	Root	Stem	Bonanno (2012), Mabhungu et al. (2019)
Al	Root, stem, leaf	Root	Stem	
As	Root, stem, leaf	Root	Stem	
Cr	Root, stem, leaf	Root	Stem	
Mn	Root, stem, leaf	Root	Stem	
Zn	Root, stem, leaf	Root	Stem	

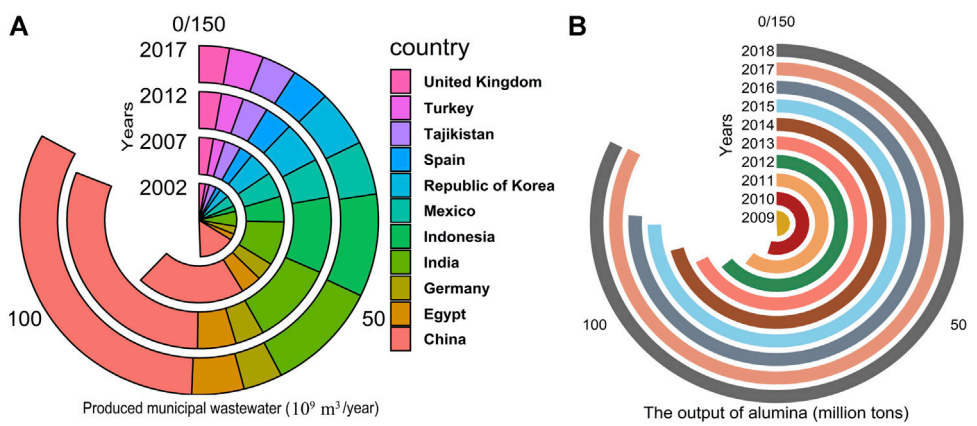

FIGURE 3 | Produced municipal wastewater in different countries **(A)** and the output of alumina in the world **(3B)**.

pollution come from industry, household, agricultural activities, and environmental and global changes. From 2002 to 2017, the total amount of municipal wastewater discharge in different countries uptrend (**Figure 3A**). In some developing countries, such as China, India, Indonesia, these countries produce much industrial wastewater and need to spend much money to treat this wastewater (This figure results from global information system on water and agriculture: http://www.fao.org/aquastat/statistics/query/results.html). Wastewater treatment had been a concern in the Bronze Age (ca 3,200–1100 BC) in Crete, Aegean Islands, and Indus Valley civilizations (Salgot and Folch, 2018). Since the 1950s, wetlands had been used for water purification around the world. Emergy assessment, a measure of the environmental and human economic resource utilization, showed that wetland systems used much fewer materials than conventional wastewater treatment. Wetland systems can rely on microbes and plants' ecological action for their efficacy and improve energy independence (Nelson et al., 2001). Wetlands are divided into natural and constructed wetlands. Because of environmental issues, natural wetlands are not always available where treatment is needed (Jenssen et al., 1993). Using constructed wetlands (CW), ecological concerns are reduced, and systems can be built on-site and more easily customized to facilitate specific treatment needs. In constructed wetlands, plants can stabilize the bed's surface, provide the right physical filtration conditions, transport gases, release oxygen to the rhizosphere, absorb inorganic compounds, organic pollutants, and plant metabolites, and release organic compounds (Stottmeister et al., 2003). Of course, not all plants are suitable for use in constructed wetlands. Plants need to meet the general requirements: 1) not causing significant weed or disease risks or risking to the ecological or genetic integrity of the surrounding natural ecosystems; 2) are well tolerant to local growing environments, pests, and diseases; 3) growing fast and having high biomass productivity; 4) removing of contaminants through direct assimilation and storage, or by enhancement of microbial transformations such as nitrification (through oxygen release from the root zone) and denitrification (by the production of carbon substrates) (Tanner, 1996).

Giant reed is an excellent plant for water purification. Wang et al. (2008) tested the removal efficiency of chemical oxygen demand (COD), total nitrogen (TN), and total phosphorus (TP) in rural domestic sewage by seven kinds of aquatic plants (*Arundo donax*, *Triarrhena sacchariflora*, *Acorus calamus*, *Phragmites communis*, *Iris pseudacorus*, *Lythrum salicaria,* and *Sagittaria trifolia*), and the result shows that giant reed has the strongest purification ability. Giant reed has higher removal rates for total suspended solids (TSS) than some aquatic plants (Toscano et al., 2015). The planted filter of giant reed allows better elimination of *Escherichia coli* (*E. coli*) than *Pennisetum purpureum* Schumach (Fidele and Audra, 2020) and previous study has shown that giant reed planted in gravel-based constructed wetlands (CWs) can remove up virtually 100% of *E. coli* (Idris et al., 2012a). It shows excellent organic pollutant removal, macronutrient, removal microbiological removal, and heavy metal (Leto et al., 2013; Jesus et al., 2017; Pu et al., 2018), giant reed can be used to treat various polluted waters (Liao et al., 2017). Giant reed shows excellent purification efficiency when used to treat micro-polluted river water, secondary municipal wastewaters for crop irrigation, dairy factory stormwater, and winery wastewater (salinity up to 9 dS/m) (Williams et al., 2008, 2009; Idris et al., 2012b; Xie et al., 2012; Barbagallo et al., 2014). Moreover, giant reed can be used as a source of biomass production when it is used to treat polluted waters. Mavrogianopoulos et al. (2002) report that giant reed stem biomass production in pig's waste is higher than the ordinary production in the soil. Irrigation with urban wastewater increased the biomass yield of three energy crops (*Typha latifolia*, *Arundo donax,* and *Phragmites australis*) and the biomass productivity of giant reed was much higher than those of *T. latifolia* and *P. australis* (Czakó and Márton, 2011; Zema et al., 2012). Giant reed can uptake pollutants from wastewater and accumulate pollutants in different parts. Cui and Wang (2013) got the nitrogen and phosphorus content of different parts of giant reed. There is a quantitive relationship of stem < root < leaves and root < stem < leaves, respectively, for the total nitrogen content and the total phosphorus content in the plant. Previous study reports the potential of giant reed for phytoextraction of heavy metals from synthetic wastewater and traces element concentrations decreased according to the pattern of root > leaf > stem (Mirza et al., 2010; Bonanno, 2012). Pollutants can be removed from wastewater by harvesting giant reed. The harvested giant reed can also be used to produce biomethane for energy and digestate for plant nutrition through anaerobic digestion process (Shilpi et al., 2019). A major barrier to the use of giant reed for water purification is its invasive properties in riparian ecosystems. Because giant reed hardly produces viable seed and its clumping rhizome growth habit, its ability to spread is limited. Giant reed's rapid clonal spread can be attributed to flood dispersal of rhizome and culm fragments. It is necessary to avoid the use of giant reed for treatment polluted rivers that are subject to flooding.

Red Mud Improvement

As the name implies, the red mud is brick red in color and slimy, with an average particle size of fewer than 10 μm, and a few particles larger than 20 μm can also be available (Paramguru et al., 2004). Red mud is the primary waste material produced during alumina production following the Bayer's process. Depending on the quality of the raw material processed, 1–2.5 tons of red mud is generated per ton of alumina produced (Paramguru et al., 2004). From 2009 to 2018, the output of alumina has nearly 40% growth in the world (An, 2019) (**Figure 3B**). China has become the leader in aluminum production and use (Hu et al., 2018). It causes the production of red mud to increase dramatically. Although many methods having been used to neutralize bauxite residues, cost remains an important consideration. Nowadays, dry stacking is one of the most popular disposal practices for red mud (Khairul et al., 2019). The main environmental impacts of red mud are its high alkalinity, salinity, and sodicity. Besides, the high alkalinity, salinity, and sodicity may be an immediate risk to plant growth. The pH of red mud can be up to 11 or more, due to presence of NaOH and Na_2CO_3 (1–6%, w/w) (Brunori et al., 2005; Sahu et al., 2010). The selected plant species should survive high salinity and alkalinity conditions to build vegetation on the residue. However,

very few plant species are able to survive on substrates with high pH, EC, and Na concentrations (Xue et al., 2016).

Without human intervention, the phytoremediation of red mud deposits is a slow process (Mishra and Pandey, 2019). Planting potentially successful plant species can accelerate ecological succession and restore soil fertility. Halophytes show the greatest potential to ameliorate bauxite residues (Xue et al., 2016). At present, giant reed is not considered to be a halophyte because it mainly invades freshwater habitats, but its salt tolerance has been confirmed (Pompeiano et al., 2017; Sánchez et al., 2017; Di Mola et al., 2018). Giant reed exhibits high tolerance to saline conditions and significant adaptability to salt accumulation in the soil (Verslues et al., 2006). Giant reed can maintain adequate K^+ and Ca^{2+} to counteract high salinity influence. The accumulation of Na^+ in leaf tissues under Na + stress was lower than that in roots during the experiment, and Na^+ decreased under leaf/root salinity (Balogh et al., 2012). However, in consideration of the accumulation of Na^+ and Cl^- in the leaves, the compartmentalization mechanism (for instance, vacuole storage) is likely to assist giant reed after exposure to salt toxicity once Na^+ and Cl^- have been inevitably absorbed and translocated to the leaf tissues (Pompeiano et al., 2017). The results of biomass production, nutrient removal, salt tolerance, weed risk, and carbon sequestration with saline brewery wastewater show that giant reed is suitable for growing on saline soil (Williams et al., 2008). More importantly, giant reed can still grow well in the alkaline soils of pH9-10 and reduce alkaline soils' pH. Giant reed has phytoremediation potential to grow in red mud containing high pH, EC, and trace metals. Red mud and red mud control soil in a 1:1 ratio positively affect on the height and biomass of reeds (Alshaal et al., 2013).

CONCLUSION AND FUTURE CHALLENGES

This paper reviews the application of giant reed in production and ecological remediation. It can absorb heavy metals, treat wastewater, improve red mud, and is a valuable raw material for many products. Genetic diversity has low among populations of giant reed that originated from different territories due to asexual reproduction (Antal et al., 2018). Therefore, it is of great significance to directly modify the expression of specific genes, making giant reed even more competitive than other energy crops.

Plant breeding can be considered a coevolution between humans and plants. People caused changes in the plants that were used for production and life. In turn, those new plant types allowed changes in human populations to take place. The core of plant breeding is to choose a better type among the varieties, yield, and quality of the edible portion; easy to grow, harvest, and process; resistance to environmental stress; and insect resistance (Breseghello and Coelho, 2013). Standard breeding methods include hybrid breeding, mutation breeding, haploid (polyploid) breeding, genetic engineering breeding. Among them, hybrid breeding is the preferred breeding method for many crops (Kempe and Gils, 2011). Hybrid breeding is a remarkable success story in maize, sunflower, sorghum, beets, and rye (Longin et al., 2012). As DNA's understanding has expanded and its importance for plant characteristics, breeders have taken matters into their own hands. Instead of waiting for spontaneous mutations to occur in DNA, they began mutation breeding in the 1930s (Bradshaw, 2017). Through this breeding, changes to plant DNA can be applied at a much higher frequency. Mutation breeding is an essential method for improving crops, with more than 3,200 mutant cultivars produced worldwide thus far (FAO/IAEA Mutant Variety Database) (Yamaguchi, 2018). Polyploidy is an intriguing phenomenon in plants that have provided an essential pathway for evolution and speciation (Bukhari and Kour, 2019). Polyploidy breeding can be used as a critical tool for developing new crop species, producing larger fruit or other parts to obtain more yield and profits, improving the resistance of plant organisms and abiotic organisms.

In the past 20 years, genetically engineered development has improved transgenic plants' speed and accuracy compared to traditional plant breeding. The knowledge of the essential genes transferred by transgenic plants is higher than that of conventional breeding. Transgenic technologies to develop cassava with enhanced resistance to viral diseases and insect pests improved nutritional content, modified and increased starch metabolism, and reduced cyanogenic content of processed roots (Taylor et al., 2004). Tobacco and *Arabidopsis* plants transformed with *Escherichia coli mtlD* encoding a mannitol-1-phosphate dehydrogenase accumulated mannitol. These plants have increased tolerance to high salinities than control plants (Bajaj et al., 1999). Liu et al. (2013) transferred the *ScNHX1* (encoding vacuolar membrane Na+/H+ antiporter from *Suaeda corniculata*) and *ScVP* (encoding vacuolar H + -PPase from *S. corniculata*) genes into alfalfa plants, and the results showed that transgenic alfalfa plants co-expressing *ScVP*/*ScNHX1* showed higher salt and saline-alkali tolerance compared with wild-type plants. Di et al. (2015) introduced the gene encoding the betaine aldehyde dehydrogenase from *Atriplex micrantha* into the maize inbred lines Zheng58 and Qi319 by *Agrobacterium*-mediated transformation. The maize ubiquitin promoter controlled them. The transgenic maize plants showed higher betaine aldehyde dehydrogenase activity and grew better than wild-type plants under NaCl stress. Compared with wild type, transgenic plants have higher fresh weight under salt stress, lower malondialdehyde content, lower relative conductivity, higher chlorophyll content, higher plant height, and higher grain. It is indicated that the expression of BADH gene in maize seedlings enhances these plants' salt tolerance. Zhang and Liu (2011) transferred a gene that simultaneously expressed human *CYP2E1* and *glutathione S-transferase* (*GST*) into alfalfa plants from hypocotyl segments by using an *Agrobacterium* transformation system. The *pKHCG* transgenic alfalfa plants' resistance to mixed contaminants (heavy metal-organic compounds) was significantly increased compared to the transgenic alfalfa plants expressing a single gene (*GST* or *CYP2E1*) and the non-transgenic control plants. The *pKHCG* alfalfa plants showed strong resistance to the mixtures of cadmium (Cd) and trichloroethylene (TCE), and these mixtures were metabolized

TABLE 2 | Giant reed and hyperaccumulator plants differ in accumulating heavy metal.

	Ni (mg/kg)	Pb (mg/kg)	Cd (mg/kg)	As (mg/kg)	Zn (mg/kg)	Cr (mg/kg)
Giant reed[a–d]	<193	<515	<64.12	<61.96	<118	<34
Hyperaccumulator plants[e]	>1,000	>1,000	>100	>1,000	>3,000	>300

[a]*Alshaal et al. (2013)*
[b]*Guo and Miao (2010)*
[c]*Barbosa et al. (2015)*
[d]*Sidella et al. (2017)*
[e]*Reeves et al. (2018)*

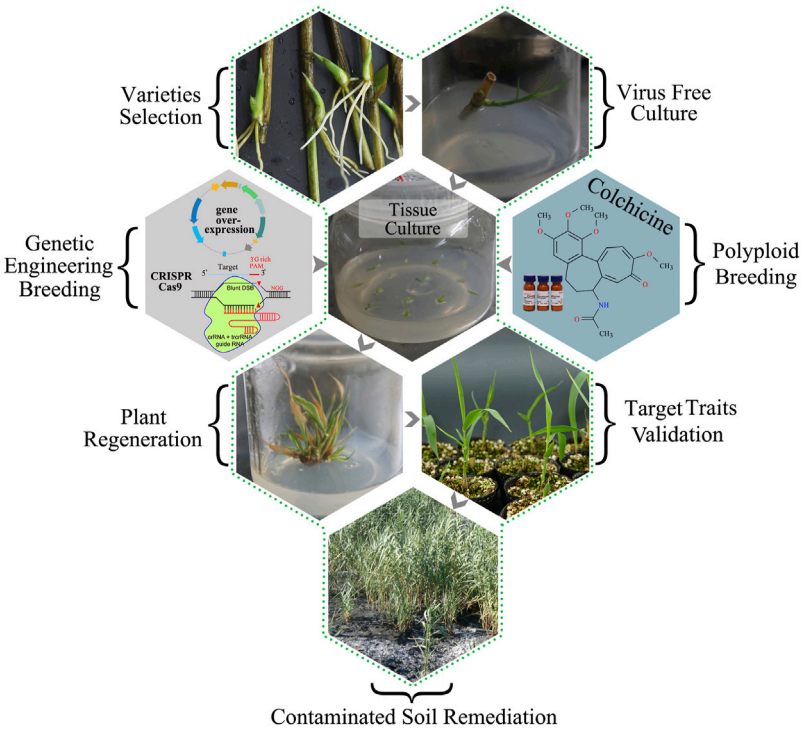

FIGURE 4 | Flow chart of breeding giant reed resistant varieties using transgenic technology.

by the combination of introduced *GST* and *CYP2E1*. He et al. (2001) introduced the bacterial mercuric reductase (*merA*) into tobacco and the transgenic tobacco plants were resistant to high levels of mercuric chloride and removed mercury from water solutions and soil by volatilization. Czako et al. (2006) co-introduced the bacterial mercuric reductase (*merA*) and organomercurial lyase (*merB*) genes into the saltmarsh cordgrass (*Spartina alterniflora*) by *Agrobaterium*-mediated transformation and the resultant heavy metal resistant transgenic tissue showed enhanced tolerance to both mercuric and phenylmercuric salts. Kim et al. (2011) transferred the *MuSI* gene into tobacco, and *Escherichia coli* cells overexpressing *MuSI* were more resistant to Cd than wild-type cells transfected with vector alone. *MuSI* transgenic plants were also more resistant to Cd. *MuSI* transgenic tobacco plants absorbed less Cd than wild type plants. In transgenic plants, cadmium transport from root to shoot was reduced, thereby avoiding the toxicity of cadmium. These results indicated that *MuSI* transgenic tobacco plants tolerate Cd by reduced translocation from roots to shoots and reduced uptake and/or increased immobilization of Cd in the roots. Peng et al. (2018) isolated a *TpNRAMP5* from dwarf Polish wheat (DPW, *Triticum polonicum* L.) and transferred it to *Arabidopsis thaliana*. The expression of *TpNRAMP5* in *Arabidopsis* significantly increased the content of Cd, Co, and Mn in roots, stems, and whole plants but did not affect the content of Fe and Zn. These results indicate that *TpNRAMP5* is a metal transporter that enhances Cd, Co, and Mn accumulation but does not enhance the accumulation of Zn and Fe. With the continuous advancement of biotechnology, it is an excellent way to improve the ecological environment by cultivating plants through genetically modified technology.

The use of plants to remove contaminants from contaminated water and soil may be a promising strategy. Giant reed can absorb heavy metals, reduce the pH of the saline soil and purify the water. It should be mentioned that some disadvantages of giant reed cannot be overlooked. There is still a gap between giant reed and

hyperaccumulator plants accumulating most of heavy metal (**Table 2**). Although recent studies report giant reed as moderately tolerant to salt stress and biomass yield was not decreased, surprisingly, high salt stress caused yield heavy losses (Di Mola et al., 2018). There is an urgent need, but it is still a significant challenge for giant reed breeding because giant reed seeds cannot breed in most areas. The reproduction only occurs by the vegetative growth of rhizomes and of stem nodes of broken canes. Because of this, the genotypic diversity among clonal populations is expected to be very low (Sicilia et al., 2019). Considering the chromosome number of giant reed is diverse and ploidy levels of giant reed may depend on the different territory in which the plant has grown and may depend on its evolutionary history, polyploidy breeding in giant reed is an excellent choice (Corno et al., 2014). As the regeneration system of giant reed has been published so far, and an optimized particle bombardment protocol for gene transfer with embryogenic calli was recently reported in giant reed (Takahashi and Takamizo, 2012), genetic engineering could represent a feasible option for giant improvement reed (**Figure 4**). Biotic and abiotic stress tolerance is the minimum required trait, which is not tricky in molecular breeding. These traits and candidate target genes are reviewed in front of this article.

AUTHOR CONTRIBUTIONS

SH, JL conceived the original structure of the review. QJ, DL helped with literature data collection. DZ prepared the manuscript. All authors have read and agreed to the published version of the manuscript.

FUNDING

This research was supported by the National Natural Science Foundation of China (41867054), the National Key R&D Program of China (2019YFC0507503), the Natural Science Foundation of Guangxi, China (2018GXNSFAA281108), Science and Technology Major Project of Guangxi (Guike AA20161004), and the Science and Technology Major Project of Guilin, China (20180101-2).

REFERENCES

Ahluwalia, S. S., and Goyal, D. (2007). Microbial and Plant Derived Biomass for Removal of Heavy Metals from Wastewater. *Bioresour. Technol.* 98, 2243–2257. doi:10.1016/j.biortech.2005.12.006

Ahmed, M. J. (2016). Potential of Arundo donax L. Stems as Renewable Precursors for Activated Carbons and Utilization for Wastewater Treatments: Review. *J. Taiwan Inst. Chem. Eng.* 63, 336–343. doi:10.1016/j.jtice.2016.03.030

Al-Snafi, A. E. (2015). The Constituents and Biological Effects of *Arundo Donax*-A Review. *Int. J. Phytopharmacy Res.* 6, 34–40.

Ali, H., Khan, E., and Sajad, M. A. (2013). Phytoremediation of Heavy Metals-Concepts and Applications. *Chemosphere* 91, 869–881. doi:10.1016/j.chemosphere.2013.01.075

Alshaal, T., Domokos-Szabolcsy, É., Márton, L., Czakó, M., Kátai, J., Balogh, P., et al. (2013). Phytoremediation of Bauxite-Derived Red Mud by Giant Reed. *Environ. Chem. Lett.* 11, 295–302. doi:10.1007/s10311-013-0406-6

Alshaal, T., Elhawat, N., Domokos-Szabolcsy, É., Kátai, J., Márton, L., Czako, M., et al. (2015). "Giant Reed (Arundo donax L.): A Green Technology for Clean Environment," in *Phytoremediation: Management of Environmental Contaminants, Vol I.* Editors A. A. Ansari, S. S. Gill, R. Gill, G. R. Lanza, and L. Newman. (Springer Science + Business Media B. V.), 3–20. doi:10.1007/978-3-319-10395-2_1

An, P. (2019). Review, analyse and Forecast for Aluminum Market. *Light Met.* 5, 1–11. doi:10.13662/j.cnki.qjs.2019.05.001

Angelini, L. G., Ceccarini, L., and Bonari, E. (2005). Biomass Yield and Energy Balance of Giant Reed (*Arundo donax* L.) Cropped in Central Italy as Related to Different Management Practices. *Eur. J. Agron.* 22, 375–389. doi:10.1016/j.eja.2004.05.004

Angelini, L. G., Ceccarini, L., Nassi o Di Nasso, N., and Bonari, E. (2009). Comparison of *Arundo donax L.* And Miscanthus X Giganteus in a Long-Term Field Experiment in Central Italy: Analysis of Productive Characteristics and Energy Balance. *Biomass and Bioenergy* 33, 635–643. doi:10.1016/j.biombioe.2008.10.005

Antal, G., Fári, M. G., and Domokos-Szabolcsy, É. (2018). Obtention of New Ornamental Leaf Variants of Giant Reed (*Arundo donax* L.) Originated from Somatic Embryogenesis and Their Photosynthetic Parameters. *Int. J. Hortic. Sci.* 24. doi:10.31421/ijhs/24/1-2./1542

Assirelli, A., Civitarese, V., Caracciolo, G., Sannino, M., and Faugno, S. (2019). Mechanical Harvesting Line Setting of Giant Reeds. *Appl. Sci.* 9, 5425. doi:10.3390/app9245425

Assirelli, A., Santangelo, E., Spinelli, R., Acampora, A., Croce, S., Civitarese, V., et al. (2013). Mechanization of Rhizome Extraction in Giant Reed (*Arundo donax* L.) Nurseries. *Appl. Eng. Agric.* 29, 489–494. doi:10.13031/aea.29.9797

Atma, W., Larouci, M., Meddah, B., Benabdeli, K., and Sonnet, P. (2017). Evaluation of the Phytoremediation Potential of *Arundo donax* L. For Nickel-Contaminated Soil. *Int. J. Phytoremediation* 19, 377–386. doi:10.1080/15226514.2016.1225291

Bajaj, S., Targolli, J., Liu, L.-F., Ho, T.-H. D., and Wu, R. (1999). Transgenic Approaches to Increase Dehydration-Stress Tolerance in Plants. *Mol. Breed.* 5, 493–503. doi:10.1023/a:1009660413133

Baker, A. J. M., Mcgrath, S. P., Sidoli, C. M. D., and Reeves, R. D. (1994). The Possibility of In Situ Heavy Metal Decontamination of Polluted Soils Using Crops of Metal-Accumulating Plants. *Resour. Conservation Recycling* 11, 41–49. doi:10.1016/0921-3449(94)90077-9

Baker, A. J. M., McGrath, S. P., Reeves, R. D., and Smith, J. A. C. (2000). "Metal Hyperaccumulator Plants: A Review of the Ecology and Physiology of a Biological Resource for Phytoremediation of Metal Polluted Soils," in *Phytoremediation of Contaminated Soil and Water*. Editors N. Terry and G. Banuelos (Boca Raton, FL: Lewis), 85–108.

Balogh, E., Herr, J. M., Jr, Czakó, M., and Márton, L. (2012). Defective Development of Male and Female Gametophytes in Arundo donax L. (POACEAE). *Biomass and Bioenergy* 45, 265–269. doi:10.1016/j.biombioe.2012.06.010

Barbagallo, S., Barbera, A. C., Cirelli, G. L., Milani, M., and Toscano, A. (2014). Reuse of Constructed Wetland Effluents for Irrigation of Energy Crops. *Water Sci. Technol.* 70, 1465–1472. doi:10.2166/wst.2014.383

Barbosa, B., Boléo, S., Sidella, S., Costa, J., Duarte, M. P., Mendes, B., et al. (2015). Phytoremediation of Heavy Metal-Contaminated Soils Using the Perennial Energy Crops *Miscanthus* Spp. And *Arundo donax* L. *Bioenerg. Res.* 8, 1500–1511. doi:10.1007/s12155-015-9688-9

Barbosa, B., Fernando, A., Lino, J., Costa, J., Sidella, S., Boléo, S., et al. (2013). "Phytoremediation Response of Arundodonax L. In Soils Contaminated with Zinc and Chromium,".in Proceedings of the 21st European Biomass Conference and Exhibition, Setting the course for a Biobased Economy, Copenhagen, Denmark, June 3–7, 2013, 3–7.

Barreca, F., and Fichera, C. R. (2013). Wall Panels of *Arundo donax* L. For Environmentally Sustainable Agriculture Buildings: Thermal Performance Evaluation. *J. Food Agric. Environ.* 11, 1353–1357.

Barreca, F., Martinez Gabarron, A., Flores Yepes, J. A., and Pastor Pérez, J. J. (2019). Innovative Use of Giant Reed and Cork Residues for Panels of Buildings in Mediterranean Area. *Resour. Conservation Recycling* 140, 259–266. doi:10.1016/j.resconrec.2018.10.005

Barreca, F. (2012). Use of Giant Reed *Arundo Donax* L. In Rural Constructions. *Agric. Eng. Int. CIGR J.* 14, 46–52.

Basso, M. C., Cerrella, E. G., Buonomo, E. L., Bonelli, P. R., and Cukierman, A. L. (2005). Thermochemical Conversion ofArundo Donaxinto Useful Solid Products. *Energ. Sourc.* 27, 1429–1438. doi:10.1080/009083190523280

Bell, G. P. (1998). Ecology and Management of *Arundo donax*, and Approaches to Riparian Habitat Restoration in Southern California. Online resource: https://www.invasive.org/gist/moredocs/arudon 01.pdf (Accessed October 2018).

Bonanno, G. (2012). *Arundo donax* as a Potential Biomonitor of Trace Element Contamination in Water and Sediment. *Ecotoxicology Environ. Saf.* 80, 20–27. doi:10.1016/j.ecoenv.2012.02.005

Borso, F. D., Di Marzo, C., Zuliani, F., Danuso, F., and Baldini, M. (2018). Harvest Time and Ensilage Suitability of Giant Reed and Miscanthus for Bio-Methane Production and Characterization of Digestate for Agronomic Use. *Agron. Res.* 16, 22–40.

Bradshaw, J. E. (2017). Plant Breeding: Past, Present and Future. *Euphytica* 213, 60. doi:10.1007/s10681-016-1815-y

Breseghello, F., and Coelho, A. S. G. (2013). Traditional and Modern Plant Breeding Methods with Examples in Rice (*Oryza Sativa* L.). *J. Agric. Food Chem.* 61, 8277–8286. doi:10.1021/jf305531j

Brunori, C., Cremisini, C., Massanisso, P., Pinto, V., and Torricelli, L. (2005). Reuse of a Treated Red Mud Bauxite Waste: Studies on Environmental Compatibility. *J. Hazard. Mater.* 117, 55–63. doi:10.1016/j.jhazmat.2004.09.010

Bukhari, R., and Kour, H. (2019). Polyploidy in Agriculture: With Special Reference to Mulberry. *J. Pharmacognosy Phytochemistry* 8, 1795–1808. doi:10.20546/ijcmas.2019.805.101

Burakov, A. E., Galunin, E. V., Burakova, I. V., Kucherova, A. E., Agarwal, S., Tkachev, A. G., et al. (2018). Adsorption of Heavy Metals on Conventional and Nanostructured Materials for Wastewater Treatment Purposes: A Review. *Ecotoxicology Environ. Saf.* 148, 702–712. doi:10.1016/j.ecoenv.2017.11.034

Cano-Ruiz, J., Ruiz Galea, M., Amorós, M. C., Alonso, J., Mauri, P. V., and Lobo, M. C. (2020). Assessing *Arundo donax L.* In Vitro-tolerance for Phytoremediation Purposes. *Chemosphere* 252, 126576. doi:10.1016/j.chemosphere.2020.126576

Castaldi, P., Silvetti, M., Manzano, R., Brundu, G., Roggero, P. P., and Garau, G. (2018). Mutual Effect of *Phragmites Australis, Arundo donax* and Immobilization Agents on Arsenic and Trace Metals Phytostabilization in Polluted Soils. *Geoderma* 314, 63–72. doi:10.1016/j.geoderma.2017.10.040

Cavallaro, V., Tringali, S., and PatanÈ, C. (2011). Large-scalein Vitropropagation of Giant Reed (Arundo donaxL.), a Promising Biomass Species. *J. Hortic. Sci. Biotechnol.* 86, 452–456. doi:10.1080/14620316.2011.11512787

Chen, C., Li, B., and Mo, H. (2016). The Establishment of Rapid Propagation Systems for *Arundo donax*. *South. Hortic.* 27, 01–05.

Clijsters, H., and Van Assche, F. (1985). Inhibition of Photosynthesis by Heavy Metals. *Photosynth. Res.* 7, 31–40. doi:10.1007/bf00032920

Coppa, E., Astolfi, S., Beni, C., Carnevale, M., Colarossi, D., Gallucci, F., et al. (2020). Evaluating the Potential Use of Cu-Contaminated Soils for Giant Reed (Arundo donax, L.) Cultivation as a Biomass Crop. *Environ. Sci. Pollut. Res.* 27, 8662–8672. doi:10.1007/s11356-019-07503-x

Corno, L., Lonati, S., Riva, C., Pilu, R., and Adani, F. (2016). Giant Cane (*Arundo donax* L.) Can Substitute Traditional Energy Crops in Producing Energy by Anaerobic Digestion, Reducing Surface Area and Costs: A Full-Scale Approach. *Bioresour. Technol.* 218, 826–832. doi:10.1016/j.biortech.2016.07.050

Corno, L., Pilu, R., and Adani, F. (2014). *Arundo donax L.*: a Non-food Crop for Bioenergy and Bio-Compound Production. *Biotechnol. Adv.* 32, 1535–1549. doi:10.1016/j.biotechadv.2014.10.006

Corno, L., Pilu, R., Tambone, F., Scaglia, B., and Adani, F. (2015). New Energy Crop Giant Cane (*Arundo donax* L.) Can Substitute Traditional Energy Crops Increasing Biogas Yield and Reducing Costs. *Bioresour. Technol.* 191, 197–204. doi:10.1016/j.biortech.2015.05.015

Cristaldi, A., Conti, G. O., Cosentino, S. L., Mauromicale, G., Copat, C., Grasso, A., et al. (2020). Phytoremediation Potential of *Arundo donax* (Giant Reed) in Contaminated Soil by Heavy Metals. *Environ. Res.* 185, 109427. doi:10.1016/j.envres.2020.109427

Cui, J., and Wang, L. (2013). Laboratory Study on the Performance of Domestic Wastewater Biofilters Made of *Arundo donax* L. *AmmApplied Mech. Mater.* 295298, 1104–1109. doi:10.4028/www.scientific.net/amm.295-298.1104

Curt, M., Sanz, M., Mosquera, F., Mauri, P., Plaza, A., Aguado, P., et al. (2013). "Harvest Mechanisation of *Arundo donax* L. In Spain," in 21st European Biomass Conference and Exhibition, Copenhagen, Denmark, June 3–7, 2013.

Czakó, M., Feng, X., He, Y., Liang, D., and Márton, L. (2006). Transgenic *Spartina Alterniflora* for Phytoremediation. *Environ. Geochem. Health* 28, 103–110. doi:10.1007/s10653-005-9019-8

Czakó, M., and Márton, L. (2011). *Subtropical and Tropical Reeds for biomassEnergy Crops*. Cambridge, United Kingdom: RSC Publishing Royal Society of Chemistry, 322–340.

Dahlawi, S., Naeem, A., Rengel, Z., and Naidu, R. (2018). Biochar Application for the Remediation of Salt-Affected Soils: Challenges and Opportunities. *Sci. Total Environ.* 625, 320–335. doi:10.1016/j.scitotenv.2017.12.257

Danelli, T., Sepulcri, A., Masetti, G., Colombo, F., Sangiorgio, S., Cassani, E., et al. (2021). *Arundo donax* L. Biomass Production in a Polluted Area: Effects of Two Harvest Timings on Heavy Metals Uptake. *Appl. Sci.* 11, 1147. doi:10.3390/app11031147

Delplace, G., Schreck, E., Pokrovsky, O. S., Zouiten, C., Blondet, I., Darrozes, J., et al. (2020). Accumulation of Heavy Metals in Phytoliths from Reeds Growing on Mining Environments in Southern Europe. *Sci. Total Environ.* 712, 135595. doi:10.1016/j.scitotenv.2019.135595

Dhiren, K., and Singh, H. B. (2015). Traditional Knowledge, Economic Prospects and Conservation Issues on Giant Reed (*Arundo donax* Linnaeus) in Manipur, Northeast India. *Pleione* 9, 481–493.

Di, H., Tian, Y., Zu, H., Meng, X., Zeng, X., and Wang, Z. (2015). Enhanced Salinity Tolerance in Transgenic Maize Plants Expressing a BADH Gene from *Atriplex Micrantha*. *Euphytica* 206, 775–783. doi:10.1007/s10681-015-1515-z

Di Mola, I., Guida, G., Mistretta, C., Giorio, P., Albrizio, R., Visconti, D., et al. (2018). Agronomic and Physiological Response of Giant Reed (*Arundo donax* L.) to Soil Salinity. *Ital. J. Agron.* 13, 31–39. doi:10.4081/ija.2018.995

Dixit, R., Wasiullah, D., Malaviya, D., Pandiyan, K., Singh, U., Sahu, A., et al. (2015). Bioremediation of Heavy Metals from Soil and Aquatic Environment: an Overview of Principles and Criteria of Fundamental Processes. *Sustainability* 7, 2189–2212. doi:10.3390/su7022189

Domokos-Szabolcsy, É., Fári, M., Márton, L., Czakó, M., Veres, S., Elhawat, N., et al. (2018). Selenate Tolerance and Selenium Hyperaccumulation in the Monocot Giant Reed (*Arundo donax*), a Biomass Crop Plant with Phytoremediation Potential. *Environ. Sci. Pollut. Res.* 25, 31368–31380. doi:10.1007/s11356-018-3127-3

Dubey, S., Shri, M., Gupta, A., Rani, V., and Chakrabarty, D. (2018). Toxicity and Detoxification of Heavy Metals during Plant Growth and Metabolism. *Environ. Chem. Lett.* 16, 1169–1192. doi:10.1007/s10311-018-0741-8

Duke, J., and Wain, K. (1981). *Medicinal Plants of the World. 3 Vol. Computer Index with More than 85,000 entriesPlants Genetics and Germplasm Institute*. Beltsville, MD: Agriculture Research Service.

El Sheikha, A. (2017). Traceability and Inspection: For Safer Food Supply. *Asia Pac. J. Food Saf. Secur.* 3, 1–2.

Etesami, H. (2018). Bacterial Mediated Alleviation of Heavy Metal Stress and Decreased Accumulation of Metals in Plant Tissues: Mechanisms and Future Prospects. *Ecotoxicology Environ. Saf.* 147, 175–191. doi:10.1016/j.ecoenv.2017.08.032

Facchini, P. (1941). *La canna gentile per la produzione della cellulosa nobile, l'impresa agricolo industriale di Torviscosa*. Milano, Italy: SNIA VISCOSA.

Fidele, M., and Audra, P. (2020). Residual Wastewater Treatment by an Aquatic Plant System in Tropical Area: Assessment of Arundo Donax and Pennisetum Purpureum Schumach. *Int. J. Water Wastewater Treat.* 6. doi:10.16966/2381-5299.168

Fiorentino, N., Fagnano, M., Adamo, P., Impagliazzo, A., Mori, M., Pepe, O., et al. (2013). Assisted Phytoextraction of Heavy Metals: Compost and *Trichoderma* Effects on Giant Reed (*Arundo donax* L.) Uptake and Soil N-Cycle Microflora. *Ital. J. Agron.* 8, e29. doi:10.4081/ija.2013.e29

Flores, J. A., Pastor, J. J., Martinez-Gabarron, A., Gimeno-Blanes, F. J., Rodríguez-Guisado, I., and Frutos, M. J. (2011). Arundo donax Chipboard Based on Urea-Formaldehyde Resin Using under 4mm Particles Size Meets the Standard Criteria for Indoor Use. *Ind. Crops Prod.* 34, 1538–1542. doi:10.1016/j.indcrop.2011.05.011

Fu, F., and Wang, Q. (2011). Removal of Heavy Metal Ions from Wastewaters: a Review. *J. Environ. Manage.* 92, 407–418. doi:10.1016/j.jenvman.2010.11.011

Ghosh, M., and Singh, S. (2005). A Review on Phytoremediation of Heavy Metals and Utilization of It's by Products. *Asian J. Energ. Environ* 6, 18

Grottola, C. M., Giudicianni, P., Pindozzi, S., Stanzione, F., Faugno, S., Fagnano, M., et al. (2019). Steam Assisted Slow Pyrolysis of Contaminated Biomasses: Effect of Plant Parts and Process Temperature on Heavy Metals Fate. *Waste Manag.* 85, 232–241. doi:10.1016/j.wasman.2018.12.028

Guarino, F., Miranda, A., Castiglione, S., and Cicatelli, A. (2020). Arsenic Phytovolatilization and Epigenetic Modifications in *Arundo donax* L. Assisted by a PGPR Consortium. *Chemosphere* 251, 126310. doi:10.1016/j.chemosphere.2020.126310

Gubišová, M., Čičková, M., Klčová, L., and Gubiš, J. (2016). *In vitro* tillering—An Effective Way to Multiply High-Biomass Plant *Arundo donax*. *Ind. Crops Prod.* 81, 123–128.

Guo, Z.-H., and Miao, X.-F. (2010). Growth Changes and Tissues Anatomical Characteristics of Giant Reed (*Arundo donax* L.) in Soil Contaminated with Arsenic, Cadmium and Lead. *J. Cent. South. Univ. Technol.* 17, 770–777. doi:10.1007/s11771-010-0555-8

Gupta, V. K., Ali, I., Saleh, T. A., Nayak, A., and Agarwal, S. (2012). Chemical Treatment Technologies for Waste-Water Recycling-An Overview. *RSC Adv.* 2, 6380–6388. doi:10.1039/c2ra20340e

Han, Z., and Wang, C. (2007). Accumulation and Distribution of Cadmium, Lead, Mercury, and Copper in *Arundo donax* of Different Ecotype. *Ecol. Environ.* 16, 1092–1097.

He, Y. K., Sun, J. G., Feng, X. Z., Czakó, M., and Márton, L. (2001). Differential Mercury Volatilization by Tobacco Organs Expressing a Modified Bacterial *merA* Gene. *Cell Res* 11, 231–236. doi:10.1038/sj.cr.7290091

Herrera-Alamillo, M. Á., and Robert, M. L. (2012). Liquid In Vitro Culture for the Propagation of *Arundo donax*. *Methods Mol. Biol.* 877, 153–160. doi:10.1007/978-1-61779-818-4_12

Hu, W., Nie, Q., Huang, B., Shu, X., and He, Q. (2018). Mechanical and Microstructural Characterization of Geopolymers Derived from Red Mud and Fly Ashes. *J. Clean. Prod.* 186, 799–806. doi:10.1016/j.jclepro.2018.03.086

Idris, S. M., Jones, P. L., Salzman, S. A., and Allinson, G. (2012b). Performance of the Giant Reed (Arundo donax) in Experimental Wetlands Receiving Variable Loads of Industrial Stormwater. *Water Air Soil Pollut.* 223, 549–557. doi:10.1007/s11270-011-0881-y

Idris, S. M., Jones, P. L., Salzman, S. A., Croatto, G., and Allinson, G. (2012a). Evaluation of the Giant Reed (*Arundo donax*) in Horizontal Subsurface Flow Wetlands for the Treatment of Recirculating Aquaculture System Effluent. *Environ. Sci. Pollut. Res.* 19, 1159–1170. doi:10.1007/s11356-011-0642-x

Jain, B., Singh, A. K., Kim, H., Lichtfouse, E., and Sharma, V. K. (2018). Treatment of Organic Pollutants by Homogeneous and Heterogeneous Fenton Reaction Processes. *Environ. Chem. Lett.* 16, 947–967. doi:10.1007/s10311-018-0738-3

Jenssen, P. D., Mæhlum, T., and Krogstad, T. (1993). Potential Use of Constructed Wetlands for Wastewater Treatment in Northern Environments. *Water Sci. Technol.* 28, 149–157. doi:10.2166/wst.1993.0223

Jesus, J. M., Cassoni, A. C., Danko, A. S., Fiúza, A., and Borges, M.-T. (2017). Role of Three Different Plants on Simultaneous Salt and Nutrient Reduction from Saline Synthetic Wastewater in Lab-Scale Constructed Wetlands. *Sci. Total Environ.* 579, 447–455. doi:10.1016/j.scitotenv.2016.11.074

Kempe, K., and Gils, M. (2011). Pollination Control Technologies for Hybrid Breeding. *Mol. Breed.* 27, 417–437. doi:10.1007/s11032-011-9555-0

Khairul, M. A., Zanganeh, J., and Moghtaderi, B. (2019). The Composition, Recycling and Utilisation of Bayer Red Mud. *Resour. Conservation Recycling* 141, 483–498. doi:10.1016/j.resconrec.2018.11.006

Kim, Y.-N., Kim, J.-S., Seo, S.-G., Lee, Y., Baek, S.-W., Kim, I.-S., et al. (2011). Cadmium Resistance in Tobacco Plants Expressing the *MuSI* Gene. *Plant Biotechnol. Rep.* 5, 323–329. doi:10.1007/s11816-011-0186-z

Leto, C., Tuttolomondo, T., Bella, S. L., Leone, R., and Licata, M. (2013). Growth ofArundo donaxL. andCyperus alternifoliusL. In a Horizontal Subsurface Flow Constructed Wetland Using Pre-treated Urban Wastewater-A Case Study in Sicily (Italy). *Desalination Water Treat.* 51, 7447–7459. doi:10.1080/19443994.2013.792134

Lewandowski, I., Scurlock, J. M. O., Lindvall, E., and Christou, M. (2003). The Development and Current Status of Perennial Rhizomatous Grasses as Energy Crops in the US and Europe. *Biomass and Bioenergy* 25, 335–361. doi:10.1016/s0961-9534(03)00030-8

Li, C., Xiao, B., Wang, Q., Yao, S., and Wu, J. (2014). Phytoremediation of Zn-And Cr-Contaminated Soil Using Two Promising Energy Grasses. *Water Air Soil Pollut.* 225, 1–12. doi:10.1007/s11270-014-2027-5

Li, P., Qian, H., and Wu, J. (2018). Conjunctive Use of Groundwater and Surface Water to Reduce Soil Salinization in the Yinchuan Plain, North-West China. *Int. J. Water Resour. Develop.* 34, 337–353. doi:10.1080/07900627.2018.1443059

Liao, J., Zhang, D., Mallik, A., Huang, Y., He, C., and Xu, G. (2017). Growth and Nutrient Removal of Three Macrophytes in Response to Concentrations and Ratios of N and P. *Int. J. Phytoremediation* 19, 651–657. doi:10.1080/15226514.2016.1278424

Liu, L., Fan, X.-D., Wang, F.-W., Wang, N., Dong, Y.-Y., Liu, X.-M., et al. (2013). Coexpression of ScNHX1 and ScVP in Transgenic Hybrids Improves Salt and Saline-Alkali Tolerance in Alfalfa (*Medicago Sativa* L.). *J. Plant Growth Regul.* 32, 1–8. doi:10.1007/s00344-012-9270-z

Liu, Y.-N., Guo, Z.-H., Xiao, X.-Y., Wang, S., Jiang, Z.-C., and Zeng, P. (2017). Phytostabilisation Potential of Giant Reed for Metals Contaminated Soil Modified with Complex Organic Fertiliser and Fly Ash: A Field Experiment. *Sci. Total Environ.* 576, 292–302. doi:10.1016/j.scitotenv.2016.10.065

Longin, C. F. H., Mühleisen, J., Maurer, H. P., Zhang, H., Gowda, M., and Reif, J. C. (2012). Hybrid Breeding in Autogamous Cereals. *Theor. Appl. Genet.* 125, 1087–1096. doi:10.1007/s00122-012-1967-7

Luo, Z., Wang, T., Yi, L.-B., Peng, X.-L., Ding, G.-X., and Liu, S.-B. (2018). Effects of Growth Regulators on the Survival Rate of Cuttings from Lateral Branches of Giant Reed (*Arundo donax*) in Summer. *J. Biol.* 35, 23. doi:10.3969/j.issn.2095-1736.2018.03.023

Mabhungu, L., Adam, E., and Newete, S. (2019). Monitoring of Phytoremediating Wetland Macrophytes Using Remote Sensing in the Case of Common Reed and Giant Reed: a Review. *Appl. Ecol. Environ. Res.* 17, 7957–7972. doi:10.15666/aeer/1704_79577972

Mahmood, N. M. Q. (2010). Phytoremediation of Arsenic (As) and Mercury (Hg) Contaminated Soil. *World Appl. Sci. J.* 8, 113–118.

Marton, L., and Czako, M. (2002). *Sustained Totipotent Regenerable Tissue Culture of Arundo donax (Giant Reed) and Totipotent Tissue and Plants Produced Therefrom*. United States Patent Application: 20020166149.

Mavrogianopoulos, G., Vogli, V., and Kyritsis, S. (2002). Use of Wastewater as a Nutrient Solution in a Closed Gravel Hydroponic Culture of Giant Reed (*Arundo donax*). *Bioresour. Technol.* 82, 103–107. doi:10.1016/s0960-8524(01)00180-8

Miao, Y., Xiao, X.-Y., Miao, X.-F., Guo, Z.-H., and Wang, F.-Y. (2012). Effect of Amendments on Growth and Metal Uptake of Giant Reed (*Arundo donax* L.) Grown on Soil Contaminated by Arsenic, Cadmium and Lead. *Trans. Nonferrous Met. Soc. China* 22, 1462–1469. doi:10.1016/S1003-6326(11)61342-3

Mir, T. A., Jan, M., and Dhyani, S. (2018). A Comprehensive Account of Ethno-Medicinal Uses of Monocot Flora (Reported from February–June) of Karwapani Forest Doon Valley-Uttarakhand. *SERBD-International J. Multidisciplinary Sci.* 1, 22–27.

Mirza, N., Mahmood, Q., Pervez, A., Ahmad, R., Farooq, R., Shah, M. M., et al. (2010). Phytoremediation Potential of *Arundo donax* in Arsenic-Contaminated Synthetic Wastewater. *Bioresour. Technol.* 101, 5815–5819. doi:10.1016/j.biortech.2010.03.012

Mishra, T., and Pandey, V. C. (2019). "Phytoremediation of Red Mud Deposits through Natural Succession," in *Phytomanagement of Polluted Sites* (Amsterdam, Netherlands: Elsevier), 409–424. doi:10.1016/b978-0-12-813912-7.00016-8

Mukhopadhyay, S., and Maiti, S. (2010). Phytoremediation of Metal Mine Waste. *Appl. Ecol. Environ. Res.* 8, 207–222.

Muradian, R., and Martinez-Alier, J. (2001). Trade and the Environment: from a "Southern" Perspective. *Ecol. Econ.* 36, 281–297. doi:10.1016/s0921-8009(00)00229-9

Nagajyoti, P. C., Lee, K. D., and Sreekanth, T. V. M. (2010). Heavy Metals, Occurrence and Toxicity for Plants: a Review. *Environ. Chem. Lett.* 8, 199–216. doi:10.1007/s10311-010-0297-8

Nelson, M., Odum, H. T., Brown, M. T., and Alling, A. (2001). "Living off the Land": Resource Efficiency of Wetland Wastewater Treatment. *Adv. Space Res.* 27, 1547–1556. doi:10.1016/s0273-1177(01)00246-0

Nikhade, C., and Makde, K. (2014). Reproductive Behavior of *Arundo donax L. Int. J. Researches Biosciences, Agric. Technol.* 2, 670–679. doi:10.29369/ijrbat.2014.02.II.0043

Nouri, H., Chavoshi Borujeni, S., Nirola, R., Hassanli, A., Beecham, S., Alaghmand, S., et al. (2017). Application of Green Remediation on Soil Salinity Treatment: A Review on Halophytoremediation. *Process Saf. Environ. Prot.* 107, 94–107. doi:10.1016/j.psep.2017.01.021

O'Connor, D., Peng, T., Zhang, J., Tsang, D. C. W., Alessi, D. S., Shen, Z., et al. (2018). Biochar Application for the Remediation of Heavy Metal Polluted Land: a Review of In Situ Field Trials. *Sci. Total Environ.* 619-620, 815–826. doi:10.1016/j.scitotenv.2017.11.132

Papazoglou, E. G., Karantounias, G. A., Vemmos, S. N., and Bouranis, D. L. (2005). Photosynthesis and Growth Responses of Giant Reed (*Arundo donax* L.) to the Heavy Metals Cd and Ni. *Environ. Int.* 31, 243–249. doi:10.1016/j.envint.2004.09.022

Paramguru, R. K., Rath, P. C., and Misra, V. N. (2004). Trends in Red Mud Utilization - a Review. *Mineral. Process. Extractive Metall. Rev.* 26, 1–29. doi:10.1080/08827500490477603

Peng, F., Wang, C., Zhu, J., Zeng, J., Kang, H., Fan, X., et al. (2018). Expression of *TpNRAMP5*, a Metal Transporter from Polish Wheat (*Triticum Polonicum L.*), Enhances the Accumulation of Cd, Co and Mn in Transgenic *Arabidopsis* Plants. *Planta* 247, 1395–1406. doi:10.1007/s00425-018-2872-3

Perdue, R. E. (1958). Arundo Donax-Source of Musical Reeds and Industrial Cellulose. *Econ. Bot.* 12, 368–404. doi:10.1007/bf02860024

Pompeiano, A., Landi, M., Meloni, G., Vita, F., Guglielminetti, L., and Guidi, L. (2017). Allocation Pattern, Ion Partitioning, and Chlorophyll a Fluorescence in *Arundo donax L.* In Responses to Salinity Stress. *Plant Biosyst. - Int. J. Dealing all Aspects Plant Biol.* 151, 613–622. doi:10.1080/11263504.2016.1187680

Pu, G., Zeng, D., Mo, L., Liao, J., Xu, G., Huang, Y., et al. (2018). Cadmium Accumulation and its Effects on Physiological Characteristics of *Arundo donax* L. In a Simulated Wetland. *Glob. NEST J.* 21, 423–429. doi:10.30955/gnj.002580

Pu, G., Zhang, D., Zeng, D., Xu, G., and Huang, Y. (2017). Physiological Response of *Arundo donax L.* To Thallium Accumulation in a Simulated Wetland. *Mar. Freshw. Res.* 69, 714–720. doi:10.1071/MF17093

Quave, C. L., Plano, L. R. W., Pantuso, T., and Bennett, B. C. (2008). Effects of Extracts from Italian Medicinal Plants on Planktonic Growth, Biofilm Formation and Adherence of Methicillin-Resistant *Staphylococcus aureus*. *J. Ethnopharmacology* 118, 418–428. doi:10.1016/j.jep.2008.05.005

Quinn, L. D., Straker, K. C., Guo, J., Kim, S., Thapa, S., Kling, G., et al. (2015). Stress-tolerant Feedstocks for Sustainable Bioenergy Production on Marginal Land. *Bioenerg. Res.* 8, 1081–1100. doi:10.1007/s12155-014-9557-y

Rabhi, M., Karray-Bouraoui, N., Medini, R., Attia, H., Abdelly, C., and Smaoui, A. (2010). Seasonal Variations in Phytodesalination Capacity of Two Perennial Halophytes in Their Natural Biotope. *J. Biol. Res.* 14, 181.

Rai, P. K., Lee, S. S., Zhang, M., Tsang, Y. F., and Kim, K.-H. (2019). Heavy Metals in Food Crops: Health Risks, Fate, Mechanisms, and Management. *Environ. Int.* 125, 365–385. doi:10.1016/j.envint.2019.01.067

Reeves, R. D., Van Der Ent, A., and Baker, A. J. M. (2018). "Global Distribution and Ecology of Hyperaccumulator Plants," in *Agromining: Farming for Metals*. Heidelberg, Germany; Springer, 75–92.

Roberto, P. (2012). Giant Reed (*Arundo donax* L.): A Weed Plant or a Promising Energy Crop? *Afr. J. Biotechnol.* 11, 9163–9174. doi:10.5897/AJB11.4182

Sahu, R. C., Patel, R. K., and Ray, B. C. (2010). Neutralization of Red Mud Using CO2 Sequestration Cycle. *J. Hazard. Mater.* 179, 28–34. doi:10.1016/j.jhazmat.2010.02.052

Salgot, M., and Folch, M. (2018). Wastewater Treatment and Water Reuse. *Curr. Opin. Environ. Sci. Health* 2, 64–74. doi:10.1016/j.coesh.2018.03.005

San Martín, C., Gourlie, J. A., and Barroso, J. (2019). Control of Volunteer Giant Reed (Arundo donax). *Invasive Plant Sci. Manag.* 12, 43–50. doi:10.1017/inp.2018.36

Sánchez, J., Curt, M. D., and Fernández, J. (2017). Approach to the Potential Production of Giant Reed in Surplus Saline Lands of Spain. *Gcb Bioenergy* 9, 105–118. doi:10.1111/gcbb.12329

Sarathambal, C., Khankhane, P. J., Gharde, Y., Kumar, B., Varun, M., and Arun, S. (2017). The Effect of Plant Growth-Promoting Rhizobacteria on the Growth, Physiology, and Cd Uptake of *Arundo donax* L. *Int. J. Phytoremediation* 19, 360–370. doi:10.1080/15226514.2016.1225289

Saxena, G., Purchase, D., Mulla, S. I., Saratale, G. D., and Bharagava, R. N. (2019). Phytoremediation of Heavy Metal-Contaminated Sites: Eco-Environmental Concerns, Field Studies, Sustainability Issues, and Future Prospects. *Rev. Environ. Contam. Toxicol.* 249, 71–131. doi:10.1007/398_2019_24

Shahid, M. J., Tahseen, R., Siddique, M., Ali, S., Iqbal, S., and Afzal, M. (2019). Remediation of Polluted River Water by Floating Treatment Wetlands. *Water Supply* 19, 967–977. doi:10.2166/ws.2018.154

Shatalov, A. A., and Pereira, H. (2006). Papermaking Fibers from Giant Reed (*Arundo donax* L.) by Advanced Ecologically Friendly Pulping and Bleaching Technologies. *BioResources* 1, 45–61.

Shilpi, S., Lamb, D., Bolan, N., Seshadri, B., Choppala, G., and Naidu, R. (2019). Waste to Watt: Anaerobic Digestion of Wastewater Irrigated Biomass for Energy and Fertiliser Production. *J. Environ. Manag.* 239, 73–83. doi:10.1016/j.jenvman.2019.02.122

Sicilia, A., Testa, G., Santoro, D. F., Cosentino, S. L., and Piero, A. R. L. (2019). RNASeq Analysis of Giant Cane Reveals the Leaf Transcriptome Dynamics under Long-Term Salt Stress. *BMC Plant Biol.* 19, 355. doi:10.1186/s12870-019-1964-y

Sidella, S., Cosentino, S. L., Fernando, A., Costa, J., and Barbosa, B. (2017). "Phytoremediation of Soils Contaminated with Lead by *Arundo donax* L," in WASTES-solutions, Treatments and Opportunities II-Selected Papers from the 4th Edition of the International Conference Wastes: Solutions, Treatments and Opportunities, Porto, Portugal, September 25–26, 2017 (London, United Kingdom: CRC Press), 25–26.

Sidella, S., Fernando, A., Barbosa, B., Costa, J., Boléo, S., Bandarra, V., et al. (2013). "Phytoremediation Response of *Arundo donax* in Soils Contaminated with Lead," in Proceedings of the 21st European Biomass Conference and Exhibition, Setting the Course for a Biobased Economy, Copenhagen. Denmark, June 3–7, 2013 (Munich, Germany: ETA-Renewable Energies and WIP-Renewable Energies, 385–387.

Singh, A., Kuhad, R. C., and Ward, O. P. (2009). "Biological Remediation of Soil: an Overview of Global Market and Available Technologies," in *Advances in Applied Bioremediation. Soil Biology*. Editors A. Singh and O. P. Ward (Berlin, Germany: Springer), 1–19. doi:10.1007/978-3-540-89621-0_1

Singh, H. B. (2003). *Herbal Medicine of Manipur A Colour Encyclopedia*. New Delhi, India: Daya Publishing House.

Sinha, S. C. (1996). *Medicinal Plants of Manipur*. Manipur, India: Mass & Sinha Publications.

Speck, O., and Spatz, H.-C. (2004). Damped Oscillations of the Giant Reed *Arundo donax* (Poaceae). *Am. J. Bot.* 91, 789–796. doi:10.3732/ajb.91.6.789

Stottmeister, U., Wießner, A., Kuschk, P., Kappelmeyer, U., Kästner, M., Bederski, O., et al. (2003). Effects of Plants and Microorganisms in Constructed Wetlands for Wastewater Treatment. *Biotechnol. Adv.* 22, 93–117. doi:10.1016/j.biotechadv.2003.08.010

Sumiahadi, A., and Acar, R. (2018). A Review of Phytoremediation Technology: Heavy Metals Uptake by Plants. *IOP Conf. Ser. Earth Environ. Sci.* 142, 012023. doi:10.1088/1755-1315/142/1/012023

Takahashi, W., and Takamizo, T. (2012). "Molecular Breeding of Grasses by Transgenic Approaches for Biofuel Production," in *Transgenic Plants–Advances And Limitations*. Editor Y. O. Çiftçi (Rijeka, Croatia: InTech), 91–116.

Tang, H. (2000). Study on Cutting Seedling Technology of Giant Reed. *For. Sci. Technol.* 2, 13–14. doi:10.13456/j.cnki.lykt.2000.02.004

Tanner, C. C. (1996). Plants for Constructed Wetland Treatment Systems - A Comparison of the Growth and Nutrient Uptake of Eight Emergent Species. *Ecol. Eng.* 7, 59–83. doi:10.1016/0925-8574(95)00066-6

Taylor, N., Chavarriaga, P., Raemakers, K., Siritunga, D., and Zhang, P. (2004). Development and Application of Transgenic Technologies in Cassava. *Plant Mol. Biol.* 56, 671–688. doi:10.1007/s11103-004-4872-x

Tejada, M., Garcia, C., Gonzalez, J. L., and Hernandez, M. T. (2006). Use of Organic Amendment as a Strategy for Saline Soil Remediation: Influence on the Physical, Chemical and Biological Properties of Soil. *Soil Biol. Biochem.* 38, 1413–1421. doi:10.1016/j.soilbio.2005.10.017

Thakur, S., Singh, L., Ab Wahid, Z., Siddiqui, M. F., Atnaw, S. M., and Din, M. F. M. (2016). Plant-driven Removal of Heavy Metals from Soil: Uptake, Translocation, Tolerance Mechanism, Challenges, and Future Perspectives. *Environ. Monit. Assess.* 188, 206. doi:10.1007/s10661-016-5211-9

Tiwari, S., and Lata, C. (2018). Heavy Metal Stress, Signaling, and Tolerance Due to Plant-Associated Microbes: an Overview. *Front. Plant Sci.* 9, 452. doi:10.3389/fpls.2018.00452

Toscano, A., Marzo, A., Milani, M., Cirelli, G. L., and Barbagallo, S. (2015). Comparison of Removal Efficiencies in Mediterranean Pilot Constructed Wetlands Vegetated with Different Plant Species. *Ecol. Eng.* 75, 155–160. doi:10.1016/j.ecoleng.2014.12.005

Ullah, A., Heng, S., Munis, M. F. H., Fahad, S., and Yang, X. (2015). Phytoremediation of Heavy Metals Assisted by Plant Growth Promoting (PGP) Bacteria: a Review. *Environ. Exp. Bot.* 117, 28–40. doi:10.1016/j.envexpbot.2015.05.001

Verslues, P. E., Agarwal, M., Katiyar-Agarwal, S., Zhu, J., and Zhu, J.-K. (2006). Methods and Concepts in Quantifying Resistance to Drought, Salt and Freezing, Abiotic Stresses that Affect Plant Water Status. *Plant J.* 45, 523–539. doi:10.1111/j.1365-313x.2005.02593.x

Wang, M., Zhang, D., Dong, J., and Tan, S. K. (2018). Application of Constructed Wetlands for Treating Agricultural Runoff and Agro-Industrial Wastewater: a Review. *Hydrobiologia* 805, 1–31. doi:10.1007/s10750-017-3315-z

Wang, Q., Duan, L., Ruihua, L., and Wu, J. (2008). Comparison of Nutrient Uptake from Rural Domestic Sewage of Aquatic Plants. *Acta Agriculturae Boreali-Sinica* 23, 217–222.

Wang, R., Li, H., and Sun, H. (2019). Bismuth: Environmental Pollution and Health Effects. *Encyclopedia Environ. Health* 1, 415–423. doi:10.1016/b978-0-12-409548-9.11870-6

Williams, C., Biswas, T., Schrale, G., Virtue, J., and Heading, S. (2008). "Use of Saline Land and Wastewater for Growing a Potential Biofuel Crop (*Arundo donax* L.)," in Proceedings of Irrigation Australia Conference, Melbourne, Australia, May 20–22, 2008

Williams, C. M. J., Biswas, T. K., Black, I. D., Marton, L., Czako, M., Harris, P. L., et al. (2009). Use of Poor Quality Water to Produce High Biomass Yields of Giant Reed (*Arundo donax* L.) on Marginal Lands for Biofuel or Pulp/paper. *Acta Hortic.* 806, 595–602. doi:10.17660/actahortic.2009.806.74

Xian, K., Su, J., Fu, C., Huang, N., Gong, Q., and He, J. (2018). Techniques for Rapid Propagation of *Arundo donax*. *Guihaia* 38, 128–134.

Xie, W., Xie, F., Huang, L., Gao, X., Chen, J., Ma, X., et al. (2012). Purification Efficiency of Micro-polluted River Water by Horizontal Subsurface-Flow Constructed Wetland with *Arundo donax*. *China Water & Wastewater* 28, 69–71. doi:10.3969/j.issn.1000-4602.2012.21.020

Xue, S., Zhu, F., Kong, X., Wu, C., Huang, L., Huang, N., et al. (2016). A Review of the Characterization and Revegetation of Bauxite Residues (Red Mud). *Environ. Sci. Pollut. Res.* 23, 1120–1132. doi:10.1007/s11356-015-4558-8

Yamaguchi, H. (2018). Mutation Breeding of Ornamental Plants Using Ion Beams. *Breed. Sci.* 68, 71–78. doi:10.1270/jsbbs.17086

Yang, L., and Li, Y. (2014). Anaerobic Digestion of Giant Reed for Methane Production. *Bioresour. Technol.* 171, 233–239. doi:10.1016/j.biortech.2014.08.051

Yang, Q., Li, Z., Lu, X., Duan, Q., Huang, L., and Bi, J. (2018). A Review of Soil Heavy Metal Pollution from Industrial and Agricultural Regions in China: Pollution and Risk Assessment. *Sci. Total Environ.* 642, 690–700. doi:10.1016/j.scitotenv.2018.06.068

Yang, Y., Wang, Y., Zhu, M., and Lu, Y. (2016). A Study on Callus Induction and Plant Regeneration in Giant Reed (*Arundo donax*). *Pratacultural Sci.* 33, 1332–1341. doi:10.11829/j.issn.10010629.20150720

Yin, K., Wang, Q., Lv, M., and Chen, L. (2019). Microorganism Remediation Strategies towards Heavy Metals. *Chem. Eng. J.* 360, 1553–1563. doi:10.1016/j.cej.2018.10.226

Zema, D. A., Bombino, G., Andiloro, S., and Zimbone, S. M. (2012). Irrigation of Energy Crops with Urban Wastewater: Effects on Biomass Yields, Soils and Heating Values. *Agric. Water Manag.* 115, 55–65. doi:10.1016/j.agwat.2012.08.009

Zhang, Y., and Liu, J. (2011). Transgenic Alfalfa Plants Co-expressing Glutathione S-Transferase (GST) and Human *CYP2E1* Show Enhanced Resistance to Mixed Contaminates of Heavy Metals and Organic Pollutants. *J. Hazard. Mater.* 189, 357–362. doi:10.1016/j.jhazmat.2011.02.042

Zhang, Y., Sivakumar, M., Yang, S., Enever, K., and Ramezanianpour, M. (2018). Application of Solar Energy in Water Treatment Processes: A Review. *Desalination* 428, 116–145. doi:10.1016/j.desal.2017.11.020

Zhao, G., Huang, X., Tang, Z., Huang, Q., Niu, F., and Wang, X. (2018). Polymer-based Nanocomposites for Heavy Metal Ions Removal from Aqueous Solution: a Review. *Polym. Chem.* 9, 3562–3582. doi:10.1039/c8py00484f

Conflict of Interest: The authors declare that the research was conducted in the absence of any commercial or financial relationships that could be construed as a potential conflict of interest.

frontiers in Environmental Science

ORIGINAL RESEARCH
published: 15 June 2021
doi: 10.3389/fenvs.2021.684887

Prediction of Cadmium Transfer From Soil to Potato in Karst Soils, China

Ke Liu, Hongyan Liu, Xianyong Zhou, Zhu Chen and Xulian Wang*

College of Agriculture, Guizhou University, Guiyang, China

Contamination of food with the heavy metal Cd is a significant global concern. In this study, a field survey was performed to investigate the characteristics of Cd transfer from soil to potato tubers (n = 105). The results showed that the bioaccumulation factor of the potato tuber ranged from about 0.1 to 1. The soil threshold of Cd derived from the cumulative probability distribution was 0.15 mg kg^{-1} in order to protect 95% of potatoes. Additionally, prediction models for Cd transfer were constructed based on soil properties and the concentration of $CaCl_2$-extractable soil Cd. The results of the analysis showed that pH was the critical factor affecting Cd uptake by potatoes. Additionally, the R^2 of different empirical models increased from 0.354 to 0.715 as the number of soil parameters was increased, and the predicted soil Cd concentration approached the measured values at values of about 0–15 mg kg^{-1}. The results of this study suggest that the probability distribution method was stricter than the empirical prediction models for estimating the ecological risk of Cd contamination of potatoes in karst soils.

Keywords: cadmium, potato, soil threshold, prediction model, probability statistics

OPEN ACCESS

Edited by:
Jun Zhou,
University of Massachusetts Lowell, United States

Reviewed by:
Jiakai Gao,
Henan University of Science and Technology, China
Hongbiao Cui,
Anhui University of Science and Technology, China

****Correspondence:***
Hongyan Liu
hyliu@gzu.edu.cn

Specialty section:
This article was submitted to Toxicology, Pollution and the Environment, a section of the journal Frontiers in Environmental Science

Received: *24 March 2021*
Accepted: *18 May 2021*
Published: *15 June 2021*

Citation:
Liu K, Liu H, Zhou X, Chen Z and Wang X (2021) Prediction of Cadmium Transfer From Soil to Potato in Karst Soils, China. Front. Environ. Sci. 9:684887. doi: 10.3389/fenvs.2021.684887

INTRODUCTION

With the development of industry and agriculture in China, contamination of food by the trace metal cadmium (Cd) has become a public concern due to its toxicity and persistence in soil. Soil Cd has negative effects on crop growth and production (e.g., wheat and rice) and can affect human health through the food chain (Diao, et al., 2005). Potatoes are an important food resource in China, which has the largest potato production in the world. In 2019, the Chinese potato planting area reached 4.7895 million hectares, and China's potato production of 91.938 million tons accounted for 24.91% of the global total. The consumption of potatoes that have accumulated Cd from contaminated soil is a major issue because potatoes are widely planted around the world. For example, excessive Cd accumulated in potatoes (about 0.18 mg kg^{-1}) was shown to be caused by Cd pollution (1.25 mg kg^{-1}) in sierozem soil in Gansu Province, China (Liu, et al., 2019). Soil minerals in karst areas have high heavy metal content, and the metals in these minerals have been brought to the soil surface by geological and biological processes. Metal elements that have migrated to the surface have weak migration ability in the soil. Moreover, human activities in karst areas lead to a certain amount of heavy metal contamination in the local soil, further increasing the content of heavy metals and eventually leading to abnormal metal content (Tang, et al., 2021; Zhang, et al., 2021). Therefore, it is necessary to study the transfer of Cd from soil to crops in order to better control soil risks and ensure food safety.

In general, plant Cd concentrations are correlated with the soil total Cd. For example, soil total Cd accounted for 64% of the variation in the Cd concentration in potato tubers based on the results of stepwise multiple regression (n = 49) when irrigation was performed with river water contaminated by mining (Carla, et al., 2007). However, McLaughlin et al., (1997) found no significant correlation

between the Cd content in soil and that in potato tubers in a study of 352 potato production sites in Australia. These contradictory results may be due to differences in study regions, experimental conditions, and plant varieties. Soil total Cd concentrations can indicate the pollution status of soil, but cannot accurately reflect the pollution risk of soil to plants. The content of bioavailable Cd in soil mainly refers to the Cd that can be absorbed by crops during the crop growth period. In fact, many researchers have found that plant Cd content is closely related to the available Cd content in soil that is extractable by chemical extractants like $CaCl_2$ or CH_3COONH_4. The Tessier sequential extraction procedure can be used to extract five fractions of Cd with different reagents. For instance, Wei et al., 2020 used the five-step batch metal fractionation method to study the influence of spent mushroom substrate on Cd immobilization and soil amendment, and Mitchell et al., 2020 employed a similar method to explore the impact of low-temperature biochar on the Cd concentration of calcareous river sediments. While single extraction methods seem to be more convenient and practical, Cd and Zn extracted by 0.01 M $CaCl_2$ were successfully used to predict Cd levels in brown rice planted in paddy fields across the western plains in Taiwan (Römkens, et al., 2009; Kara et al., 2004) assessed the soil Cd content in sowing regions of potato fields from a total of 45 different sampling stations in Turkey by using HCl + H_2SO_4. 0.01 M $CaCl_2$ is a commonly used chemical extractant in various extraction methods used to research the bioavailability of Cd because 0.01 M $CaCl_2$ solution matches the soil with respect to pH, concentration, and composition (Zhou, et al., 2019). Additionally, the physical and chemical properties of soil also have a great influence on the accumulation and absorption of Cd by crops. For example, soil pH and concentrations of Cl and Zn were found to be the main factors affecting the Cd concentration of potato tubers in Australia (McLaughlin et al., 1997). Furthermore, using a stepwise regression model, Rafiq et al., 2014 showed that the Cd phytoavailability of pak choi grown in Chinese soils was dependent on soil properties such as pH and organic matter content.

Empirical models such as Freundlich-type models have been widely used to study the accumulation and transfer of heavy metals between soil and plants. The Cd concentrations of plants and soil, as well as bioaccumulation factors (BAFs), could be added to Freundlich-type models in order to predict the phytoavailability of metals for the evaluation of environmental quality. For example, the Freundlich relationship was applied to the empirical modeling of soil parameters including clay content, soil organic matter, cation exchange capacity, and soil Cd to predict the Cd content in wheat grain (François, et al., 2009). Additionally, multiple linear regression models have been used to predict the metal content of plants. For instance, the uptake and transfer of Cd in potatoes (n = 10) was predicted based on metal bioavailability (ethylenediamine tetraacetic acid extract) and soil properties in two contaminated regions of Kosovo (Zogaj and Düring, 2016). Moreover, Xu et al., 2019 used a polynomial model to derive Cd soil–plant relationships and soil criteria in order to provide suggestions for food safety and soil management. In recent years, the cumulative probability distribution method has been applied to study the soil threshold Cd concentrations in order to improve crop protection. For example, species sensitivity distribution (SSD) methodology is mainly used to determine the concentration of a toxicant that is protective of different ratios of species (50, 90, or 95%) in the environment. At present, the probability distribution functions used to fit the toxicological data of pollutants include log-normal, log-logistic, and Burr III type models. Liu et al., 2015 derived the soil threshold of Cd in a wheat-producing area of China (n = 18) based on probability estimation using the log-normal function. Moreover, Ding et al., 2016 used the SSD to obtain the soil thresholds of Pb for root vegetables with a BAF-based prediction model depending on the combination of soil pH and cation exchange capacity (CEC). Additionally, Ding et al., 2018 applied a similar cumulative probability distribution (SSD) to determine the soil threshold of Cd based on 12 root vegetable cultivars fitted by a Burr type III distribution with three different Cd treatments in various types of soil. These studies show that linear regression models can be used to describe the transport and enrichment of heavy metals, and the relationships between heavy metals in soil and plants. Therefore, probability statistics such as the SSD method can be used to perform risk assessment of pollutants at the level of the whole ecosystem and set soil thresholds.

Paired soil and plant samples (n = 105) were collected, and concentrations of Cd were measured. The present study aimed to 1) investigate the characteristics of Cd transfer from soil to potato tubers in a karst area of Guizhou Province, China, 2) obtain the soil Cd threshold based on the cumulative probability distribution using the log-normal function, and 3) explore an empirical prediction model based on plant and soil Cd concentrations and soil factors like pH and organic matter in order to improve soil environmental quality and protect food safety and human health.

MATERIALS AND METHODS

Sample Collection

Field research was carried out in farmland in Guizhou Province, China. This province has a high background content of Cd due to the prevalent karst geochemical conditions, and the problem of soil Cd pollution is particularly prominent. For example, the relationships between soil properties and the accumulation of heavy metals in *Brassica campestris* L. in a karst area of Guizhou Province showed that the background levels of heavy metals in the soil of Guizhou Province are generally high due to the influence of topography and the presence of soil parent material (Zhang, et al., 2020). An analysis of the risk posed by eight typical heavy metals in soils in Guizhou Province using province-wide data available in the literature revealed that Cd showed a very high potential ecological risk (Yu, et al., 2021). We selected the counties of Weining, Hezhang, Ceheng, Changshun, and Leigong, each of which contains a large proportion of carbonate rocks, for sampling. Soil was collected from the upper layer of the soil (0–20 cm). The distance between the sampling point and the local trunk road was more than 100 m.

TABLE 1 | Basic soil properties.

Soil property	Number	Average	Standard deviation	Median	Minimum	Maximum
pH	105	6.53	1.12	6.79	4.27	8.61
Organic matter ($g \cdot kg^{-1}$)	105	40.22	14.07	37.55	7.26	79.68

Sample Analysis

The collected soil samples were air-dried and then crushed with wooden sticks before being passed through a nylon sieve with a diameter of 0.149 mm. The collected potato samples were washed with tap water to remove surface soil particles and were then washed with distilled water, put into an oven at 105–110°C for 15 min, and dried to a constant weight at 70–90°C in the oven. Finally, the samples were smashed for the subsequent analysis. The soil physical and chemical properties were determined by routine methods (Liu, et al., 2015), soil pH was determined by a glass electrode at a soil:water ratio of 1:2.5 ($g\ ml^{-1}$), organic matter content was measured based on an oil bath heating method (potassium dichromate oxidation), and the results are shown in **Table 1**.

The total Cd in soil was determined as follows: we accurately weighed 0.1 g (accurate to 0.0001 g) of the sieved soil sample and placed it in a polytetrafluoroethylene (PTFE) tank, added 3 ml HNO_3 and 3 ml HCl, and placed the capped tank in a matched steel pipe, which was sealed. The steel pipe was placed in an incubator and heated at 185°C at a pressure of 790 kPa for 8 h. After cooling to room temperature, the digestion solution was removed from the pipe, placed on an electric heating plate, heated to 160°C, and steamed until it was viscous. The residual digestion solution was transferred to a 50 ml volumetric flask and diluted to 50 ml with ultrapure water.

Soil bioavailable Cd was determined by $CaCl_2$ extraction. A soil sample (2.00 g) was passed through a 0.2 mm sieve and placed in a 50 ml centrifuge tube. Then, 0.01 mol L^{-1} $CaCl_2$ solution was added and the tube was shaken for 2 h and centrifuged at 3,500 $r \cdot min^{-1}$ for 5 min. The level of Cd in the supernatant was detected. We accurately weighed 0.3 g (accurate to 0.0001 g) of each plant sample, placed it in a PTFE tank, and soaked it in 6 ml of HNO_3 overnight. Then, 2 ml of H_2O_2 solution was mixed into the above solution and the tank was covered and placed in a supporting steel pipe and sealed. Plant Cd was determined as follows: the steel pipe was placed in an oven and heated at 100°C for 2 h. Next, the temperature was raised to 140°C for 2 h, after which it was raised to 160°C for 4 h. The method for solution transferal and detection of the plant Cd concentration was the same as that used for the soil samples. A total of 10 ml of each digested sample solution was analyzed by inductively coupled plasma mass spectrometry to determine its Cd concentration (ICP-MS; Thermo Fisher Scientific, Waltham, MA, United States, and x2). Reference material GSS-5 and GSB-1 was adopted to ensure the quality control and the detected Cd concentration in soil and plant deviated about 15% from the true value.

Modeling

Statistical analysis was performed using Microsoft Excel 2010 and SPSS 22.0 software. The log-normal function was applied to fit the cumulative probability distribution curve (SSD curve) using SSD Generator V1 software. The cumulative probability distribution was obtained from the toxicological data for pollutants based on the concept of BAFs (C_{soil} = 0.1/BAF, 0.1 mg kg^{-1} was the limit of the Chinese food safety standard (GB 2762-2017) for Cd). The soil threshold values corresponding to different levels of protection or risk were obtained from the curve.

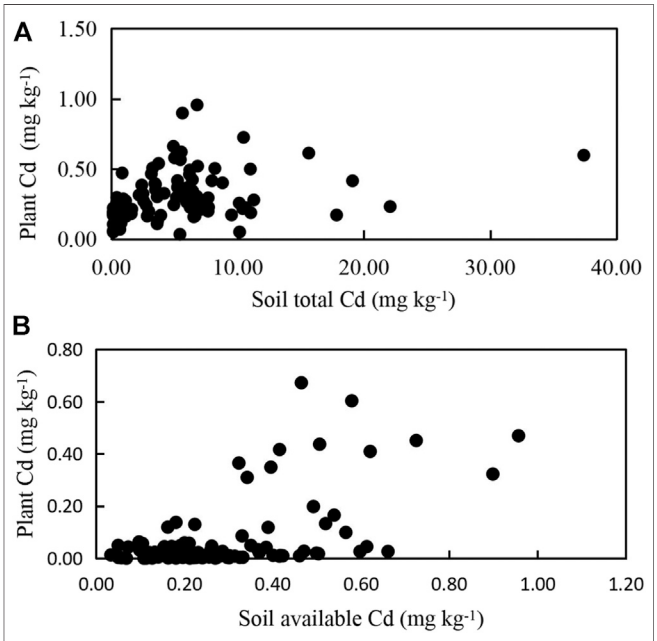

FIGURE 1 | Relationship between the plant Cd concentration and soil total Cd **(A)**, and the relationship between the plant Cd concentration and soil available Cd **(B)**.

The BAF is the ratio of the metal concentration in plant tissues to that in the soil, and is calculated as follows:

$$BAF = \frac{C_{plant}}{C_{soil}}, \quad (1)$$

where C_{plant} is the Cd concentration in the tuber of the test plant and C_{soil} is the Cd concentration in the test soil.

The relationships among soil Cd, plant Cd concentration, and soil properties were expressed by an empirical model as follows:

$$\text{Log } C_{soil} = a \times \log C_{plant} + b \times pH + c \times \log(\text{other soil properties}) + k, \quad (2)$$

where a, b, and c reflected the relationships among soil Cd, soil plant Cd, and soil properties, while k was the intercept.

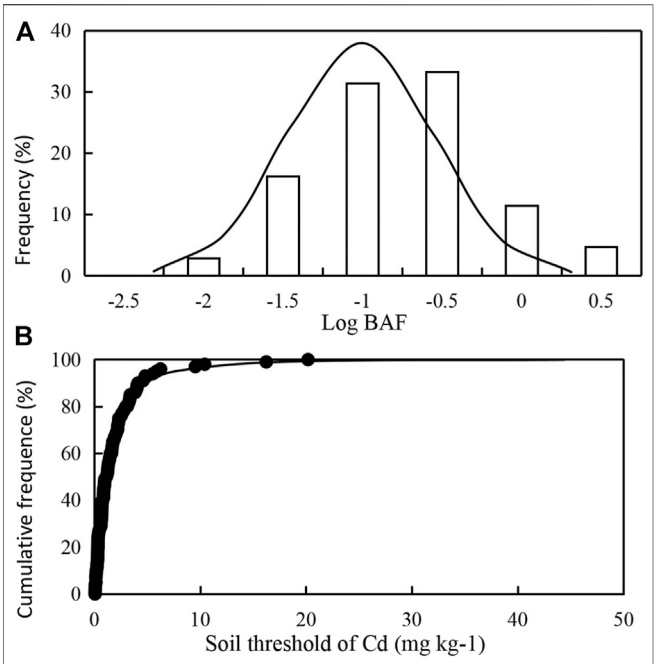

FIGURE 2 | Frequency distribution of the bioaccumulation factor (BAF) **(A)** and the cumulative probability distribution of the soil Cd threshold (**B**).

RESULTS AND DISCUSSION

Probability Statistics for Soil Cd Threshold

The total Cd concentration of the soil samples varied between 0.15 and 37.4 mg kg^{-1}, with an average value of 4.98 mg kg^{-1}, and the Cd concentration of the potato samples varied between 0.03 and 0.96 mg kg^{-1}, with an average value of 0.29 mg kg^{-1} (**Figure 1A**). The soil and plant Cd concentrations generally exceeded the Chinese soil environmental quality risk control standard for soil contamination of agricultural land (GB 15618-2018; soil screening levels of 0.3 and 0.6 mg kg^{-1}, respectively, for pH ≤ 7.5 and pH > 7.5) and food hygiene standards (GB 2762-2017, <0.1 mg kg^{-1}). The soil available Cd concentration varied between 0.0003 and 0.67 mg kg^{-1}, with an average value of 0.07 mg kg^{-1} (**Figure 1B**). The extractable Cd was far less than the soil total Cd; the average soil total Cd concentration was about 71 times that of the average extractable Cd concentration. Although the total Cd concentration in the soil was high, only a small proportion of this Cd could be absorbed by plants. The variation in soil total Cd and soil available Cd concentration are shown in **Figures 1A,B**. Previous studies found that the soil Cd significantly affected the Cd content of plants; for example, Liu et al., 2010 observed a significant difference ($p < 0.05$) in the Cd concentration of 40 Chinese cabbage shoots (from 0.88 to 7.76 mg kg^{-1}) when the soil Cd concentration increased from 1.0 to 5.0 mg kg^{-1}. However, Christopher et al., 2019 found that the Cd concentration in the flesh of potato was 0.2 mg kg^{-1} when the soil Cd concentration was lower than the detection limit. The results of experiments assessing the relationship between soil Cd content and plant Cd content have been inconsistent. Some studies have found that soil Cd levels were significantly related to plant Cd levels, while others have reported no relationship between these factors, perhaps due to the differences in plant species, climate, and other conditions.

The variation in BAFs calculated by **Eq. 1** was relatively large (about three orders of magnitude), facilitating the study of Cd transfer from soil to plants (**Figure 2A**). This large variation may be due to the fact that the external environment, including soil properties, plant varieties, irrigation, and fertilizer management, differed among the various study fields (Liu, et al., 2015). Statistical methods have been used to describe the probability distribution characteristics of BAFs in order to analyze Cd accumulation in potatoes. In the present study, it was found that the major BAF of Cd for plant uptake was in the range of 0.005–1.40, which is close to the BAF range found in a field survey of potatoes in four regions of New Zealand (Gray, et al., 2019). The critical value of the Cd concentration in soil may be deduced in terms of the limit of the Cd concentration in plants according to the measured bioaccumulation value (BAF = Cplant/Csoil, Cplant is 0.1 mg kg^{-1}, which is the maximum value of Cd in potato tubers according to Chinese national food safety standards, and the corresponding Csoil is the soil Cd criteria) (Diao, et al., 2005). The soil Cd critical value of sampling soil sites can be used to fit the cumulative distribution curve of the soil threshold in order to prevent Cd contamination of potatoes in karst areas. In the present study, the soil Cd concentration that protected potatoes in 95% of soil sites was taken as the soil threshold of Cd. The resulting probability cumulative distribution can be built in many ways. For example, probability cumulative distribution functions, such as log-normal, log-logistic, or Burr type III, have been applied to study the cumulative distribution of the soil or water threshold of Cd. In general, it is necessary to estimate the potential risk of pollutants more conservatively for the risk assessment and derivation of soil environmental thresholds. In a previous study, the soil threshold of As for eight Chinese wheat varieties was calculated for 18 soils using cumulative probability distribution methods, including the Burr type III function, based on the protection of 95% of wheat varieties (Dai et al., 2016). In addition, hazardous concentrations of nonylphenol in the soil environment were estimated using probabilistic approaches based on acute and chronic species sensitivity distributions (Kwak, et al., 2017).

The cumulative probability distribution curve shown in **Figure 2B** characterizes the ecological risk to ecosystems; the potential affected fraction of Cd for the environment was calculated according to a given soil threshold Cd concentration (such as 0.3 or 0.6 mg kg^{-1}). Furthermore, the distribution curve was also used to determine the soil threshold Cd concentration based on a given protection probability. For example, when the cumulative frequency was 20, 80% (100–20%) of soil sites have a safe soil Cd concentration below the soil Cd threshold. In the present study, it was found that the soil Cd threshold for the study area was 0.15 mg kg^{-1} to protect the plant samples in 95% of the soil sites based on the cumulative probability distribution (cumulative frequency = 5%) (**Figure 2B**). The cumulative probability distribution can also

TABLE 2 | Pearson correlations between soil total Cd (Cd_{total}), soil $CaCl_2$-extractable Cd (Cd_{CaCl2}), and plant Cd concentration (Cd_{plant}).

	Log Cd_{total}	Log Cd_{CaCl2}	Log Cd_{plant}
Log Cd_{total}	1	0.083	0.499[a]
Log Cd_{CaCl2}		1	0.434[a]
Log Cd_{plant}			1

** $p < 0.01$.

be used to obtain other soil Cd thresholds for protecting different proportions of potatoes. The soil Cd threshold determined in this study as sufficient for protection of 95% of soil sites in karst areas was slightly lower than the Chinese soil environmental quality risk control standard for the contamination of agricultural soil (GB 15618-2018). These results indicate that potatoes grown in karst areas, in which tubers may more easily accumulate Cd from soil, may be more susceptible to soil Cd pollution in comparison with those grown in other areas.

Prediction Model for Soil and Plant Cd Concentration

Since the biochemical behavior of Cd in soil is complex, and many factors affect Cd uptake by plants, it is important to study the toxicity of Cd in mature crops in order to protect human health. Empirical regression can be used to estimate the rate of accumulation or transfer of heavy metals from soil to crops based on soil properties. For example, Liang et al., 2013 log-transformed the Cd content of spinach and soil to normalize variance and match a Freundlich-type function, and they added soil properties such as pH to the prediction model to improve its fitting accuracy. Liu et al., 2015 used a similar empirical method to fit a soil Cd threshold model using 18 Chinese soil types to prevent contamination of wheat by Cd. In the present study, we found that log Cd_{CaCl2} and log Cd_{total} were both extremely significantly positively correlated with log Cd_{plant} ($p < 0.01$). The Pearson correlation coefficient was 0.434 for both log Cd_{CaCl2} and log Cd_{plant}, where it was 0.499 for log Cd_{total} and log Cd_{plant} (**Table 2**). These results indicate that both the soil total Cd and the $CaCl_2$-extracted Cd played an important role in Cd absorption by potato tubers. These findings are similar to those reported by Jun et al., 2018 from a study of the effects of alkaline amendment on Cd bioavailability in two Chinese cultivars of polished rice (Xiangwanxian 13 and Zhongyou 9,918) grown in paddy soil. A recent study using single extraction procedures, including methods utilizing EDTA, DTPA, CH_3COOH, and HCl, revealed that the extractable Cd in soil was linearly correlated with the Cd concentration in wheat grains (Liu et al., 2019). These results are consistent with our findings, which showed a similar relationship between Cd in soil and plant samples.

A stepwise linear regression was performed to establish the relationship between log Cd_{soil} (soil total Cd), log Cd_{CaCl2} (soil $CaCl_2$-extracted Cd), and soil pH and organic matter (OM) (n = 105) based on **Eq. 2**. The results of the prediction models showed that Cd_{total} was significantly correlated with the soil pH and OM, soil-extractable Cd_{CaCl2}, and Cd_{plant}; the R^2 value of the prediction model increased from 0.354 to 0.715 as the number of independent variables was increased (**Table 3**). Linear regression equations were obtained to describe the relationships between the total Cd concentration in soil and the Cd concentrations in wheat grains and roots (R^2 = 0.62, 0.71 for grains and roots, respectively), as well as between the $CaCl_2$-extracted Cd concentration in soil and the Cd concentrations in wheat grains and roots (R^2 = 0.58, 0.49 for grains and roots, respectively). A recent study indicated that the soil total Cd and $CaCl_2$-extracted Cd were useful predictors of the Cd transfer from soil to plants (Qu, et al., 2020), which was in agreement with the results described in the present study. Soil pH was an important predictive factor, as shown by its presence in every prediction model in **Table 3**, and, among the independent variables in equation (4), pH contributed approximately 47% of the variance in the dependent variables.

Prediction of soil threshold Cd values by linear equations is more convenient than prediction by the cumulative probability analysis method. The soil threshold calculated by the empirical prediction equation was greater than that calculated by the probability statistic method. For example, the soil thresholds of Cd were 0.35, 0.97, and 1.60 mg kg^{-1} when the soil pH was 5.5, 6.5, and 7, respectively, and the $soil_{CaCl2}$, OM, and Cd_{plant} were 0.1 mg kg^{-1}, 10 g kg^{-1}, and 0.1 mg kg^{-1}, according to equation (4) in **Table 3**. Previous studies have shown that soil properties, especially pH, are crucial factors influencing the transport of Cd between soil and vegetables. pH mainly affects the equilibrium distribution of heavy metal ions at the two-phase interface of soil and water, as well as the formation and dissolution of soil carbonate. Soil organic matter has a large number of functional groups, and its ability to adsorb Cd is much higher than that of other mineral colloids. Humic acid formed by decomposition can chelate (complex) with heavy metals, inhibiting the absorption of metals by plants. Using a stepwise regression model, Rafiq et al., 2014 concluded that Cd phytoavailability to pak choi was significantly affected by soil pH, organic matter, and total Zn and Cd concentrations, and the R^2 of the stepwise regression model in their report was 0.977. Furthermore, through stepwise forward multiple regressions, McLaughlin et al. (1997) found that soil parameters such as pH and Cl were important influences on the Cd concentration of potato tubers. Furthermore, the measured soil Cd concentrations in the present study were close to the values predicted using equation (4) (**Table 3**) for a certain soil Cd concentration range (about 0–15 mg kg^{-1}). The predicted soil Cd concentrations were greater than the measured values for higher soil Cd concentrations (**Figure 3**). In contrast with our results, a recent study reported no significant relationships between soil properties and the Cd concentration in potatoes in three field sites across New Zealand (Gray, et al., 2019). A recent study in Hunan province reported a soil Cd threshold of 1.819–3.272 mg kg^{-1} based on the safety limit of Cd in cereals (0.2 mg kg^{-1}), which was higher than that permitted

TABLE 3 | Prediction models for soil Cd concentration.

Prediction equation	R^2	*p*
Log Cd_{total} = 0.321pH−1.694	0.354	<0.01
Log Cd_{total} = 0.521pH + 0.481log $soil_{CaCl2}$−2.159	0.629	<0.01
Log Cd_{total} = 0.491pH + 0.469log $soil_{CaCl2}$+0.864log OM−3.346	0.679	<0.01
Log Cd_{total} = 0.436pH + 0.348log $soil_{CaCl2}$+0.804log OM+0.519log Cd_{plant}−2.785	0.715	<0.01

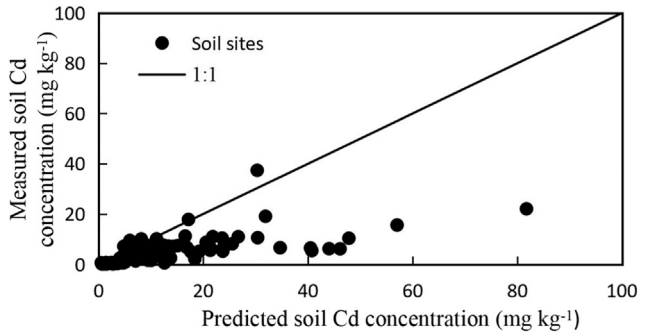

FIGURE 3 | Relationship between the measured and predicted soil Cd concentrations for different soil sites.

by the national soil environmental standards of China (Chen, et al., 2019). Using a prediction model, the threshold of soil total Cd in rootstalk vegetable fields in Guangdong was calculated to be 0.94 mg kg^{-1}, which was also higher than the national soil Cd threshold in China (Sun, et al., 2013). Although the threshold values of Cd from studies performed in non-karst area were higher than those from our research, these differences are likely due to differences in soil conditions, pollution conditions, plant species, and other factors. Further research is required to compare Cd uptake rates and soil threshold values for karst and non-karst areas.

CONCLUSION

In the frequency distribution of the BAF of potato tubers, BAF values from 0.1 to 0.3 occurred relatively frequently for soil Cd concentrations ranging from 0.15 to 37.4 mg kg^{-1}. The transfer of Cd from soil with a high Cd concentration to potato tubers was found to be highly positively correlated with soil pH, OM, and $CaCl_2$-extractable Cd (R^2 = 0.715). The log-transformed plant Cd concentration was highly significantly correlated with the soil total Cd and soil $CaCl_2$-extractable Cd concentrations, with Pearson correlations of 0.499 and 0.434, respectively. The log-normal function was used to establish the cumulative probability distribution of the soil Cd threshold. Our results show that the probability model and empirical model can each adequately describe the transfer of Cd from soil to crops.

DATA AVAILABILITY STATEMENT

The original contributions presented in the study are included in the article/Supplementary Material, and further inquiries can be directed to the corresponding author.

AUTHOR CONTRIBUTIONS

KL analyzed the data and wrote the manuscript, HL revised the manuscript, XZ collected the samples, and ZC and XW provided important suggestions for the manuscript.

FUNDING

This research was supported by the Joint Projects of the National Natural Science Foundation of China (42067028) and the Science and Technology Planning Project of Guizhou Province, China (Qiankehejichu no. (2019)1103, Qiankehehoubuzu no. (2020) 3001).

REFERENCES

Carla, O., Carlo, V., and Erik, S. (2007). Elevated Cadmium Concentrations in Potato Tubers Due to Irrigation with River Water Contaminated by Mining in Potosí, Bolivia. *J. Environ. Qual.* 36, 1181–1186. doi:10.1016/j.ecoenv.2016.04.031

Chen, Q., Peng, P., Hou, H., Ding, X., Long, J., au, X., et al. (2019). Effects of Soil Properties on the Cd Threshold in Typical Paddy Soils Using BCR Sequential Extraction. *Hum. Ecol. Risk Assess. Int. J.* 25, 2160–2173. doi:10.1080/10807039.2018.1490998

Christopher, N., Shiv, P., Eman, E., Jaskaran, D., Ali, M., and Ramanbhai, P. (2019). Effect of Biochar on Heavy Metal Accumulation in Potatoes from Wastewater Irrigation. *J. Environ. Manage.* 232, 153–164. doi:10.1016/j.ecoenv.2016.04.031

Dai, Y., Lv, J., Liu, K., Zhao, X., and Cao, Y. (2016). Major Controlling Factors and Prediction Models for Arsenic Uptake from Soil to Wheat Plants. *Ecotoxicology Environ. Saf.* 130, 256–262. doi:10.1016/j.ecoenv.2016.04.031

Diao, W.-P., Ni, W.-Z., Ma, H.-Y., and Yang, X.-E. (2005). Cadmium Pollution in Paddy Soil as Affected by Different Rice (Oryza Sativa L.) Cultivars. *Bull. Environ. Contam. Toxicol.* 75, 731–738. doi:10.1007/s00128-005-0812-y

Ding, C., Ma, Y., Li, X., Zhang, T., and Wang, X. (2016). Derivation of Soil Thresholds for lead Applying Species Sensitivity Distribution: A Case Study for Root Vegetables. *J. Hazard. Mater.* 303, 21–27. doi:10.1016/j.jhazmat.2015.10.027

Ding, C., Ma, Y., Li, X., Zhang, T., and Wang, X. (2018). Determination and Validation of Soil Thresholds for Cadmium Based on Food Quality Standard

and Health Risk Assessment. *Sci. Total Environ.* 619-620, 700–706. doi:10.1016/j.scitotenv.2017.11.137

François, M., Grant, C., Lambert, R., and Sauvé, S. (2009). Prediction of Cadmium and Zinc Concentration in Wheat Grain from Soils Affected by the Application of Phosphate Fertilizers Varying in Cd Concentration. *Nutr. Cycl Agroecosyst* 83, 125–133. doi:10.1007/s10705-008-9204-0

Gray, C. W., Yi, Z., Lehto, N. J., Robinson, B. H., Munir, K., and Cavanagh, J.-A. E. (2019). Effect of Cultivar Type and Soil Properties on Cadmium Concentrations in Potatoes. *New Zealand J. Crop Hortic. Sci.* 47, 182–197. doi:10.1080/01140671.2019.1599028

Jun, M., Libin, Z., Lu, W., Xingmei, L., Caixian, T., Hongjin, C., et al. (2018). Contrasting Effects of Alkaline Amendments on the Bioavailability and Uptake of Cd in rice Plants in a Cd-Contaminated Acid Paddy Soil. *Environ. Sci. Pollut. Res. Int.* 25, 8827–8835. doi:10.1007/s11356-017-1148-y

Kara, E. E., Pirlak, U., and Özdılek, H. G. (2004). Evaluation of Heavy Metals' (Cd, Cu, Ni, Ph, and Zn) Distribution in Sowing Regions of Potato Fields in the Province of Niğde, Turkey. *Water Air Soil Pollut.* 153, 173–186. doi:10.1023/b:wate.0000019942.37633.31

Kwak, J. I., Moon, J., Kim, D., Cui, R., and An, Y.-J. (2017). Species Sensitivity Distributions for Nonylphenol to Estimate Soil Hazardous Concentration. *Environ. Sci. Technol.* 51, 13957–13966. doi:10.1021/acs.est.7b04433

Liang, Z., Ding, Q., Wei, D., Li, J., Chen, S., and Ma, Y. (2013). Major Controlling Factors and Predictions for Cadmium Transfer from the Soil into Spinach Plants. *Ecotoxicology Environ. Saf.* 93, 180–185. doi:10.1016/j.ecoenv.2013.04.003

Liu, K., Lv, J., He, W., Zhang, H., Cao, Y., and Dai, Y. (2015). Major Factors Influencing Cadmium Uptake from the Soil into Wheat Plants. *Ecotoxicology Environ. Saf.* 113, 207–213. doi:10.1016/j.ecoenv.2014.12.005

Liu, W., Zhou, Q., An, J., Sun, Y., and Liu, R. (2010). Variations in Cadmium Accumulation Among Chinese Cabbage Cultivars and Screening for Cd-Safe Cultivars. *J. Hazard. Mater.* 173, 737–743. doi:10.1016/j.jhazmat.2009.08.147

Liu, Z., Bai, Y., and Yang, T. (2019). Effect of Cd on the Uptake and Translocation of Pb, Cu, Zn, and Ni in Potato and Wheat Grown in Sierozem. *Soil Sediment. Contam.* 28, 650–669. doi:10.1080/15320383.2019.1643289

McLaughlin, M. J., Maier, N. A., Rayment, G. E., Sparrow, L. A., Berg, G., au, A., et al. (1997). Cadmium in Australian Potato Tubers and Soils. *J. Environ. Qual.* 26, 1644–1649. doi:10.2134/jeq1997.00472425002600060026x

Mitchell, K., Mendoza-González, C. V., Ramos-Gómez, M. S., Yamamoto-Flores, L., Guerrero-Barrera, A. L., Macias-Medrano, R., et al. (2020). The Effect of Low-Temperature Biochar and its Non-pyrolyzed Composted Biosolids Source on the Geochemical Fractionation of Pb and Cd in Calcareous River Sediments. *Environ. Earth Sci.* 79. doi:10.1007/s12665-020-08908-5

Qu, X., Xu, W., Ren, J., Zhao, X., Li, Y., and Gu, X. (2020). A Field Study to Predict Cd Bioaccumulation in a Soil-Wheat System: Application of a Geochemical Model. *J. Hazard. Mater.* 400, 123135. doi:10.1016/j.jhazmat.2020.123135

Rafiq, M. T., Aziz, R., Yang, X., Xiao, W., Stoffella, P. J., Saghir, A., et al. (2014). Phytoavailability of Cadmium (Cd) to Pak Choi (Brassica Chinensis L.) Grown in Chinese Soils: A Model to Evaluate the Impact of Soil Cd Pollution on Potential Dietary Toxicity. *PLoS One* 9, e111461. doi:10.1371/journal.pone.0111461

Römkens, P. F. A. M., Guo, H. Y., Chu, C. L., Liu, T. S., Chiang, C. F., and Koopmans, G. F. (2009). Prediction of Cadmium Uptake by Brown rice and Derivation of Soil-Plant Transfer Models to Improve Soil protection Guidelines. *Environ. Pollut.* 157, 2435–2444. doi:10.1016/j.envpol.2009.03.009

Sun, F. F., Wang, F. H., Wang, X., He, W., Wen, D., Wang, Q. F., et al. (2013). Soil Threshold Values of Total and Available Cadmium for Vegetable Growing Based on Field Data in Guangdong Province, South China. *J. Sci. Food Agric.* 93, 1967–1973. doi:10.1002/jsfa.6000

Tang, M., Lu, G., Fan, B., Xiang, W., and Bao, Z. (2021). Bioaccumulation and Risk Assessment of Heavy Metals in Soil-Crop Systems in Liujiang Karst Area, Southwestern China. *Environ. Sci. Pollut. Res.* 28, 9657–9669. doi:10.1007/s11356-020-11448-x

Wei, Y., Jin, Z., Zhang, M., Li, Y., Huang, S., au, X., et al. (2020). Impact of Spent Mushroom Substrate on Cd Immobilization and Soil Property. *Environ. Sci. Pollut. Res.* 27, 3007–3022. doi:10.1007/s11356-019-07138-y

Xu, G., Zhang, S., Song, J., Brewer, R., and Gao, H. (2019). Cadmium Uptake in Radish (Raphanus Sativus L.) and Surficial Contamination: Implications for Food Safety and Local Soil Management. *J. Soils Sediments* 19, 3585–3596. doi:10.1007/s11368-019-02290-x

Yu, G., Chen, F., Zhang, H., and Wang, Z. (2021). Pollution and Health Risk Assessment of Heavy Metals in Soils of Guizhou, China. *Ecosystem Health and Sustainability* 7. doi:10.1080/20964129.2020.1859948

Zhang, J., Mu, G., Zhang, Z., Huang, X., and Fang, H. (2021). Speciation Variation and Bio-Activation of Soil Heavy Metals (Cd and Cr) in Rice-Rape Rotation Lands in Karst Regions. *Int. J. Env. Res. Pub. He.* 18. doi:10.3390/ijerph18031364

Zhang, Z., Wu, X., Tu, C., Huang, X., Zhang, J., Fang, H., et al. (2020). Relationships between Soil Properties and the Accumulation of Heavy Metals in Different Brassica Campestris L. Growth Stages in a Karst Mountainous Area. *Ecotox. Environ. Safe.* 206. doi:10.1016/j.ecoenv.2020.111150

Zhou, W., Zhang, J., Zou, M., Liu, X., Di, X., Wang, Q., et al. (2019). Feasibility of Using rice Leaves Hyperspectral Data to Estimate CaCl2-Extractable Concentrations of Heavy Metals in Agricultural Soil. *Sci. Rep.-UK* 9. doi:10.1038/s41598-019-52503-z

Zogaj, M., and Düring, R.-A. (2016). Plant Uptake of Metals, Transfer Factors and Prediction Model for Two Contaminated Regions of Kosovo. *J. Plant Nutr. Soil Sci.* 179, 630–640. doi:10.1002/jpln.201600022

Conflict of Interest: The authors declare that the research was conducted in the absence of any commercial or financial relationships that could be construed as a potential conflict of interest.

frontiers in Environmental Science

ORIGINAL RESEARCH
published: 07 July 2021
doi: 10.3389/fenvs.2021.638324

The Combination of Lime and Plant Species Effects on Trace Metals (Copper and Cadmium) in Soil Exchangeable Fractions and Runoff in the Red Soil Region of China

Lei Xu[1,2], Xiangyu Xing[3], Hongbiao Cui[4], Jing Zhou[5], Jun Zhou[5], Jianbiao Peng[6], Jingfeng Bai[1], Xuebo Zheng[7] and Mingfei Ji[2]**

[1]College of Environmental Science and Tourism, Nanyang Normal University, Nanyang, China, [2]Henan Key Laboratory of Ecological Security for Water Source Region of Mid-Line of South-to-North Diversion Project, Nanyang, China, [3]College of Non-Major Foreign Language Teaching, Nanyang Normal University, Nanyang, China, [4]School of Earth and Environment, Anhui University of Science and Technology, Huainan, China, [5]Key Laboratory of Soil Environment and Pollution Remediation, Chinese Academy of Science, Institute of Soil Science, Nanjing, China, [6]School of Environment, Henan Normal University, Xinxiang, China, [7]The Key Laboratory of Tobacco Biology and Processing, Ministry of Agriculture and Rural Affairs, Tobacco Research Institute of Chinese Academy of Agricultural Sciences, Qingdao, China

OPEN ACCESS

Edited by:
Ravi Naidu,
University of Newcastle, Australia

Reviewed by:
Bhabananda Biswas,
University of South Australia, Australia
Varenyam Achal,
Guangdong Technion-Israel Institute of Technology (GTIIT), China

***Correspondence:**
Xuebo Zheng
zhengxuebo@caas.cn
Mingfei Ji
jimfdy@gmail.com

Specialty section:
This article was submitted to Toxicology, Pollution and the Environment, a section of the journal Frontiers in Environmental Science

Received: *06 December 2020*
Accepted: *28 June 2021*
Published: *07 July 2021*

Citation:
Xu L, Xing X, Cui H, Zhou J, Zhou J, Peng J, Bai J, Zheng X and Ji M (2021) The Combination of Lime and Plant Species Effects on Trace Metals (Copper and Cadmium) in Soil Exchangeable Fractions and Runoff in the Red Soil Region of China. Front. Environ. Sci. 9:638324. doi: 10.3389/fenvs.2021.638324

The water-soluble heavy metal ions in contaminated soil may enter aquatic ecosystem through runoff, thus causing negative impact on the water environment. In this study, a two-year *in situ* experiment was carried out to explore an effective way to reduce the runoff erosion and water-soluble copper (Cu) and cadmium (Cd) in a contaminated soil (Cu: 1,148 mg kg^{-1}, Cd: 1.31 mg kg^{-1}) near a large Cu smelter. We evaluated the ability to influence soil properties by four Cu-tolerance plant species (*Pennisetum sp., Elsholtzia splendens, Vetiveria zizanioides, Setaria pumila*) grown in a contaminated acidic soil amended with lime. The results show that the addition of lime can significantly reduce the exchangeable fraction (EXC) of Cu and Cd in soil (81.1–85.6% and 46.3–55.9%, respectively). Plant species cannot change the fraction distributions of Cu and Cd in the lime-amended soils, but they can reduce the runoff generation by 8.39–77.0%. Although water-soluble Cu concentrations in the runoff were not significantly differed and water-soluble Cd cannot be detected among the four plant species, the combined remediation can significantly reduce 35.9–63.4% of Cu erosion to aquatic ecosystem, following the order: *Pennisetum sp.* > *Elsholtzia splendens* > *Vetiveria zizanioides* > *Setaria pumila*. The implication of this study would provide valuable insights for contaminated soil management and risk reduction in the Cu and Cd contaminated regions.

Keywords: soil contamination, lime, phytoremediation, soil erosion, runoff

INTRODUCTION

Increasing anthropogenic activities such as smelting and irrigation using waste water and atmospheric deposition have caused severe heavy metal contamination in soil around the world (Xu X et al., 2018). Heavy metals entering the soil will harm human health through the food-chain (Ouyang et al., 2018a). Meanwhile, Soil erosion has been a worldwide land degradation process and a

serious threat to the sustainability of agriculture (Borrelli et al., 2015; Wang R et al., 2016; Wang Y et al., 2016). In China, 28.3% of the total soil loss occurs on agricultural lands, which account for only 6.8% of the total area of soil loss (MWR, 2007) (Li et al., 2014). The researches show that heavy metals mainly accumulate in the surface layer of soil and heavy metals in the surface layer can enter the surface runoff with the process of soil erosion (Devi and Bhattacharyy, 2018). Moreover, the migration of heavy metals with surface runoff will cause the expansion of heavy metal pollution area (Ouyang et al., 2018b).

In order to reduce the mobility and bioavailability of heavy metals in agricultural soils, many cost-effective and environmentally friendly techniques have been developed during the past decades (He et al., 2019). Lime has been used for *in situ* remediation of metal contaminated soil because it is cheap and easy to get (Guo et al., 2018; Zhang et al., 2019). At the same time, phytoremediation has been widely used in remediation of heavy metal contaminated soil because it is considered as an environmentally friendly and economic method to treat the pollutant (Ashraf et al., 2019; Liu et al., 2020).

The previous studies have greatly contributed to the knowledge of runoff and soil loss in red soil region of China (Xu Y et al., 2018). Many scholars have also done research on remediation of soil heavy metal pollution in this area (Liu et al., 2019). Nevertheless, changes of soil runoff after pollution remediation have received relatively little attention. The existing research mainly focuses on the soil heavy metal pollution situation, pollution sources, hazards and remediation measures. Unfortunately, the relationships between these remediation measures and runoff such as runoff and concentration of heavy metals in runoff have seldom been discussed. Meanwhile, few studies have compared the different remediation measures for optimisation purposes.

This study explores the various effects of the combined remediation of lime and *Pennisetum sp.*, *Elsholtzia splendens*, *Vetiveria zizanioides* on speciation and availability of heavy metals in soil and runoff and concentration of heavy metals in runoff. *Setaria pumila*, an indigenous plant didn't need to be planted artificially and could grow normally after the lime was applied in our previous studies, but would not grow in the soil without lime (Xu et al., 2017). So our study included five treatments: untreated soil, lime and native *Setaria lutescens* (indigenous plant, didn't need to be planted artificially), lime and *Elsholtzia splendens*, lime and *Vetiveria zizanioides*, lime and *Pennisetum sp*. We hypothesised that the combined remediation would reduce surface runoff and concentration of heavy metals in runoff. Specifically, the objectives are to define the relationship between plant species and runoff generation and to identify the best remediation activity for contaminated soil.

MATERIALS AND METHODS

Study Site

The study site is located in Guixi City, Jiangxi Province, China (116°55′ E, 28°12′ N). The area has a subtropical monsoon climate, with an average annual precipitation of 1808 mm. Farmers had used water containing heavy metals to irrigate for a long time, which lead to heavy metal contamination in soil (mainly Cu and Cd) and Cd concentrations in rice exceeding the National food health standards (0.2 mg kg^{-1}, GB 15201-94). The soil texture is sandy loam and the basic soil properties are listed in **Table 1**.

Lime and Plant Species

The Cu and Cd concentrations in the lime (particle size 0.25 mm, purchased from building materials market, Jiangxi, China) were 1.36 and 0.873 mg kg^{-1}, respectively; the pH was 12.2. Four phytoextractors were selected, including a Cu-tolerant plant (*Elsholtzia splendens*), energy plant (*Pennisetum sp.* and *Vetiveria zizanioides*) and a native weed (*Setaria pumila*). All the plants used in the experiment were obtained by indoor cultivation.

Plot Design

Five treatments were set up in this study: untreated soil (CK), lime and native *Setaria lutescens* (LW), lime and *Elsholtzia splendens* (LE), lime and *Vetiveria zizanioides* (LV), lime and *Pennisetum sp.* (LP), and every treatment was design with three replicates. The field plots were designed as 200 cm (length) × 200 cm (width) and were separated by plastic plates. 0.2% lime (based on the 0–17 cm soil weight) was applied every plot on December 23, 2012, then the lime was mixed thoroughly with the soil by rotary tillage. *Elsholtzia splendens* (planting density 20 × 20 cm), *Vetiveria zizanioides* (planting density 30 × 30 cm), and *Pennisetum sp.* (planting density 50 × 50 cm) were planted on 26 April each year (2013, 2014). Weeds (mainly *Setaria lutescens*) were cleared from all plots before planting every year and no more weeding after planting. All field plots were managed in the same management. Runoff was collected at the bottom of the slope in a channel that was connected to a 50 L plastic bucket, the runoff after each rainfall was calculated by weighing. The average slope gradient for the plots was approximately 3°.

Sample Collection

All the aboveground parts (shoots) of the plants were harvested in the middle of December each year. Some plant samples were brought back to the laboratory, and washed with tap water and then with ultrapure water. Thereafter, the plant samples were weighted after drying to constant weight in an oven at 80°C, subsequently, plant samples were crushed by a grinder and used for heavy metal analysis.

After the plant samples were harvested, five soil samples were collected in each plot and fully mixed to form a composite soil sample (about 1 kg), then the samples were air-dried and ground for physicochemical analysis.

We mainly study the runoff from April to June, because this period is rainy season and plants grown vigorously, which can have a significant impact on the runoff process. The runoff after each heavy rainfall was calculated by weighed, after the water sample in the plastic bucket was mixed, and 1 L water sample was taken out and shipped to our laboratory. After the sample was stationary for 3 days, the supernatant was separated by siphon method and prepared for chemical analysis.

TABLE 1 | Soil characteristics in the study site prior to this study (SOC = soil organic carbon).

Bulk density (g cm^{-3})	pH	SOC mg kg^{-1}	Total nitrogen g kg^{-1}	Total phosphorus g kg^{-1}	Total potassium g kg^{-1}	CEC cmol kg^{-1}	Total Cu mg kg^{-1}	Total Cd μg kg^{-1}
1.25	5.65	16.5	1.08	0.173	2.18	8.25	1,148	1.31×10^3

TABLE 2 | Surface soil properties after treatments (SOC = soil organic carbon, CK = untreated soil, LW, lime + *Setaria lutescens*; LE, lime + *Elsholtzia splendens*; LV, lime + *Vetiveria zizanioides*; LP, lime + *Pennisetum sp.*, Different lowercase letters indicate significant differences between treatments, $n = 3$, $p < 0.05$).

Time	Treatment	pH	SOC g kg^{-1}	Total Cu mg kg^{-1}	Total Cd μg kg^{-1}
2013	CK	5.65 ± 0.0651c	17.1 ± 0.765a	1.15×10^3 ± 35.4a	1.31×10^3 ± 135a
	LW	6.32 ± 0.133ab	17.0 ± 0.768a	1.19×10^3 ± 7.49a	1.32×10^3 ± 86.5a
	LV	6.11 ± 0.293ab	17.9 ± 1.43a	1.12×10^3 ± 111a	1.32×10^3 ± 166a
	LE	6.70 ± 0.202a	18.2 ± 2.82a	1.18×10^3 ± 44.3a	1.31×10^3 ± 114a
	LP	6.63 ± 0.0586a	18.0 ± 1.60a	1.22×10^3 ± 115a	1.32×10^3 ± 168a
2014	CK	5.40 ± 0.0608b	16.9 ± 0.370b	1.15×10^3 ± 33.5a	1.32×10^3 ± 95.6a
	LW	6.13 ± 0.0462a	17.2 ± 0.587ab	1.20×10^3 ± 25.3a	1.32×10^3 ± 132a
	LV	6.27 ± 0.155a	18.6 ± 0.958a	1.16×10^3 ± 88.6a	1.33×10^3 ± 22.6a
	LE	6.18 ± 0.176a	18.7 ± 0.359a	1.19×10^3 ± 48.8a	1.33×10^3 ± 181a
	LP	6.39 ± 0.333a	19.1 ± 1.09a	1.22×10^3 ± 96.2a	1.32×10^3 ± 94.1a

Sample Analysis

The soil pH was measured with a glass electrode at a water soil ratio of 2.5:1 (PHS-2CW-CN, Bante, Shanghai, China). Walkley–Black procedure was used to measure the soil organic carbon (SOC), total nitrogen (TN) and total phosphate (TP) (Walkley and Black, 1934). The soil total potassium (TN) was measured according to Olsen (1954).

The Cu and Cd in soil was measured by atomic absorption spectrophotometry (SpectrAA-220) after the samples were digested (Xu et al., 2016). In order to ensure the reliability of the experimental data, a standard soil sample (GBW07405, National Research Center for Certified Reference Materials, China) was used during the experiment. The fractions of Cu and Cd were determined by the modified Tessier sequential chemical extraction procedures which divided soil fractions into five grades (Xu et al., 2016). The Cu and Cd in the runoff were measured by atomic absorption spectrophotometry after filtered by 0.45 μm filter membrane.

Statistical Analysis

SPSS20.0 (IBM SPSS, Somers, NY, United States) was used for one-way ANOVA and correlation analysis and all the graphics were plotted by Sigmaplot 12.5.

RESULTS AND DISCUSSION

Surface Soil Properties

The properties of surface soil in plots of the five treatments are summarized in **Table 2**. The soil pH were significantly improved after the lime was applied, the range of improvement was 0.46–0.98. The addition of lime increased soil pH, mainly because lime was an alkaline substance, and its $CaCO_3$ content was high which contributed greatly to the improvement of soil pH (Li et al., 2019). There were difference during the different treatments of plants, but the effect of plants on soil pH was not significant in 2013 and 2014. At the same time, there was a reduction of the soil pH 1 year after the lime application, and the decreasing range was 0.16–0.52. This might be due to that the area was located in an acid deposition area, and a large amount of acid gas was emitted from the smelters and fertilizer plants. The soil organic carbon contents were similar among the five treatments in 2013 but variable in 2014. The highest soil organic carbon content in 2014 was found in the lime–*Pennisetum sp* (LP) treatment (19.1 g kg^{-1}). This result might be related to three factors: first, vegetation restoration in soil erosion areas increased vegetation coverage and reduced soil erosion and nutrient loss (Tao et al., 2020); at the same time, the presence of plant residues, roots and root exudates also increased the input of organic matter to the soil (Lu et al., 2019); last, after the combined remediation, the changes of microbial community structure and function related to organic carbon turnover might affect the accumulation of organic carbon (Zhao et al., 2015). These changes in soil ultimately affect the concentration of soil organic carbon. Compared with the CK, the combined treatment of lime and plants did not significantly change the total Cu and Cd in soil.

Chemical Fractions of Cd and Cu

Heavy metals in soil can be divided into solid and solution phases according to their existing forms, and they mainly exist in the solid phase (Xiao et al., 2017). Moreover, heavy metals in solid-phase can be divided into different fractions according to their solubility, mobility, bioavailability, and potential environmental toxicity, therefore, a single extraction step cannot fully evaluate the toxicity and migration of heavy metals in soil (Hou et al., 2017). In order to evaluate the migration and bioavailability of heavy metals in soil, a sequential extraction procedure was used in the present study. The fractions of Cu and Cd in soil were listed in **Table 3**. The total Cu concentration was 1.15×10^3 mg kg^{-1} in the soil of CK, The Fe-Mn fraction of Cu (409 mg kg^{-1}, 35.6%) was most abundant, followed by the OM fraction (275 mg kg^{-1},

TABLE 3 | Soil Cu and Cd fractions after the treatments (CK, untreated soil; LW, lime + *Setaria lutescens*; LE, lime + *Elsholtzia splendens*; LV, lime + *Vetiveria zizanioides*; LP, lime + *Pennisetum sp*.; EXC, exchangeable fraction; CA, carbonate-bound fraction, Fe–Mn, Fe–Mn oxides-bound fraction; OM, organic matter-bound fraction; RES, residual fraction. Different lowercase letters indicate significant differences between treatments, $n = 3$, $p < 0.05$).

Heavy metal	Time	Treatment	EXC mg kg^{-1}	CA mg kg^{-1}	Fe-Mn mg kg^{-1}	OM mg kg^{-1}	RES mg kg^{-1}	Total mg kg^{-1}
Cu	2013	CK	77.3 ± 11.0a	217 ± 8.86a	409 ± 11.8a	275 ± 25.0a	143 ± 15.7b	1.15×10^3 ± 35.4a
		LW	12.3 ± 3.44b	218 ± 11.6a	418 ± 31.1a	296 ± 15.5a	195 ± 8.10ab	1.19×10^3 ± 7.49a
		LV	11.4 ± 3.30b	221 ± 13.4a	488 ± 59.5a	256 ± 27.8a	209 ± 14.4a	1.12×10^3 ± 111a
		LE	14.6 ± 7.19b	207 ± 19.7a	458 ± 64.2a	260 ± 22.9a	168 ± 15.4ab	1.18×10^3 ± 44.3a
		LP	11.1 ± 2.84b	208 ± 28.3a	462 ± 13.3a	270 ± 45.1a	216 ± 37.7a	1.22×10^3 ± 116a
	2014	CK	82.6 ± 6.94a	218 ± 8.86a	431 ± 27.9a	273 ± 34.0a	154 ± 38.8a	1.15×10^3 ± 33.5a
		LW	20.0 ± 5.09b	221 ± 13.5a	445 ± 30.1a	291 ± 17.5a	173 ± 22.0a	1.12×10^3 ± 25.3a
		LV	19.4 ± 0.80b	224 ± 28.1a	483 ± 44.3a	255 ± 11.0a	202 ± 30.7a	1.16×10^3 ± 88.6a
		LE	19.7 ± 4.78b	207 ± 19.7a	461 ± 23.3a	250 ± 23.3a	169 ± 15.2a	1.19×10^3 ± 48.8a
		LP	16.6 ± 3.72b	208 ± 28.3a	470 ± 45.0a	264 ± 14.9a	217 ± 40.6a	1.22×10^3 ± 96.2a
Heavy metal	**Time**	**Treatment**	**EXC μg kg^{-1}**	**CA μg kg^{-1}**	**Fe-Mn μg kg^{-1}**	**OM μg kg^{-1}**	**RES μg kg^{-1}**	**Total μg kg^{-1}**
Cd	2013	CK	564 ± 82.6a	101 ± 12.2b	144 ± 22.0a	24.5 ± 3.78b	562 ± 40.0a	1.31×10^3 ± 135a
		LW	298 ± 36.4b	175 ± 17.3a	235 ± 12.4a	42.9 ± 7.17ab	629 ± 31.9a	1.33×10^3 ± 86.5a
		LV	297 ± 60.0b	191 ± 35.1a	241 ± 48.2a	38.2 ± 7.93ab	675 ± 44.5a	1.32×10^3 ± 166a
		LE	249 ± 25.1b	194 ± 21.1a	242 ± 33.2a	44.6 ± 7.99a	589 ± 39.4a	1.3110^3 ± 114a
		LP	303 ± 96.7b	183 ± 36.2a	232 ± 68.0a	35.9 ± 6.64ab	566 ± 123a	1.32×10^3 ± 168a
	2014	CK	567 ± 60.2a	101 ± 12.2b	151 ± 15.8b	24.6 ± 2.90b	570 ± 14.2a	1.32×10^3 ± 95.6a
		LW	307 ± 55.4b	174 ± 6.01a	236 ± 9.77a	45.0 ± 9.99a	626 ± 53.5a	1.3210^3 ± 132a
		LV	299 ± 18.1b	193 ± 35.6a	245 ± 30.5a	38.2 ± 2.65ab	726 ± 188a	1.33×10^3 ± 226a
		LE	255 ± 26.7b	197 ± 9.96a	245 ± 50.8a	45.9 ± 6.52a	585 ± 55.6a	1.33×10^3 ± 181a
		LP	303 ± 45.7b	184 ± 14.6a	224 ± 27.6ab	36.2 ± 4.01ab	546 ± 20.5a	1.32×10^3 ± 94.1a

23.9%) and CA fraction (217 mg kg^{-1}, 18.9%); the RES fraction (143 mg kg^{-1}, 12.4%) and EXC fraction (77.3 mg kg^{-1}, 6.72%) were the lowest. When the lime was added to the soil, the EXC fractions of all the other four treatments were reduced significantly in 2013 and 2014. Both of the most maximum reduction in 2013 and 2014 were found in LP, where EXC fraction with 85.6% reduction from 77.3 to 11.1 mg kg^{-1} and a 82.4% reduction from 82.6 to 16.6 mg kg^{-1}, respectively. Conversely, the RES fractions were significantly improved in the combined remediation compared with CK. Just as the EXC fraction, the most maximum promotion of RES fractions in 2013 and 2014 were found in LP, and the RES fraction was increased by 51.0 and 40.9%, respectively. While there was no significant difference of the CA fraction, Fe-Mn fraction and OM fraction among the five treatments. It is worth noting that there was no significant difference in Cu fractions among the four different plant treatments (LW, LV, LE, LP), in other words, almost all the changes of Cu fractions were caused by the addition of lime but not the cultivation of plant.

The total Cd concentration in soil was 1.31×10^3 μg kg^{-1}, but different from the distribution of Cu, the Cd in the soil of CK was mainly present in the EXC fraction (564×10^3 μg kg^{-1}, 43.1%), which indicated that the bioavailability of Cd was higher than that of Cu in this area. Additionally, the RES fraction (562×10^3 μg kg^{-1}, 42.9%) was abundant and followed by the Fe-Mn and CA fraction which were 144×103 μg kg^{-1} (11.0%) and 101×103 μg kg^{-1} (7.71%), respectively. The OM fraction (24.5×10^3 μg kg^{-1}, 1.87%) was the least in the soil of CK. With lime application, the total Cd concentration was almost unchanged, but the EXC fraction of Cd was significantly by 46.3–55.9% and 45.9–55.0% in 2013 and 2014, respectively. While the CA fraction was markedly increased, the decrease rates in 2013 and 2014 were 73.3–92.1% and 72.3–95.0%, respectively. However, the addition of lime had no significant effect on Fe-Mn, OM and RES fraction of Cd in soil. Similar to the fraction of Cu in soil, there was no significant difference in Cd fractions among the four different plant treatments (LW, LV, LE, LP).

The EXC fraction of heavy metals is considered as a phase which is much easier to migrate and has higher bioavailability (Markovic et al., 2019). The EXC fraction of Cd is often present at low concentrations (<10% of total Cd) in uncontaminated soil (Wong et al., 2002). However, in this study, the EXC fraction of Cd constituted 43.1% of the total Cd in the soil of CK, which far more than that in uncontaminated soil. We speculated that the high EXC fraction of Cd was not only related to irrigation, but also introduced from atmospheric deposition of the nearby copper smelter. Research shows that the Cd which enters the soil through atmospheric deposition has high activity and bioavailability (Zhou et al., 2019). Additionally, the EXC fraction can be used to evaluate the bioavailability and environmental toxicity of heavy metals (Mohamed et al., 2017). In this study, the EXC fraction of Cu and Cd were significantly decreased by the combine remediation, meanwhile the RES and CA fractions were increased after the application. At the same time, the percentages of EXC fraction of both Cd and Cu were significantly decreased after the combine remediation. This demonstrated that lime could be used as an effective amendment to decrease the bioavailability and mobility of Cd and Cu in the contaminated soil. Meanwhile, the reduction of EXC fraction Cu (85.6%) by application of lime was much greater than that of Cd (55.9%) in terms of the reduction range, which indicated that the ability of lime to reduce the bioavailability and mobility of Cu was better than that of Cd.

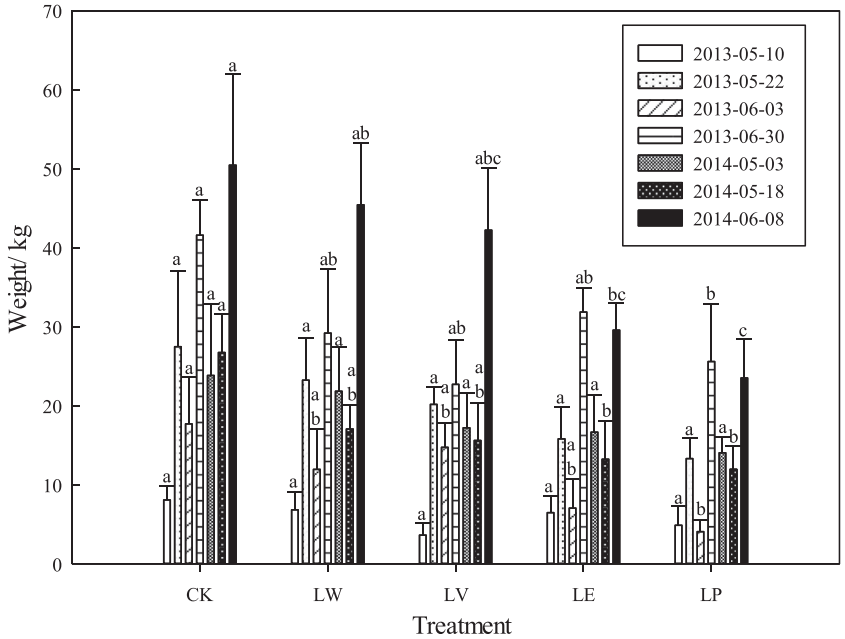

FIGURE 1 | Cumulative runoff of single rainfall for different treatments in 2013 and 2014(CK, untreated soil; LW, lime + *Setaria lutescens*; LE, lime + *Elsholtzia splendens*; LV, lime + *Vetiveria zizanioides*; LP, lime + *Pennisetum sp*., Different lowercase letters indicate significant differences between treatments, $n = 3$, $p < 0.05$).

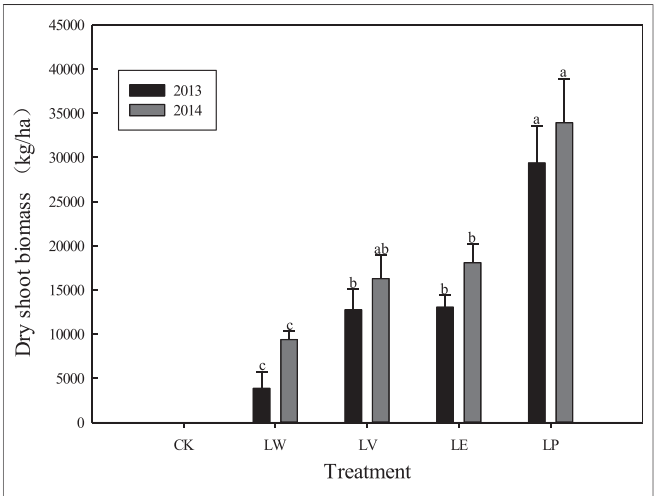

FIGURE 2 | Dry shoot biomass of each treatment (CK = untreated soil, LW = lime + *Setaria lutescens*, LE, lime + *Elsholtzia splendens*; LV, lime + *Vetiveria zizanioides*; LP, lime + *Pennisetum sp*., Different lowercase letters indicate significant differences between treatments in the same year, $n = 3$, $p < 0.05$).

Runoff Generation Response

A total of seven rainfall events greater than 50 mm were record during 2013 and 2014. The runoff generation was shown **Figure 1**, the runoff was significantly different among the five treatments. There was no significant difference of the runoff generation among the different treatments in 2013-05-10, 2013-05-22 and 2014-05-03. In the other four rainfall events, the CK treatment showed the largest runoff generation in every rainfall event among all of the plots, while the minimum runoff generation was LP treatment. Compared with CK, LW treatment can reduce runoff generation by approximately 9.95–32.6%. The runoff reduction rates of LV, LE and LP were calculated as 16.8%–53.4%, 23.3%–60.1% and 38.4–77.0%, respectively. While we found that the larger the shoot biomass, the smaller the runoff generation (**Figures 1**, **2**). The results showed that the combined remediation of lime and plants could effectively reduce the runoff generation in the process of rainfall. However, this effect only appears after the plant had grown for a period of time. The above ground part of hedgerow had the function of mechanical blocking to retain runoff and reduce runoff and sediment; the root system of underground part could fix soil and improve soil physical and chemical properties (Cao et al., 2015). After planting plants, the runoff generation time of the slope land could be lagged behind than control, and the more vigorous the aboveground part of the plants grow, the more obvious of the lag time of runoff generation was. The aboveground part of the plant had the mechanical blocking function to retain runoff and reduce runoff and sediment, the underground part of the root system could fix the soil and improve the soil physical and chemical properties (Wang et al., 2017; Wang et al., 2018).

Water-soluble metal concentration and pH in runoff are listed in the **Table 4**. Based on the analysis, we found that the runoff pH was significantly increased by the combined remediation of lime and plant in runoff events of 2013-06-03, 2014-05-03, 2014-05-18 and 2014-06-08. However, the effect of plant on the pH of runoff was not significant after lime was applied. Similar to the pH of runoff, the addition of lime in soil could significantly reduce the water-soluble Cu concentration in runoff, but the plant had no significant effect on the water-soluble Cu concentration. The reduction rates of water-soluble Cu concentration in each rainfall

TABLE 4 | Water-soluble metal concentration and pH in runoff of different remediation measures (CK, untreated soil; LW, lime + *Setaria lutescens*; LE, lime + *Elsholtzia splendens*; LV, lime + *Vetiveria zizanioides*; LP, lime + *Pennisetum sp.*, Different lowercase letters indicate significant differences between treatments, n = 3, $p < 0.05$).

Treatment	CK		LW		LV		LE		LP	
Time	pH	Cu mg kg^{-1}	pH	Cu mg kg^{-1}	pH	Cu mg kg^{-1}	pH	Cu mg kg^{-1}	pH	Cu mg kg^{-1}
2013-05-10	5.27 ± 0.25a	0.23 ± 0.025a	5.37 ± 0.19a	0.19 ± 0.012ab	5.53 ± 0.03a	0.19 ± 0.009ab	5.50 ± 0.20a	0.19 ± 0.020b	5.45 ± 0.19a	0.18 ± 0.007b
2013-05-22	5.09 ± 0.65a	0.21 ± 0.020a	6.02 ± 0.36a	0.16 ± 0.015b	5.59 ± 0.64a	0.18 ± 0.010ab	6.08 ± 0.24a	0.18 ± 0.022ab	5.87 ± 0.37a	0.18 ± 0.012ab
2013-06-03	5.17 ± 0.14b	0.22 ± 0.026a	5.66 ± 0.28a	0.17 ± 0.011ab	5.68 ± 0.03a	0.17 ± 0.027ab	5.72 ± 0.06a	0.13 ± 0.033b	5.61 ± 0.15a	0.15 ± 0.043ab
2013-6-30	5.27 ± 0.31a	0.19 ± 0.022a	5.38 ± 0.20a	0.15 ± 0.027ab	5.57 ± 0.32a	0.16 ± 0.025ab	5.81 ± 0.04a	0.12 ± 0.030b	5.50 ± 0.17a	0.12 ± 0.022b
2014-05-03	5.07 ± 0.28b	0.22 ± 0.029a	5.88 ± 0.22a	0.19 ± 0.020ab	5.67 ± 0.11ab	0.19 ± 0.016ab	6.08 ± 0.28a	0.17 ± 0.014b	5.55 ± 0.17ab	0.17 ± 0.014ab
2014-05-18	5.01 ± 0.28b	0.25 ± 0.028a	5.51 ± 0.25ab	0.18 ± 0.011b	5.54 ± 0.26ab	0.19 ± 0.016b	5.80 ± 0.30a	0.19 ± 0.010b	5.35 ± 0.20ab	0.18 ± 0.013b
2014-06-08	4.91 ± 0.09b	0.22 ± 0.017a	5.22 ± 0.12ab	0.19 ± 0.014ab	5.29 ± 0.18ab	0.19 ± 0.013ab	5.50 ± 0.31a	0.17 ± 0.011b	5.19 ± 0.18ab	0.17 ± 0.007b

was quite different, and the maximum reduction rate occurred in LE in 2013-06-03 (40.9%), the minimum reduction rate occurred in LW and LV in 2014-06-08 (13.6%). Combined with the data of runoff and Cu concentration in runoff, we found that the combine remediation could significantly reduce 35.9–63.4% of Cu erosion to aquatic ecosystem, following the order: *Pennisetum sp.* > *Elsholtzia splendens* > *Vetiveria zizanioides* > *Setaria pumila*. In this study, Cd was not detected in the runoff which might be due to the low concentration of Cd in soil compared with Cu, thus failed to reach the limit of instrument detection.

Numerous studies have shown that the activity and mobility of heavy metal can be significantly affected by soil pH (Zhai et al., 2018). The bioavailability and toxicity of heavy metals in soils are mainly depending on the activity of free ions rather than total amount. Soil pH is the most important factor affecting Cu and Cd availability among all parameters. The lower the environmental pH value is, the higher the mobility and activity of Cu and Cd is (Fei et al., 2018). Therefore, it is an effective measure to reduce the mobility and activity of Cu and Cd by adding lime to increase soil pH in acidic areas polluted by Cu and Cd (Rees et al., 2014). The EXC fraction of Cu in soil was reduced, and the water-soluble Cu concentration in runoff was reduced by increasing soil pH (**Table 3**, **Table 4**). The result is similar to Liu who found that the mass concentration of water-soluble Cd in runoff samples was significantly lower than that of other treatments after increasing soil pH by adding biochar in the same rainfall event (Liu et al., 2016). At the same time, previous study had shown that, the available Cu was converted to the stable component due to the decrease of redox potential (Eh) and the increase of pH under flooding condition, thus reducing the Cu activity (Cui et al., 2018). The results of correlation analysis showed that there was a significant correlation between Cu concentration in runoff and EXC fraction of Cu in soil ($p = 0.621$). This indicated that reducing the mobility and mobility of heavy metals in soil was an effective way to reduce the concentration of heavy metals in runoff. The addition of lime could significantly reduce the EXC fraction of Cu in soil, which might be the direct reason for the decrease of Cu concentration in runoff. At the same time, plant planting reduced the runoff generation, the combined effect of reduction of copper concentration in runoff and runoff generation decreased Cu erosion to aquatic ecosystem.

CONCLUSION

Five treatments were compared in terms of soil characteristics, runoff generation, water-soluble metal concentration and pH in runoff in this study. The results supported our hypothesis that four combine remediation (LW, LV, LE, and LP) could enhance the soil pH, SOC and reduce the EXC fraction of Cu and Cd in soil, while the water-soluble Cu concentration could be reduced and pH in runoff could be increased by this four remediation. Three combine remediation (LV, LE, LP) could reduce the surface runoff generation, which was vital to preventing sediment and heavy metal loss during water flow. However, the runoff generation cannot be significantly reduced by only lime application. Meanwhile, the LP treatment had the best performance in reducing runoff generation among the four treatments. As a result, the water-soluble Cu which into the river with the runoff is greatly reduced. Thus, the combine

remediation can improve soil quality, decrease heavy metal availability and mobility in the soil and can be effective in reducing heavy metal loss. However, because the main purpose of our study was to explore the effect of combined phytoremediation and lime on the exchangeable fractions and migration of heavy metals with water, we mainly considered the possible effect when designed the experiment, so the research on the mechanism was lacking. We will add indoor simulation experiments and pay more attention to the mechanism in the future field trials.

DATA AVAILABILITY STATEMENT

The original contributions presented in the study are included in the article/supplementary material, further inquiries can be directed to the corresponding authors.

AUTHOR CONTRIBUTIONS

LX is responsible for the writing of the paper and the conduct of the experiment, XX has made contributions to the revision of the language of the paper, HC, JGZ, JNZ, JP, JB, XZ, and MJ share the ideas and logic modification of the paper.

FUNDING

The research was funded by the PhD Special Project of Nanyang Normal University (2018ZX018), Scientific and Technological Research Projects in Henan Province (212102310844), the National Natural Science Foundation of China (31901195, 41601340) and scientific research and service platform fund of Henan province (2016151).

REFERENCES

Ashraf, S., Ali, Q., Zahir, Z. A., Ashraf, S., and Asghar, H. N. (2019). Phytoremediation: Environmentally Sustainable Way for Reclamation of Heavy Metal Polluted Soils. *Ecotoxicology Environ. Saf.* 174, 714–727. doi:10.1016/j.ecoenv.2019.02.068

Borrelli, P., Märker, M., and Schütt, B. (2015). Modelling Post-Tree-Harvesting Soil Erosion and Sediment Deposition Potential in the Turano River Basin (Italian Central Apennine. *Land Degrad. Develop.* 26, 356–366. doi:10.1002/ldr.2214

Cao, L., Zhang, Y., Lu, H., Yuan, J., Zhu, Y., and Liang, Y. (2015). Grass Hedge Effects on Controlling Soil Loss from Concentrated Flow: A Case Study in the Red Soil Region of China. *Soil Tillage Res.* 148, 97–105. doi:10.1016/j.still.2014.12.009

Cui, H., Zhang, W., Zhou, J., Xu, L., Zhang, X., Zhang, S., et al. (2018). Availability and Vertical Distribution of Cu, Cd, Ca, and P in Soil as Influenced by Lime and Apatite with Different Dosages: a 7-year Field Study. *Environ. Sci. Pollut. Res.* 25, 35143–35153. doi:10.1007/s11356-018-3421-0

Devi, U., and Bhattacharyy, K. G. (2018). Mobility and Bioavailability of Cd, Co, Cr, Cu, Mn and Zn in Surface Runoff Sediments in the Urban Catchment Area of Guwahati, India. *Appl. Water Sci.* 8, 18–32. doi:10.1007/s13201-018-0651-8

Fei, Y., Yan, X. L., and Li, Y. H. (2018). Stabilization Effects of Fe-Mn Binary Oxide on Arsenic and Heavy Metal Co-contaminated Soils under Different pH Conditions. *Environ. Sci.* 3, 1430–1437. doi:10.13227/j.hjkx.201707101

Guo, F., Ding, C., Zhou, Z., Huang, G., and Wang, X. (2018). Stability of Immobilization Remediation of Several Amendments on Cadmium Contaminated Soils as Affected by Simulated Soil Acidification. *Ecotoxicology Environ. Saf.* 161, 164–172. doi:10.1016/j.ecoenv.2018.05.088

He, L., Zhong, H., Liu, G., Dai, Z., Brookes, P. C., Xu, J., et al. (2019). Remediation of Heavy Metal Contaminated Soils by Biochar: Mechanisms, Potential Risks and Applications in China. *Environ. Pollut.* 252, 846–855. doi:10.1016/j.envpol.2019.05.151

Hou, D., O'Connor, D., Nathanail, P., Tian, L., and Ma, Y. (2017). Integrated GIS and Multivariate Statistical Analysis for Regional Scale Assessment of Heavy Metal Soil Contamination: A Critical Review. *Environ. Pollut.* 231, 1188–1200. doi:10.1016/j.envpol.2017.07.021

Li, Q. Y., Fang, H. Y., Sun, L. Y., and Cai, Q. G. (2014). USING THE 137 Cs TECHNIQUE TO STUDY THE EFFECT OF SOIL REDISTRIBUTION ON SOIL ORGANIC CARBON AND TOTAL NITROGEN STOCKS IN AN AGRICULTURAL CATCHMENT OF NORTHEAST CHINA. *Land Degrad. Develop.* 25, 350–359. doi:10.1002/ldr.2144

Li, Y., Cui, S., Chang, S. X., and Zhang, Q. (2019). Liming Effects on Soil pH and Crop Yield Depend on Lime Material Type, Application Method and Rate, and Crop Species: a Global Meta-Analysis. *J. Soils Sediments* 19, 1393–1406. doi:10.1007/s11368-018-2120-2

Liu, B., Wu, C., Pan, P., Fu, Y., He, Z., Wu, L., et al. (2019). Remediation Effectiveness of Vermicompost for a Potentially Toxic Metal-Contaminated Tropical Acidic Soil in China. *Ecotoxicology Environ. Saf.* 182, 109394–109402. doi:10.1016/j.ecoenv.2019.109394

Liu, H. L., Zhou, J., Li, M., Hu, Y. M., Liu, X., and Zhou, J. (2019). Study of the Bioavailability of Heavy Metals from Atmospheric Deposition on the Soil-Pakchoi (Brassica Chinensis L.) System. *J. Hazard. Mater.* 362, 9–16. doi:10.1016/j.jhazmat.2018.09.032

Liu, S., Yang, B., Liang, Y., Xiao, Y., and Fang, J. (2020). Prospect of Phytoremediation Combined with Other Approaches for Remediation of Heavy Metal-Polluted Soils. *Environ. Sci. Pollut. Res.* 27, 16069–16085. doi:10.1007/s11356-020-08282-6

Liu, X. L., Zeng, Z. X., Tie, B. Q., Chen, Q. W., and Wei, X. D. (2016). Cd Runoff Load and Soil Profile Movement after Implementation of Some Typical Contaminated Agricultural Soil Remediation Strategies. *Environ. Sci.* 37, 734–739. doi:10.13227/j.hjkx.2016.02.044

Lu, J., Dijkstra, F. A., Wang, P., and Cheng, W. (2019). Roots of Non-woody Perennials Accelerated Long-Term Soil Organic Matter Decomposition through Biological and Physical Mechanisms. *Soil Biol. Biochem.* 134, 42–53. doi:10.1016/j.soilbio.2019.03.015

Markovic, J., Jovic, M., Smiciklas, I., Sljivic-Ivanovic, M., Onjia, A., Trivunac, K., et al. (2019). Cadmium Retention and Distribution in Contaminated Soil: Effects and Interactions of Soil Properties, Contamination Level, Aging Time and *In Situ* Immobilization Agents. *Ecotoxicology Environ. Saf.* 174, 305–314. doi:10.1016/j.ecoenv.2019.03.001

Mohamed, B. A., Ellis, N., Kim, C. S., and Bi, X. (2017). The Role of Tailored Biochar in Increasing Plant Growth, and Reducing Bioavailability, Phytotoxicity, and Uptake of Heavy Metals in Contaminated Soil. *Environ. Pollut.* 230, 329–338. doi:10.1016/j.envpol.2017.06.075

Olsen, S. R. (1954). *Estimation of Available Phosphorus in Soils by Extraction with Sodium Bicarbonate*. Washington: Us Department of Agriculture Circ.

Ouyang, W., Wang, Y., Lin, C., He, M., Hao, F., Liu, H., et al. (2018a). Heavy Metal Loss from Agricultural Watershed to Aquatic System: A Scientometrics Review. *Sci. Total Environ.* 637-638, 208–220. doi:10.1016/j.scitotenv.2018.04.434

Ouyang, W., Yang, W., Tysklind, M., Xu, Y., Lin, C., Gao, X., et al. (2018b). Using River Sediments to Analyze the Driving Force Difference for Non-point Source Pollution Dynamics between Two Scales of Watersheds. *Water Res.* 139, 311–320. doi:10.1016/j.watres.2018.04.020

Rees, F., Simonnot, M. O., and Morel, J. L. (2014). Short-term Effects of Biochar on Soil Heavy Metal Mobility Are Controlled by Intra-particle Diffusion and Soil pH Increase. *Eur. J. Soil Sci.* 65, 149–161. doi:10.1111/ejss.12107

Tao, W., Wang, Q., Guo, L., and Lin, H. (2020). A New Analytical Model for Predicting Soil Erosion and Nutrient Loss during Crop Growth on the Chinese Loess Plateau. *Soil tillage Res.* 199, 104585–1045943. doi:10.1016/j.still.2020.104585

Walkley, A., and Black, I. A. (1934). An Examination of the Degtjareff Method for Determining Soil Organic Matter, and a Proposed Modification of the Chromic

Acid Titration Method. *Soil Sci.* 37, 29–38. doi:10.1097/00010694-193401000-00003

Wang, R., Guo, J., Xu, Y., Ding, Y., Shen, Y., Zheng, X., et al. (2016). Evaluation of Silkworm Excrement and Mushroom Dreg for the Remediation of Multiple Heavy Metal/metalloid Contaminated Soil Using Pakchoi. *Ecotoxicology Environ. Saf.* 124, 239–247. doi:10.1016/j.ecoenv.2015.10.014

Wang, Y., Cao, L., Fan, J., Lu, H., Zhu, Y., Gu, Y., et al. (2017). Modelling Soil Detachment of Different Management Practices in the Red Soil Region of China. *Land Degrad. Develop.* 28, 1496–1505. doi:10.1002/ldr.2658

Wang, Y., Fan, J., Cao, L., and Liang, Y. (2016). Infiltration and Runoff Generation under Various Cropping Patterns in the Red Soil Region of China. *Land Degrad. Develop.* 27, 83–91. doi:10.1002/ldr.2460

Wang, Y., Fan, J., Cao, L., Zheng, X., Ren, P., and Zhao, S. (2018). The Influence of Tillage Practices on Soil Detachment in the Red Soil Region of China. *Catena* 165, 272–278. doi:10.1016/j.catena.2018.02.011

Wong, S. C., Li, X. D., Zhang, G., Qi, S. H., and Min, Y. S. (2002). Heavy Metals in Agricultural Soils of the Pearl River Delta, South China. *Environ. Pollut.* 119, 33–44. doi:10.1016/s0269-7491(01)00325-6

Xiao, R., Wang, S., Li, R., Wang, J. J., and Zhang, Z. (2017). Soil Heavy Metal Contamination and Health Risks Associated with Artisanal Gold Mining in Tongguan, Shaanxi, China. *Ecotoxicology Environ. Saf.* 141, 17–24. doi:10.1016/j.ecoenv.2017.03.002

Xu, L., Cui, H., Zheng, X., Zhou, J., Zhang, W., Liang, J., et al. (2017). Changes in the Heavy Metal Distributions in Whole Soil and Aggregates Affected by the Application of Alkaline Materials and Phytoremediation. *RSC Adv.* 7, 41033–41042. doi:10.1039/c7ra05670b

Xu, L., Cui, H., Zheng, X., Zhu, Z., Liang, J., and Zhou, J. (2016). Immobilization of Copper and Cadmium by Hydroxyapatite Combined with Phytoextraction and Changes in Microbial Community Structure in a Smelter-Impacted Soil. *RSC Adv.* 6, 103955–103964. doi:10.1039/c6ra23487a

Xu, X., Zheng, F., Wilson, G. V., He, C., Lu, J., and Bian, F. (2018). Comparison of Runoff and Soil Loss in Different Tillage Systems in the Mollisol Region of Northeast China. *Soil Tillage Res.* 177, 1–11. doi:10.1016/j.still.2017.10.005

Xu, Y., Seshadri, B., Sarkar, B., Wang, H., Rumpel, C., Sparks, D., et al. (2018). Biochar Modulates Heavy Metal Toxicity and Improves Microbial Carbon Use Efficiency in Soil. *Sci. Total Environ.* 621, 148–159. doi:10.1016/j.scitotenv.2017.11.214

Zhai, X., Li, Z., Huang, B., Luo, N., Huang, M., Zhang, Q., et al. (2018). Remediation of Multiple Heavy Metal-Contaminated Soil through the Combination of Soil Washing and *In Situ* Immobilization. *Sci. Total Environ.* 635, 92–99. doi:10.1016/j.scitotenv.2018.04.119

Zhang, W.-h., Sun, R.-b., Xu, L., Liang, J.-n., and Zhou, J. (2019). Assessment of Bacterial Communities in Cu-Contaminated Soil Immobilized by a One-Time Application of Micro-/nano-hydroxyapatite and Phytoremediation for 3 Years. *Chemosphere* 223, 240–249. doi:10.1016/j.chemosphere.2019.02.049

Zhao, Y. L., Guo, H. B., Xue, Z. W., Mu, X. Y., and Li, C. H. (2015). [Effects of Tillage and Straw Returning on Microorganism Quantity, Enzyme Activities in Soils and Grain Yield]. *Ying Yong Sheng Tai Xue Bao* 26, 1785–1792.

Conflict of Interest: The authors declare that the research was conducted in the absence of any commercial or financial relationships that could be construed as a potential conflict of interest.

Advantages of publishing in Frontiers

OPEN ACCESS
Articles are free to read for greatest visibility and readership

FAST PUBLICATION
Around 90 days from submission to decision

HIGH QUALITY PEER-REVIEW
Rigorous, collaborative, and constructive peer-review

TRANSPARENT PEER-REVIEW
Editors and reviewers acknowledged by name on published articles

Frontiers
Avenue du Tribunal-Fédéral 34
1005 Lausanne | Switzerland

Visit us: www.frontiersin.org
Contact us: frontiersin.org/about/contact

REPRODUCIBILITY OF RESEARCH
Support open data and methods to enhance research reproducibility

DIGITAL PUBLISHING
Articles designed for optimal readership across devices

FOLLOW US
@frontiersin

IMPACT METRICS
Advanced article metrics track visibility across digital media

EXTENSIVE PROMOTION
Marketing and promotion of impactful research

LOOP RESEARCH NETWORK
Our network increases your article's readership